NOTICE

The quality of this microform is heavily dependent upon the quality of the original thesis submitted for microfilming. Every effort has been made to ensure the highest quality of reproduction possible.

If pages are missing, contact the university which granted the degree.

Some pages may have indistinct print especially if the original pages were typed with a poor typewriter ribbon or if the university sent us an inferior photocopy.

Reproduction in full or in part of this microform is governed by the Canadian Copyright Act, R.S.C. 1970, c. C-30, and subsequent amendments.

AVIS

La qualité de cette microforme dépend grandement de la qualité de la thèse soumise au microfilmage. Nous avons tout fait pour assurer une qualité supérieure de reproduction.

S'il manque des pages, veuillez communiquer avec l'université qui a conféré le grade.

La qualité d'impression de certaines pages peut laisser à désirer, surtout si les pages originales ont été dactylographiées à l'aide d'un ruban usé ou si l'université nous a fait parvenir une photocopie de qualité inférieure.

La reproduction, même partielle, de cette microforme est soumise à la Loi canadienne sur le droit d'auteur, SRC 1970, c. C-30, et ses amendements subséquents.

THE UNIVERSITY OF ALBERTA

THE ORIGIN OF DRYLAND SALINITY NEAR NOBLEFORD, ALBERTA

BY

JAMES JOHN MILLER

A THESIS

SUBMITTED TO THE FACULTY OF GRADUATE STUDIES AND RESEARCH

IN PARTIAL FULFILMENT OF THE REQUIREMENTS FOR THE DEGREE

OF DOCTOR OF PHILOSOPHY

IN

SOIL GENESIS AND CLASSIFICATION

DEPARTMENT OF SOIL SCIENCE

EDMONTON, ALBERTA

SPRING, 1989

ISBN 0-315-52862-1

THE UNIVERSITY OF ALBERTA

RELEASE FORM

NAME OF AUTHOR: JAMES JOHN MILLER

TITLE OF THESIS: THE ORIGIN OF DRYLAND SALINITY NEAR NOBLEFORD, ALBERTA

DEGREE: DOCTOR OF PHILOSOPHY

YEAR THIS DEGREE GRANTED: SPRING 1989

Jim Miller

10919 - 63rd Ave.
Edmonton
Alberta T6H 1R1

Date: April 14, 1989

THE UNIVERSITY OF ALBERTA

FACULTY OF GRADUATE STUDIES AND RESEARCH

The undersigned certify that they have read, and recommended to the Faculty of Graduate Studies and Research for acceptance, a thesis entitled The Origin of Dryland Salinity Near Nobleford, Alberta submitted by James John Miller in partial fulfilment of the requirements for the degree of Doctor of Philosophy in Soil Science.

(Supervisor)

Date: February 7, 1989

DEDICATION

to

Elmer and Marge Miller

ABSTRACT

The major objective of this study was to determine the origin of dryland salinity near Nobleford, Alberta, using field and laboratory techniques. Evaporite mineralogy, soil solution and groundwater chemistry of one saline seep were studied in detail. The soil solution and groundwater chemistry were dominated by Na and SO_4 ions. Dissolution of gypsum and bassanite contributed SO_4 ions to the soil solution, whereas Na ions were probably derived from the bedrock, or dissolution of mirabilite and cation exchange in the drift. Gypsum, bassanite, and calcite were the only evaporite minerals identified within the soil profile. Simulations with a geochemical model (SOLMNEQ) revealed that more soluble minerals such as mirabilite and epsomite could only precipitate in soil solutions of extremely high ionic strength. The mineral sequence observed in the soil profile could not be solely explained by mineral precipitation, as predicted by the Hardie-Eugster model. However, the common-ion effect involving decalcification and gypsum and/or bassanite precipitation may be an important factor.

Four saline seeps in the study area were investigated using hydrogeological methods to ascertain possible sources of excess water contributing to soil salinization. These sources were: artesian discharge from shallow and deep bedrock aquifers; flow through the upper, weathered bedrock zone; confined flow through coarse-textured drift deposits; and infiltration of surface water at lower elevations. Greater quantities of groundwater were

discharged at saline seeps via local flow at shallow depths (< 20 m) than from artesian discharge from deep bedrock aquifers (30 - 69 m).

The generation and transport of soluble salts to saline seeps on the lower slopes of bedrock ridges was generally from relatively shallow depths (< 20 m), and from short distances away (< 2,000 m). In closed topographic depressions (such as the Studhorse Lake basin), however, salts may be transported from the deeper bedrock (30 - 69 m), but only over a long period of time or if fracture-dominated flow was assumed to have occurred.

ACKNOWLEDGEMENTS

I gratefully acknowledge the contribution of the following people and organizations to this research:

- My supervisors, Dr. S. Pawluk and Dr. G. J. Beke, for their guidance and advice.
- Dr. M. J. Dudas, Dr. D. S. Chanasyk, and Dr. J. Toth (committee members) for their interest and contributions.
- Dr. H. R. Krouse and the staff in the Isotope Laboratory in the Department of Physics, University of Calgary.
- Alberta Environment in Edmonton (Groundwater Branch) for providing the rotary drill rig and personnel for deep drilling operations.
- Alberta Environment (Soils Branch) in Lethbridge for providing the auger drill rig and personnel for shallow drilling operations, and for allowing use of piezometers and wells adjacent to Keho Lake. In particular, the cooperation of J. Forster was much appreciated.
- Alberta Agriculture (Drainage Branch) in Lethbridge for allowing use of piezometers and wells near the Monarch Branch Canal. In particular, the cooperation of Dr. M. J. Hendry was greatly appreciated. Dr. Hendry offered many helpful suggestions during the course of this study.
- Dr. L. D. Arnold and staff of the Isotope Laboratory at the Alberta Environment, Environmental Research Centre in Vegreville for tritium analyses.

- R. Stein of the Alberta Research Council for many helpful discussions on hydrogeology.
- M. Ableу, P. Yee and G. Braybrook of the University of Alberta for preparation of thin sections (and help with computing), soil chemical analyses, and assistance in SEM analyses, respectively.
- The Soil Science Section of Agriculture Canada, Lethbridge, for its support. The field and laboratory assistance of D. Campbell, D. Graham, and D. Murray was much appreciated. Thanks is also extended to F. Anderson and the staff of the Soil Chemistry Laboratory for performing the chemical analyses.
- The office staff in the Department of Soil Science (M. Calvert, M. Goh, and S. Nakashima) for assistance in day-to-day tasks, and for providing good cheer.
- All landowners in the Nobleford area who kindly allowed use of their land for this study. In particular, the cooperation of Mr. G. Withage and Mr. B. Spencer was greatly appreciated.
- P. Geib for performing the excellent drafting of many of the tables and figures.
- M. Laverty for her competent typing of the thesis.
- D. Ophori for his many helpful suggestions and advice on flow-net modelling using computers.
- G. Spiers, J. Warren, and C. Maule for trying to answer all my questions.
- My fellow graduate students in the Department of Soil Science, for their friendship and support.
- To Kelly Ostermann, I wish to extend a heartfelt thanks for her friendship and support.

This research was made possible by the cooperation between the University of Alberta, Agriculture Canada, Alberta Environment, Alberta Agriculture, and the Department of Physics, University of Calgary. Financial support for this study was provided by a grant from the Natural Sciences and Engineering Research Council to S. Pawluk, and by contributions from Agriculture Canada in Lethbridge. This support is gratefully acknowledged.

TABLE OF CONTENTS

TABLE OF CONTENTS (continued)

TABLE OF CONTENTS (continued)

LIST OF TABLES

LIST OF TABLES (continued)

LIST OF FIGURES

LIST OF FIGURES (continued)

LIST OF FIGURES (continued)

LIST OF PLATES

1. INTRODUCTION

Dryland salinity is considered to be the major soil degradation problem in the prairie provinces of Canada (Prairie Farm Rehabilitation Administration 1983; Sparrow 1984). The widespread occurrence and growth of saline seeps has become one of the most serious conservation problems in the Great Plains region of North America (Miller et al. 1981). Dryland salinity causes the loss of productive agricultural land and a general deterioration of the environment. The total annual loss of crop revenue from salinity alone in the prairie provinces is estimated to be at least $260 million (Sparrow 1984).

It is generally accepted that water-soluble salts, particularly the sodium salts, are responsible for the low fertility of salt-affected soils. In defining the units of the World Map of Salt-Affected Soils, two classes of soils were recognized: (1) a saline class dominated by neutral chloride and sulfate salts; and (2) an alkali class dominated by exchangeable sodium, and/or by sodium bicarbonate and sodium carbonate salts capable of alkaline hydrolysis (Szabolcs 1978). Saline soils are also commonly referred to as solonchak or white alkali soils; whereas alkali soils are referred to as black-alkali or Solonetzic soils. Saline seeps are a type of saline soil. Seeps are areas of recently developed salinity in non-irrigated soils that are wet some or all of the time, often with white salt crusts where crop or grass production is reduced or eliminated (Miller et al. 1981).

Most of the research on the evaporite mineralogy of saline soils has focussed on the identification and characterization of these minerals in salt crusts or efforescences (Keller et al. 1986a and b), or within the soil profile (Tursina and Yamnova 1986). Other studies have attempted to predict the mineralogical sequence as saline groundwaters migrate upward to the soil surface (Hardie and Eugster 1970; Timpson et al. 1986; Skarie et al. 1987).

The solubility of evaporite minerals is the major factor controlling their occurrence. It is difficult, however, to predict evaporite mineral precipitation or dissolution because of a lack of reliable thermodynamic data (ΔG^o_f = standard free energy of formation values) for these minerals. In addition, researchers may use different thermodynamic data bases that have slightly different ΔG^o_f values. Consequently, Ksp (solubility product constant) values calculated for minerals from ΔG^o_f data may vary and can result in inconsistent predictions of mineral precipitation and dissolution.

Another problem is predicting mineral precipitation or dissolution in soil solutions or groundwaters of high ionic strength. Many geochemical models that use the extended Debye-Hückel equation to calculate activity coefficients are inaccurate for solutions of high ionic strength (Harvie and Weare 1980). Recent geochemical models use Pitzer equations to accurately determine activity coefficients in solutions of high ionic strength (Crowe 1988).

Although considerable information is being revealed about the identity and morphology of evaporite minerals in saline soils,

few studies have tried to relate evaporite mineralogy to the hydrological and chemical conditions under which these minerals form. Kovda (1947) recognized that soil salinization is a complex process involving the groundwater, soil solution and solid phase of the soil. Most research, however, has focussed on the study of each phase as a separate entity. Considerable work needs to be done on the effect of groundwater and soil solution chemistry on evaporite mineralogy.

Determining possible sources of excess water in saline soils requires a knowledge of both hydrology and hydrogeology. Unconfined flow systems may be local, intermediate or regional; and are driven by gravity-induced flow by differences in the elevation of the water table (Tóth 1962). Geological heterogeneity, however, can result in anomalous groundwater discharge, particularly from confined groundwater flow in highly porous lenses (Tóth 1962), or via permeable aquifers (Freeze and Witherspoon 1967). Frequently, discharge from confined aquifers may be unrelated to the contour of the land.

Local, unconfined groundwater flow (Stein 1987), and artesian discharge from confined glacial and bedrock aquifers (Henry et al. 1985) have both been implicated in causing dryland salinity. The two-year crop/fallow rotation has been cited as the major cultural factor causing increased shallow groundwater flow and saline seeps (Brown et al. 1983). Reclamation usually consists of lowering the shallow water table in the discharge area, or preventing excess water from entering the recharge area (Miller et al. 1981).

Few soil scientists have examined the problem of dryland salinity from a regional hydrogeological perspective. Consequently, many studies simply attempted to prove the hypothesis that local groundwater flow was causing soil salinity. Many studies failed to ascertain any contribution from intermediate or regional, unconfined groundwater flow, or from artesian discharge from deeper confined aquifers. As pointed out by Pawluk (1982), much of the confusion regarding salinization reflects devotion by pedologists to the study of physico-chemical properties and/or morphology within the pedon, with little regard given to the dynamics of the land system as a single unit of study.

Part of the problem has been that soil scientists studying soil salinity have not had sufficient training in hydrogeology. This is evident in the literature by frequent misuse of basic groundwater terminology. Tóth (1984) has noted that certain fundamental concepts have been poorly understood or rejected outright by workers who had entered hydrogeology from other disciplines.

Many workers have also considered the unweathered till or bedrock as a lower impermeable boundary to groundwater flow, thus ignoring or rejecting the concept of regional hydraulic continuity. Regional hydraulic continuity, however, is not a self-evident property of the rock framework, and the proposition that it even exists is opposed by some earth scientists (Tóth 1984). The role of fracture-dominated flow in transporting water and salts has also not been adequately addressed in the study of soil salinity. This is probably because fracture-flow is a poorly understood process.

Few soil salinity studies have utilized flow net constructions of groundwater flow on a regional scale. This has resulted in an incomplete understanding of the hydraulics of groundwater flow. In addition, most flow nets have generally been of a qualitative nature (equipotential lines). In the future, there needs to be more emphasis on quantitative flow nets (streamlines) (van Schilfgaarde 1981), that will reveal where specific quantities of groundwater are moving in the flow region. This should be a high priority in soil salinity research.

Soil salinization results from a combination of hydrogeological, cultural and climatic factors (Miller et al. 1981). Research has shown how important these factors are, but also how difficult it is to fully document them (Hendry and Schwartz 1982). Recent work by Stein (1987) has shown that dryland salinity cannot be explained by the relatively simple conceptual models proposed in the past. The Blackspring Ridge study revealed the complexity and variety of the causes of salinity. Now, research is required to adequately define the interactions of these causes of salinity.

Various theories have been proposed to account for the primary source of salts (mainly sulfate) within drift deposits of the Great Plains region of North America. These include: brine squeezing (Cherry 1972), oxidation of organic sulfur (Wallick 1981; Hendry et al. 1986), oxidation of pyrite (Mermut and Arshad 1987), and groundwater discharge from deep regional groundwater flow (Pawluk 1982). Redistribution of soluble salts occurred when postglacial groundwater flow systems adjusted to the new topography (Tóth 1984).

The excess salts in saline soils that are derived from the redistribution of salts may originate from drift or bedrock deposits, or both. As groundwater moves along its flow paths in the saturated zone, increases of total dissolved solids and most of the major ions normally occur (Freeze and Cherry 1979). Consequently, groundwater tends to evolve chemically toward the composition of seawater (Chebotarev 1955). Primary chemical processes enrich the groundwater in dissolved mineral matter by a direct attack of water on rock, whereas secondary processes modify the chemical character of the water (Tóth 1984).

Various chemical and isotopic species may reveal the possible sources of soluble salts in saline soils. High Na concentrations are generally indicative of a bedrock source of salts (Greenlee et al. 1968; Eilers 1973; Stein 1987). The oxygen isotopic composition of sulfate has been suggested as a possible indicator of sources of salt (Hendry and Krouse 1987). In addition, high Br and I contents are associated with relatively deep formation waters (Hitchon et al. 1971), and may indicate a bedrock source of salts.

This study will attempt to approach the problem of dryland salinity using an interdisciplinary approach and from a regional perspective. The three papers in this study attempt to address the following objectives:

1) To investigate the nature and distribution of evaporite minerals in a saline seep from southern Alberta and to ascertain the relationships between the evaporite minerals and soil solution and groundwater chemistry.

2) To ascertain the possible sources of excess water causing high water tables and dryland salinity in a study area in southern Alberta.

3) To determine if the excess salts in saline soils of this study area are originating from the drift and/or bedrock deposits.

1.1 BIBLIOGRAPHY

BROWN, P.L., HALVORSON, A.D., SIDDOWAY, F.H., MAYLAND, H.F. and MILLER, R.M. 1983. Saline-seep diagnosis, control and reclamation. United States Dept. of Agric., Conservation Research Report No. 30.

CHEBOTAREV, I.I. 1955. Metamorphism of natural waters in the crust of weathering. Geochim. Cosmochim. Acta. 8: 22-212.

CHERRY, J.A. 1972. Geochemical processes in shallow groundwater flow systems in five areas in southern Manitoba, Canada. Proc. 24th Intern. Geol. Congr., Sec. 11. Montreal, Quebec. p. 208-221.

CROWE, A.S. 1988. A numerical model for simulating mass transport and reactions during diagenesis in clastic sedimentary basins. Unpubl. Ph.D. Thesis. Dept. of Geology, Univ. of Alberta, Edmonton, Alberta. 270 pp.

EILERS, R.G. 1973. Relations between hydrogeology and soil characteristics near Deloraine, Manitoba. Unpubl. M.Sc. Thesis. Dept. of Soil Science, Univ. of Manitoba, Winnipeg, Manitoba. 202 pp.

FREEZE, R.A. and CHERRY, J.A. 1979. Groundwater. Prentice-Hall, Inc., Englewood Cliffs, N.J.

FREEZE, R.A. and WITHERSPOON, D.A. 1967. Theoretical analysis of regional groundwater flow: 2. Effect of water table configuration and subsurface permeability variation. Water Resources Res. 3: 623-634.

GREENLEE, G.M., PAWLUK, S. and BOWSER, W.E. 1968. Occurrence of soil salinity in drylands of southwestern Alberta. Can. J. Soil Sci. 48: 65-75.

HARDIE, L.A. and EUGSTER, H.P. 1970. The evolution of closed-basin brines. Mineral. Soc. Amer. Spec. Pap. 3: 273-290.

HARVIE, E. and WEARE, J.H. 1980. The prediction of mineral solubilities in natural waters: The Na-K-Mg-Ca-Cl-SO_4-H_2O system from zero to high concentration at 25°C. Geochim. Cosmochim. Acta. 44: 981-997.

HENDRY, M.J., CHERRY, J.A. and WALLICK, E.I. 1986. Origin and distribution of sulfate in a fractured till in southern Alberta, Canada. Water Resources Res. 22(1): 45-61.

HENDRY, M.J. and KROUSE, H.R. 1987. A technique to identify source areas of groundwater causing saline seeps. Proc. of Alberta Soil Science Workshop, Calgary, Alberta. p. 164-169.

HENDRY, M.J. and SCHWARTZ, F. 1982. Hydrogeology of saline seeps. 1st Annual Western Provincial Conference on Rationalization of Water and Soil Research and Management: Soil Salinity. Lethbridge, Alberta. p. 25-40.

HENRY, J.L., BULLOCK, P.R., HOGG, T.J. and LUBA, L.D. 1985. Groundwater discharge from glacial and bedrock aquifers as a soil salinization factor in Saskatchewan. Can. J. Soil Sci. 65(4): 749-768.

HITCHON, B., BILLINGS, G.K. and KLOVAN, J.E. 1971. Geochemistry and origin of formation waters in the western Canada sedimentary basin - III. Factors controlling chemical composition. Geochim. Cosmochim Acta. 35: 567-598.

KELLER, L.P., McCARTHY, G.J. and RICHARDSON, J.L. 1986a. Mineralogy and stability of soil evaporites in North Dakota. Soil Sci. Soc. Am. J. 50: 1069-1071.

KELLER, L.P., McCARTHY, G.J. and RICHARDSON, J.L. 1986b. Laboratory modelling of northern great plains salt efflorescence mineralogy. Soil Sci. Soc. Am. J. 50: 1363-1367.

KOVDA, V.A. 1947. Origin and regime of salt-affected soils. Vol. 1 and 2. Moscow, Izd. Ak. Nauk. SSSR.

MERMUT, A.R. and ARSHAD, M.A. 1987. Significance of sulfide oxidation in soil salinization in southeastern Saskatchewan, Canada. Soil Sci. Soc. Am. J. 51: 247-251.

MILLER, M.R., BROWN, P.L., DONOVAN, J.J., BERGANTINE, R.N., SONDEREGGER, J.L. and SCHMIDT, F.A. 1981. Saline-seep development and control in the North American Great Plains: Hydrogeological aspects. Agric. Water Management 4: 115-141.

PAWLUK, S. 1982. Salinization and Solonetz formation. Proc. 19th Annual Alberta Soil Sci. Workshop, Edmonton, Alberta. p. 1-24.

PRAIRIE FARM REHABILITATION ADMINISTRATION. 1983. Land degradation and soil conservation issues on the Canadian prairies. Agriculture Canada, Regina, Saskatchewan.

SKARIE, R.L., RICHARDSON, J.L., McCARTHY, G.J. and MAIANU, A. 1987. Evaporite mineralogy and groundwater chemistry associated with saline soils in eastern North Dakota. Soil Sci. Soc. Am. J. 51: 1372-1377.

SPARROW, H.O. 1984. Soil at risk (Canada's Eroding Future). Standing Senate Committee on Agriculture, Fisheries and Forestry, Ottawa, Canada.

STEIN, R. 1987. A hydrogeological investigation of the origin of saline soils at Blackspring Ridge, southern Alberta. Unpubl. M.Sc. Thesis. Dept. of Geology, Univ. of Alberta, Edmonton, Alberta. 272 pp.

SZABOLCS, I. 1978. Extent, nature and control measures of soil salinity and alkalinity in Europe. Proc. Sub-Commission on Salt-Affected Soils, 11th Inter. Soil Sci. Soc. Congr., Edmonton, Canada. p. 1-1 to 1-22.

TIMPSON, M.E., RICHARDSON, J.L., KELLER, L.P. and McCARTHY, G.J. 1986. Evaporite mineralogy associated with saline seeps in southwestern North Dakota. Soil Sci. Soc. Am. J. 50: 490-493.

TÓTH, J. 1962. A theory of groundwater motion in small drainage basins in central Alberta, Canada. J. Geophy. Res. 67(11): 4375-4387.

TÓTH, J. 1984. The role of regional gravity flow in the chemical and thermal evolution of ground water. p. 3-39. In Hitchon, B. and Wallick, E.I. (eds.). Proc. First Canadian/American Conference on Hydrogeology, Practical Applications on Ground Water Geochemistry. 22-26 June, Banff, Alberta, Canada. National Water Well Assoc., Worthington, Ohio, U.S.A.

TURSINA, T.V. and YAMNOVA, I.A. 1986. Identification of salt minerals in soils. Soviet Soil Sci. p. 97-109.

VAN SCHILFGAARDE, J. 1981. Dryland management for salinity control. Agric. Water Management 4: 383-391.

WALLICK, E.I. 1981. Chemical evolution of groundwater in a drainage basin of holocene age, east-central Alberta, Canada. J. Hydrol. 54: 245-283.

2. EVAPORITE MINERALOGY, AND SOIL SOLUTION AND GROUNDWATER CHEMISTRY OF A SALINE SEEP FROM SOUTHERN ALBERTA

2.1 INTRODUCTION

Early research by Kovda (1947) showed that soil salinization is a complex process involving groundwater, and the solution and solid phase of the soil. Knowledge of the interactions between evaporite minerals and the chemistry of the soil solution and shallow groundwater will help in understanding the nature of soil salinity, and subsequently aid in the reclamation of these soils.

Precipitation of evaporite minerals is controlled by the solubility of each mineral. Consequently, as saline groundwater migrates upwards to the soil surface, less soluble evaporite minerals such as calcite and gypsum precipitate wit' .he soil profile (Timpson et al. 1986; Skarie et al. 1987), whereas more soluble Na-Mg-type evaporites precipitate on the soil surface as efflorescence (Keller et al. 1986a and b).

When salinization occurs on a larger scale within closed basins, playas or saline lakes may occur (Last and Schweyen 1983). A model based on mineral precipitation was developed by Hardie and Eugster (1970) to predict the evaporite mineral sequence for evolution of closed-basin brines; and has been successfully used to predict mineralogical changes in saline soils in North Dakota

(Timpson et al. 1986; Skarie et al. 1987). Mineral precipitation, however, is only one of several solute fractionation mechanisms involved in the geochemical evolution of saline water (Eugster and Jones 1979).

Erroneous interpretations may result when the composition of evaporite minerals is inferred from water extracts. Consequently, the solid phase should be investigated directly to determine the actual minerals present (Tursina and Yamnova 1986). In Europe and Russia, considerable work has been done on the morphology of evaporite minerals. The scanning electron microscope has been used to study the morphology of evaporite minerals in efflorescences (Driessen and Schoorl 1973; Gumuzzio et al. 1982); whereas micromorphological techniques have been used to examine the morphology of evaporite minerals within the soil profile (Barzanji and Stoops 1974; Eswaran et al. 1981; Tursina and Yamnova 1986). Similar studies have been conducted in North America (Nettleton et al. 1982).

The objective of this study was to investigate the nature and distribution of evaporite minerals in a seep from southern Alberta, and to ascertain the relationship between the evaporite minerals, soil solution and shallow groundwater chemistry.

2.2 MATERIALS AND METHODS

2.2.1 Site Description and Sampling

The soil pedon examined in this study is from a side-hill, saline seep, about 48 km northwest of Lethbridge, Alberta (NW 1/4 Sec. 34, Tp 10, Rg 23, W4 M). The soil was classified as a saline Gleyed Regosol; however, the dominant soil in this area is an Orthic Dark Brown of the Lethbridge and Whitney Soil Series (Alberta Institute of Pedology 1977). The parent material at the site consists of the following sequence of layers with increasing depth: glaciolacustrine (0-160 cm), glaciofluvial (160-175 cm), glaciolacustrine (175-200 cm) and morainal (200+ cm). The vegetation (non-virgin) at the site is a mixture of tall wheat grass (Agropyron elongatum) and crested wheat grass (Agropyron cristatum).

A backhoe was used for digging a fresh soil pit to facilitate soil sampling during the spring and summer of 1985. Bulk soil samples were collected from all recognizable horizons and layers. A monolith box 7 cm x 7 cm x 50 cm was used to sample the soil pedon from the surface to 50 cm; thereafter, small Kubiena boxes 8 cm x 6 cm x 5 cm were used to obtain soil monoliths from selected horizons for preparation of thin sections. Evaporite crystals were sampled in the field and stored in vials prior to analyses. Shallow groundwater samples for chemical analyses were taken from an observation well 2.94 m in depth every one or two weeks from May 23 to August 16 in 1985. Soil moisture was measured using the neutron scattering method, and soil temperature was measured using psychrometers and thermistors.

2.2.2 Laboratory Measurements

The following chemical analyses were performed on the groundwater samples taken from the well and on the saturation extracts of the bulk soil samples: Ca, Mg, Na and K (Chang and van Schaik 1966), SO_4 (American Public Health Association 1980), CO_3 and HCO_3 (Bower and Wilcox 1965), Cl (Adriano and Doner 1982), and electrical conductivity (EC) and pH (Rhoades 1982). The percent $CaCO_3$ equivalent was determined using the method of Bundy and Bremner (1972).

X-ray analyses were conducted on selected bulk soil samples, on evaporite crystals removed from impregnated soil monoliths, and on evaporite minerals obtained from the soil pit. The X-ray diffractograms were prepared using Cokα radiation at 50 kv and 25 mA, and at a scan speed of $1^{o}2\theta$ min^{-1}. Soil monoliths were air-dried in the laboratory, impregnated with epoxy resin and cut into 7 x 5 cm thin sections using procedures described by Brewer and Pawluk (1975). Surface morphology of the unimpregnated salt minerals was investigated using the scanning electron microscope.

The solution-mineral equilibrium model SOLMNEQ (Kharaka and Barnes 1973) was used to calculate the ion activity product (IAP) of the solution species composing the evaporite mineral of interest. Analytical concentrations of soluble cations (Ca, Mg, Na) and anions (SO_4, Cl, HCO_3, CO_3), and a groundwater or soil temperatur· 25°C, were used as input parameters. The K_{sp} of the mineral wa* ·· lated separately using thermodynamic data obtained from ··· compiled by Robie et al. (1978). Calculated K_{sp} values ·· 25°C

of selected evaporite minerals used in this paper are listed in Table 2.1. The IAP calculated using SOLMNEQ was then compared to the mineral's K_{sp} value in Table 2.1 to obtain the saturation index (SI) value (log IAP/K_{sp}). In logarithmic form, $SI < 0$, $SI = 0$, and $SI > 0$ refer to undersaturation, saturation, and supersaturation, respectively, with respect to the mineral in question.

2.3 RESULTS AND DISCUSSION

2.3.1 Groundwater Chemistry

The groundwater was dominated by Na and SO_4 during the period May 23 to August 16, 1985 (Table 2.2). The range in Na and SO_4 concentration was from approximately 77 to 135 mmole $(\pm)L^{-1}$, and from 94.2 to 142.8 mmole $(\pm)L^{-1}$, respectively. The mean EC of the groundwater was 11.3 dS m^{-1}, and the pH ranged from 7.2 to 8.6. The relative concentrations of the cationic and anionic species followed the order Na >> Mg > Ca >> K, and SO_4 >> HCO_3 > Cl > CO_3, respectively. The depth to water table from May, 1985, to May, 1987, ranged from 1.68 to 2.34 m.

The type of evaporite mineral possibly forming below the water table was investigated using the solution-mineral equilibrium model SOLMNEQ (Kharaka and Barnes 1973). Three simulations were run using SOLMNEQ. The input data consisted of the groundwater chemical and temperature values for the three sampling dates shown in Table 2.2. The ion concentrations in the groundwater at these times generally represented the range in values encountered.

The simulations predicted that the groundwater was undersaturated with respect to bassanite, epsomite, mirabilite, and thenardite, undersaturated to nearly saturated with respect to gypsum and anhydrite, and saturated to moderately supersaturated with respect to calcite (Table 2.3). SI values for the groundwater in this study indicated that calcite, and possibly gypsum and anhydrite, could theoretically precipitate below the water table.

2.3.2 Soil Solution Chemistry

The dominant ion species in the soil solution, from saturation paste extracts of the soil profile, were Na and SO_4 (Fig. 2.1). The relative concentrations of the cationic species followed the order Na >> Mg > Ca in the upper pedon (< 160 cm), and Na >> Mg = Ca in the lower pedon (160–220 cm). K concentrations were < 2 mmole ($\pm$)L^{-1} and were not considered. The relative concentrations of anionic species followed the sequence SO_4 > Cl > HCO_3 + CO_3, except in the surface horizon (0–7 cm) where HCO_3 + CO_3 > Cl. The relatively high HCO_3 and CO_3 concentrations in the surface horizon may be related to high root respiration, organic matter decay, and dissolution of calcite at this depth.

The similarity between the ionic composition of the soil solution and groundwater suggested a genetic connection via the capillary fringe. The quantities of the various ion species increased upward from a depth of 220 cm to a maximum in the 13 to 24 cm horizon, then decreased to a minimum in the surface 0 to 7 cm

horizon (Fig. 2.1). The shape of the salt profile reflected net upward movement of water and salts; however, some downward leaching occurred as evidenced by depletion of soluble salts in the surface horizon.

The degree of ion pairing was calculated for the soil solutions (saturation paste extracts) of two selected soil horizons (13–24 and 175–184 cm) and for the groundwater, using SOLMNEQ. The simulations predicted that the degree of ion pairing for the cationic species was relatively high for Mg, slightly less for Ca, and low for Na (Table 2.4). Sulfate had the highest degree of ion pairing for the anionic species. This was followed by HCO_3. Ion pairing of Cl was < 1%; these values are not shown in Table 2.4. The dominant pair species were neutral $CaSO_4^o$ and $MgSO_4^o$. Similar findings were reported by Alzubaidi and Webster (1983) and Timpson and Richardson (1986).

The high degree of ion pairing of Mg and Ca relative to Na (Table 2.4) indicated that the sodium adsorption ratio calculated from analytical data (SAR_p) likely underestimated the sodicity of the soil solution. A more accurate SAR value was obtained when corrections for ion pairs and ion complexes were made to the SAR_p, and only the activities of the free ionic species were used in the calculation of the theoretical SAR_t (Sposito and Mattigod 1977; Alzubaidi and Webster 1983; Timpson and Richardson 1986). The SAR corrected for ion pairing (SAR_t) gave a considerably higher estimate of the sodicity status of the soil solution than the uncorrected SAR_p (Table 2.5).

The exchangeable sodium percentage (ESP) is another index of soil sodicity. This value (ESP = ESR x 100) was estimated from the SAR_p of the solution using the equation ESR = -0.01 + 0.015 (SAR_p) (U.S. Salinity Laboratory Staff 1954). This theoretical approach is considered to be more accurate than measuring the ESP experimentally. A maximum ESP of 68.3% was determined for the 24 to 30 cm horizon (Table 2.5) indicating high quantities of exchangeable Na^+ in the upper profile of this soil. The EC, pH, and SAR values in this profile (Table 2.5) would qualify this soil as a saline-sodic soil. Sommerfeldt and MacKay (1982) also reported saline-sodic soils at this study site.

2.3.3 Evaporite Mineralogy

X-ray analyses of evaporite crystals and bulk soil samples were used to identify the types of evaporite minerals present. Gypsum ($CaSO_4 \cdot 2H_2O$) and bassanite ($CaSO_4 \cdot 1/2H_2O$) were the only two sulfate minerals identified (Table 2.6). The presence of calcite was verified by measuring the percent $CaCO_3$ equivalent (Table 2.5). Gypsum was found only in the lower profile (> 160 cm) whereas bassanite was present in both the upper (0-30 cm) and lower profile (> 88 cm). Calcite occurred in all horizons. Nettleton et al. (1982) found that gypsum was the only sulfate mineral in some gypsiferous soils in the western United States. The presence of both gypsum and bassanite in soils has also been reported (Eswaran et al. 1981; Tsarevskiy et al. 1984; Bullock et al. 1985).

Timpson et al. (1986) found that the sequence calcite-gypsum-and mixed Na-Mg-(SO_4) minerals occurred from the lower to

upper profiles of four saline seeps in North Dakota, and proposed that the mineralogical changes could be explained by the Hardie-Eugster model of closed-basin brine evolution (Hardie and Eugster 1970). Similar findings were reported by Skarie et al. (1987). In contrast, the mineral sequence observed in this study cannot be explained by the Hardie-Eugster model. Slight downward leaching, an absence of a salt crust on the soil surface, vegetation (pasture), depth of water table, and the soil profile located on the upslope periphery of the seep may have been important factors why the mineral sequence observed here could not be predicted using the Hardie-Eugster model. In addition, a major limitation of the Hardie-Eugster model is that mineral precipitation is the only mechanism considered; and when saturation occurs, the solids are removed from interaction with the brine. However, as noted by Eugster and Jones (1979), additional mechanisms may also be involved. These include selective dissolution of efflorescent crusts and sediment coatings, sorption, de-gassing, and redox reactions.

A possible mechanism that may be partially responsible for the mineral sequence observed in this study may be calcite dissolution and gypsum and/or bassanite precipitation (common-ion effect). The 0 to 7 cm and 175 to 200 cm depths were depleted of carbonates (Table 2.5). The depletion of carbonates in the surface and deeper horizons may be related to the presence of numerous gypsum and/or bassanite crystals at these depths. Previous researchers have proposed that growing gypsum crystals acquire their

calcium from carbonate minerals, as evidenced by distinct zones of decalcification adjacent to growing gypsum crystals that were observed in thin section (Barzanji and Stoops 1974; Turaina et al. 1980). This phenomena was also observed in thin sections of this study (Plate 2.1).

To determine what evaporite minerals could theoretically form in the upper and lower soil profile, the soil solution chemistry derived from saturation paste extracts of two selected soil horizons (13–24 cm and 184–200 cm) were used as input data for SOLMNEQ. In addition, to simulate increasing evapotranspiration (ET) and/or concentrations in the 13 to 24 cm horizon, simulations were run using concentrations 2x and 4x the concentrations of the saturation extract values. These concentration factors seem reasonable because in this horizon the saturation percentage value for water was about 2.4x the value of the lowest soil moisture reading during this study. Soil in the 184 to 200 cm depth was constantly saturated during this study; therefore, the use of saturation paste extract values (1x) for this horizon is justified.

The model predicted that calcite could form in the 13 to 24 cm depth (Table 2.7). SI values for anhydrite, gypsum, and bassanite in the 13 to 24 cm depth showed a trend towards mineral precipitation with increasing ET and/or concentrations. The SI values for epsomite and mirabilite also showed a trend towards saturation with increasing concentration factor suggesting that these two minerals may possible form, but only if the ionic strength of the soil solution increases significantly. Precipitation of

these minerals, however, is dependent on temperature; winter temperatures will favour precipitation of mirabilite over epsomite (Timpson et al. 1986). In the 184 to 200 cm depth, SI values for calcite, anhydrite, and gypsum were close to saturation, suggesting that these minerals may possible form. SI values for the remaining sulfate minerals did not indicate precipitation.

Last and Schweyen (1983) reported similar findings for saline lakes of the Great Plains region of North America. Lake waters were supersaturated with respect to calcite and gypsum; and had ionic strengths similar to the soil solutions used here (0.1-1.5). Only lake waters with ionic strengths between 1 and 5 showed supersaturation with respect to Na_2SO_4 minerals whereas an ionic strength of 4 was necessary for supersaturation with respect to Mg_2SO_4 minerals. This suggests that soil solutions must contain extremely high concentrations of Na, Mg, and SO_4 before evaporite minerals comprising these species can precipitate.

As noted by Stoops et al. (1978), even though a large number of evaporite minerals are theoretically possible, the number encountered in soils is low. Na_2SO_4 minerals such as mirabilite and thenardite were not identified in this study; however, G. J. Beke (personal communication) has identified the occurrence of mirabilite at a depth of approximately 1 m in a soil near Enchant in southern Alberta.

Although the most common crystal habit of $CaSO_4$ was lenticular (Plate 2.2 b,g) rod-like (Plate 2.2 c), granular (Plate 2.2 d,f), and tabular (Plate 2.2 h) shapes also occurred. The

$CaSO_4$ crystals in the upper profile (0–24 cm) were found mainly in craze planes. In the lower profile (175–200 cm) the crystals were found in craze planes, vughs, and channels. Bassanite was also observed in the upper profile as coatings along root channels.

The size of the gypsum and bassanite crystals was determined on thin sections using an image analysis system. The mean maximum diameter of the bassanite crystals was 0.02 mm (medium-coarse silt) in the 0 to 24 cm depth, and the mean maximum diameter of the gypsum and bassanite crystals was 0.14 mm (medium sand) in the 175 to 184 cm depth. The crystals ranged in size from · dium silt to very fine sand in the upper profile, and from very fine sand to very coarse sand size in the lower profile. Gypsum and/or bassanite crystals generally range from coarse clay to coarse sand size, and typically increase in size with depth (Barzanji and Stoops 1974; Eswaran et al. 1981; Nettleton et al. 1982; Tsarevskiy et al. 1984; Bullock et al. 1985; Tursina and Yamnova 1986).

In this study the finer bassanite crystals in the upper horizons were associated with variable soil moisture that ranged from very dry (< permanent wilting point) to near-saturated or saturated conditions, with variable soil temperatures, and with high concentrations of soluble Na. In contrast, larger bassanite and gypsum crystals in the lower horizons were associated with near-saturated or saturated conditions, with relatively constant soil temperatures, and with relatively low concentrations of soluble Na. Gypsum crystals of small size have been attributed to large temperature and solution volume changes, high soluble concentrations

of Na and a high degree of supersaturation (Edinger 1973). In contrast, large gypsum crystals have been attributed to accretion under stable hydrochemical conditions that allow uninterrupted growth (Edinger 1973), such as would occur with solute precipitation from groundwater (Tsarveskiy et al. 1984).

Various forms of gypsum and/or bassanite were observed in this study: aggregated closely-packed clusters (Plate 2.2 a,g), non-aggregated loosely-packed clusters (Plate 2.2 c), gypsans (Plate 2.2 d), clusters within roots (Plate 2.2 e), and cluster-rosettes (Plate 2.2 f). Previous studies have reported that these various forms of $CaSO_4$ reflect either a recent or relic, water-salt regime (Tursina et al. 1980; Tsarevskiy et al. 1984; Tursina and Yamnova 1986).

The surface morphology of the evaporite minerals was examined using the SEM (Plate 2.3). Lenticular or discoid crystals were the most common (Plate 2.3 a,b,c,d), although some prismatic forms were also observed. Similar findings have been reported by Stoops et al. (1978) and Eswaran et al. (1981).

An increase in weathering through dissolution of the evaporite minerals was observed with an increase in depth; from initial stages represented by weathering of crystals edges (Plate 2.3 b), through an intermediate stage showing weathering along cleavage planes (Plate 2.3 d), to development of "comb-like" features (Plate 2.3 e,f). Increased cracking and de-lamination, and the development of fissures and a "comb-like" shape reflects increased weathering or dissolution of gypsum crystals in soils (Stoops et al. 1978; Tsarevskiy et al. 1984; Tursina and Yamnova 1986).

2.4 SUMMARY AND CONCLUSIONS

The chemistry of the groundwater was dominated by Na and SO_4. Simulations with a geochemical model predicted that calcite, and possibly gypsum and anhydrite, could theoretically precipitate below the water table. Bassanite, gypsum, and calcite, however, were the only evaporite minerals identified below the water table. The presence of "comb-like" weathering features on the surfaces of bassanite and gypsum crystals found below the water table indicated that dissolution of these minerals may be a major source of soluble Ca and SO_4 in the groundwater. Possible sources of the relatively high concentrations of Na in the groundwater may have been the more soluble Na_2SO_4 minerals that are transient in nature, cation exchange within the drift, or Na influx from groundwater flow systems. The contribution of soluble salts from groundwater flow will be assessed in subsequent papers.

The chemical composition of the soil solution and groundwater were similar, suggesting that soluble salts in the soil pedon were derived from the shallow groundwater. Additional evidence was the observed increase in soluble salts from a depth of 220 cm to a maximum in the 13 to 24 cm horizon. Slight downward leaching of soluble salts also occurred, as evidenced by a depletion of ionic species in the surface horizon. Net upward movement of water and salts in this profile, and only slight leaching, was consistent with minimal pedogenic development (shallow solum) and this profile meeting the limits of a saline Gleyed Regosolic soil.

Greater ion pairing of Mg and Ca relative to Na suggested that the SAR_p may underestimate the sodicity of a soil solution. A more accurate measure of the SAR is obtained when the SAR_t is used. Because Mg and Ca tend to form related $MgSO_4^o$ and $CaSO_4^o$ ion pairs, and Na^+ remains in the free ionic form in solution, sodium adsorption should be high. This was reflected by a maximum ESP value of 68.3% in the 24 to 30 cm depth. Evidence of slight dissolution of bassanite was observed in the surface horizon and evidence of strong dissolution of bassanite and gypsum was observed in the lower profile, suggesting that dissolution of bassanite and gypsum may be a major source of Ca and SO_4 in the soil solution of the pedon.

Evaporite mineral composition in the solid phase appeared to be dominated by gypsum and bassanite. The evaporite mineral sequence observed in this profile cannot be accounted for by the Hardie-Eugster model. The descrepancy may be due to various site factors which prohibit the application of the Hardie-Eugster model, and/or to the fact that when saturation occurs in the model, the solids are removed from interaction with the brine. The evidence from this study suggested that dissolution of calcite and precipitation of gypsum and/or bassanite (common-ion effect) may be an important mechanism controlling the mineral sequence observed here. In addition, an increase in $CaSO_4$ crystal size with depth could be related to a shift from dynamic to stable hydrochemical conditions. Discrepancies between what minerals were actually identified and what minerals the geochemical model SOLMNEQ predicted

to be theoretically possible can be attributed to various factors. These include the models thermodynamic data base and equation (extended Debye-Hückel) used to calculate the activity coefficients; and limitations in sampling, preserving and identifying the more soluble evaporite minerals which may be present in the soil in small amounts but are difficult to detect using X-ray and micromorphological techniques. Evaporite mineralogy is extremely dynamic and varies seasonally and even daily.

2.5 BIBLIOGRAPHY

ADRIANO, D.C. and DONER, M.E. 1982. Bromine, chlorine, and fluorine. p. 449-479. In A.L. Page (ed.) Methods of soil analysis. Agronomy 9(2). Am. Soc. Agron., Madison, Wisconsin.

ALBERTA INSTITUTE OF PEDOLOGY. 1977. Soils of the Lethbridge area (NW82H) M-77-3. Alberta Inst. Pedol., Edmonton, Alberta. Scale 1:126,720.

ALZUBAIDI, A. and WEBSTER, G.R. 1983. Ion pairs in a Solonetzic soil. Can. J. Soil Sci. 63: 479-484.

AMERICAN PUBLIC HEALTH ASSOCIATION. 1980. Standard methods for the examination of water and wastewater. Method 426D: automated methylthymol blue method. 15th ed. APHA-AWWA-WPCF, Washington, D.C.

BARZANJI, A.G. and STOOPS, G. 1974. Fabric and mineralogy of gypsum accumulations in some soils of Iraq. Proc. 10th Int. Cong. Soil Sci., Moscow. Vol. 7: 271-277.

BOWER, A.A. and WILCOX, L.V. 1965. Soluble salts. p. 933-951. In C.A. Black (ed.) Methods of soil analysis. Agronomy 9. Am. Soc. Agron., Madison, Wisconsin.

BREWER, R. and PAWLUK, S. 1975. Investigations of some soils developed in hummocks of the Canadian Sub-Arctic and southern Arctic regions. Can. J. Soil Sci. 55: 301-309.

BULLOCK, P., FEDOROFF, N., JONGERIUS, A., STOOPS, G., TURSINA, T. and BABEL, U. 1985. Handbook for soil thin section description. Int. Soc. Soil Sci. Waine Research Publ., England. p. 70-71.

BUNDY, L.G. and BREMNER, J.M. 1972. A simple titrimetric method for determination of inorganic carbon in soils. Soil Sci. Soc. Am. Proc. 36: 273-275.

CHANG, P.C. and VAN SCHAIK, J.C. 1966. Automated method for soil salinity studies. p. 94-95. In Automation in analytical chemistry. Technicon Symposia. Ardsley (Chauncey), New York.

DARAB, K., CSILLAG, J. and PINTER, I. 1979. Studies on the ion composition of salt solutions and of saturation extracts of salt-affected soils. Geoderma 23: 95-111.

DRIESSEN, P.M. and SCHOORL, R. 1973. Mineralogy and morphology of salt efflorescences on saline soils in the Great Konya Basin, Turkey. J. Soil Sci. 24: 436-442.

EDINGER, S.E. 1973. The growth of gypsum: an investigation of the factors which affect the size and growth rates of the habit faces of gypsum. J. Crystal Growth 18: 217-224.

ESWARAN, H., ILAIWI, M. and OSMAN, A. 1981. Mineralogy and micromorphology of aridisols. Proc. 3rd Int. Soil Classif. Workshop, The Arab Center for the Studies of Arid Zones and Drylands (ACSAD), Damascus, Syria. p. 153-174.

EUGSTER, H.P. and JONES, B.F. 1979. Behaviour of major solutes during closed-basin brine evolution. Amer. J. of Sci. 279: 609-631.

GUMUZZIO, J., BATLLE, J. and CASAS, J. 1982. Mineralogical composition of salt efflorescences in a Typic Salorthid, Spain. Geoderma 28: 39-51.

HARDIE, L.A. and EUGSTER, H.P. 1970. The evolution of closed-basin brines. Mineral. Soc. Amer. Spec. Pap. 3: 273-290.

KELLER, L.P., McCARTHY, G.J. and RICHARDSON, J.L. 1986a. Mineralogy and stability of soil evaporites in North Dakota. Soil Sci. Soc. Am. J. 50: 1069-1071.

KELLER, L.P., McCARTHY, G.J. and RICHARDSON, J.L. 1986b. Laboratory modeling of northern great plains salt efflorescence mineralogy. Soil Sci. Soc. Am. J. 50: 1363-1367.

KHARAKA, Y.K. and BARNES, I. 1973. SOLMNEQ: solution-mineral equilibrium computation. U.S. Dept. Commerce, Nat. Tech. Info. Service, PB 215399, U.S. Geol. Surv., Menlo Park, California.

LAST, W.M. and SCHWEYEN, T.H. 1983. Sedimentology and geochemistry

of saline lakes of the northern great plains. p. 107-125. In U.T. Hammer (ed.) 2nd International Symposium on Saline Lakes, Proc. Dr. W. Junk Publishers, The Hague, Netherlands.

KOVDA, V.A. 1947. Origin and regime of salt-affected soils. Vol. 1 and 2. Moscow, Izd. Ak. Nauk. SSSR.

McKEAGUE, J.A. (ed.) 1978. Manual of soil sampling and methods of analysis. Can. Soc. Soil Sci., Ottawa, Ontario. 212 pp.

NETTLETON, W.D., NELSON, R.E., BRASHER, B.R. and DERR, P.S. 1982. Gypsiferous soils in the western United States. p. 147-168. In J.A. Kittrick et al. (eds.) Acid sulfate weathering. Spec. Publ. 10. Soil Sci. Soc. Amer., Madison, Wisconsin.

RHOADES, J.D. 1982. Soluble salts. p. 167-179. In A.L. Page (ed.) Methods of soil analysis. Agronomy 9. Am. Soc. Agron., Madison, Wisconsin.

ROBIE, R.A., HEMINGWAY, B.S. and FISHER, J.R. 1978. Thermodynamic properties of minerals and related substances at 298.15 K and 1 Bar (10^5 Pascals) pressure and at higher temperatures. Geol. Survey Bull. 1452, U.S. Gov. Printing Office. p. 1-29.

SKARIE, R.L., RICHARDSON, J.L., McCARTHY, G.J. and MAIANU, A. 1987. Evaporite mineralogy and groundwater chemistry associated with saline soils in eastern North Dakota. Soil Sci. Soc. Am. J. 51: 1372-1377.

SOMMERFELDT, T.G. and MacKAY, D.C. 1982. Dryland salinity in a closed drainage basin at Nobleford, Alberta. J. Hydrol. 55: 25-41.

SPOSITO, G. and MATTIGOD, S.U. 1977. On the sodium adsorption ratio. Soil Sci. Soc. Am. J. 41: 323-329.

STOOPS, G., ESWARAN, H. and ABTAHI, A. 1978. Scanning electron microscopy of authigenic sulphate minerals in soils. p. 1093-1113. In M. Delgado (ed.) Proc. 5th Int. Working Meeting on Soil Micromorphology, Granada, Spain.

TIMPSON, M.E. and RICHARDSON, J.L. 1986. Ionic composition and distribution in saline seeps of southwestern North Dakota, U.S.A. Geoderma 37: 295-305.

TIMPSON, M.E., RICHARDSON, J.L., KELLER, L.P. and McCARTHY, G.J. 1986. Evaporite mineralogy associated with saline seeps in southwestern North Dakota. Soil Sci. Soc. Am. J. 50: 490-493.

TSAREVSKIY, V.V., SOKOLOVA, T A., PAVLOV, V.A. and SELETSKIY, G.I. 1984. Gypsum neoformations in soils of the Turgay Solonetz complexes. Soviet Soil Sci. 16(5): 34-44.

TURSINA, T.V., YAMNOVA, I.A. and SHOBA, S.A. 1980. Combined stage-by-stage morphological, mineralogical, and chemical study of the composition and organization of saline soils. Soviet Soil Sci. p. 81-94.

TURSINA, T.V. and YAMNOVA, I.A. 1986. Identification of salt minerals in soils. Soviet Soil Sci. p. 97-109.

U.S. SALINITY LABORATORY STAFF. 1954. Diagnosis and improvement of saline and alkali soils. U.S. Dept. Agric., Washington, D.C. Handb. 60.

Table 2.1. Chemical formulae and solubility product constants of selected evaporite minerals.

Mineral	Chemical formula	Log Ksp (@ 25 °C)
Calcite	$CaCO_3$	−8.30
Gypsum	$CaSO_4 \cdot 2H_2O$	−4.33
Anhydrite	$CaSO_4$	−4.12
Bassanite	$CaSO_4 \cdot 0.5H_2O$	−3.53
Epsomite	$MgSO_4 \cdot 7H_2O$	−2.07
Mirabilite	$Na_2SO_4 \cdot 10H_2O$	−1.17
Thenardite	Na_2SO_4	−0.27

Table 2.2. Chemistry and temperature of the groundwater at three selected sampling dates in 1985.

Chemistry and temperature	Concentration in mmole (±) / L		
	May 23	June 20	July 25
Na	77.0	121.8	135.0
Ca	1.8	16.9	14.6
Mg	11.2	24.6	24.6
K	0.4	0.7	0.4
SO_4	94.2	115.2	142.8
CO_3	1.2	1.7	1.0
HCO_3	8.9	16.6	10.0
Cl	3.7	5.0	4.3
EC (dS/m)	8.3	11.9	11.8
pH	8.6	7.8	7.2
Temp. (°C)	9.0	9.0	12.0

Table 2.3. Saturation indices of the groundwater with respect to calcite (calc.), gypsum (gyp.), anhydrite (anhy.), bassanite (bass.), epsomite (epso.), mirabilite (mirab.), and thenardite (then.), at three selected sampling dates in 1985.

	log IAP/Ksp *						
Date	Calc.	Gyp.	Anhy.	Bass.	Epso.	Mirab.	Then.
May 23	0.49	-1.31	-1.52	-2.11	-2.80	-3.21	-4.11
June 20	0.93	-0.36	-0.57	-1.16	-2.49	-2.87	-3.77
July 25	0.04	-0.39	-0.60	-1.19	-2.45	-2.72	-3.62

* at 25°C

Table 2.4. Percent ion pairing in the soil solution of the 13 to 24 cm and 175 to 184 cm horizons, and in the groundwater.

Depth (cm)	Mg	Ca	Na	SO_4	HCO_3
	% ion pairing				
13-24	[illegible]5	56.7	15.8	37.8	26.5
175-184	[illegible]	42.4	2.1	11.6	5.7
295 †	54.3	48.7	5.4	22.9	1.4

†Groundwater

Table 2.5. Selected chemical properties of the soil horizons.

Horizon	Depth in cm	pH (H_2O)	EC dS/m	$CaCO_3$ g / 100 g soil	SAR_p*	SAR_t**	ESP
Apksgj	0–7	7.5	2.8	3.7	4.3	5.2	5.5
AC	7–13	8.0	23.5	9.8	33.3	45.3	49.0
Ccasa1	13–24	8.6	32.5	22.0	42.9	59.2	63.4
Ccasa2	24–30	8.6	21.1	22.7	46.2	61.9	68.3
Ccasa3	30–49	8.6	15.6	20.5	39.7	52.4	58.6
Cksa1	49–63	8.7	13.2	14.5	34.5	44.5	50.8
Cksa2	63–88	8.5	12.4	13.1	28.6	36.9	41.9
Cksa3	88–160	8.5	11.1	14.3	24.8	31.7	36.2
IICksag	160–175	8.2	9.4	12.7	24.0	30.0	35.0
IIICksg	175–184	8.3	4.7	5.8	20.4	24.3	29.6
IIICksa	184–200	8.0	7.8	3.3	17.5	21.5	25.3
IVCks	200+	8.4	5.7	11.7	23.0	27.8	33.5

* SAR_p = practical

** SAR_t = theoretical

Table 2.6. Occurrence of evaporite mineral in soil horizon; (+) denotes presence and (-) denotes absence.

Horizon	Depth (cm)	Gypsum	Bassanite	Calcite
Ap1ksgj	0-7	-	+	+
AC	7-13	-	+	+
Ccasa1	13-24	-	+	+
Ccasa2	24-30	-	+	+
Ccasa3	30-49	-	-	+
Cksa1	49-63	-	-	+
Cksa2	63-88	-	-	+
Cksa3	88-160	-	+	+
IICksag	160-175	+	+	+
IIICksg	175-184	+	+	+
IIICksa	184-200	+	+	+
IVCks	200+	+	+	+

Table 2.7. Saturation indices (at 25°C) of selected evaporite minerals in the 13 to 24 cm, and 184 to 200 cm horizons.

Depth (cm)	Conc. factor	log IAP/Ksp *						
		Calc.	Anhy.	Epso.	Gyp.	Bass.	Mirab.	Then.
13-24	1x	1.05	-0.09	-1.74	0.12	-0.68	-1.77	-2.63
13-24	2x	1.55	0.26	-1.38	0.47	-0.33	-1.20	-2.02
13-24	4x	2.10	0.63	-0.99	0.84	0.04	-0.71	-1.43
184-200	1x	0.28	-0.40	-2.77	-0.19	-0.99	-3.27	-4.16

* The concentration factor refers to 1x, 2x, and 4x the concentration of the saturation paste extract.

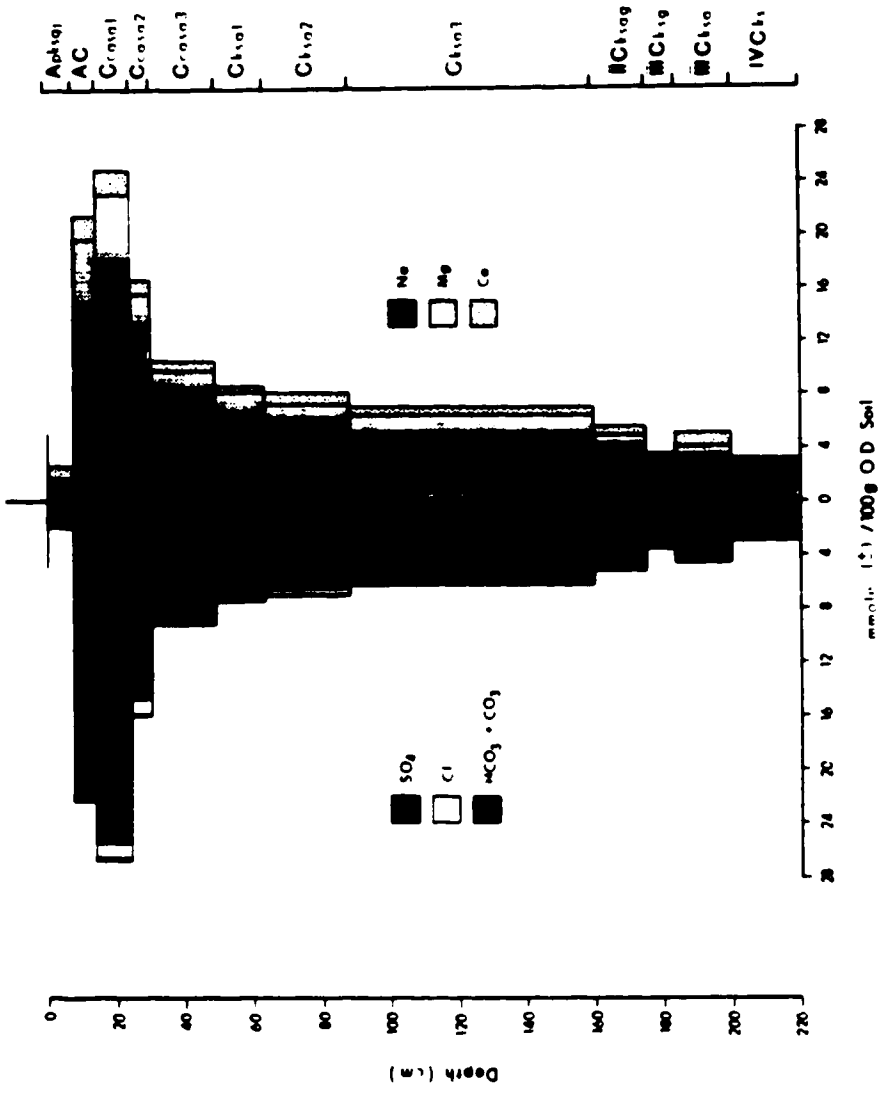

Figure 2.1. Ionic composition of saturation extracts from horizons and layers of the soil profile at Site C2.

Plate 2.1. Photographs of thin section slides showing:

(a) nearly complete decalcification (darker areas on photograph) of the surface horizon (0-7 cm) with a few remaining zones of crystic plasma (lighter area of zone 1 on photograph).

(b) decalcified zones (darker areas of zones 1, 2, and 3 on photograph) associated with the presence of bassanite crystals in the 7 to 13 cm horizon.

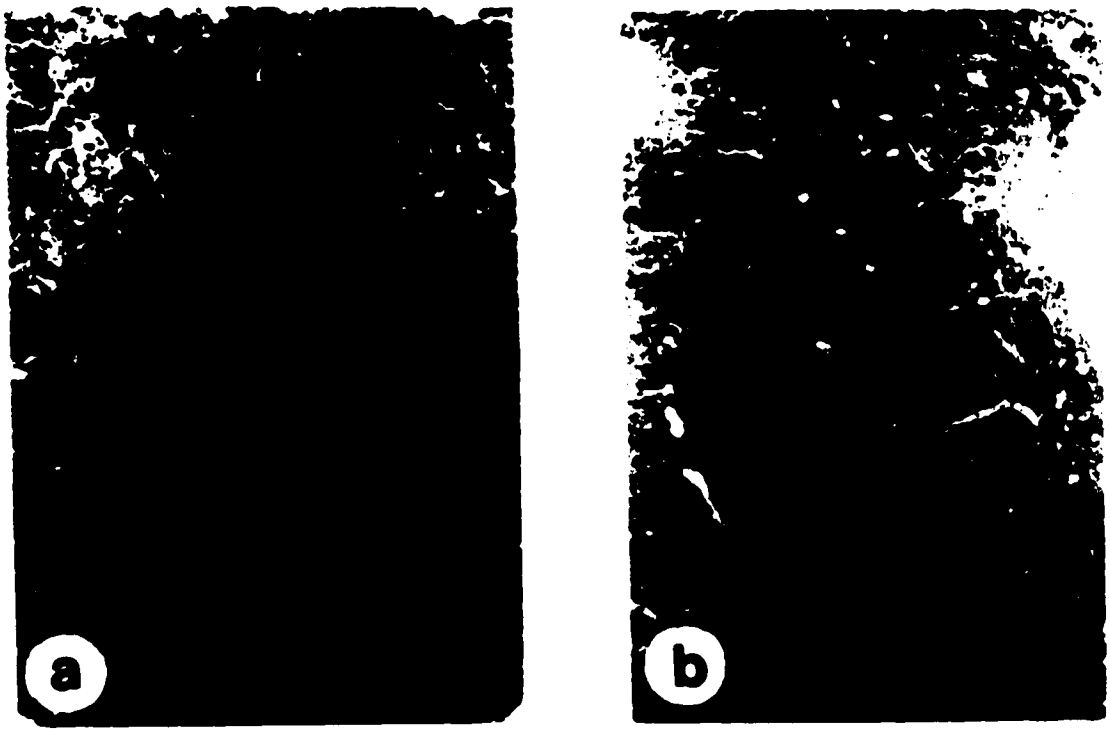
a
b

Plate 2.2. Micrographs (crossed nicols) of bassanite and/or gypsum crystals in the soil showing:

(a) aggregated cluster of bassanite in the 0 to 24 cm horizon (2.5x).

(b) enlargement of (a) showing lenticular crystals (40x).

(c) non-aggregated cluster of bassanite in the 0 to 24 cm horizon illustrating rod-shaped crystals (10x).

(d) gypsans of bassanite coating both walls of a root channel in the 0 to 24 cm horizon (10x).

(e) clusters of bassanite crystals within a root of the 0 to 24 cm horizon (2.5x).

(f) cluster-rosette of bassanite from the 0 to 24 cm horizon (10x).

(g) large lenticular gypsum and/or bassanite crystals from the 175 to 184 cm horizon (10x).

(h) massive tabular gypsum and/or bassanite crystals from the 175 to 184 cm horizon (2.5x).

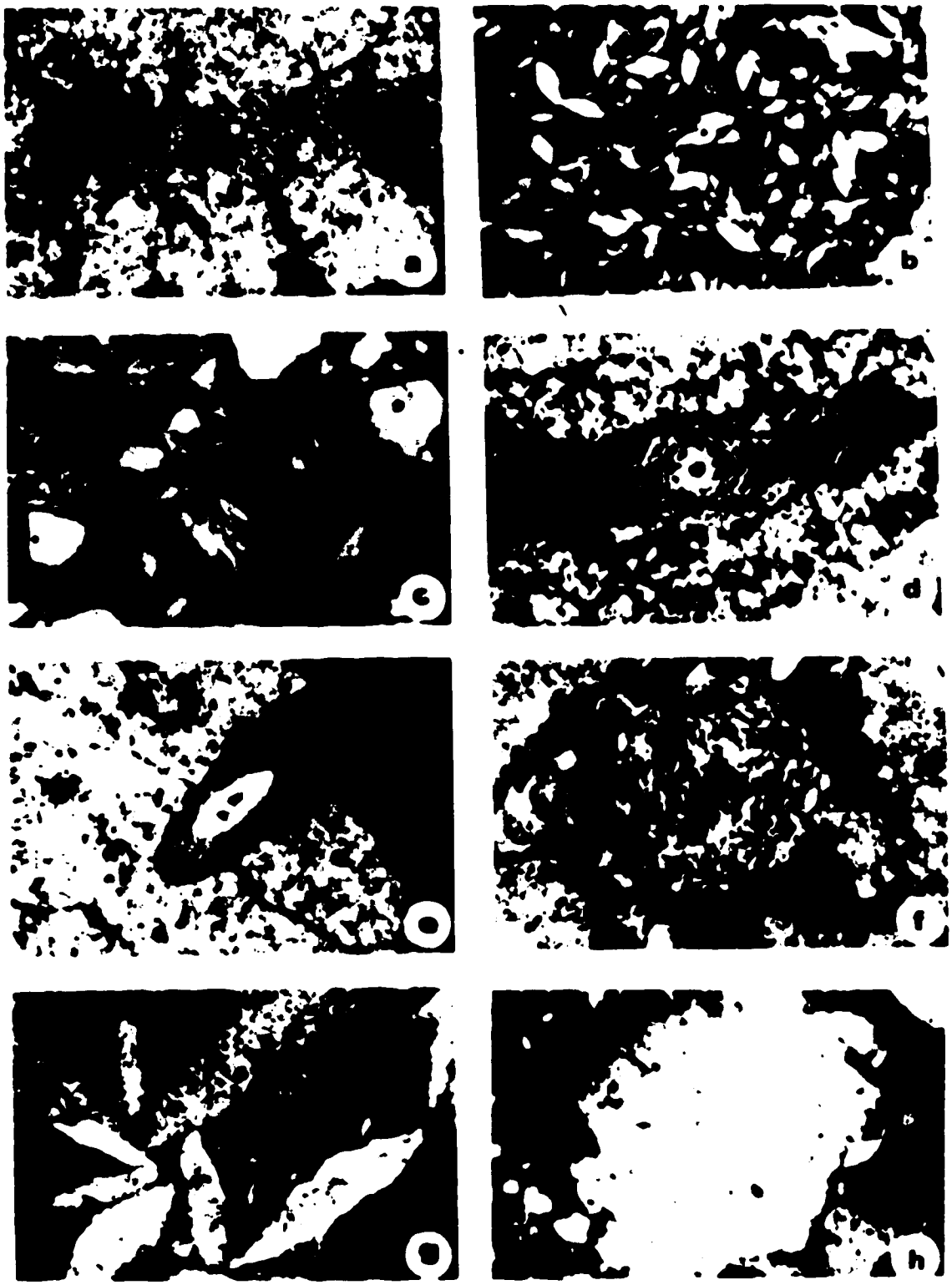
a
b
c
d
e
f
g
h

Plate 2.3. Scanning electron micrographs of soil bassanite and/or gypsum crystals showing:

(a) lenticular or discoid bassanite crystal from the 0 to 7 cm horizon.

(b) weathering along crystal edges of bassanite in the 0 to 7 cm horizon.

(c) lenticular bassanite or gypsum crystal in the 175 to 184 cm horizon.

(d) initiation of "comb-like" features on bassanite and/or gypsum crystals from the 175 to 184 cm horizon.

(e) well-developed "comb-like" features of bassanite and/or gypsum from the 184 to 200 cm horizon.

(f) enlargement of (e) showing weathering along cleavage planes.

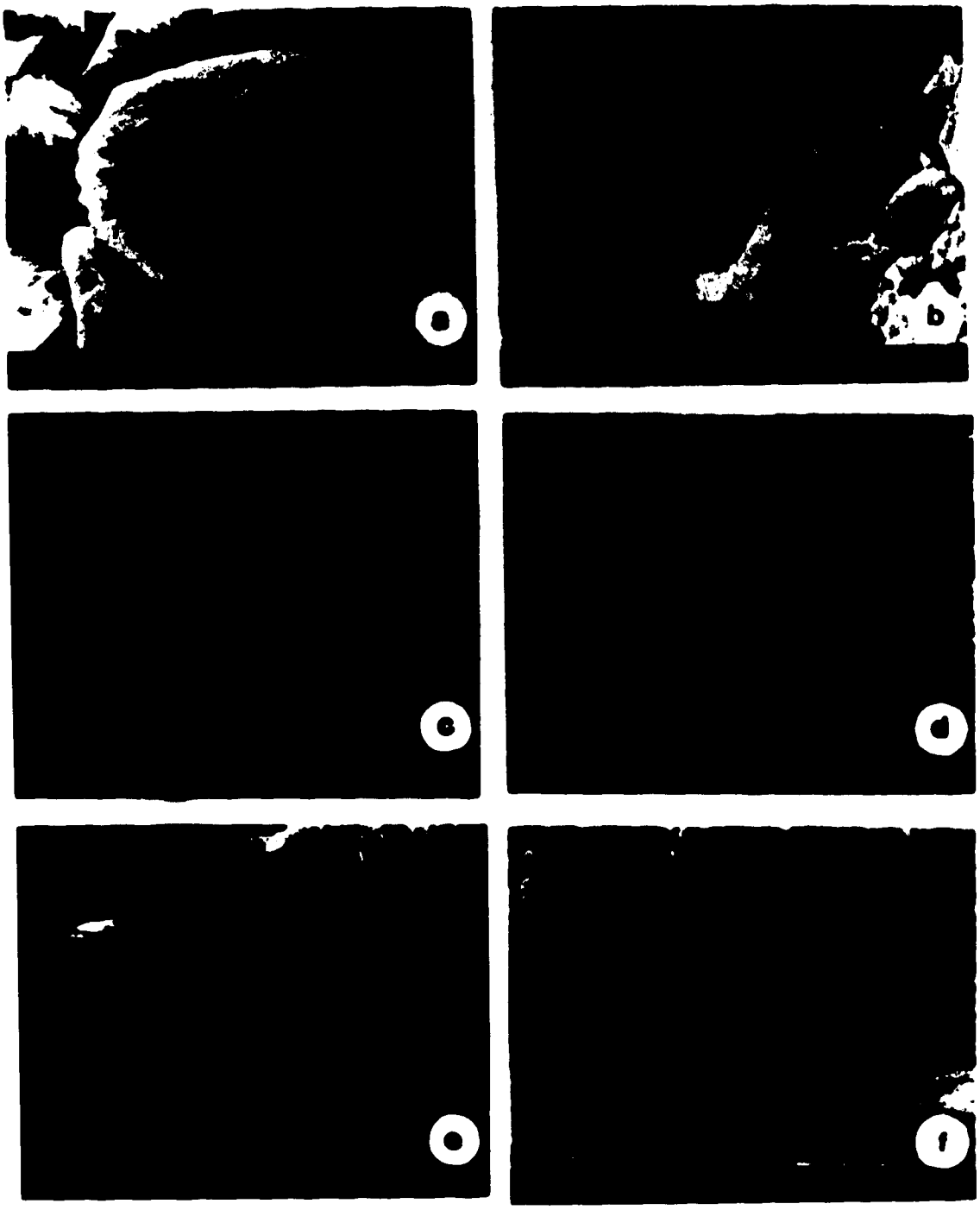

3. SOURCES OF EXCESS WATER CAUSING DRYLAND SALINITY NEAR NOBLEFORD, ALBERTA

3.1 INTRODUCTION

Dryland salinity has been identified as a major soil degradation problem in the Great Plains region of North America (Prairie Farm Rehabilitation Administration 1983). Saline soils are caused by high water tables and a surplus of salts. The excess water and salts are determined by a combination of hydrogeological, cultural and climatic factors.

Discharge from shallow groundwater flow through permeable, coarse-textured drift deposits (Greenlee et al. 1968; Brown et al. 1983; Stein 1987), lignite layers (Doering and Sandoval 1976), or fractured and weathered till (Hendry and Schwartz 1982) has been shown to be a possible source of excess water contributing to high water tables and soil salinization. In addition, discharge from shallow groundwater flow in the weathered zone immediately below the drift-bedrock contact has been reported as another possible source of excess water (Halvorson and Black 1974; Sommerfeldt and MacKay 1982; Hendry 1983; Forster 1984; Chan and Hendry 1985; Stein 1987). In contrast, discharge from deeper bedrock aquifers under artesian conditions can cause shallow water tables and extensive areas of saline soils (Meyboom 1966; Doering and Benz 1972). Henry et al. (1985) reported that groundwater discharge from glacial and bedrock

aquifers was a factor in soil salinization at 15 sites in Saskatchewan.

The two-year crop/fallow rotation has been cited as the major cultural factor causing increased shallow groundwater flow and saline seeps in the North American Great Plains Region (Halvorson and Black 1974; Miller et al. 1981; Hendry and Schwartz 1982; Brown et al. 1983). Several researchers (Halvorson and Black 1974; Sommerfeldt and MacKay 1982) have reported water percolating below the root zone in summerfallow fields. Other management practices that cause water and snow accumulation can also locally contribute to saline seep growth (Sommerfeldt and MacKay 1982). A major hydrologic factor contributing excess water for soil salinization is infiltration of surface runoff water at lower elevations. Sommerfeldt and MacKay (1982) identified surface runoff as a major source of excess water in the lowland of a closed drainage basin near Nobleford, Alberta. Stein (1987) also reported that surface runoff water from spring snowmelt and post-growing season rainfall were the primary sources of excess water causing high water tables in low-lying portions of the lacustrine plain at the base of Blackspring Ridge near Vulcan, Alberta.

Reclamation of saline soils caused by shallow groundwater flow may involve lowering the high water table in the discharge area and/or decreasing the quantity of water entering the local recharge area by various management practices (Brown et al. 1983). Reclamation of saline soils caused by discharge from deeper drift and bedrock aquifers can be accomplished by pumping the water from the aquifer to decrease the pressure head (Doering and Benz 1972).

The objective of this study was to ascertain the possible sources of excess water causing high water tables and dryland salinity in a study area in southern Alberta. Subsequent recommendations could then be made as to suitable management practices for dealing with the sources of excess water in these saline soils.

3.2 MATERIALS AND METHODS

3.2.1 Site Location and Physiography

The study area is located in southwestern Alberta near the village of Nobleford, about 48 km northwest of Lethbridge, Alberta (Plate 3.1). A large bedrock ridge covered by a thin veneer of glacial drift, and trending approximately southwest to northeast through Nobleford, bisects the study area. North of the ridge, the topography gently decreases towards Keho Lake which is about 31 m lower in elevation than the ridge. Immediately south of the bedrock ridge the topography decreases sharply. Thereafter (south of Monarch Branch Canal), the topography decreases gently to the southern limit of the study area which is about 53 m lower in elevation than the bedrock ridge. Closed topographic basins exist around Keho Lake, Studhorse Lake (saline slough northwest of Nobleford), and a small depressional area near the southern limit of the study area. The remainder of the study region has undulating topography with nearly level to very gentle slopes (Class 2 and 3), except for the

southern portion of the bedrock ridge which has very gentle to gentle slopes (Class 3 and 4).

The dominant soil in this area is an Orthic Dark Brown of the Lethbridge and Whitney Soil Series (Alberta Institute of Pedology 1977). In the northern portion of the study area, saline soils are found west of Keho Lake and adjacent to the saline Studhorse Lake. Dark Brown Solodized Solonetz soils of the Kehol Soil Series have also been found in the basin around Studhorse Lake (Alberta Institute of Pedology 1977). In the southern portion of the study area, saline soils (mainly due to side-hill seepage) are found immediately south of the bedrock ridge southeast of Nobleford, and just downslope from the Monarch Branch Canal. In addition, some minor areas of saline soils (including Solonetzic soils) are scattered throughout the southern portion of the study area. Salinity was recognizable by a salt crust on the soil surface, by salt-tolerant vegetation such as Salicornia rubra (samphire), Hordeum jubatum (wild barley) and Kochia scoparia (kochia), and by poor crop growth and/or bare patches in cropped fields. Generally, the dominant farming practice in the study area was dryland, cereal-crop production.

The climate of the region is semi-arid and continental. Long-term (1949-1987), mean annual total precipitation for the region is approximately 410 mm, 70 percent of which falls from April to September. Long-term (1951-1980), mean monthly total evaporation from a class "A" pan for this region ranges from between 78 mm (October) and 184 mm (July); mean annual total evaporation is approximately 943 mm.

3.2.2 Field Methods

Two cross-section lines (A- and B-Lines) and one cross-section line (C-Line) were chosen for regional and local investigations of groundwater flow, respectively (Plate 3.1). The three lines were generally perpendicular to the topographic gradient, traversed the bedrock ridge and major areas of salinity.

Test drilling and geologic sampling of drift and bedrock materials for the local investigation at Sites C1 and C2 were performed using Alberta Environment's B40L rotary drilling rig. This rig utilizes a 10.2-cm O.D. continuous-flight auger and a push-pull sampling technique. Test drilling and geologic sampling for the regional investigations of the A- and B-Lines were performed using Alberta Environment's conventional rotary drilling equipment. All test holes were initially drilled using air; however, mud was used when test holes began yielding water. Spontaneous potential, resistivity, and gamma logs were run at Sites A4, B1 and B2. Spontaneous potential and resistivity logs were run at Site A1. The lithology of the samples from all test holes were described in the field.

Piezometers installed at Sites C1 and C2 consisted of either 3.8-cm or 5.1-cm I.D. PVC pipe and well screen (Schedule 40), solvent welded, with well screens (0.05 cm slot diameter) ranging in length from about 1.4 to 3.0 m. Piezometers installed on the A- or B-Lines consisted of 4.9-cm I.D. PVC pipe or well screen (Schedule 80), with threaded connections and with well screens (0.03 cm slot diameter) ranging in length from about 0.66 to 1.45 m. The

piezometers were installed in open boreholes, a sandpack was added to cover the well screen and the intake zone sealed with peltonite. In addition, benseal was added after the peltonite for boreholes on the A- and B-Lines. The remainder of the borehole was backfilled with drill cuttings.

Water table wells were constructed of 3.8- or 5.1-cm I.D. PVC pipe (Schedule 40 or 80). The casing was perforated with a hacksaw along its length below ground, installed in the open borehole, and backfilled with drill cuttings. A bentonite plug was placed at the ground surface to prevent entry of surface runoff water.

Several shallow piezometers and water table wells from previous studies (Sommerfeldt and MacKay 1982; Forster 1984; Chan and Hendry 1985) were utilized for this study. Site B3 corresponded to Site 8 in the study by Sommerfeldt and MacKay (1982). Sites A1 and B1 corresponded to piezometer nests 352 (water table well 1320) and 366 (water table well 1331), respectively, in the study by Forster (1984). Sites A4, A5 and A6 corresponded to the test holes 5220-M, 5221-M and 5224-M, respectively, in the study by Chan and Hendry (1985). The piezometers in this study were designated by symbols such as A1-76. This means that this piezometer was located at Site A1 and the piezometer tip was 76 m below the ground surface. A total of 46 piezometers ranging in depth from 3 to 99 m, and a total of 12 water table wells ranging in depth from 3 to 7 m, were utilized in this study.

All piezometers were developed by filling the pipes with

water to overflowing. Water in the pipes and some formation water were then removed using an air compressor (Sommerfeldt and Campbell 1975). All water table wells were developed by filling with water and subsequent bailing. Bail or slug tests were performed on all piezometers, and the hydraulic conductivity calculated from recovery data using the methodology of Hvorslev (1951).

The water levels in the piezometers and water table wells were recorded every one to two weeks from May to October during 1985, 1986 and 1987; and approximately every one to two months during the winter of these three years. A battery-operated Spohr tape graduated in centimeters was used to locate the water level from the top of the groundwater installation. The accuracy of the sounder used to measure the water levels was approximately $\pm$25 mm. The water table was estimated from the presence or absence of water in piezometers at nests where the water table well was dry. Water samples for tritium analyses were taken from piezometers in May 1987.

Soil moisture was measured using the neutron scattering method. Initially, an access tube of 122 cm length was used; however, shortly thereafter this was replaced by a longer access tube of 300 cm so as to obtain moisture readings to at least the water table. Moisture readings were taken sequentially at 23 and 30 cm, at 15 cm intervals to 122 cm, at 150 cm and then at 50 cm intervals to 300 cm. The moisture status of the following depths are reported in this study (23, 46, 76, 133, 200, and 250 cm). Generally, readings were every one or two weeks from May to October during 1985 and 1986.

Electrical conductivity was measured at various intervals along the A- and B-Line sections using a Geonics EM-38 ground conductivity meter. The readings were taken with both transmitter and receiver ends in contact with the ground surface; the vertical and horizontal readings representing the 0 to 120 cm and 0 to 60 cm depth intervals, respectively. EM-38 values (dS m^{-1}) reported in this study are direct readings taken by the probe in the field.

3.2.3 Laboratory Methods

Vertical and horizontal saturated hydraulic conductivities were determined with semi-disturbed cores using modified Tempe cells (Sommerfeldt et al. 1984). The percent soil water at saturation, field capacity (-33 kPa), and permanent wilting point (-1500 kPa) of semi-disturbed cores, and particle size distribution (hydrometer) of the soil horizons and layers at Sites C1 and C2 were determined by methods outlined by McKeague (1978). Bulk density values of semi-disturbed cores were used in the conversion of gravimetric to volumetric moisture values. Tritium analysis was performed by the Environmental Isotopes Section at the Alberta Environmental Centre at Vegreville, Alberta. Most of the water samples were enriched to increase the precision of low level tritium measurements.

A finite-difference groundwater flow model (McDonald and Harbaugh 1984) was used to construct steady-state, two-dimensional qualitative flow nets (equipotential distribution) in the regional investigation of groundwater flow in the A- and B-Line cross-sections. A finite-element computer code (Frind 1971) was used to

generate a steady-state, two-dimensional quantitative flow net (stream functions) in the local investigation of groundwater flow in the C-Line cross-section. The finite-element computer code can be easily altered to calculate stream functions, as outlined by Frind and Matanga (1985). Conversion and use of the modified code in the Geology Department at the University of Alberta has been documented by Freeman (1981) and Ophori (1986).

3.3 RESULTS AND DISCUSSION

3.3.1 Geology

3.3.1.1 Surficial geology

Surficial deposits in the study area consisted of glaciolacustrine, till, and glaciofluvial materials. A veneer or thin blanket of till covered the bedrock ridge near Nobleford. Till was also found in the upland areas of the northern portion of the study area. The till consisted of a fine-loamy to fine-silty lacustrine blanket or veneer over fine-loamy morainal material (Alberta Institute of Pedology 1977). The remainder of the study area was covered by glaciolacustrine deposits that ranged in texture from fine-loam to clay. Glaciofluvial deposits were found below the surface glaciolacustrine materials in some southern portions of the study area. The thickness of the overburden in the study area was extremely variable, ranging from < 1 m on the bedrock ridge to 20 to 30 m in the southernmost region of the study area.

On the A-Line cross-section (Fig. 3.1), till deposits were found at Site A1 and to just north of Site A3. The dominant texture of these materials was silty clay loam; however, textures ranged from loam to clay. These deposits ranged in thickness from 2 to 9 m. Forster (1984) previously reported that the upland areas adjacent to the Keho Lake basin consisted of a thin blanket or veneer of coarse to moderately coarse-textured drift, and that fine clay, clay loam and sandy clay loam materials were found at lower elevations closer to the lake.

In the closed basin surrounding Studhorse Lake near Site A3, glaciolacustrine deposits were found. The texture of these materials was dominantly silty clay loam in soils surrounding the slough, but increased in texture to clay loam or heavy clay towards the dry lake bottom. These lake deposits were generally < 6 m in thickness.

The veneer of till on the flanks and top of the bedrock ridge extending south of Site A3 to just north of Site A5 ranged in texture from sandy loam to clay. The sandy loam materials were found where weathered sandstone was close to the soil surface. The till was generally < 5 m in thickness, and was only 43 cm thick at Site A4.

The glaciolacustrine deposits at and south of Site A5 were dominantly silty clay loam in texture and ranged in thickness from 4 m to a maximum of about 8 m. The underlying fluvial deposits consisted of poorly sorted, fine clayey sands interbedded with coarse sands and gravels (Chan and Hendry 1985).

On the B-Line cross-section (Fig. 3.2), the glaciolacustrine deposits in the Keho Lake basin near Site B1 were dominantly silty clay loam in texture and generally < 12 m in th[illegible]ess. Till deposits extending from just south of Site B1, and traversing Sites B2 and B3, were dominantly clay loam in texture. A trend of increasing coarser texture (sandy clay loam to sandy loam) with depth was observed at Sites B2 and B3 and may be related to the shallower, weathered sandstone at these sites. The thickness of the till ranged from < 2 m at Site B2 to a maximum of about 12 m on the northern flank of the bedrock ridge. Glaciolacustrine deposits at the southernmost portion of the B-Line near Site B4 were dominantly silty clay loam to clay in texture and generally < 18 m in thickness.

On the C-Line cross-section (Fig. 3.3), the surficial deposits consisted of glaciolacustrine, fluvial or till deposits. Two thin layers of fluvial sandy and gravelly material extended from north of Site C1, through Site C1, and merged to one layer at Site C2. At Site C1 the texture of the glaciolacustrine material overlaying the shallowest fluvial layer was dominantly loam, with some clay loam lenses. The till material between the two fluvial layers at Site C1 had a dominant texture of clay loam with some minor lenses of sandy clay loam.

At Site C2 there was only one fluvial layer observed, and it was located immediately above the drift-bedrock contact. The glacial material above this sand and gravel layer at Site C2 was characterized by finer-textured material (loam to clay loam)

overlaying coarser-textured materials (sandy loam to sandy clay loam). Sommerfeldt and MacKay (1982) have previously reported the presence of coarse-textured materials extending southward from the kame near Site C1. They have also identified thin layers of sand within finer-textured material in the area near Site C2. Similar findings have also been reported by G. J. Beke (personal communication).

3.3.1.2 Bedrock geology

Bedrock of the area consisted of non-marine shale, sandstone, mudstone, siltstone, bentonitic sandstone, coal, and carbonaceous shale strata of the St. Mary Formation (Figs. 3.1, 3.2 and 3.3). The Bearpaw and Blood Reserve Formation may also occur in this area (Geological Survey of Canada 1967); however, these formations were not encountered during drilling operations. Generally, the dominant geology encountered was interbedded strata of the above bedrock units. These layers of alternating strata, usually < 2 m in thickness, were dominated by shale and to a lesser extent sandstone. Other bedrock strata, however, also occurred within this geologic unit. Potential aquifers within the relatively impermeable interbedded shale and sandstone units consisted of the upper weathered bedrock (shale or sandstone), sandstone strata, and carbonaceous shale and/or coal strata.

The weathered zone of the uppermost bedrock was recognizable by fracturing and oxidizing staining, and by the brown or tan color of the bedrock material. In contrast, the color of the

unweathered bedrock below was more gray. The weathered zone ranged from approximately 5 to 18 m below the ground surface. Similar findings in this study area have been reported by Forster (1984), and Chan and Hendry (1985).

The permeable sandstone strata found in this study area ranged in thickness from about 2 to 12 m. Some of the shallower sandstone strata were fractured. Many of the sandstone beds were lenticular in nature. This is a feature characteristic of the St. Mary Formation (Geological Survey of Canada 1967). The carbonaceous shale and/or coal beds found on the C-Line cross-section (Fig. 3.3) were generally < 2 m thick; however, significant quantities of water were encountered upon drilling through these strata.

The dip of the permeable sandstone and carbonaceous shale and/or coal aquifers was determined by extrapolating structure contours on the base of the Cretaceous Fish Scale Formation (Energy Resources Conservation Board 1969). For the A-Line cross-section (Fig. 3.1), the dip was level between Sites A3 and A4. North of Site A3, and south of Site A4, the beds inclined upwards at a rate of approximately 4 m km^{-1}. For the B-Line cross-section (Fig. 3.2), the beds were level in the central portion of the section and inclined upwards at a rate of about 19 m km^{-1} and 11 m km^{-1} under the northern (Site B1) and southern (Site B4) portions of the section, respectively.

3.3.2 Hydrogeology

3.3.2.1 Hydraulic conductivity

The saturated hydraulic conductivity (Ks) values determined from response tests on piezometers in various geologic materials are shown in Fig. 3.4. These values represent horizontal Ks values, except those from piezometers B3-6 and B3-16 which represent vertical Ks values. The Ks values for the glaciolacustrine deposits ranged from 2.8×10^{-11} to 1.2×10^{-8} m s^{-1} (n=5). The geometric mean was 6.0×10^{-10} m s^{-1}. In addition, Ks values were determined with semi-disturbed cores using modified Tempe cells. Horizontal Ks values (geometric means) for the cores ranged from 8.3×10^{-10} to 3.4×10^{-6} m s^{-1} (n=39). The geometric mean was 1.1×10^{-8} m s^{-1}. The vertical Ks values ranged from 1.4×10^{-9} to 3.8×10^{-6} m s^{-1} (n=37). The geometric mean was 1.2×10^{-7} m s^{-1}. All glaciolacustrine core samples were taken from Sites C1 and C2; and the higher Ks values probably reflected the coarser textures of the materials found in this area.

Forster (1984) reported that lacustrine deposits of the Keho Lake basin had horizontal Ks values that ranged from 10^{-10} to 10^{-12} m s^{-1}. In contrast, Buckland et al. (1986) found that for the medium to fine textured glaciolacustrine deposits in the southern portion of the study area (southeast of Site A5), the horizontal Ks values (geometric means) ranged from 3.0×10^{-7} to 2.3×10^{-6} m s^{-1}, and vertical Ks (geometric means) ranged from 9.3×10^{-8} to 4.4×10^{-6} m s^{-1} (n=144). In addition, Ks values for

the 0 to 1.0 m depth were generally an order of magnitude greater than the values for the 1.0 to 2.0 m depth.

No Ks values were determined for till deposits in this study; however, several previous studies have reported Ks values for till in southern Alberta. Hendry (1982) found that Ks of the weathered till matrix was approximately 10^{-10} m s^{-1}. In contrast, the Ks values of small- and large-scale fractures in the till were on average 5 x 10^{-9} and 2 x 10^{-7} m s^{-1}, respectively. Geometric mean Ks values of approximately 10^{-8} m s^{-1} have been determined for weathered tills in southern Alberta (Hendry 1983; Stein 1987); and values of 9.1 x 10^{-10} m s^{-1} have been reported for unweathered tills (Stein 1987).

The horizontal Ks values of the various geologic strata in the St. Mary Formation were extremely variable, ranging from approximately 10^{-12} to 10^{-5} m s^{-1} (Fig. 3.4). In comparison, Chan and Hendry (1985) reported Ks values that ranged from 10^{-10} to 10^{-6} m s^{-1} for this formation.

The hydraulic conductivity of the fractured and/or weathered sandstone strata ranged from 1.1 x 10^{-7} to 6.4 x 10^{-5} m s^{-1}. The geometric mean was 3.5 x 10^{-6} m s^{-1}. Forster (1984) found that Ks values for weathered sandstone ranged from 6.2 x 10^{-7} to 2.8 x 10^{-4} m s^{-1}. Stein (1987) reported a geometric mean value of 1.0 x 10^{-6} m s^{-1} for similar strata within the equivalent Horseshoe Canyon Formation.

The unweathered and/or bentonitic sandstone exhibited Ks values from 1.3 x 10^{-9} to 1.1 x 10^{-6} m s^{-1}. The geometric mean

was 6.1 x 10^{-8} m s^{-1}. Forster (1984) found values ranging from 6.0 x 10^{-13} to 7.1 x 10^{-8} m s^{-1}, and Stein (1987) reported a geometric mean value of 7.6 x 10^{-10} m s^{-1} for this strata. In addition, Chan and Hendry (1985) noted Ks values of 10^{-10} m s^{-1} for bentonitic sandstone.

Interbedded shale, sandstone, siltstone and mudstone was the dominant strata of the St. Mary Formation. The Ks values for this unit were extremely variable. Two groups of values were visible after plotting on Fig. 3.4; there was a low Ks and a high Ks group. The low Ks group had values that ranged from 2.1 x 10^{-12} to 4.4 x 10^{-9} m s^{-1}. The geometric mean was 3.9 x 10^{-11} m s^{-1}. Generally, these low Ks values were from the deeper piezometers (> 50 m). In contrast, the high Ks group had values that ranged from 8.1 x 10^{-8} to 5.8 x 10^{-6} m s^{-1}. The geometric mean value was 3.2 x 10^{-7} m s^{-1}. All four of the piezometers in this high Ks group were at depths < 50 m. Higher Ks values at shallower depths most likely reflected weathering and/or fracturing of the upper bedrock.

The Ks values of the carbonaceous shale and/or coal strata ranged from 7.4 x 10^{-8} to 1.1 x 10^{-6} m s^{-1}. The geometric mean was 1.7 x 10^{-7} m s^{-1}. These four values were all from Sites C1 or C2. Similar Ks values for these strata have been cited by Stein (1987).

3.3.2.2 Qualitative flow nets of regional investigations

The equipotential distribution along the A- and B-Line cross-sections was simulated using a finite-difference groundwater

flow model (MacDonald and Harbaugh 1984). The model grids for the A- and B-Lines consisted of 24 rows and 45 columns, and 22 rows and 50 columns, respectively (Figs. 3.5 and 3.6). Boundary conditions were specified hydraulic head values. These head values remained constant during the computer simulation. Hydraulic head values for the upper water table boundary were taken from water table wells in the field. Hydraulic head values between observation wells were interpolated. Hydraulic head values along the two vertical boundaries and along the bottom boundary were derived from field measurements of hydraulic head in piezometers. Head values between piezometer nests were interpolated.

The hydraulic conductivity values assigned to each hydrostratigraphic unit are listed in Table 3.1. The Ks values assigned to the geologic units in the simulations were generally within the range of values determined in this and other studies. An anisotropy factor (k_h/k_v) of 10:1 was assigned to both the bedrock and drift deposits for the simulations in this study.

Using a trial and error procedure, adjustments were made to the specified hydraulic head boundary along the water table, and to the Ks values assigned to various hydrostratigraphic units, until a reasonable fit was attained with measured head values determined from piezometers. The difference between the calculated and measured pressure heads for the best-fit simulations are presented in Table 3.2.

The simulated equipotential distribution for the A-Line cross-section is shown in Fig. 3.1. The field hydraulic head value

of the deepest piezometer at Site A3 was assumed to be representative of head values at this depth within the Studhorse Lake basin. This assumption appeared reasonable as the simulated equipotential distribution was in relatively close agreement with the flow net manually contoured using only field hydraulic head data.

Groundwater flow in the A-Line cross-section was characterized by: predominantly downward flow beneath the bedrock ridges (Sites A2 and A4), and in the Keho Lake basin at Site A1; lateral flow in the southern lowlands between Sites A5 and A6, and a large stagnant and/or sink area of upward flow beneath Studhorse Lake at Site A3. The large sink area below Site A3 appeared to receive water from lateral flow in the upper bedrock. The source of this shallow flow was the bedrock ridges to the north (Site A2) and south (Site A4). This zone of active, shallow groundwater flow was within the weathered and/or fractured shale. This stratum was also found to contain many layers or lenses of highly permeable carbonaceous shale and/or coal. A hydraulic conductivity value of 10^{-6} m s^{-1} was assigned to this upper weathered shale unit for the simulation.

The sink area was also characterized by a hydraulic head value in the deepest piezometer at Site A3 (970.0 m) that was considerably greater than the head values in the deepest piezometers underneath the adjacent bedrock ridges at Sites A2 (934.8 m) and A4 (953.9 m). This suggested that the high hydraulic head value at depth below Studhorse Lake at Site A3 can probably not be accounted for by groundwater flow within 91 m of the ground surface in the

A-Line section. This inferred a possible deeper source of groundwater flow beneath Site A3. The Studhorse Lake basin has been mapped previously as a major artesian basin (Tokarsky 1973).

The major areas of saline soils along the A-Line cross-section were found at Sites A1, A3 and south of Site A5. The EM-38 readings plotted on Fig. 3.1 illustrated the near-surface salinity (0-120 cm) in the Studhorse Lake basin at Site A3 (> 2 dS m^{-1}), and in the lowlands south of Site A5 (> 2 dS m^{-1}). Slight salinity (1 dS m^{-1}) was indicated at Site A1. The salinity at Site A1 appeared to have been caused by shallow flow through the upper weathered bedrock from the adjacent bedrock ridge to the south (Site A2). This was evident by the equipotential distribution in Fig. 3.1. The soil salinity within the Studhorse Lake basin at Site A3 can probably be attributed to shallow flow through the upper weathered bedrock and/or to deeper discharge (> 91 m) from regional flow or confined aquifers under artesian conditions. The upward hydraulic gradient below this basin may have also acted as a hydraulic perch by keeping the water table close to the soil surface. Soil salinity in the lowlands south of Site A5 was probably due to shallow flow in the upper weathered bedrock and/or to leakage from the Monarch Branch Irrigation Canal that is located just south of Site A5. Chan and Hendry (1985) reported similar findings. In addition, discharge from confined aquifers under artesian conditions may be a possible source of excess water in these lowlands as this area has also been mapped as a major artesian basin (Tokarsky 1973).

The correlation between the vertical Darcy flux and EM-38 readings was generally poor, except for the Studhorse Lake basin (Fig. 3.1). The high degree of soil salinity within the lake basin was associated with a total discharge in the basin of approximately 3.7 m^3 yr^{-1} (1.2 mm yr^{-1}). The total discharge was calculated as the area under the horizontal zero line in the recharge-discharge profile of the basin.

The simulated equipotential distribution for the B-Line cross-section is shown in Fig. 3.2. Generally, groundwater flow was downward throughout the northern portion of the section (Site B1 to B3), lateral flow predominated south of Site B3, and upward flow occurred below Site B4. The saline soils found along the B-Line occurred in the southern portion of the section. This was evident by high EM-38 readings (> 2 dS m^{-1}). Immediately south of the bedrock ridge was an extensive area of soil salinity and saline seeps (Site B3). Some small patches of soil salinity were also found further south at lower elevations between Sites B3 and B4.

The equipotential distribution indicated that the soil salinity found in the lowlands at and between Sites B3 and B4 was probably caused by shallow groundwater flowing in the upper weathered bedrock. A shallow and relatively thick, sandstone aquifer that was truncated, and subcropped below Site B3, was found to be permeable ($K_s = 10^{-5}$ m s^{-1}). This aquifer may be a major conduit for groundwater flow and a source of excess water causing soil salinization in this area. The bedrock ridge also had a very thin overburden overlaying extremely weathered sandstone. The

soils also tended to become coarser in texture with depth, because of the influence of the weathered sandstone material. In addition, there was a sharp break in topographic gradient (from steep to shallow) just upslope from Site B3. These conditions would be conducive to shallow, local flow systems originating from the bedrock ridge. The correlation between the vertical Darcy flux and EM-38 readings was generally poor for the B-Line section.

3.3.2.3 Quantitative flow net of local investigation

A finite-element code (Frind 1971) was modified to calculate stream functions for the C-Line cross-section (Fig. 3.3). Initially, however, a finite-difference code (McDonald and Harbaugh 1984) that facilitated easy adjustment of input parameters was used to derive acceptable hydraulic conductivity values for the hydrostratigraphic units on the C-Line cross-section. The hydraulic conductivity values for the best-fit simulation of the C-Line section using the finite-difference code are shown in Table 3.1. These hydraulic conductivity values were then used as input parameters for the simulation of the stream functions using the finite-element code.

The finite-element grid for the C-Line consisted of 906 linear-triangular elements and 496 nodes. Boundary conditions consisted of a combination of no-flow and specified flux boundaries. The former were specified as constant values of stream functions and were equal to zero. Specified flux values at a node along the water table boundary were calculated as the hydraulic head difference between adjacent nodes on the boundary, divided by two.

For the simulation, all boundaries except the water table were assumed to be no-flow. The water table was a specified flux boundary. The vertical no-flow boundaries below Site B2 and just south of Site C2 seemed reasonable because Site B2 was located on a groundwater divide on top of the bedrock ridge, and south of Site C2 was in a local depression. The lower horizontal boundary was taken just below a relatively thick and highly permeable (Ks = 10^{-5} m s^{-1}) sandstone layer. Relatively impermeable, interbedded shale and sandstone occurred below this sandstone stratum. Groundwater flow was probably dominantly lateral in this sandstone stratum, thereby satisfying the conditions of parallel flow adjacent to the lower impermeable boundary.

The simulation of the stream functions on the C-Line cross-section revealed that a possible source of excess groundwater at the saline seep (Site C2) was from confined groundwater discharge from highly permeable (Ks = 10^{-5} m s^{-1}) sandstone strata at the 6 and 12 m depths. The source of the groundwater appeared to be from a local recharge area just south of Site B2. The shallow overburden (< 2 m) and highly weathered sandstone in this recharge area would be conducive to significant potential recharge.

Two stream tubes contributed to groundwater discharge at Site C2 (Fig. 3.3). The quantity of groundwater that discharged was calculated to be approximately 25.6 m^3 yr^{-1} (88 mm yr^{-1}). Discharge from this shallow, local flow system was much greater than artesian discharge from deep bedrock aquifers below the closed

topographic depression (3.7 m^{-3} yr^{-1}; 1.2 mm yr^{-1}) at Studhorse Lake (Fig. 3.1).

3.3.2.4 Tritium content of groundwaters from saline areas

The tritium concentration of groundwater samples from piezometers and water table wells in saline arcas (Sites A1, A3, B3, and C2) are shown in Table 3.3. The tritium content of precipitation at Ottawa, Canada, before 1953 was < 20 TU (Freeze and Cherry 1979). Since the half-life of tritium is 12.3 years, the tritium content of groundwater recharged by precipitation prior to 1953 should have a tritium concentration of < 2 TU. Relatively deep piezometers (> 30 m) that exhibited high tritium values (> 2 TU) were likely due to incomplete flushing of the drilling water and/or surface water used to develop the piezometers. This was probably the case for piezometer A1-76 (Table 3.3).

The tritium data for the groundwater samples from piezometers at Site A1 showed likely contamination of the piezometer at 76 m (A1-76) and pre-1953 water at 9 and 24 m (A1-9, A1-24). At Site A3, adjacent to Studhorse Lake, stratification of the groundwater with respect to tritium was evident. Pre-1953 water (< 2 TU) occurred at 30 and 69 m (A3-30, A3-69), whereas post-1953 water (46 TU) was present at 5 m (A3-5W), just below the water table. This stratification of post-1953 shallow groundwater overlaying pre-1953 deeper groundwater was also evident at Sites B3 and C2. Stein (1987) previously found zones of high tritium content in the upper 2 to 3 m of the saturated zone in areas of

groundwater discharge, and attributed this condition to recharge to the water table by infiltration of precipitation and snowmelt water. The tritium results from this study supported these previous findings.

3.3.2.5 Water table levels

The water table levels determined from observation wells in this study area ranged from 1.14 to 7.11 m. The shallowest and deepest water tables were found in the southern lowlands at Site A6, and below the bedrock ridge at Site A4, respectively.

The water table levels at Site C1 and Site C2 are shown in Fig. 3.7. The water table in the saline seep (Site C2) exhibited marked fluctuations within the range 1.68 to 2.34 m. Sharp increases in the water table level at Site C2 were attributed to above-average precipitation during that or the previous month. This was evident by water table peaks in September 1985, September and November 1986, and in July 1987. This phenomena was also observed in water table wells from the A- and B-Lines (Appendix 6.4). Precipitation-induced, time lag responses of water tables are a commonly reported phenomena (Maclean and Pawluk 1975; Stein 1987).

The water table in the bedrock ridge at Site C1 ranged from 5 to 24 m below the ground surface during this study. In the fall (September 13 to October 25, 1985) and spring (May 13, 1986), the water table was 5.2 to 5.3 m from the soil surface. At this time, water was present in the well at 5 m, but no water was

present in the piezometers at 24 or 25 m (C1-24, C1-25). This indicated the presence of a perched water table.

On the A-Line cross-section, the water table level on the northern bedrock ridge at Site A2 ranged from 3 to 14 m. On the southern bedrock ridge at Site A4, the water table ranged from 7 to 20 m for most of the study; however, from July 9 to August 7, 1986, the water table was at 7 m. The water table on the flank of the bedrock ridge at Site A5 ranged from 3 to 8 m for most of the monitoring period, except from July 16 to September 12, 1986, when the water table was from 2.5 to 2.8 m below the ground surface. The water table levels at the saline Sites A1 and A3 ranged from 4 to 9 m and 2.6 to 3.8 m, respectively. In the southern lowlands at Site A6, the water table ranged from 1.1 to 2.0 m below the soil surface.

The water table on the bedrock ridge at Site B2 was from 5 to 34 m below the soil surface, as determined by the presence or absence of water in the well or piezometers. The water table at Sites B1 and B3 ranged from 3 to 6 m below the ground surface. At Site B4 the water table was from 2.8 to 3.5 m below the ground surface.

3.3.2.6 Water levels in piezometers

Hydrographs for the piezometers used in this study are given in Appendix 6.4. Basic time lags (To) were > 200 days for some piezometers (A1-76, A2-84, A4-99, 56, 20, B1-6 and B1-9). This indicated that these piezometers may not have fully recovered

to their equilibrium water levels. In addition, the piezometer screen at A4-39 was suspected of being plugged and the bentonite seal on A5-8 was broken during development, rendering this piezometer inoperative.

The water levels in piezometers could generally be grouped into two categories: piezometers that exhibited static to slight fluctuations (A1, A2, A4, A6, B1 and B2), and piezometers that showed marked fluctuations (A3, A5, A6, B3, B4, C1 and C2). Some of the water level fluctuations were likely due to precipitation events. This was evident in piezometers at Sites C1 and C2. Stein (1987) reported similar findings.

A comparison of the hydraulic head in piezometers within confined aquifers and the elevation of the top of the aquifer was performed to ascertain if the aquifers existed under artesian conditions. If the water level in a well in a confined aquifer is at the top of the aquifer, the aquifer is said to exist under artesian conditions (Freeze and Cherry 1979). Estimates of artesian conditions were calculated as the difference between the hydraulic head in a piezometer within a confined aquifer and the elevation of the top of the aquifer. The calculated values for confined sandstone, carbonaceous shale and/or coal strata, and a fluvial aquifer, are shown in Table 3.4.

Four sandstone aquifers in the A-Line cross-section that ranged from 24 to 69 m in depth below ground surface had pressure heads that ranged from 12 to 50 m above the top of the sandstone strata. Artesian conditions were lowest (12 m) in the Keho Lake

basin at Site A1 (A1-24) and increased southward to a maximum value (50 m) at 69 m below the flank of the bedrock ridge at Site A5. Artesian conditions were also found at the 20 m depth, in the fluvial deposit overlain by finer-textured lacustrine material, in the southern lowlands at Site A6. The artesian conditions here, however, were much weaker (3 m) than in the sandstone aquifers.

In contrast, an opposite trend was observed for artesian conditions in sandstone aquifers on the B-Line. Here artesian conditions were greatest (34 m) at the 41 m depth in the Keho Lake basin at Site B1, and then decreased southward, to pressure heads of only 2 m above the shallow aquifer (6 m), just south of the bedrock ridge at Site B3.

Sandstone aquifers below the saline seep at Site C2 showed the greatest artesian conditions at the 30 m depth. The pressure head values in two piezometers at this depth were 21 m above the top of the aquifer. In contrast, artesian conditions at the 6 and 7 m depth within the sandstone strata were only 4 m.

Carbonaceous shale and/or coal aquifers were also present along the C-Line cross-section. Artesian conditions at the 34 and 35 m depth below the bedrock ridge at Site C1 were 17 and 16 m, respectively. At the 24 m depth, the pressure head was only 7 m above the aquifer. Similar artesian conditions were also found at the 10 m depth at Site C2.

3.3.3 Soil Moisture Regime

3.3.3.1 Soil moisture regime on the bedrock ridge

The soil moisture regime on the bedrock ridge at Site C1 was investigated to ascertain if drainage of soil water was causing local recharge from the ridge, and contributing excess water to the saline seep downslope at Site C2. The soil moisture regime at Site C1 during the spring to fall periods of 1985, 1986 and 1987, in relation to precipitation, is shown in Fig. 3.8.

Soil moisture at 23 cm during the three years was generally below field capacity (-33 kPa). For short periods, however, soil moisture was above field capacity. This occurred in May to June and September to October of 1985, in May and October of 1986, and near the end of July 1987. Soil moisture at 46 cm was at or above field capacity during 1985. Soil moisture at 46 cm in 1986 and 1987 was generally below field capacity, except from the middle of May to the end of June of 1986, when it was above field capacity. Soil moisture at 76 cm was above field capacity during 1985, from May to July 1986, and in June and early July 1987. Soil moisture at 122 and 200 cm during the three years was below field capacity. In contrast, soil moisture at 250 cm was greater than at 122 and 200 cm, and was generally above field capacity during the study.

High soil moisture at 250 cm may be related to the presence of a fluvial sand and gravel layer at this depth. An observation well penetrating this confined fluvial layer revealed the presence of a perched water table in the fall of 1985

(Fig. 3.7). The perched water table and high soil water content of this fluvial layer indicated that lateral saturated flow may have occurred within this confined glacial aquifer.

The soil water balance at the 76 cm depth was calculated to obtain a general approximation of how much water was draining downward and/or laterally, and possibly contributing excess water to the saline seep downslope (Site C2). The limitations of calculating the water balance at one specific depth were recognized; however, other methods that determine the water balance for the entire soil profile also incorporate many assumptions. The water balance at the 76 cm depth was chosen because decreases in soil moisture storage at this depth should reflect deep drainage out of the soil profile, and may possibly indicate potential for recharge to the water table.

The drainage component for the 76 cm depth was calculated using the equation:

$$D = P - \Delta S - Et \qquad (1)$$

where D is drainage, P is precipitation, ΔS is the change in soil moisture between two successive measurements, and Et is the actual evapotranspiration.

Time periods when soil moisture declined ($-\Delta S$) were used to determine the drainage component for the 76 cm depth. Only decreases in soil moisture that occurred above field capacity (-33 kPa) were used in the calculation. The ΔS values were taken from Fig. 3.8. Daily precipitation values for the selected time periods were taken from the meteorological station records for the Lethbridge Airport. Daily Class "A" pan evaporation values (Ep)

measured at the study site were converted to potential evapotranspiration values (Et_o) by using Kp coefficients of 0.7 and 0.8 (Doorenbos and Pruitt 1977); Et_o values were then converted to actual evapotranspiration values (Et) by using a kc coefficient of 0.9 (Penman 1948).

The soil water balance at 76 cm for the three years of this study is shown in Table 3.5. The assumption was made that when the deep drainage was a negative value, decreases in soil moisture were due only to evapotranspiration, and deep drainage was assumed to be zero. Net downward and/or lateral drainage was 91.3, 8.5, and 0 mm in 1985, 1986, and 1987, respectively. In comparison, Maule and Chanasyk (1987) used the field capacity method and reported total drainage values of 95 and 93 mm under fallow and barley within the Black soil zone near Edmonton, Alberta. Deep drainage in this study was highest in the fall during periods when precipitation was high and evapotranspiration was low. A high drainage component (91.3 mm) during September, 1985, may partially explain the perched water table at a shallow depth (5.2 m) during this time period. A high soil water content found in the fluvial sand and gravel layer at 2.50 m below the ground surface may be further evidence of deep drainage on the bedrock ridge.

3.3.3.2 Soil moisture regime at the saline seep

The soil moisture regime for the saline seep at Site C2 is shown in Fig. 3.9. Soil moisture at 23 cm during the three-year monitoring period ranged from above field capacity (-33 kPa) to less than the permanent wilting point (-1500 kPa). Soil moisture

at 23 cm during 1985 was generally below field capacity, except from the middle of May to late June, and in September when it was above field capacity. Soil moisture at 23 cm in 1986 was generally between field capacity and the permanent wilting point, except for short periods in late May and early October, when it was above field capacity. In contrast, soil moisture at 23 cm during 1987 was generally less than the permanent wilting point. In late July, however, soil moisture increased to field capacity for a very brief period. Soil moisture at 46 and 76 cm during the three years was always greater than field capacity. This reflected relatively wet conditions at these depths. Soil moisture at 122 cm during the three years was either slightly below or at saturation. This suggested that the top of the capillary fringe was close to 122 cm. Soil moisture at 200 and 250 cm indicated constantly saturated conditions during this study.

Increases in soil moisture at specific depths could be related to above-average precipitation during that month. This was evident by the simultaneous increase in soil moisture at 23, 46 and 76 cm in September of 1985, and at 23 cm in July of 1987.

3.3.4 Air Photo History of Saline Soils

Black and white aerial photographs were examined to ascertain any historical trends in the development of soil salinity at Sites A1, A3, B3, and C2. Photographs for five different years (1951, 1961, 1970, 1977, and 1985) were used (Plates 3.2, 3.3, and 3.4). Soil salinity was recognizable by white areas on the photographs.

Salinity was first apparent near Sites C2 and B3 in 1961 (Plate 3.2); however, these sites were not saline until 1970. The extent of salinity decreased at both sites in 1977 and increased again in 1985, but only at Site B3.

Ponding of surface water was evident in the depressional lowland near Sites C2 and B3 in 1951 and 1970 (Plate 3.2 a and c). The ponded water in 1951 can probably be attributed to above-average precipitation during 1951 (Fig. 3.10). Sommerfeldt and Ma Kay (1982) previously determined that some of this surface runoff accumulated in the lowland was recharging the water table below. Similar findings were also reported by Stein (1987).

The surface expression of the coarse-textured fluvial materials encountered at a shallow depth (250 cm) on the bedrock ridge at Site C1 was visible on the air photograph in 1961 (Plate 3.2 b). These sand and gravel fluvial deposits trended from slightly northwest to southeast through Site C1 and into the lowlands below the bedrock ridge. Results from this study suggested that it was highly probable that these fluvial materials were conducting water laterally through the glacial deposits as confined flow.

No soil salinity was visible on the aerial photographs for the five different years at Site A1; however, some white areas visible east of Site A1 in 1961 and 1970 may possibly have indicated salinity (Plate 3.3 b, c). Surface salinity was most apparent in the Studhorse Lake basin (Site A3) after 1951 (Plate 3.4 b, c, d, e).

Soil salinity was visible near or at Sites A1, A3, B3, and C2 in 1961. This suggested that salinization of these sites became visible on the soil surface sometime between 1951 and 1961. Precipitation records indicated that between 1951 and 1961, 7 of the 11 years had total annual precipitation values that were above the long-term (1949-1987) mean (Fig. 3.10). The salinity visible on the soil surface in 1961 may have been related to the relatively high precipitation between 1951 and 1961.

3.4 SUMMARY AND CONCLUSIONS

Various possible sources of excess water could have contributed to the development of saline soils and saline seeps in this study area (Sites A1, A3, B3, and C2). The most likely source of excess water at Site A1 was from shallow groundwater flow through the upper highly weathered bedrock from the adjacent bedrock ridge at Site A2. The weathered zone of the upper bedrock was approximately 15 to 17 m thick at Sites A1 and A2, respectively. The qualitative flow net (Fig. 3.1) showed that lateral groundwater flow occurred through this weathered zone. This weathered zone was fractured and contained thin layers of carbonaceous shale and/or coal, and had a relatively high hydraulic conductivity (10^{-6} m s^{-1}). In addition, it was possible that lateral flow from the bedrock ridge occurred through thin layers of sandy glacial material. The finer textured glacial materials

downslope at Site A1 would create a damming effect resulting in an increase of excess water at Site A1. This phenomenon was previously reported by Forster (1984). Other contributing factors here could have been the shallow overburden (1 to 2 m thick) and the sharp break in topography (from steep to shallow) from the bedrock ridge at Site A2 to the lower slope position at Site A1. The water table at Site A1 during this study, however, was from 4 to 9 m below the ground surface. This suggested that either very little soil salinization occurred during this study because of the relatively deep water table, or that excess water originated above the water table as lateral, unsaturated flow through coarse textured glacial deposits. Little soil salinization occurs under dryland conditions when the water table is greater than 3 m from the soil surface (Peck 1978). In addition, previous research has shown that there is a strong lateral component to unsaturated flow on a hillslope, even in the absence of apparent sublayers of much lower permeability (McCord and Stephens 1987).

There were three possible sources of excess water at Site A3 adjacent to Studhorse Lake. These included: discharge from deep confined aquifers under artesian conditions; lateral and shallow groundwater flow through the upper highly weathered bedrock zone; and infiltration of surface runoff and/or precipitation water. The qualitative flow net (Fig. 3.1) revealed that the high hydraulic head values found at depth below the Studhorse Lake basin could not be accounted for by the flow net within 91 m of the ground surface. Discharge from deeper confined aquifers under

strong artesian conditions was indicated by water levels in the piezometers above the level of the water table (near-flowing artesian conditions). The quantity of groundwater that discharged within the Studhorse Lake basin was calculated to be about 3.7 m^3 yr^{-1} (1.2 mm yr^{-1}). Studhorse Lake has also been mapped as a major artesian basin (Tokarsky 1973). Lateral and shallow groundwater flow through the upper highly weathered bedrock zone was indicated by the qualitative flow net (Fig. 3.1). This lateral flow appeared to have originated from the bedrock ridges at Site A2 and Site A4. Infiltration of surface and precipitation water was indicated by the tritium data (Table 3.3). This was evident by stratification of post-1953 shallow groundwater overlaying pre-1953 deeper groundwater. These three possible sources of excess water at Site A3 resulted in a shallow water table that ranged from 2.6 to 3.8 m below the soil surface.

There were four possible sources of excess water at Site B3. These were: lateral and shallow groundwater flow through the upper weathered bedrock zone; lateral flow through coarse-textured glacial deposits; infiltration of surface and precipitation water; and discharge from a shallow but relatively thick sandstone aquifer. Lateral and shallow groundwater flow through the upper bedrock was indicated by the qualitative flow net (Fig. 3.2). There was a trend of increasing coarser texture (sandy clay loam to sandy loam) with depth in the shallow glacial deposits covering the adjacent bedrock ridge near Site B2. The sandy loam materials just above the bedrock contact reflected the influence of the highly

weathered sandstone capping the bedrock ridge. Lateral flow of water may have occurred through these sandy loam glacial materials. Infiltration of surface and precipitation water was indicated by the tritium data (Table 3.3). It was also possible that the relatively thick and permeable (10^{-5} m s^{-1}) sandstone aquifer subcropping just downslope from Site B3 may have contributed excess water via discharge under artesian conditions. The water table at Site B3 was from 3 to 6 m during the study. This suggested that probably little salinization occurred during this time, or that excess water from lateral flow in the coarse textured glacial materials and/or infiltration of surface and precipitation water were likely the major sources of excess water during this study. Other contributing factors to excess water at Site B3 could have been the relatively thin overburden (1 to 4 m) capping the bedrock ridge, and the sharp break in topographic gradient (from steep to shallow) from the bedrock ridge to the lower slope position at Site B3.

There were three possible sources of excess water at the saline seep at Site C2. These included: infiltration of surface and precipitation water; confined flow through sand and gravel fluvial layers; and discharge from shallow, confined sandstone aquifers under artesian conditions. Infiltration of surface and precipitation water was indicated by the tritium data and by the presence of ponded water visible on air photographs in 1951 and 1970. Lateral flow through confined sand and gravel fluvial layers from the bedrock ridge to the north at Site C1 was indicated by a

perched water table in a well penetrating a shallow fluvial layer at Site C1, and by a relatively high soil water content in this sand and gravel layer. During periods of above-average precipitation, temporarily saturated conditions may have existed in these fluvial layers, and contributed excess water downslope via lateral flow. Evidence for discharge from shallow confined sandstone aquifers under artesian conditions was provided by the quantitative flow net (Fig. 3.3). The local recharge area for this flow appeared to be just south of Site B2 on the bedrock ridge. Artesian conditions in the sandstone aquifer at the 30 m depth below Site C2 were observed. The pressure heads here were 31 m above the top of the aquifer. The quantity of groundwater discharging from the sandstone aquifers was approximately 25.6 m^3 yr^{-1} (88 mm yr^{-1}). The contribution of excess water at Site C2 resulted in a water table that ranged from 1.68 to 2.34 m, and a top of a capillary fringe that was at approximately 1.22 m.

The results from this study were used to develop five models that represented the various possible sources of excess water contributing to high water tables and soil salinity (Fig. 3.11). These five possible sources of excess water were:

1. Discharge below closed topographic depressions from deep, confined bedrock aquifers under near-flowing artesian conditions.
2. Discharge from shallow, confined bedrock aquifers (sandstone, carbonaceous shale and/or coal) under artesian conditions.
3. Shallow groundwater flow through the upper highly weathered bedrock zone.

4. Lateral confined flow through sand and gravel fluvial layers (or coarse textured glacial materials) under temporarily saturated conditions.
5. Infiltration of surface water and precipitation at lower elevations.

Managing soil salinity becomes feasible when the possible sources of excess water contributing to high water tables are known. Shallow groundwater flow through the upper weathered bedrock or through permeable glacial materials can be dealt with using traditional management practices that emphasize utilization of excess water in the local recharge area. These practices may include continuous cropping the recharge area, interceptor cropping using alfalfa, and draining water from topographic depressions in the recharge area. Infiltration of surface and precipitation water at lower elevations in the discharge area, however, may require special management techniques to minimize runoff from snowmelt and precipitation to lower elevations. Some of these management practices have been suggested by Sommerfeldt and MacKay (1982). Pumping water from deep bedrock aquifers to decrease the pressure head within the aquifer is not economically feasible; however, pumping may be a possible alternative for shallower aquifers (Doering and Benz 1972).

3.5 BIBLIOGRAPHY

ALBERTA INSTITUTE OF PEDOLOGY. 1977. Soils of the Lethbridge area (NW82H) M-77-3. Alberta Inst. Pedol., Edmonton, Alberta. Scale 1:126,720.

BROWN, P.L., HALVORSON, A.D., SIDDOWAY, F.H., MAYLAND, H.F., and MILLER, R.M. 1983. Saline-seep diagnosis, control and reclamation. United States Dept. of Agric., Conservation Research Report No. 30.

BUCKLAND, G.D., HARKER, D.B., and SOMMERFELDT, T.G. 1986. Comparison of methods for determining saturated hydraulic conductivity and drainable porosity of two southern Alberta soils. Can. J. Soil Sci. 66(2): 249-259.

CHAN, G.W. and HENDRY, M.J. 1985. Impact of irrigation expansion on salinity adjacent to the Monarch Branch canal. Alberta Agriculture, Drainage Branch. 38 pp.

DOERING, E.J. and BENZ, L.C. 1972. Pumping an artesian source for water table control. J. Irrig. Drain. Div., ASCE 98: 275-287.

DOERING, E.J. and SANDOVAL, F.M. 1976. Hydrology of saline seeps in the northern Great Plains. Trans. ASAE (Am. Soc. Agric. Eng.) 19: 856-861, 865.

DOORENBOS, J. and PRUITT, W.O. 1977. Guidelines for predicting crop water requirements. FAO Irrigation and Drainage Paper No. 24. Food and Agriculture Organization of the United Nations, Rome, Italy. 144 pp.

ENERGY RESOURCES CONSERVATION BOARD. 1969. Structure contours on the base of the Fish Scales Formation for Area No. Two, Alberta. Calgary, Alberta. Scale: 1 inch:4 miles.

FORSTER, J.T. 1984. Soils and hydrogeologic investigation, Keyhoe Lake reservoir enlargement project. Alberta Environment, Lethbridge, Alberta. 23 pp.

FREEMAN, J.T. 1986. Modelling regional groundwater flow with environmental isotopes: Ross Creek Basin, Alberta. M.Sc. Thesis, Dept. of Geology, Univ. of Alberta, Edmonton, Alberta. 224 pp.

FREEZE, R.A. and CHERRY, J.A. 1979. Groundwater. Prentice-Hall, Inc., Englewood Cliffs, N.J. p. 136-137.

FRIND, E.O. 1971. Finite element model for steady-state potential distribution in a two-dimensional cross-section. Unpublished paper and computer code. Dept. of Earth Sciences, Univ. of Waterloo, Waterloo, Ontario.

FRIND, E.O. and MATANGA, G.B. 1985. The dual formulation of flow for contaminant transport modelling. 1. Review of theory and accuracy aspects. Water Resour. Res. 21(2): 159-169.

GEOLOGICAL SURVEY OF CANADA. 1967. Bedrock geology map 20-1967. Scale 1:253,440.

GREENLEE, G.M., PAWLUK, S. and BOWSER, W.E. 1968. Occurrence of soil salinity in drylands of southwestern Alberta. Can. J. Soil Sci. 48: 65-75.

HALVORSON, A.D. and BLACK, A.L. 1974. Saline seep development in dryland soils of northwestern Montana. J. Soil Water Conserv. 29: 77-81.

HENDRY, M.J. 1982. Hydraulic conductivity of a glacial till in Alberta. Ground Water 20(2): 162-169.

HENDRY, M.J. 1983. Origin of groundwater causing soil salinization in the Horsefly Lake area. Alberta Agriculture, Drainage Branch, Lethbridge, Alberta. 52 pp.

HENDRY, M.J. and SCHWARTZ, F. 1982. Hydrogeology of saline seeps. 1st Annual Western Provincial Conf. on Rationalization of Water and Soil Research and Management: Soil Salinity. Lethbridge, Alberta. p. 25-40.

HENRY, J.L., BULLOCK, P.R., HOGG, T.J. and LUBA, L.D. 1985. Groundwater discharge from glacial and bedrock aquifers as a soil salinization factor in Saskatchewan. Can. J. Soil Sci. 65(4): 749-768.

HVORSLEV, M.J. 1951. Time lag and soil permeability in groundwater observations. U.S. Army Corps Engineers. Waterways Exp. Station. Bull. No. 36, Vicksburg, Miss.

MACLEAN, A.H. and PAWLUK, S. 1975. Soil genesis in relation to groundwater and soil moisture near Vegreville, Alberta. J. Soil Sci. 26: 278-293.

MAULE, C.P. and CHANASYK, D.S. 1987. A comparison of two methods for determining the evapotranspiration and drainage components of the soil water balance. Can. J. Soil Sci. 67(1): 43-54.

McCORD, J.T. and STEPHENS, D.B. 1987. Lateral moisture flow beneath a sandy hillslope without an apparent impeding layer. Hydrological Processes I: 225-238.

McDONALD, M.G. and HARBAUGH, A.W. 1984. A modular three-dimensional finite-difference groundwater flow model. U.S. Dept. of the Interior, U.S. Geological Survey, National Center, Reston, Virginia. 528 pp.

McKEAGUE, J.A. (ed.) 1978. Manual of soil sampling and methods of analysis. Can. Soc. Soil Sci., Ottawa, Ontario. 212 pp.

MEYBOOM, P. 1966. Groundwater studies in the Assiniboine River Drainage Basin, Part I: The evaluation of a flow system in southcentral Saskatchewan. Geol. Surv. Can. Bull. 139.

MILLER, M.R., BROWN, P.L., DONOVAN, J.J., BERGANTINE, R.N., SONDEREGGER, J.L. and SCHMIDT, F.A. 1981. Saline seep development and control in North American Great Plains: Hydrogeological aspects. Agri. Water Management 4: 115-141.

OPHORI, D.U. 1986. A numerical simulation analysis of regional groundwater flow for basin management: plains region, Alberta. Ph.D. Thesis, Dept. of Geology, Univ. of Alberta, Edmonton, Alberta. 327 pp.

PECK, A.J. 1978. Note on the role of a shallow aquifer in dryland salinity. Australian J. Soil Res. 16: 237-240.

PENMAN, H.L. 1948. Natural evaporation from open water, bare soil and grass. Proc. R. Soc. A 193: 120-145.

PRAIRIE FARM REHABILITATION ADMINISTRATION. 1983. Land degradation and soil conservation issues on the Canadian prairies. Agriculture Canada, Regina, Saskatchewan. p. 41.

SOMMERFELDT, T.G. and CAMPBELL, D.E. 1975. A pneumatic system to pump water from piezometers. Ground Water 13: 293.

SOMMERFELDT, T.G. and MacKAY, D.C. 1982. Dryland salinity in a closed drainage basin at Nobleford, Alberta. J. Hydrol. 55: 25–41.

SOMMERFELDT, T.G., SCHAALJE, G.B. and HULSTEIN, W. 1984. Use of Tempe cell modified to restrain swelling, for determination of hydraulic conductivity and soil water content. Can. J. Soil Sci. 64: 265–272.

STEIN, R. 1987. A hydrogeological investigation of the origin of saline soils at Blackspring Ridge, southern Alberta. Unpubl. M.Sc. Thesis, Dept. of Geology, Univ. of Alberta, Edmonton, Alberta. 272 pp.

TOKARSKY, O. 1973. Hydrogeology of the Lethbridge–Fernie area, Alberta. Alberta Research Council Report 74–1, Edmonton, Alberta. 18 pp.

Table 3.1. Horizontal hydraulic conductivity values of the different hydrostratigraphic units used in the computer modelling of the qualitative and quantitative flow nets.

Hydrostratigraphic Unit	A – Line	B – Line	C – Line
		($m\ s^{-1}$)	
Glacial units			
Glaciolacustrine	10^{-9}	10^{-9}	–
Till	10^{-8}	10^{-8}	–
Fluvial	10^{-8}	–	–
Bedrock units			
Upper weathered and/or fractured shale	10^{-6}	–	10^{-6}
Upper weathered sandstone	10^{-7}	10^{-5}	10^{-5}
Lower unweathered and /or bentonitic sandstone	10^{-9}	10^{-7}	–
Interbedded shale and sandstone	10^{-9}	10^{-9}	10^{-8}
Carbonaceous shale and/or coal	–	–	10^{-6}

Table3.2. Difference in pressure head (Ψ_d) between field value from piezometer (Ψ_f) and calculated value (Ψ_c) from best – fit simulations of A – ,B – , and C – Line cross – sections using the finite – difference model.

Piezometer	$\Psi_d = \Psi_f - \Psi_c$ (m)
A2 – 14	+ 4.7
A2 – 42	+ 0.1
A3 – 30	+ 0.4
A4 – 20	+ 3.8
A4 – 56	+ 2.9
A5 – 8	+ 0.1
A5 – 30	+ 1.7
B2 – 34	– 0.4
B2 – 63	+ 1.9
B3 – 6	0
B3 – 16	+ 1.4
C1 – 24	+ 1.2
C1 – 25	+ 1.3
C1 – 35a, b	+ 0.2

Table 3.3. Tritium activity (TU = Tritium Units) of groundwater samples taken in May 1987, from piezometers and water – table wells in saline areas.

Piezometer or Well	Activity(TU)
A1 – 76	10 (+/– 1)
A1 – 24	<2
A1 – 9	<2
A3 – 69	2 (+/– 1)
A3 – 30	<2
A3 – 5W	46 (+/– 1)
B3 – 16	<2
B3 – 6	18 (+/– 1)
C2 – 30a	<2
C2 – 10	7 (+/– 1)
C2 – 7	10 (+/– l)
C2 – 3W	11 (+/– 1)
C2 – 30b	<2
C2 – 9	11 (+/– 1)
C2 – 6	11 (+/– 1)

Table 3.4. Artesian conditions (hydraulic head of piezometer in aquifer minus the elevation of the top of the aquifer) in three different types of confined aquifers within the study area.

Piezometer	Sandstone	Fluvial	Carbonaceous shale and / or coal
	Artesian conditions (meters)		
A1-24	12	–	–
A2-42	19	–	–
A3-30	23	–	–
A5-69	50	–	–
A6-20	–	3	–
B1-41	34	–	–
B2-34	11	–	–
B3-6	2	–	–
C2-30a,b	21	–	–
C2-7	4	–	–
C2-6	4	–	–
C1-34	–	–	17
C1-35	–	–	16
C1-24	–	–	7
C2-10	–	–	7

Table 3.5. Water balance at the 76 cm depth on the bedrock ridge (Site C1).

Date	Precipitation (P)	Evapo-transpiration (Et)	Change in Storage (ΔS)	Deep Drainage (D)
			mm	
1985				
31 May - 23 June	4.8	109.4	-3.0	0 (-101.6)
5 Sept. - 22 Sept.	107.3	23.0	-7.0	91.3
Subtotal	112.1	132.4	-10.0	91.3
Net drainage				
1986				
27 June - 18 July	82.2	78.7	-5.0	8.5
Subtotal	82.2	78.7	-5.0	8.5
Net drainage				8.5
1987				
25 July - 29 July	0	17.5	-2.0	0 (-15.5)
Subtotal	0	17.5	-2.0	0
Net drainage				0

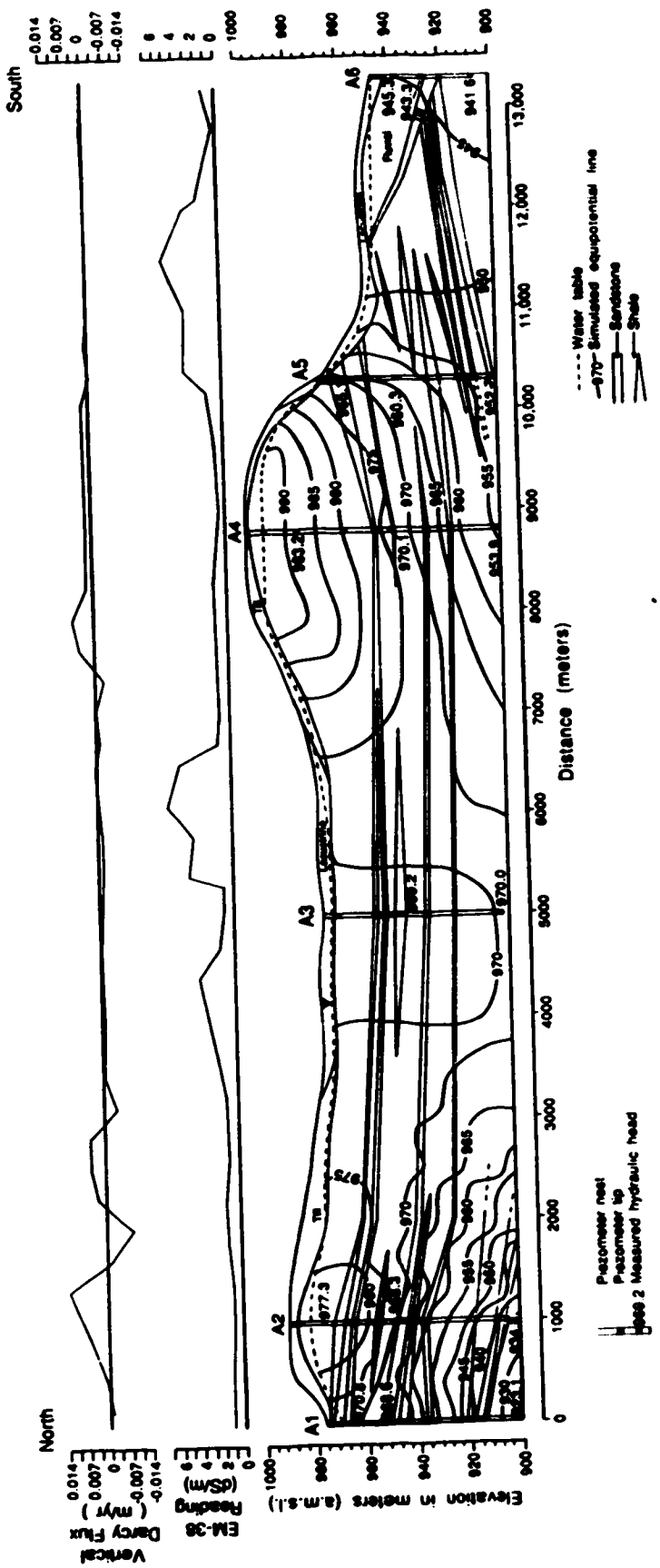

Figure 3.1. Geology, equipotential distribution, and recharge-discharge profile of the A-Line vertical cross-section.

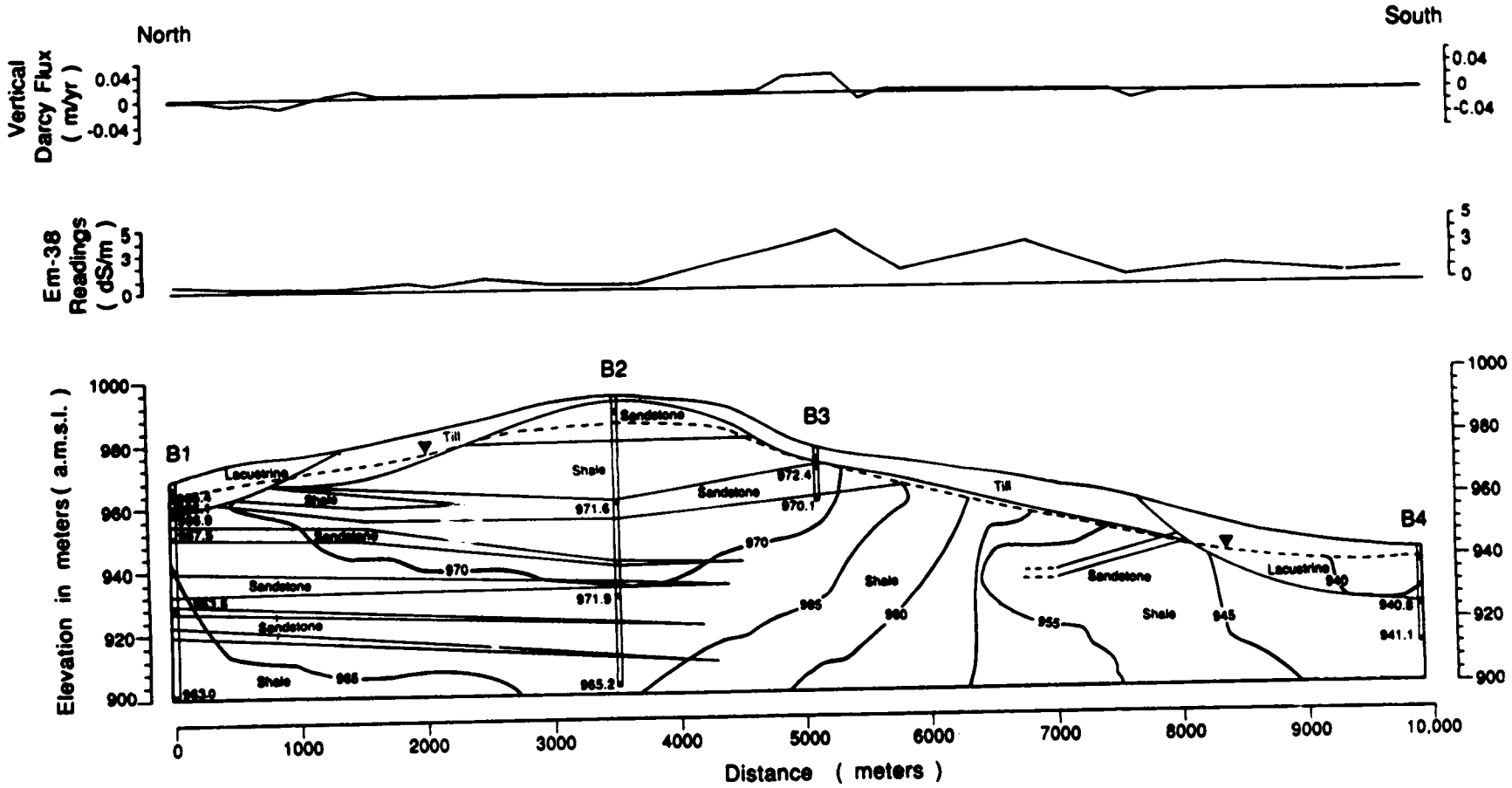

Figure 3.2. Geology, equipotential distribution, and recharge-discharge profile of the B-Line vertical cross-section.

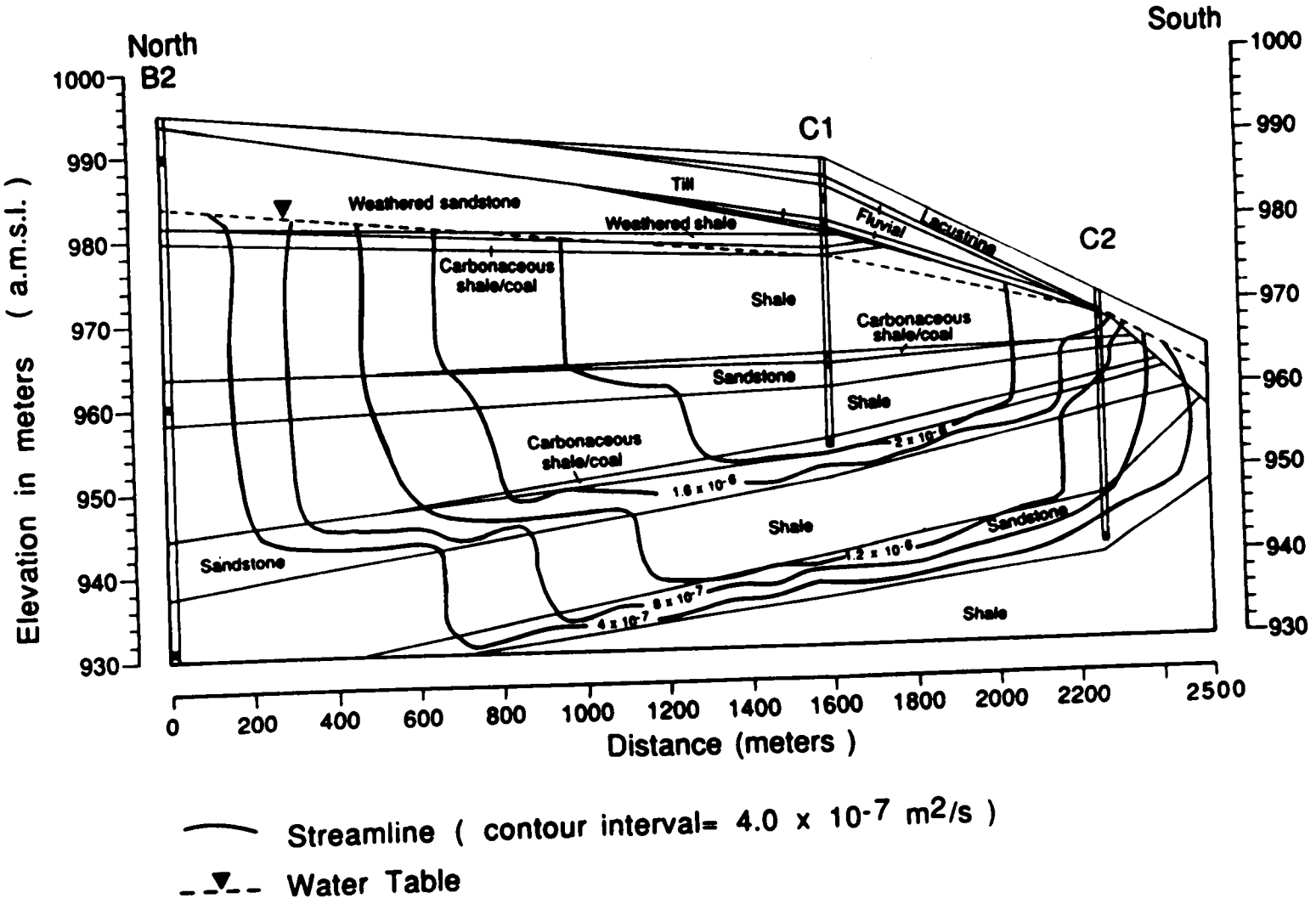

Figure 3.3. Geology and streamline distribution of the C-Line vertical cross-section.

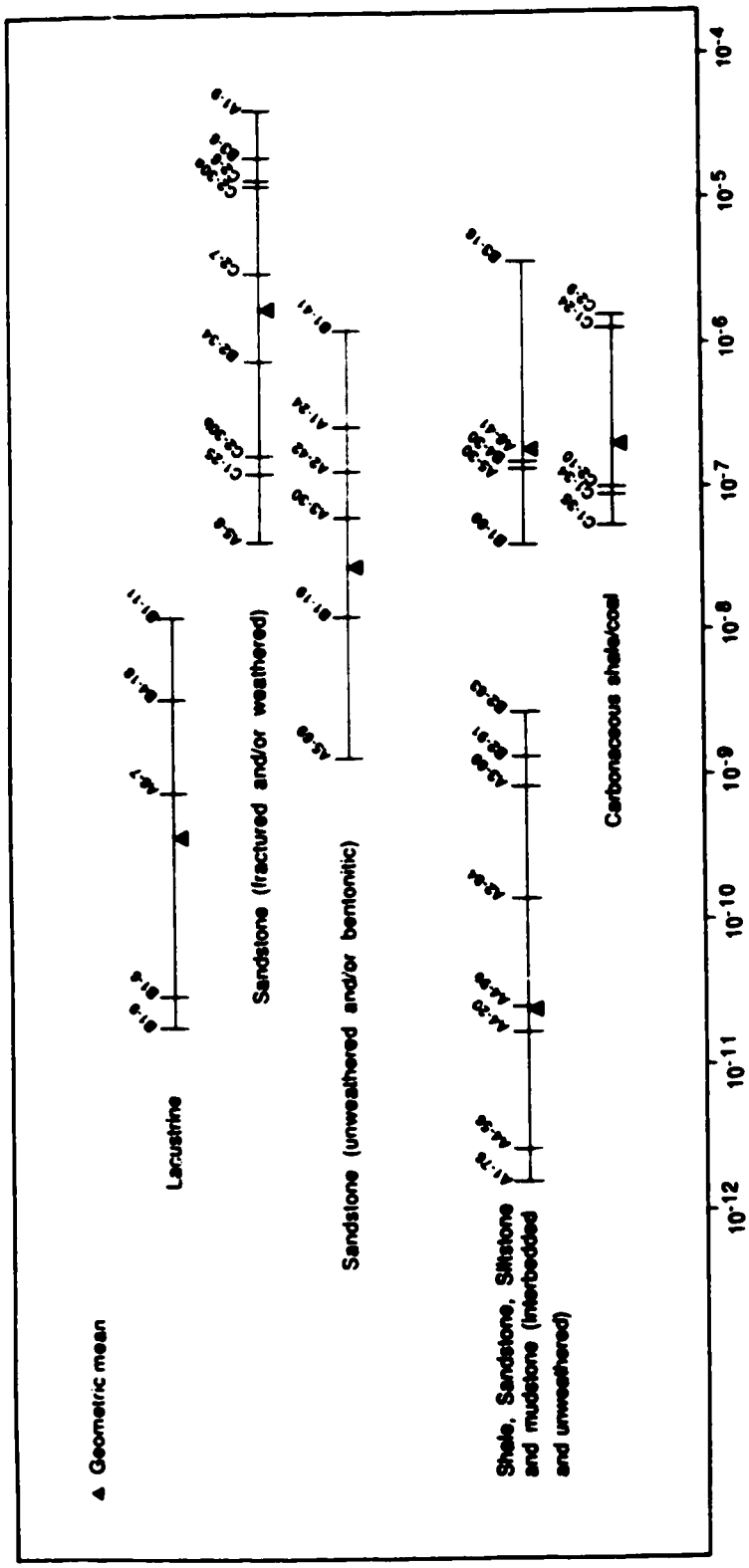

Figure 3.4. Hydraulic conductivity values of lacustrine and bedrock hydrostratigraphic units along the A-, B-, and C-Lines.

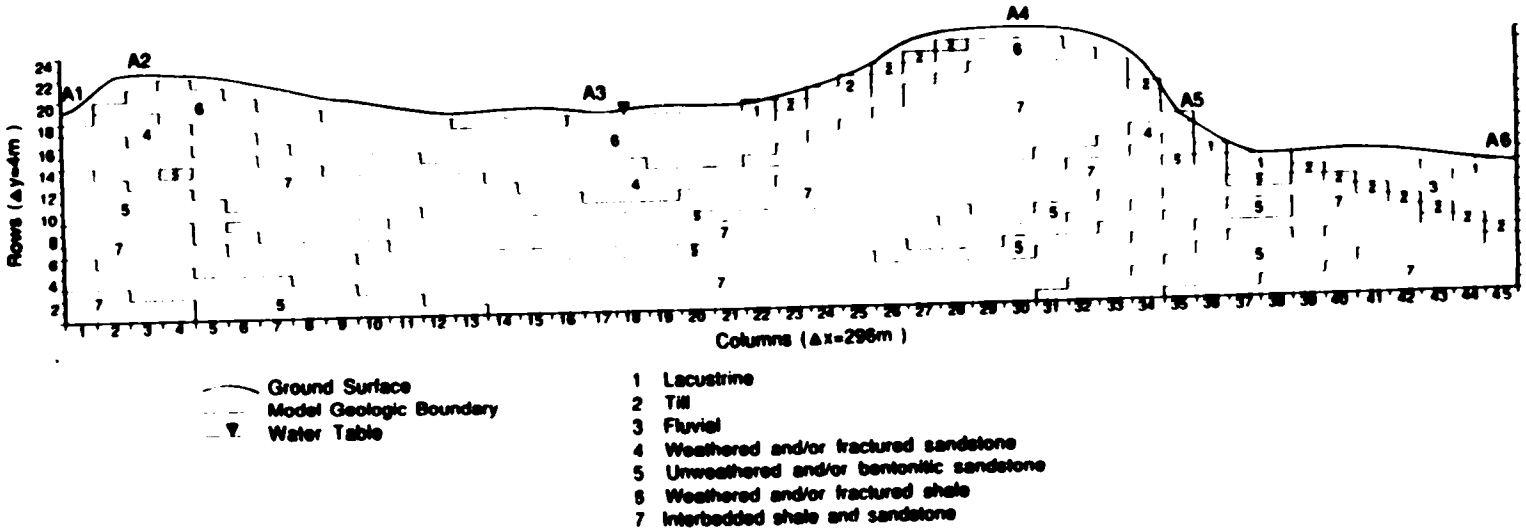

Figure 3.5. Finite-difference grid and discretization of hydrostratigraphic units along the A-Line section.

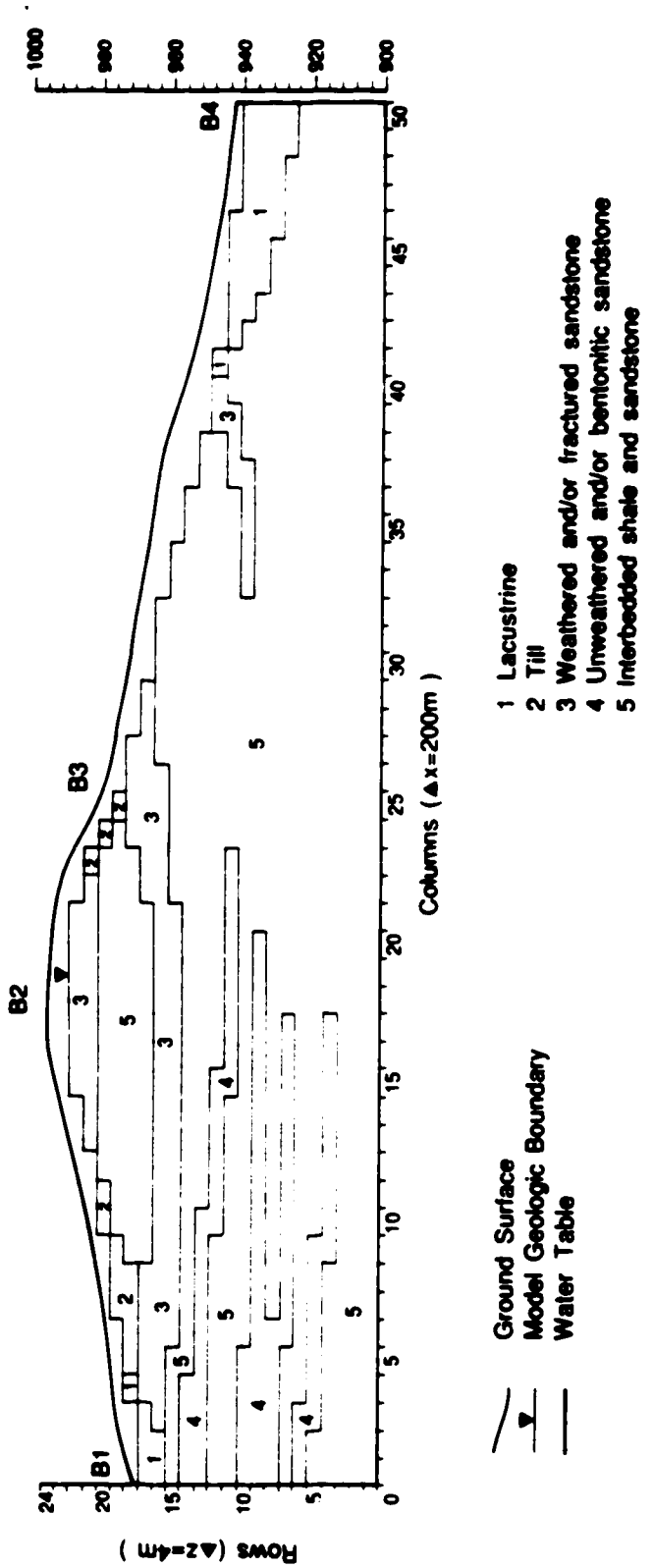

Figure 3.6. Finite-difference grid and discretization of hydrostratigraphic units along the B-Line section.

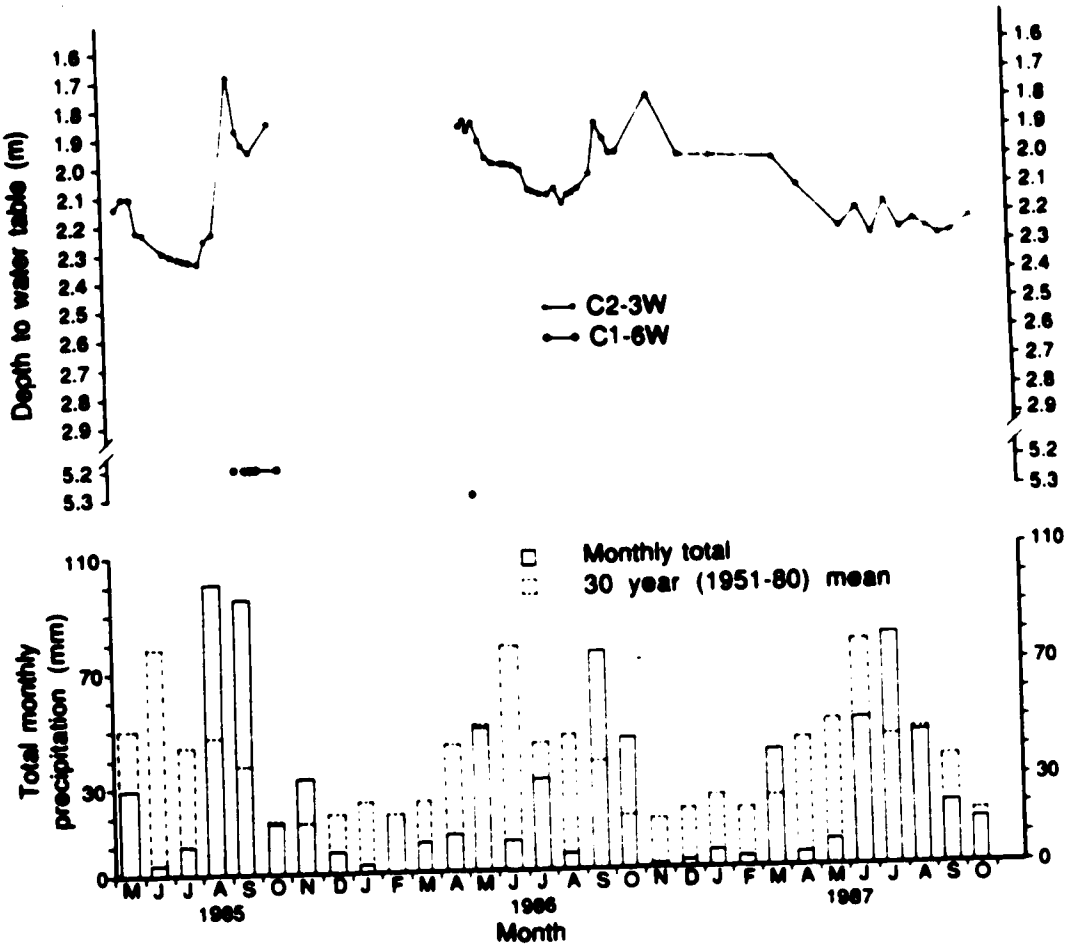

Figure 3.7. Water-table levels at Sites C1 and C2 in relation to time (months) and precipitation (mm).

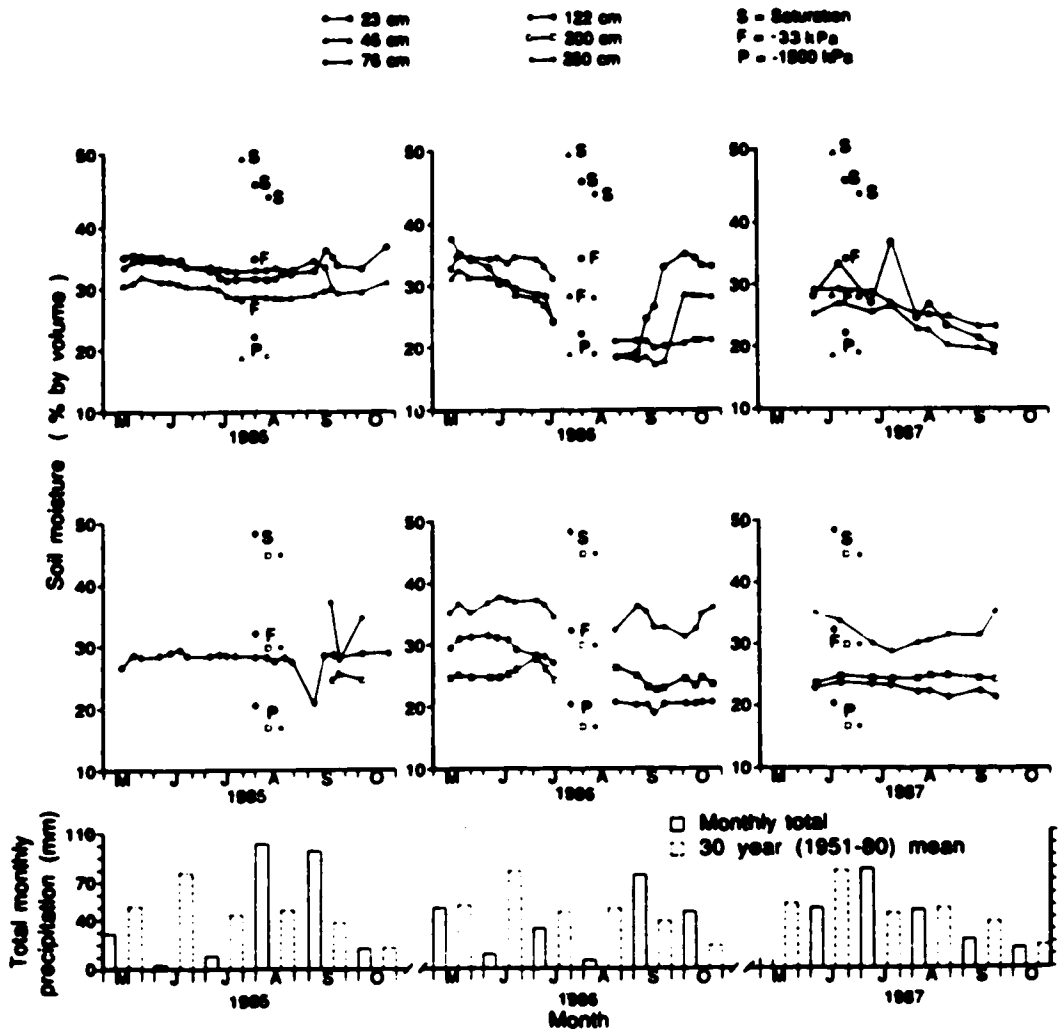

Figure 3.8. Soil moisture status at Site C1 from spring to fall in relation to time (months) and precipitation (mm).

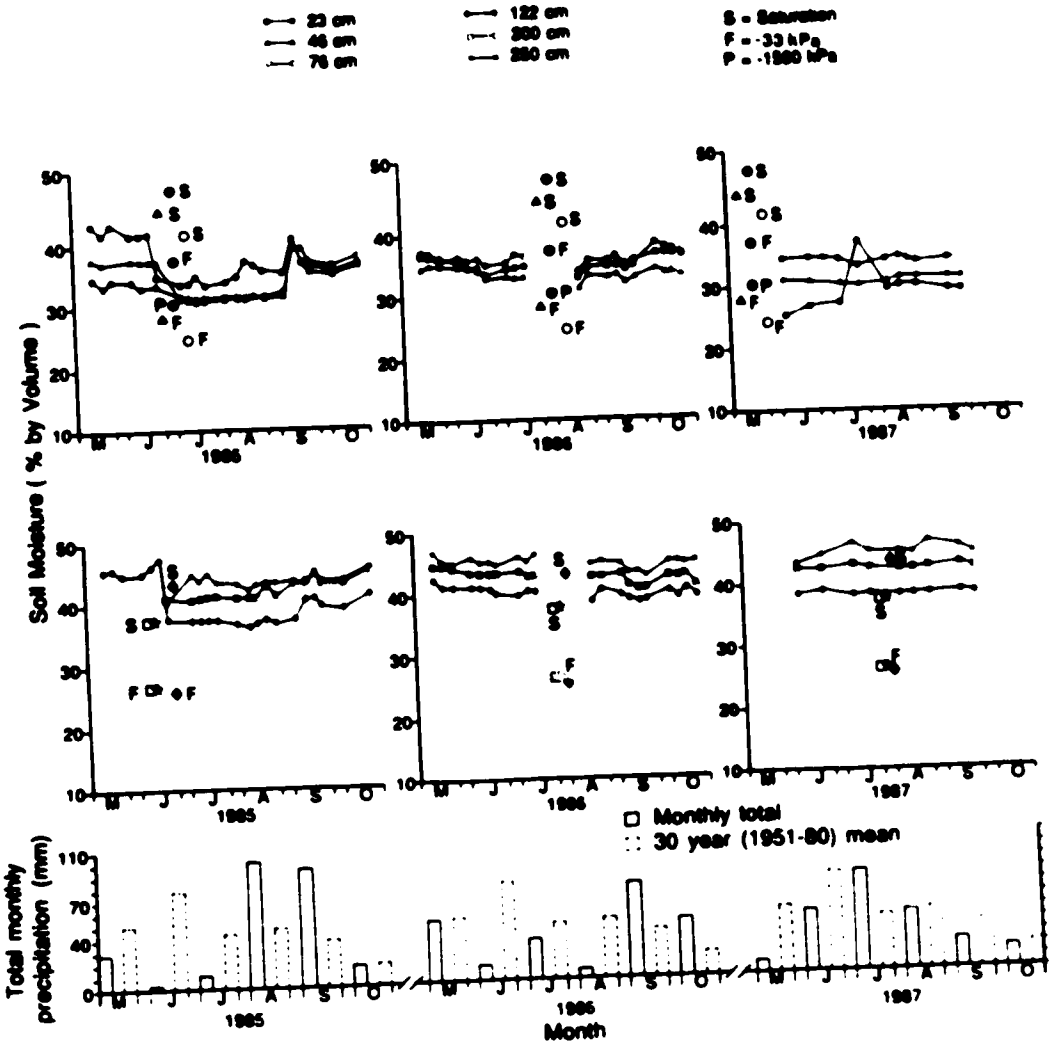

Figure 3.9. Soil moisture status at Site C2 from spring to fall in relation to time (months) and precipitation (mm).

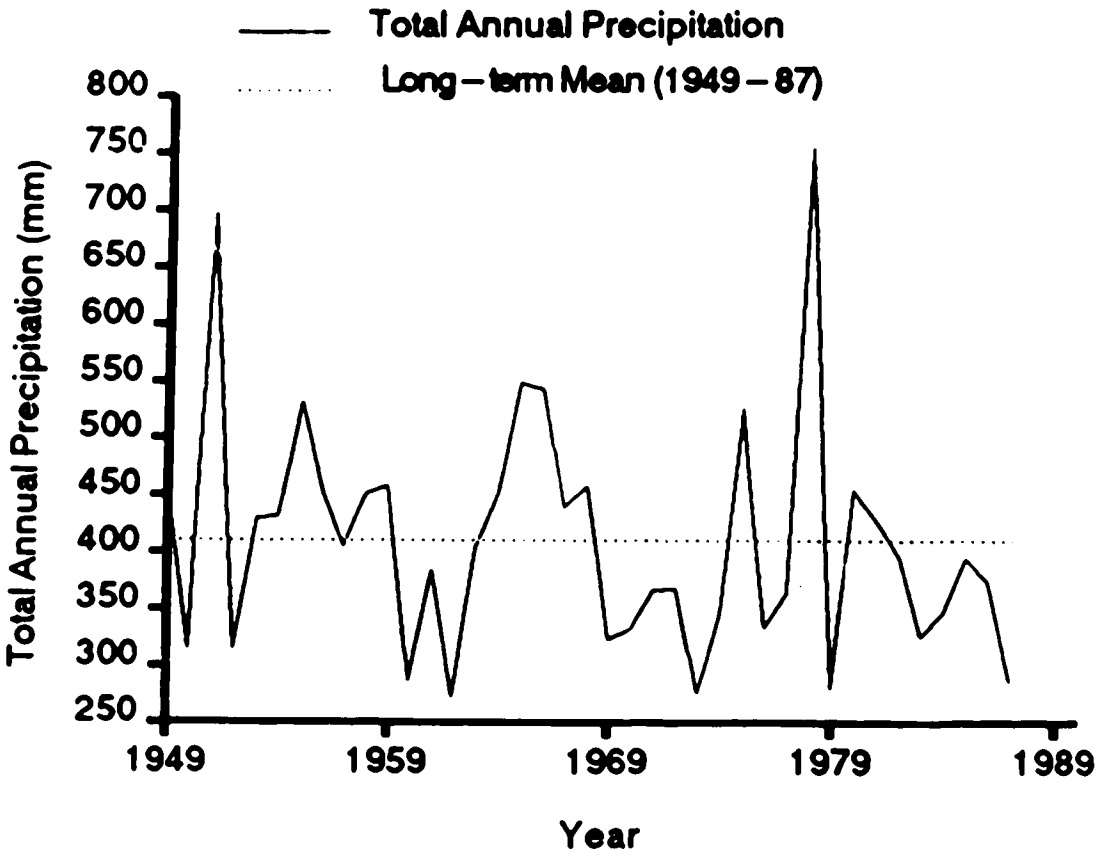

Figure 3.10. Total annual precipitation and long – term mean value (1949 – 1987) at the Lethbridge Airport.

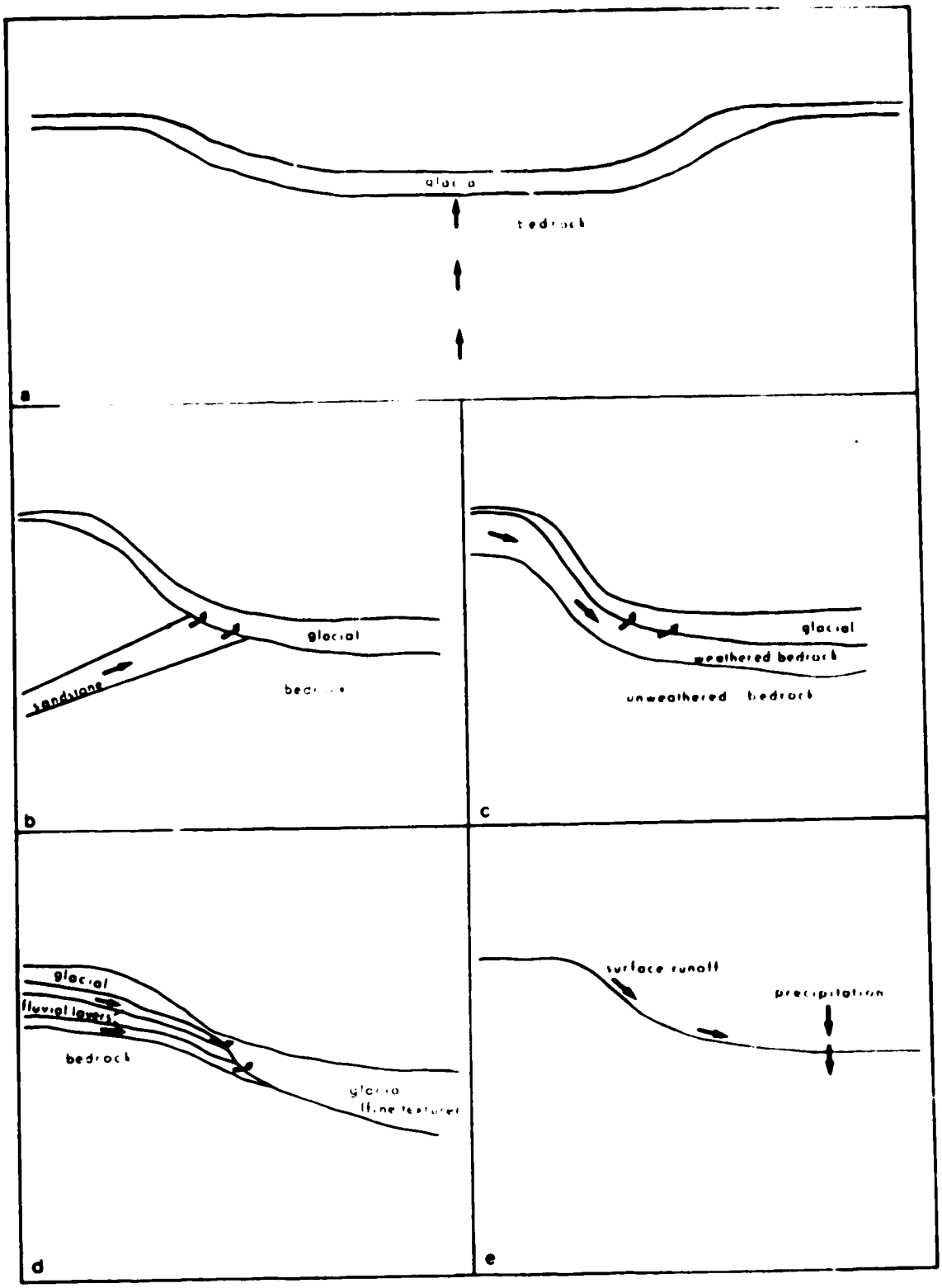

Figure 3.11. Five models representing possible sources of excess water contributing to soil salinity in the Nobleford study area.

Plate 3.1. Study site locations, topography, and areas of saline soils (s) near Nobleford. The air photo is from 1985, and the scale is 1:30,000.

Plate 3.2. Air photo history of soil salinity at Sites C2 and B3 during five different years (1951, 1961, 1970, 1977, and 1985).

(a) 1951

(b) 1961

(c) 1970

(d) 1977

(e) 1985

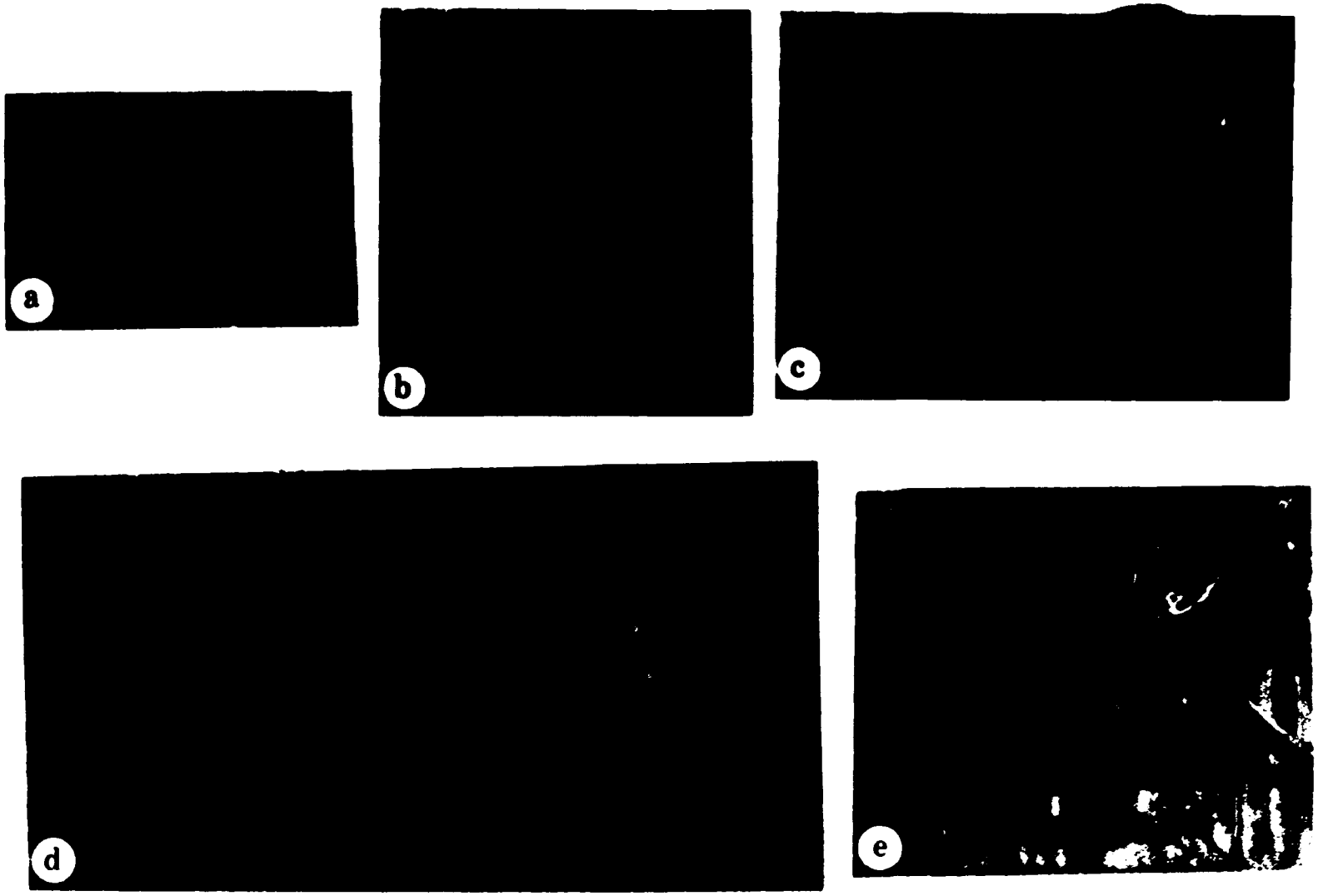
a
b
c
d
e

Plate 3.3. Air photo history of soil salinity west of Keho Lake (Site A1) during five different years (1951, 1961, 1970, 1977, and 1985).

(a) 1951

(b) 1961

(c) 1970

(d) 1977

(e) 1985

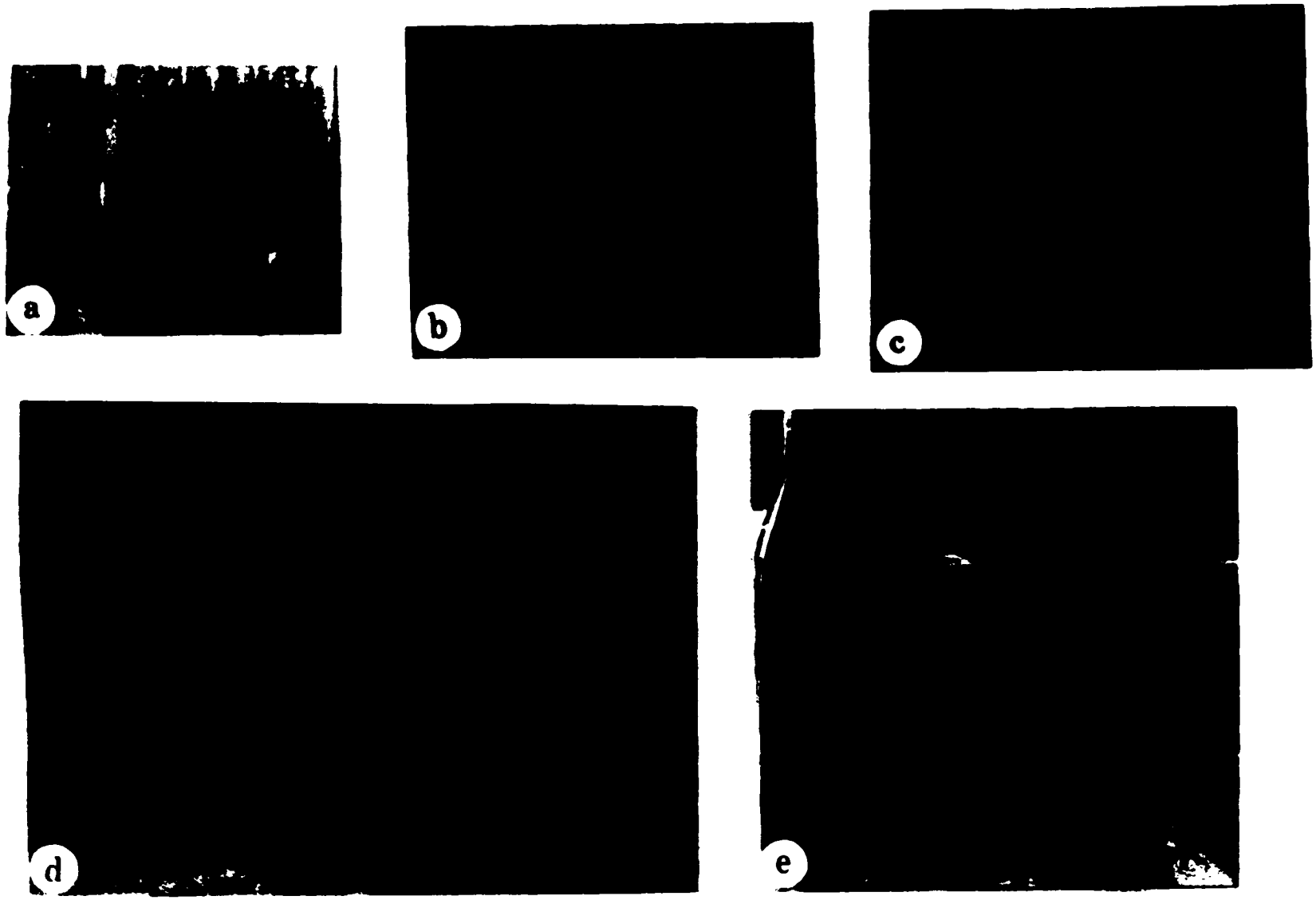
a
b
c
d
e

Plate 3.4. Air photo history of soil salinity within the Studhorse Lake basin (Site A3) during five different years (1951, 1961, 1970, 1977, and 1985).

(a) 1951

(b) 1961

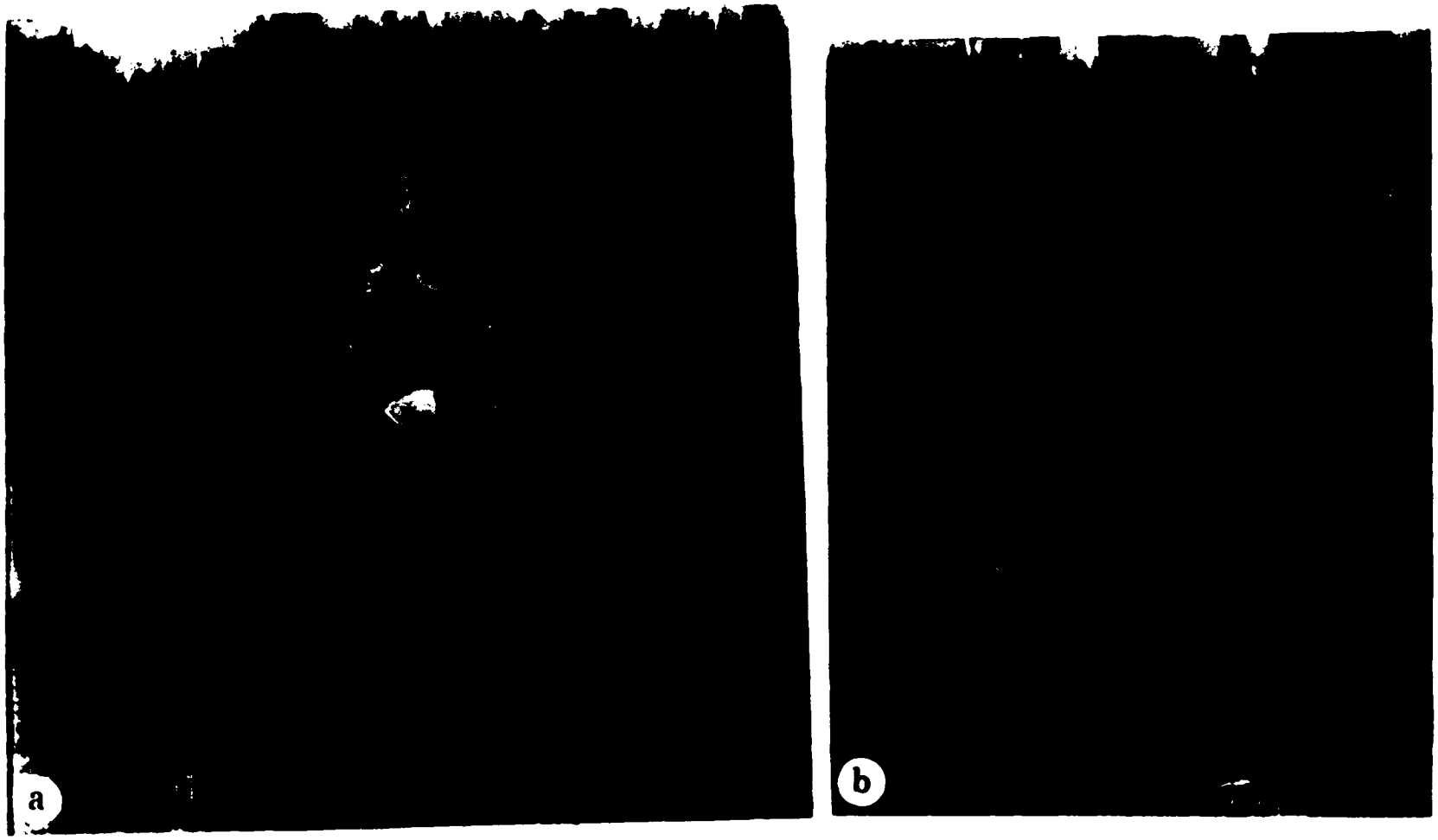
a
b

Plate 3.4(cont.) Air photo history of soil salinity within the Studhorse Lake basin (Site A3) during five different years (1951, 1961, 1970, 1977, and 1985).

(c) 1970

(d) 1977

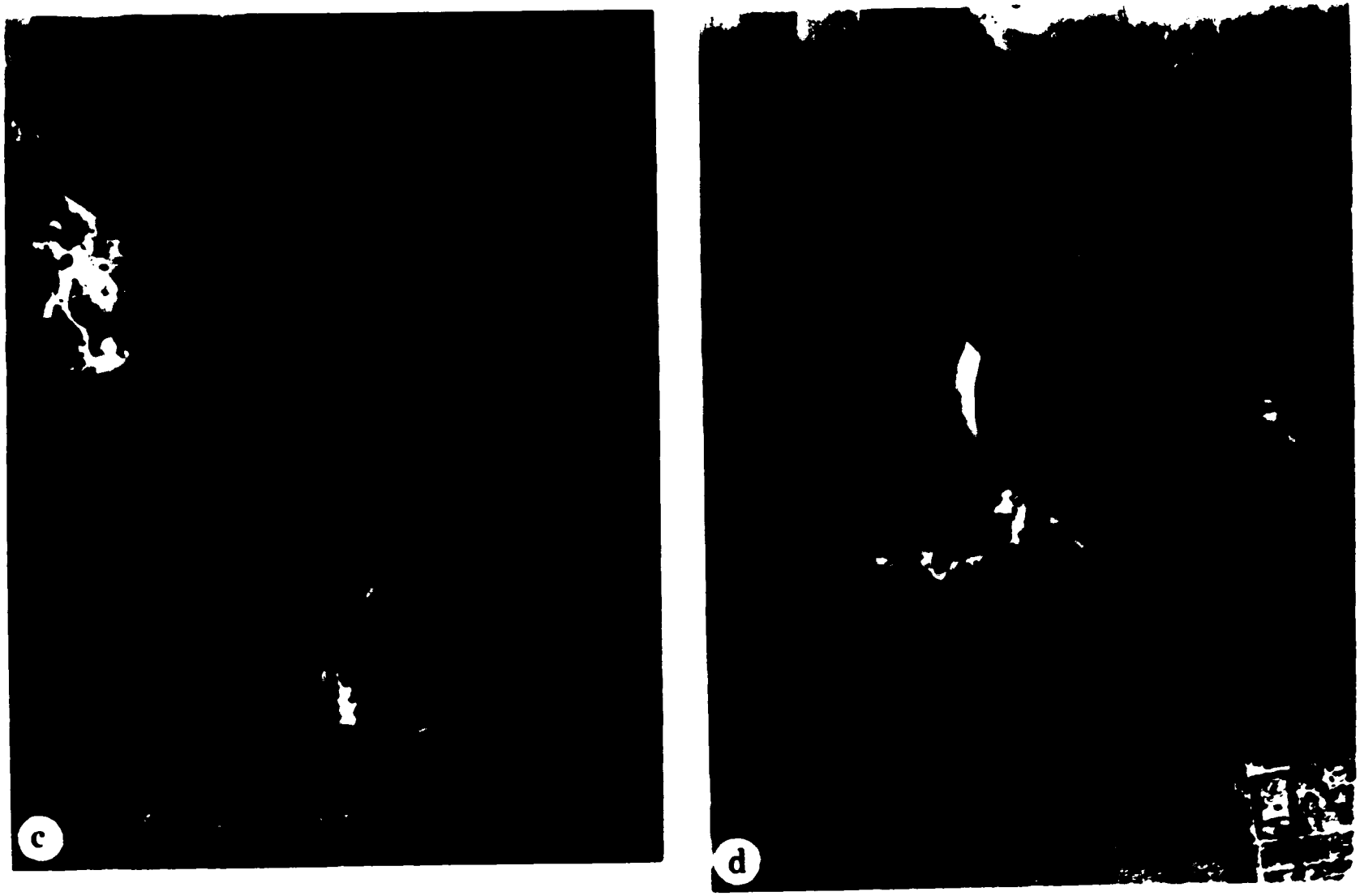
c
d

Plate 3.4(cont.) Air photo history of soil salinity within the Studhorse Lake basin (Site A3) during five different years (1951, 1961, 1970, 1977, and 1985).

(e) 1985


e

4. THE ORIGIN OF SOLUBLE-SALTS CAUSING DRYLAND SALINITY NEAR NOBLEFORD, ALBERTA

4.1 INTRODUCTION

Soil salinization results from a combination of excess water and excess soluble salts (hereafter referred to as salt). If the source of the excess water is from within the glacial drift, this implies that the salts would be derived from the drift. If the source of the excess water is from the bedrock, however, then the source of the salts could be from the bedrock and/or the drift. Research on soil salinization has focussed on the possible sources of excess water contributing to high water tables because management practices are most directly applicable to preventing the buildup of excess water. Knowledge of the source of salts, however, can provide additional information regarding the origin of soil salinity.

Some workers have proposed that the source of the salts causing soil salinization is the drift. Ferguson and Bateridge (1982) reported that up to 90 t ha^{-1} of salt was leached from soils in recharge areas, on glacial till in Montana. They attributed the increased leaching of salts and development of saline seeps to the crop-fallow system of farming. Except for the upper meter, the entire till profile contains an extremely abundant supply of water-soluble salts that are capable of maintaining

existing saline seeps for the next 25 to 100-plus years (Miller et al. 1981).

In southern Alberta the main salt reservoir has been reported to be glacial till (Hendry and Schwartz 1982). The content of water-soluble salts typically ranges from 15 to 30 meq 100 g^{-1} of air-dried till, with Na and SO_4 most abundant. Few studies, however, have determined the salt reservoir in the underlying bedrock in this region.

In a study in southern Manitoba, Eilers (1973) found that most of the soluble salts in the soil and groundwater of the study area were derived from the glacial till. Soils in one area, however, were affected by Na salts from the underlying Riding Mountain Formation. Henry et al. (1985) reported that discharge from glacial and bedrock aquifers under artesian conditions was a factor in soil salinization in Saskatchewan. They found that the source of near-surface salts could have been the aquifers and/or weathered till. In a study of the origin of saline soils at Blackspring Ridge in southern Alberta, Stein (1987) found that excess salts were derived from glacial and/or bedrock sources. Mixing and subsequent evaporation of drift and shallow bedrock sources was suggested as a possible mechanism.

Various chemical constituents have been used as tools to identify the source areas of soluble salts. High concentrations of Na and Cl ions in saline soils generally reflect a bedrock source (Greenlee et al. 1968; Eilers 1973; Henry et al. 1985; Stein 1987). Sulfur and oxygen isotopes of soluble sulfates have also

been used as indicators of sources of salt. Buylov (1976) and Kovda et al. (1980) found that the sulfur isotopic composition of sulfates from saline soils and deep artesian groundwaters of bedrock origin were similar. This suggested a hydraulic connection between the soil and artesian waters. Hendry and Krouse (1987) noted significant differences in the oxygen isotopic composition of soluble sulphate from weathered till and the underlying bedrock. They suggested that by comparing these isotope values to the values of soil sulfates, the source of the sulfate causing the salinity may be revealed. This technique, however, has not been applied to saline soils.

The oxygen isotopic composition of soluble sulfates is potentially more useful as a tracer than the sulfur isotope because the half-time of exchange between ^{18}O in the sulfate and the ^{18}O in the associated groundwater is about 10,000 years (Lloyd 1968; Mizutani and Rafter 1969); at the temperature and pH of the groundwaters of southern Alberta (Hendry and Krouse 1987).

The objective of this paper was to determine the origin of excess soluble-salts in selected saline soils in an area of dryland salinity in southern Alberta. The origin of the salts (drift and/or bedrock) will be assessed by using sulfur and oxygen isotopes, hydrochemical data, and chemistry of the soil, drift and bedrock materials.

4.2 MATERIALS AND METHODS

4.2.1 Site Description

The study area is located in southwestern Alberta near the village of Nobleford, about 48 km northwest of Lethbridge, Alberta. The location, site instrumentation and physiography of the study area have been previously described in Section 3.2.1.

4.2.2 Field Methods

Test drilling and installation of piezometers and water table wells at ten sites along the A-, B- and C-Lines was performed as outlined in Section 3.2.2. Bulk soil samples were collected from all recognizable horizons and layers at the ten sites, and also from five selected saline and Solonetzic soils throughout the study area. Drift and bedrock materials were described and sampled during auger or rotary drilling. At Sites C1 and C2, drill cuttings from the auger were sampled whenever a change in geology occurred. At sites along the A- and B-Lines, cuttings from the rotary drill were generally sampled every 3 m.

Groundwater samples were taken from piezometers or water table wells only after pumping or bailing considerable standing water from the pipe. The pH was measured in the laboratory the same day samples were taken. Groundwater samples were taken to the laboratory and stored at 4°C for later chemical and/or isotope analyses.

4.2.3 Laboratory Methods

Soil, drift and bedrock samples were air-dried and crushed to pass a 2-mm sieve. Chemical analyses were performed on saturation paste extracts from horizons and layers of the two soil profiles at Sites C1 and C2; and on the drift and bedrock samples from the auger drilling at Sites C1 and C2. Chemical analyses were also performed on 1:5 (soil:water) extracts of soil, drift and bedrock samples from the rotary drilling at sites on the A- and B-Lines. The following chemical analyses were performed on the saturation paste extracts, 1:5 (soil:water) extracts, and the groundwater samples: Ca, Mg, Na, and K (Chang and van Schaik 1965); SO_4 (American Public Health Association 1980); CO_3 and HCO_3 (Bower and Wilcox 1965); Cl (Adriano and Doner 1982); and electrical conductivity (EC) and pH (Rhoades 1982). Concentration of Br and I in the groundwaters were determined by neutron activation analyses.

Sixteen soil, drift and bedrock samples, ten groundwater samples and five samples of evaporite crystals (visually identified as probably gypsum and/or bassanite) were analyzed for the oxygen and sulfur isotopic composition of the SO_4. In addition, ten groundwater samples were analyzed to determine the oxygen isotopic composition of the water. Isotope analyses were performed in the Department of Physics (Dr. H.R. Krouse) at the University of Calgary.

The sulfate in each solid sample (soil, drift or bedrock) was dissolved using a 1:10 (soil:water) ratio. The aqueous SO_4

in each sample of groundwater and 1:10 extract was then precipitated as $BaSO_4$ using the Gravimetric Method with Ignition of Residue Technique (426A), as outlined by the American Public Health Association (1980). $BaSO_4$ and evaporite crystals were analyzed for $\delta\,^{34}S$ and $\delta\,^{18}O$ using techniques outlined by Shakur (1982). The analytical precisions for the $\delta\,^{34}S$ and $\delta\,^{18}O$ analyses were $\pm$ 0.3 and $\pm$ 0.5‰, respectively.

Stable isotope abundances were reported in the δ notation. This refers to how the abundance ratio of two isotopes in a sample differ in parts per thousand (‰) from that of an internationally accepted standard:

$$\delta \text{ sample} = \frac{R_{sample} - 1}{R_{standard}} \times 1{,}000 \qquad (1)$$

where R is the abundance ratio ($^{18}O/^{16}O$ or $^{34}S/^{32}S$). The standard for reporting $\delta\,^{34}S$ values was troilit eS) from the Canyon Diablo Meteorite (CDT). The standard for reporting $\delta\,^{18}O$ values was Standard Mean Ocean Water (SMOW).

4.3 RESULTS AND DISCUSSION

4.3.1 Sulfur and Oxygen Isotope Chemistry

The results of the isotope analyses are presented in Tables 4.1, 4.2 and 4.3. The mean $\delta\,^{34}S$ (SO_4) values for drift ($x = 0.25$‰, $n=4$) and bedrock ($x = 1.22$‰, $n=16$) were relatively

similar for all three sites. This precluded the use of the sulfur isotope as a possible tool to identify the source of soil sulfates, because the sulfur isotope values of the two possible source areas (drift and bedrock) were similar. In contrast, other workers (Wallick 1981; Shakur 1982; Hendry et al. 1986) have reported greater differences in $\delta\,^{34}S\ (SO_4)$ values between the drift and Cretaceous bedrock from other locations in Alberta. They found that $\delta\,^{34}S\ (SO_4)$ values were close to or above 0‰ in the bedrock, and decreased to greater negative values (-10 to -20‰) in the overlaying drift.

The mean $\delta\,^{18}O\ (SO_4)$ values for drift ($x = -8.0$‰, n=4) and bedrock ($x = 1.1$‰, n=16) showed a greater difference than the $\delta\,^{34}S\ (SO_4)$ values; however, the difference was not sufficient to serve as a basis for ascertaining possible source areas of salt. Hendry and Krouse (1987) reported that the $\delta\,^{18}O\ (SO_4)$ values of groundwater from weathered till ($x = -14.6$‰, n=29) were significantly less than groundwater from the Cretaceous bedrock ($x = 0.2$‰, n=6) at two study areas in southern Alberta; and proposed that this technique could be applied elsewhere to ascertain source areas of salts.

This technique, however, can only differentiate between drift and bedrock sources of salt at locations where the drift and bedrock exhibit different $\delta\,^{18}O\ (SO_4)$ values. This would result when the drift was derived from bedrock some distance away. Similar $\delta^{18}O\ (SO_4)$ values in the drift and bedrock in the Nobleford study area indicated that the drift was probably derived from the

local, underlying bedrock. Similar oxygen isotope values in both the drift and bedrock prevented differentiation of either geologic unit as the primary source of salts.

Some interesting trends, however, were observed in the isotope data (Tables 4.1, 4.2 and 4.3). These were variable $\delta^{18}O$ (SO_4) values, and relatively constant $\delta^{34}S$ (SO_4) values, of soluble sulfates and evaporite crystals (gypsum and bassanite) from different depths. The $\delta^{18}O$ (SO_4) and $\delta^{34}S$ (SO_4) values of soluble sulfates were plotted versus depth, and clearly illustrate these trends (Fig. 4.1, 4.2 and 4.3).

The $\delta^{34}S$ (SO_4) profiles in Fig. 4.1, 4.2 and 4.3 exhibited relatively constant values with depth. Values were slightly above or below 0‰. Shakur (1982) and Hendry et al. (1986) reported a trend of increasing $\delta^{34}S$ (SO_4) values with increasing depth from the till to the bedrock. They found that $\delta^{34}S$ (SO_4) values in the till were generally between -10 to -20‰ whereas values in the bedrock typically increased to near 0 or slightly positive values. An enrichment in $\delta^{34}S$ (SO_4) at depth in the bedrock was attributed to microbial reduction, as the lighter $^{32}SO_4$ is preferentially converted to sulfide during bacterial reduction of sulphate. Reduction of sulfates may partially explain the $\delta^{34}S$ (SO_4) values close to or above 0 found in this study. The presence of H_2S gas, which is indicative of sulfate reduction, was detected in some of the piezometers during the study.

The $\delta^{18}O$ (SO_4) profiles exhibited extremely variable

values with depth (Fig. 4.1, 4.2, 4.3). Negative $\delta^{18}O$ (SO_4) values (-8 to -10‰) found at shallow depths or in permeable aquifers (30 m at Site A3; 10 m at Site C2) may have indicated interaction with light meteoric water during transport of sulfate in solution and/or reoxidation of sulfides. These processes can result in negative $\delta^{18}O$ (SO_4) values because of incorporation of oxygen from meteoric groundwater which is depleted in ^{18}O. The ^{18}O (H_2O) values of the groundwater in this study ranged from -15.3 to -21.5‰ (Tables 4.1, 4.2, 4.3). Shakur (1982) found negative $\delta^{18}O$ (SO_4) values near -11‰ in shallow strata in southern Alberta, and attributed the isotope depletion to re-oxidation of ascending sulfides and incorporation of groundwater with negative $\delta^{18}O$ (H_2O) values near -20‰. Similar findings were also reported by Hendry et al. (1986).

Different $\delta^{18}O$ (SO_4) and $\delta^{18}O$ (H_2O) values found in this study indicated that $\delta^{18}O$ was not in isotopic equilibrium between SO_4 and H_2O. This phenomena was also found in non-weathered tills at two locations in southern Alberta, and was attributed to a lack of contact time between the porewater and the sulfate (Hendry et al. 1986, personal communication).

The $\delta^{18}O$ and $\delta^{34}S$ values of sulfates were plotted on a scatter diagram (Fig. 4.4) to determine if values for soil, drift, bedrock and evaporite crystals exhibited characteristic "isotopic signatures". The scatter of the isotope values was mainly due to the wide variability in $\delta^{18}O$ (SO_4) values (-11 to 17‰). The $\delta^{34}S$ (SO_4) values exhibited much less scatter (-3 to 8‰).

Isotope values showed little scatter for the soil and drift, moderate scatter for evaporite crystals, and the most scatter for bedrock (Fig. 4.4). The $\delta^{18}O$ (SO_4) values were negative (-9 to -4‰) in the soil and drift, both negative and positive (-11 to 12‰) in the bedrock, and positive (2 to 17‰) in evaporite crystals (gypsum and/or bassanite) from the soil and drift. In comparison, Hendry et al. (1986) found considerable scatter in both $\delta^{18}O$ and $\delta^{34}S$ values of soluble sulfates from till and bedrock in southern Alberta. They found differences in ^{34}S between the bedrock (-3 to 2‰) and till (-15 to 17‰); and high variability in the ^{18}O of the tills (-17 to 3‰).

Negative $\delta^{18}O$ (SO_4) values may have been related to interaction with light meteoric groundwater, and/or to reoxidation (Shakur 1982). A possible explanation for the enrichment in $\delta^{18}O$ content of the evaporite crystals (Fig. 4.4) may be repeated cycles of dissolution-reprecipitation. The enrichment may occur during crystallization, when ^{34}S and ^{18}O are favoured in gypsum by 1.65 ± 0.12 and 3.6 ± 0.9‰, respectively (Thode and Monster 1965; Lloyd 1967; Holser et al. 1979). Shakur (1982) also reported an enrichment in $\delta^{18}O$ content of evaporite crystals (mainly gypsum).

The isotope values of soil and drift samples on the scatter diagram (Fig. 4.4) showed a tendency toward linear behaviour. The slopes of such lines may indicate specific processes contributing to that linear behaviour. Mixing of two waters with SO_4 of different isotopic compositions, crystallization of sulfate minerals

(slope = 2), adsorption of sulfate by sediments (slope = 0.7), and sulfur redox reactions (slope = 0.25 or variable), have been cited as four possible mechanisms that may be related to linear behaviour (H.R. Krouse, personal communication). The linear behaviour of the soil and drift, isotope values in Fig. 4.4, had slopes indicative of crystallization of sulfate minerals.

4.3.2 Hydrochemical Facies of Soil, Drift and Bedrock

The groundwater chemistry of bedrock and drift deposits, and chemistry of soil saturation paste extracts from saline soils (Sites A1, A3, B3 and C2), were plotted on Piper diagrams to determine if the ion facies of the soil was more similar to the drift or bedrock materials (Fig. 4.5 to 4.8). At Sites A1, A3 and B3, the ion facies of the soil saturation extracts were more similar to the ion facies of the groundwater from the drift compared to the ion facies of the groundwater from the bedrock. This suggested that the source area for soluble salts in these three soils was derived mainly from the groundwater of the drift. In contrast, the ion facies of the soil saturation extracts and groundwater from the drift and bedrock were similar at Site C2 (Fig. 4.8). This inferred that the soluble salts in the soil were derived from the drift and/or bedrock groundwaters.

If mixing of both drift and bedrock groundwaters occurred, then the apparent mixture (soil) must plot on straight lines between the plottings of its two inferred components (Piper 1944). This phenomena was not apparent in the Piper diagram at Site C2

(Fig. 4.8) or at any of the other saline sites (Fig. 4.5 to 4.7). Stein (1987) has shown by geochemical modelling, however, that saline, shallow groundwaters may result from mixing and evaporation of shallow drift and bedrock groundwaters. Wallick (1981) suggested that because of groundwater movement induced by post-glacial hummocky topography, water from drift aquifers mixed with water from deep bedrock aquifers in discharge areas. This resulted in mixed groundwaters with a range of intermediate compositions.

The ion facies of the soil saturation extracts were Ca + Mg, Na - SO_4 at Sites A1 and B3; Na, Ca + Mg - HCO_3, SO_4 and Ca + Mg, Na - HCO_3, SO_4 at Site A3; and Ca + Mg, Na - HCO_3, SO_4 and Na, Ca + Mg - SO_4 at Site C2. Five other saline and Solonetzic soils in the study area exhibited Na, Ca + Mg - SO_4 ion facies (Appendix 6.7). The facies classification scheme outlined by Back (1961) was used in this study.

If it could be assumed that these saline soils were saturated and connected to the underlying groundwater flow system when discharge of salts occurred, then a comparison of the anion facies can be made to the Chebotarev (1955) sequence to reveal if the anions reflected local, intermediate or regional groundwater flow. The anion facies of saline soils was either HCO_3, SO_4 or SO_4. This inferred local or intermediate flow systems in this study area.

The ion facies of all groundwater samples taken from the drift were plotted on one Piper diagram (Appendix 6.7). All groundwaters plotted within the SO_4, HCO_3 or SO_4 anion facies,

but exhibited variable cation facies. Groundwater from the bedrock of the A- and B-Lines (Appendix 6.7) showed a trend of plotting mainly within the Na cation facies; however, some waters plotted within the Na, Ca + Mg and Ca + Mg, Na facies. The anion facies of the bedrock were mainly of the HCO_3, SO_4 or SO_4, HCO_3 type. Groundwaters from the bedrock at Sites C1 and C2 (Appendix 6.7) were generally dominated by Na or Na, Ca + Mg cation facies, and SO_4, HCO_3 or SO_4 anion facies.

The ion facies of the soil saturation extracts were most similar to the ion facies of the groundwater from the drift at Sites A1, A3, and B3 (Fig. 4.5 to 4.7). This implicated the drift deposits as the major source of soluble salts contributing to soil salinity at these sites. In contrast, the ion facies of the soil saturation extracts were similar to both the ion facies of the drift and bedrock at Site C2 (Fig. 4.8). This suggested that the drift and/or bedrock were possible sources of salt contributing to soil salinity at this site. In addition, the groundwater in this study area did not evolve to the Cl, SO_4 or Cl anion facies which is characteristic of deep, regional groundwater flow systems. Local and/or intermediate flow systems probably dominated in this area. Stein (1987) reported similar trends in the ion facies of drift and bedrock groundwaters.

4.3.3 Hydrochemistry of the Groundwater

The concentrations of the major ions (Na, Ca, Mg, SO_4, HCO_3 and Cl) in the groundwaters from water table wells and

piezometers along the A-, B- and C-Lines were plotted on Stiff diagrams to ascertain the distribution patterns of the ions and to possibly reveal information regarding potential source areas of salts. These results are shown in Figs. 4.9, 4.10 and 4.11.

A common trend observed in all three sections was an increase in the quantities of soluble salts in the groundwater with a decline in site elevation. In contrast, Sommerfeldt and Mackay (1982) found no such trend in the same study area and attributed this condition to poor lateral continuity of the groundwater from high to low elevations. Maclean (1974) found that both TDS and Na + K increased with a decline in site elevation and attributed this to an increase in the length of flow paths and/or time of contact between water and rock.

On the C-Line cross-section (Fig. 4.9), the patterns of the Stiff diagrams showed that the most likely sources of groundwater contributing to high Na and SO_4 ion concentrations (Na = 118.6; SO_4 = 130.1 mmole ($\pm$) L^{-1}) at the saline seep (Site C2) were from shallow groundwaters (6 - 10 m) at Site C2, and from saline groundwaters at the 24 to 35 m depth at Site C1. These groundwaters typically had high concentrations of Na (78.7 - 138.0 mmole ($\pm$) L^{-1}) and SO_4 (76.5 - 129.1 mmole ($\pm$) L^{-1}) ions. Groundwaters at Site B2 had low concentrations of all ions, indicating slight mineralization of the groundwater. The relatively non-saline (2.0 - 2.7 dS m^{-1}) groundwater here would have contributed little to salinity downslope at Site C2.

The Stiff diagrams along the C-Line illustrated that the excess salts at the saline seep were most likely derived from very short distances away and from relatively shallow depths. Because Site C1 was a local recharge area and the shallow groundwater here was highly saline (7.8 - 11.8 dS m^{-1}), the evidence pointed to this site as a likely source of salinity. Local groundwater flow was also indicated by the flow net of the C-Line section (Fig. 3.3). Stein (1987) reported that the majority of dissolved salts within the groundwater flow region of a local investigation were generated and transported within the shallow region less than 30 m below the water table. In addition, generation of SO_4 was found to have occurred over very short distances of vertical travel.

Along the A-Line section (Fig. 4.10), there was a noticeable trend of highest concentrations of ions occurring in the shallowest piezometers. Relatively low ion concentrations were found in deeper groundwaters, especially in the deeper piezometers at and between Sites A4 and A6. Similar findings in this study area were previously reported by Sommerfeldt and Mackay (1982); however, they also found that some groundwaters with high EC values were sandwiched between waters of low EC. In contrast, Wallick (1981) found an increase in TDS of groundwaters with increasing depth from drift to bedrock in east-central Alberta. Maclean (1974) reported that shallow groundwaters in the drift within the upper study area near Vegreville, Alberta, had the highest TDS values.

The shallowest piezometer at Site A1 (9 m) exhibited the highest Na (222.8 mmole ($\pm$) L^{-1}) and SO_4 (251.3 mmole ($\pm$) L^{-1}) concentrations of all groundwaters sampled in this study. The most probable source of the high Na and SO_4 salts causing soil salinity at Site A1 was the saline (EC = 9.2 dS m^{-1}) groundwater at the 14 m depth (shallowest piezometer) at the adjacent Site A2. Groundwater flow modelling indicated that the most likely source of excess water at Site A1 was from shallow groundwater flow through the drift or upper weathered bedrock zone, within 15 to 17 m of the soil surface. These previous findings agreed with the hydrochemical evidence presented here. The soil salinity at Site A1 was attributed to the highly saline groundwater in the upper, weathered bedrock.

At Site A3, the [illegible] diagrams showed that the most probable source of salts was the saline (EC = 6.8 dS m^{-1}) groundwater just below the water table. Previous work has revealed strong artesian discharge from depth (30 and 69 m) below this site. The groundwater in the piezometers at 30 m and 69 m at Site A3, however, contained relatively low concentrations of soluble ions (EC = 3.4 and 3.1 dS m^{-1}, respectively). Therefore, the source of the excess salts at Site A3 was probably from the shallow drift and/or upper weathered bedrock. Repeated cycles of leaching of salts from the soil following wet periods, and upward flow gradients induced by evapotranspiration during dry periods, may also partially explain the high salinity of the shallow groundwater in the closed basin at Site A3.

The soil salinity downslope from Site A5 also appeared to be caused by shallow groundwater. These saline (EC > 6.3 dS m^{-1}) groundwaters exhibited relatively high concentrations of Na and SO_4 (> 50 mmole (±) L^{-1}). In contrast, the deeper groundwaters had relatively low quantities of Na and SO_4 ions (<50 mmole (±) L^{-1}). These deeper waters of low salinity (EC <4 dS m^{-1}) formed an extensive zone from below Site A4 to Site A6. This area was therefore characterized by a shallow groundwater zone of high salinity, and a deeper zone of low salinity.

On the B-Line section (Fig. 4.11), shallow groundwater typically had the highest concentrations of Na and SO_4 ions. This was evident by highly saline (EC = 10.8 dS m^{-1}) water from the shallowest piezometer (6 m), in a permeable sandstone aquifer at Site B3.

Significant Ca + Mg concentrations (> 20 mmole (±) L^{-1}) were also present in these groundwaters. The Ca + Mg in the sandstone aquifer at Site B3 may be indicative of fracture flow. Stein (1987) proposed that significant Ca + Mg in groundwater of the upper bedrock zone was caused by fracture-dominated flow because such flow would result in restricted cation exchange processes that deplete Ca + Mg and increase Na in the groundwater. Skarie et al. (1987) found that Ca concentrations of sulfatic groundwaters and soil saturation extracts were limited to the solubility of gypsum in water (28 mmol (±) L^{-1}). In contrast, it was likely that the Ca + Mg found in the lacustrine material (Site B1) reflected the higher salt reservoir of these cations in the

drift. Similar findings have been previously reported (Maclean 1974; Wallick 1981; Stein 1987).

The source of the soil salinity at Site B3 was probably from the permeable sandstone aquifer at 6 m below the soil surface. The groundwater at this depth had considerable quantities of both Na and SO_4 ions (107.3 and 153.5 mmole ($\pm$) L^{-1}, respectively). In addition, the groundwater at the 16 m depth also had significant concentrations of Na and SO_4 ions (94.5 and 60.3 mmole ($\pm$) L^{-1}, respectively).

In summary, shallow groundwater in the drift and/or upper bedrock constituted the main salt reservoir for Na and SO_4 ions. Deeper bedrock groundwaters typically had much lower ion concentrations.

4.3.4 Soluble-Salt Profiles in Recharge and Discharge Areas

The concentrations of the major ions in 1:5 (soil:water) or saturation paste extracts were plotted versus depth for three sites located in recharge areas (Sites A2, B2 and C1), and for three sites located in discharge areas (Sites A1, A3 and C2). The results are shown in Figs. 4.12 to 4.17. The following trends were observed:

1) Leaching of soluble salts from the upper profiles of two of the three recharge sites (Sites B2 and C1) was indicated by an increase in salts with depth (Fig. 4.13, 4.14). Slight leaching was only evident at Site A2 (Fig. 4.12).
2) Redistribution of soluble salts to the saline soils at two

discharge sites (Sites A3 and C2) was reflected by maximum soluble salt accumulations within 3 m of the soil surface (Fig. 4.16, 4.17). At Site A1, redistribution of salts towards the soil surface was indicated by an increase in soluble salts with decreasing depth to a maximum at the 6.1 to 9.1 m depth (Fig. 4.15).

3) The highest concentrations of Ca + Mg ions were typically found within 10 to 20 m of the soil surface. The salt reservoir of Ca + Mg generally coincided with the presence of drift.
4) Concentrations of Na were extremely variable; however, low concentrations often correlated with drift and higher concentrations with bedrock. The exception was Site C2 where concentrations of Na were highest in the drift.
5) Concentrations of SO_4 ions were usually highest within 10 to 20 m of the ground surface.
6) Concentrations of HCO_3 were low at shallow depths (< 10 - 20 m), whereas higher concentrations were found at greater depths in the bedrock. A decrease in SO_4 and increase in HCO_3 in the deeper bedrock was probably due to sulfate reduction.
7) Concentrations of Cl were low and relatively constant at all sites (Cl ion salt profiles shown only for Sites C1 and C2).

The observed trends in the six salt profiles were used to ascertain potential sources of the soluble salts in the three saline soils or discharge areas. The assumption was made that the maximum accumulations of soluble salts near the soil surface at Sites C2, A1 and A3 represented salts that had been redistributed

by groundwater flow. This assumption seemed reasonable considering that the shape of the salt profiles reflected discharge conditions.

Cation concentrations in the salt accumulation layer near the soil surface at Site C2 were higher in Na compared to Ca + Mg (Fig. 4.17). This suggested a bedrock source of Na. Previous workers have reported that high Na concentrations indicated a bedrock source for this cation (Eilers 1973; Maclean 1974; Pawluk 1982; Stein 1987). Wallick (1981) found that high Na concentrations in groundwaters were only found in deeper drift and bedrock at depths greater than 30 m. In contrast, the high concentrations of SO_4 near the soil surface at Site C2 suggested a shallow source for SO_4. The salt profile therefore implicated both shallow drift and/or deeper bedrock as possible sources of salt.

Other evidence found in this study also supported both a shallow and deeper source of salts at Site C2. A shallow gravel layer (2.5 m) at a local recharge area (Site C1) just upslope from the saline seep at Site C2 was found to possibly have been conducting soil water laterally to the seep. As shown in the salt profile at Site C1 (Fig. 4.14), the soluble salts above 2.5 m were depleted. Soluble salts leached from the drift, above the gravel layer at Site C1, would then be transported laterally via the gravel layer to the seep at Site C2. The small but significant concentrations of Ca + Mg and high SO_4 values near the soil surface at Site C2 may have reflected such a process because these ions are typically found in greatest quantities in shallow drift deposits. Ferguson and Bateridge (1982) have reported considerable

leaching of soluble salts from drift deposits and attributed this phenomenon to the practice of grain-fallow farming. This was the farming practice in use at Site C1. The isotope and hydrochemical data of the groundwater also pointed to a shallow source of salts from within 10 m of the soil surface.

In contrast, groundwater flow modelling revealed that groundwater was discharged from two confined sandstone aquifers (at 6 and 12 m depths) below Site C2. A high concentration of soluble salts between 7.6 and 9.1 m (Fig. 4.17), and artesian discharge from the sandstone aquifer at 12 m, suggested that the 7.6 to 9.1 m depth may have been a major salt reservoir. The groundwater at 10 m, however, was already considerably mineralized before the water passed upwards through the shallower salt accumulation layer (7.6 to 9.1 m). Therefore, groundwater discharged from the sandstone aquifer at 12 m was already saline, and salts may have originated from somewhere else.

The cation concentration in the salt accumulation layer near the soil surface at Site A3 had higher concentrations of Ca + Mg relative to Na (Fig. 4.16). This suggested a shallow source of salts. Further evidence was the high concentrations of SO_4 in this layer. The isotope data also pointed to a shallow source of salts (< 5.5 m). The isotope data, however, also showed that another possible source of salinity was from a sandstone aquifer at 30 m. Hydraulic heads in the piezometers at 30 and 69 m were both above the water table level. This reflected strong artesian discharge from these two depths. Although the groundwater was

relatively non-saline at 30 m (EC = 3.4 dS m^{-1}), the ^{18}O (SO_4) value here showed a genetic connection to similar values in the soil. Groundwater at 69 m was also low in soluble salts (EC = 3.1 dS m^{-1}). Similar EC values between 30 and 69 m indicated little mineralization of the groundwater as it ascended between these two depths.

Over a long period of time, however, even groundwaters that contain relatively low concentrations of soluble salts may contribute significant quantities of soluble salts to the soil surface. The rate of salt flux to the water table from 30 and 69 m at Site A3, and the time required for soil salinization, was calculated to investigate this hypothesis. The equation utilized by Stein (1987) was used to calculate the salt flux at Site A3. This equation is:

$$Q_s = \frac{3.16 \times 10^7 \, \Delta h \, (TDS)}{\sum d_i/k_i} \qquad (3)$$

where Q_s is the salt flux in kg $yr^{-1}m^{-2}$, Δh is the head loss (m) across thickness d (m), TDS is the total dissolved solids (kg m^{-3}) of the source water, d_i is the thickness of each individual layer (m), and k_i is the hydraulic conductivity (m s^{-1}) of each individual layer.

The head loss (Δh) was 0.9 and 0.1 m at 69 and 30 m, respectively. The TDS values were 1.9 kg m^{-3} and 2.2 kg m^{-3} at 69 and 30 m, respectively. The vertical k_i values used for the various layers ranged from 10^{-7} to 10^{-9} to 10^{-11} m s^{-1} for weathered and non-weathered interbedded shale and sandstone, and

10^{-9} m s^{-1} for sandstone layers. The salt fluxes calculated for the 69 and 30 m depth using equation 3 were 2.53 x 10^{-5} and 1.02 x 10^{-4} kg yr^{-1} m^{-2}, respectively. These were extremely low fluxes. Stein (1987) reported salt flux values that ranged from 0.03 to 2.4 kg yr^{-1} m^{-2}. The low vertical hydraulic conductivity values of the layers at this site were mainly responsible for the low fluxes determined here.

Because groundwater under such strong artesian pressure may ascend through fracture-dominated flow, this process was assumed to have occurred at Site A3, and the vertical k_i values of the entire stratigraphic column were increased to a value of 10^{-7} m s^{-1}. This value was typical for fractured bedrock in this area. Assuming fracture-dominated flow, the recalculated salt fluxes were 0.08 and 0.02 kg yr^{-1} m^{-2} at 69 and 30 m, respectively. These salt fluxes are considerably higher than those values found for non-fracture flow. This indicated the strong dependency of salt fluxes on the hydraulic conductivity of the individual layers in the stratigraphic column. Stein (1987) noted that where low K geologic layers were absent in areas of upward flow, salinity often developed.

The time required to salinize the upper 1 m depth above the water table at Site A3, to an EC of 4 dS m^{-1}, was also calculated. Chang et al. (1983) found the following relationship between TDS (mg L^{-1}) and EC (dS m^{-1}):

$$TDS = 765.1\ EC^{1.08} \qquad (4)$$

Use of this equation yielded a TDS value of approximately 3,450 mg L^{-1} (3.45 kg m^{-2}) for an EC of 4 dS m^{-1}. The time required to obtain this salt load (using the initial salt fluxes for non-fracture flow), was determined to be about 1.4 x 10^5 and 3.4 x 10^4 years at the 69 and 30 m depths, respectively; and about 44 and 150 years at the 69 and 30 m depths, respectively (using salt fluxes for fracture-flow). Stein (1987) determined various salt flux values and calculated that 1.5 to 480 years were required for soil salinization to an EC of 4 dS m^{-1}. Henry et al. (1985) calculated that observed salt loads for three sites in Saskatchewan could accumulate in time periods from 500 to 5,300 years.

Previous calculations, assuming fracture-flow, showed that the groundwater at 69 m could contribute the highest salt load, and in a shorter period of time, than groundwater from 30 m. This was probably due to the greater head loss at 69 m (0.9 m) compared to 30 m (0.1 m). Although much of the evidence pointed to a shallow source of salts at Site A3 (< 5.5 m or from 30 m), calculations that assumed fracture flow continuity from 69 m revealed that, over time (44 years), salts could accumulate to significant levels (4 dS m^{-1}) in this soil.

The cation concentration in the salt accumulation layer (3.1 - 15.2 m) at Site A1 was highest in Na relative to Ca and Mg (Fig. 4.15). This suggested a major contribution of salts from the bedrock. Significant quantities of Ca + Mg cations, and high SO_4 concentrations, however, pointed to a shallow source. Isotopic

data, groundwater flow modelling and hydrochemistry results revealed that shallow groundwater was most likely dissolving salts as water moved laterally through the upper weathered bedrock zone within 15 to 17 m of the soil surface. Ponding of surface runoff by a railroad track located between Sites A1 and A2, and subsequent lateral flow in the drift, may have also been a contributing factor to soil salinity at Site A1. No upward hydraulic head gradients were found in the piezometers below this site. Therefore, the source of salts at Site A1 appeared to be from shallow depths (< 20 m).

4.3.5 Bromine and Iodine Content of Groundwaters

The halogens Br and I have been suggested as possible indicators of a deep origin of soil salinity. These two elements are typically found in high concentrations in formation waters of the western Canada sedimentary basin (Billings et al. 1969), particularly in association with oil and gas fields, and in association with Devonian salt deposits (Br only) (van Everdingen 1968; Hitchon et al. 1971). Billings et al. (1969) cited mean concentrations for Br and I of 292 and 15 mg L^{-1}, respectively, in formation waters. Hitchon et al. (1971) found that for five samples of formation waters from the Upper Cretaceous bedrock of Alberta, Br and I concentrations ranged from 13 to 92, and 4 to 39 mg L^{-1}, respectively. In addition, these same authors reported that 34 water samples from the Upper Devonian Formation had Br and I concentrations that ranged from 20 to 1,120 and 1 to 30 mg L^{-1}, respectively.

The Br and I contents of groundwaters sampled in this study are reported in Table 4.4. The concentrations of both Br and I were extremely low or non-detectable in all but one sample (B2-91). The detection limits of Br and I were 0.05 and 0.005 ppm, respectively. Surprisingly, the one sample that had significant concentrations of Br (9.7 ppm) and I (5.1 ppm) was from groundwater at a depth of 91 m below Site B2. This site was located at the groundwater divide on a large bedrock ridge, and groundwater flow beneath this site was downward. If Br and/or I were ascending from oilfield brines or formation waters derived from the Devonian formation, then the accumulations of these halogens would have been expected in discharge basins such as Keho or Studhorse Lake. This, however, was not the case. This was noteworthy because the Keho Lake basin is a major oilfield area; and strong artesian discharge was evident from the 69 m depth adjacent to Studhorse Lake. The Br and I data inferred a shallow source of salts affecting the saline soils in this study basin. Previous data seemed to substantiate this.

4.4 SUMMARY AND CONCLUSIONS

Similar $\delta^{34}S$ (SO_4) values between drift and bedrock deposits, but different $\delta^{18}O$ (SO_4) values, indicated that the latter isotope may be a useful tool in identifying the source of salts causing soil salinization. Mean $\delta^{18}O$ (SO_4) values of

soil, drift and bedrock, however, were not as useful as plotting the isotope values versus depth. This was because $\delta^{18}O$ (SO_4) values may vary significantly within these three deposits.

Plots of $\delta^{34}S$ versus $\delta^{18}O$ of SO_4 showed definite trends. Soil, drift and bedrock soluble-sulfates and evaporite crystal sulfates plotted in defined regions on the scatter diagram. A slight linear behavior of the soil and drift values was evident. Mixing, crystallization of sulfate minerals, and sulfate reduction were proposed as three possible mechanisms contributing to the linear behavior. Calculations of the theoretical $\delta^{18}O$ values of soil sulfates using an equation for mixing, revealed that mixing of shallow drift and deeper sources of salt may have contributed to the observed $\delta^{18}O$ values for soil sulfates. Sulfate reduction was indicated by $\delta^{34}S$ (SO_4) values close to or above 0‰. Enrichment of $\delta^{18}O$ (SO_4) of evaporite crystals relative to soluble-sulfates from similar depths was observed. This was attributed to the crystallization process and/or to bedrock sources that exhibited similar $\delta^{18}O$ (SO_4) values.

The ion facies of soil saturation paste extracts were compared to the ion facies of drift and bedrock groundwaters to ascertain possible source areas of salt. The soil and drift anion facies were mainly of the SO_4, HCO_3 or SO_4 type (variable cation facies); whereas bedrock groundwaters were mainly of the Na or Na, Ca + Mg cation facies (variable anion facies). Mixing of bedrock and drift groundwaters was not indicated on the Piper diagrams. The SO_4, HCO_3 or SO_4 anion facies of soil saturation extracts

suggested that, according to the Chebotarev sequence, these anions were redistributed by local or intermediate groundwater flow systems. Generally, the ion facies of soil saturation extracts were most similar to the ion facies of groundwater from the drift. This suggested a shallow origin of salinity.

The concentrations of soluble salts in the groundwaters were plotted on Stiff diagrams. Excess salts at saline seeps were most likely generated from very short distances away and from relatively shallow depths. The shallow groundwater in the drift and/or upper bedrock contributed the main salt reservoir for Na and SO_4 ions. Deeper groundwaters had much lower concentrations of these ions.

The soluble-salt profiles of 1:5 (soil:water) and saturation paste extracts showed leaching of near-surface salts in recharge areas, and accumulations of salts in discharge areas. High concentrations of Ca, Mg and SO_4 ions were found mainly within 10 to 20 m of the soil surface. The Na content was variable, but typically increased in the bedrock. The HCO_3 ion content increased with depth, and Cl contents were low and relatively constant. High Ca + Mg and SO_4 ion concentrations in the drift, and high Na ion contents in the bedrock, were used as possible indicators of the sources of salts.

Calculations of salt fluxes from the 30 and 69 m depth at Site A3 showed that, because of the low vertical hydraulic conductivities of various aquitards, salt fluxes would be extremely low (10^{-4} - 10^{-5} kg yr^{-1} m^{-2}), and soil salinization would

take a very long time (10^4 to 10^5 years). By assuming fracture-dominated flow, however, significant quantities of salts (0.08 - 0.02 kg yr^{-1} m^{-2}) may be transported from the deeper bedrock in relatively short periods of time (44 to 150 years).

All the evidence presented in this paper was considered in trying to identify possible sources of salt at Sites A3, A1 and C2. The source of salinity at Sites A1 and C2 was drift and/or bedrock from shallow depths (< 20 m); whereas the source of salinity at Site A3 was the drift and/or bedrock, at depths $\leq$ 69 m from the soil surface. Low or non-detectable Br and I contents in the groundwaters of this study area inferred the absence of any contribution from deep groundwater flow. This suggested that shallow flow systems were dominant in this area.

4.5 BIBLIOGRAPHY

ADRIANO, D.C. and DONER, M.E. 1982. Bromine, chlorine and fluorine. p. 449-479. In A.L. Page (ed.) Methods of soil analysis. Agronomy 9. Am. Soc. Agron., Madison, Wis.

AMERICAN PUBLIC HEALTH ASSOCIATION. 1980. Standard methods for the examination of water and wastewater. Method 4260: automated methylthymol blue method. 15th ed. APHA-AWWA-WPCF, Washington, D.C.

BACK, W. 1961. Techniques for mapping of hydrochemical facies. U.S. Geol. Surv. Prof. Paper 424-D, p. 380-382.

BILLINGS, G.K., HITCHON, B. and SHAW, D.R. 1969. Geochemistry and origin of formation waters in the western Canada sedimentary basin, 2. Alkali metals. Chem. Geol. 4: 211-223.

BOWER, A.A. and WILCOX, L.V. 1965. Soluble salts. p. 933-951. In C.A. Black (ed.) Methods of soil analysis. Agronomy 9 (2). Am. Soc. Agron., Madison, Wis.

BUYLOV, V.V. 1976. Sodium-carbonate salinization of soils and groundwaters. Soviet Soil Sci. 229(2): 465-468.

CHANG, P.C. and VAN SCHAIK, J.C. 1965. Automated method for soil salinity studies. p. 94-95. In Automation in analytical chemistry. Technicon Symposia. Ardsley (Chauncey), N.Y.

CHANG, C, SOMMERFELDT, T.G., CAREFOOT, J.M. and SCHAALJE, G.B. 1983. Relationships of electrical conductivity with total dissolved salts and cation concentration of sulfate-dominated soil extracts. Can. J. Soil Sci. 63: 79-86.

CHEBOTAREV, I.I. 1955. Metamorphism of natural waters in the crust of weathering. Geochim. Cosmochim. Acta. 8: 22-212.

EILERS, R.G. 1973. Relations between hydrogeology and soil characteristics near Deloraine, Manitoba. Unpubl. M.Sc. Thesis, Soil Science Dept., Univ. of Manitoba, Winnipeg, Man. 202 pp.

FERGUSON, H. and BATERIDGE, T. 1982. Salt status of glacial till soils of north-central Montana as affected by the crop-fallow system of dryland farming. Soil Sci. Soc. Am. J. 46: 807-810.

GREENLEE, G.M., PAWLUK, S. and BOWSER, W.E. 1968. Occurrence of soil salinity in drylands of southwestern Alberta. Can. J. Soil Sci. 48: 65–75.

HENDRY, M.J. CHERRY, J.A. and WALLICK, E.I. 1986. Origin and distribution of sulfate in a fractured till in southern Alberta, Canada. Water Resour. Res. 22(1): 45–61.

HENDRY, M.J. and KROUSE, H.R. 1987. A technique to identify source areas of groundwater causing saline seeps. Alberta Soil Science Workshop, Calgary, Alberta. p. 164-169.

HENDRY, M.J. and SCHWARTZ, F. 1982. Hydrogeology of saline seeps. First Annual Western Provincial Conference on Rationalization of Water and Soil Research and Management: Soil Salinity. Province of Alberta, Lethbridge, Alberta, 29 Nov. - 2 Dec. p. 164–169.

HENRY, J.L., BULLOCK, P.R., HOGG, T.J. and LUBA, L.D. 1985. Groundwater discharge from glacial and bedrock aquifers as a soil salinization factor in Saskatchewan. Can. J. Soil Sci. 65(4): 749–768.

HITCHON, B., BILLINGS, G.K. and KLOVAN, J.E. 1971. Geochemistry and origin of formation waters in the western Canada sedimentary basin. III. Factors controlling chemical composition. Geochim. Cosmochim. Acta. 35: 567-598.

HOLSER, W.T., KAPLAN, I.R., SAKAI, H. and ZAK, I. 1979. Isotope geochemistry of oxygen in the sedimentary sulphate cycle. Chem. Geol. 25: 1-7.

KOVDA, V.A., BUYLOV, V.V. and RYSKOV, Y.G. 1980. The role of underground pressure water in landscape salinization. Proc. of Int. Symp. on Salt-Affected soils. Karnal, India, 18-21 Feb.

LLOYD, R.M. 1967. Oxygen-18 composition of oceanic sulphate. Science 156: 1228-1231.

LLOYD, R.M. 1967. Oxygen isotope behaviour in the sulfate water system. J. Geophys. Res. 73: 6099-6110.

MACLEAN, A.H. 1974. Soil genesis in relation to groundwater and soil moisture regimes near Vegreville, Alberta. Ph.D. Thesis, Dept. of Soil Science, Univ. of Alberta, Edmonton, Alberta. 229 pp.

MILLER, M.R., BROWN, P.L., DONOVAN, J.J., BERGATINO, R.N., SONDEREGGER, J.L. and SCHMIDT, F.A. 1981. Saline seep development and control in the North American Great Plains - hydrogeological aspects. Agri. Water Management 4: 115-141.

MIZUTANI, Y. and RAFTER, T.A. 1969. Oxygen isotopic composition of sulfates, 3, Oxygen isotopic fractionation in the bisulfate ion-water system. N.Z. J. Sci. 12: 54-59.

PAWLUK, S. 1982. Salinization and solonetzic formation. Proc. 19th Annual Alberta Soil Sci. Workshop, Edmonton, Alberta. p. 1-24.

PIPER, A.M. 1944. A graphic procedure in the geochemical interpretation of water-analyses. Am. Geophys. Union Trans. 25: 914-923.

RHOADES, J.D. 1982. Soluble salts. p. 167-179. In A.L. Page (ed.) Methods of soil analysis. Agronomy 9 (2). Am. Soc. Agron., Madison, Wis.

SHAKUR. M.A. 1982. ^{34}S and ^{18}O variations in terrestrial sulfates. Ph.D. Thesis. Dept. of Physics, Univ. of Calgary, Calgary, Alberta. 229 pp.

SKARIE, R.L., RICHARDSON, J.L., McCARTHY, G.J. and MAIANU, A. 1987. Evaporite mineralogy and groundwater chemistry associated with saline soils in Eastern North Dakota. Soil Sci. Soc. Am. J. 51: 1372-1377.

SOMMERFELDT, T.G. and MacKAY, D.C. 1982. Dryland salinity in a closed drainage basin at Nobleford, Alberta. J. Hydrol. 55: 25-41.

STEIN, R. 1987. A hydrogeological investigation of the origin of saline soils at Blackspring Ridge, southern Alberta. Unpubl. M.Sc. Thesis. Dept. of Geology, Univ. of Alberta, Edmonton, Alberta. 272 pp.

THODE, H.G. and MONSTER, J. 1965. Sulfur isotope geochemistry of petroleum, evaporites, and ancient seas. p. 367-377. In A. Young and J.E. Galley (eds.) Fluids in subsurface environments. Vol. 4. AAPG Memoirs.

VAN EVERDINGEN, R.O. 1968. Studies of formation waters in western Canada: geochemistry and hydrodynamics. Can. J. Earth Sci. 5: 523-543.

WALLICK, E.I. 1981. Chemical evolution of groundwater in a drainage basin of Holocene age, east-central Alberta, Canada. J. Hydrol. 54: 245-283.

Table 4.1. Sulfur and oxygen isotopic composition of soluble sulfates, evaporite crystals, and groundwaters from the soil, drift, and bedrock deposits at Site A3.

Depth (m) or depth and piezometer	Sulfate form	SO_4 Ion Conc. mmole (-) / L	$\delta^{34}S$ (SO_4) (CDT)	$\delta^{18}O$ (SO_4) (SMOW)	$\delta^{18}O$ (H_2O) (SMOW)
			Per mil		
Soil					
0 - 0.13	evap. crystal		-1.07	7.6	-
0 - 0.13	soluble sulfate	6.5 (s)	-2.03	-5.4	-
0.13 - 0.27	soluble sulfate	4.4 (s)	-1.44	-6.8	-
Mean			-1.74	-6.1	-
Glacial					
1.60 - 1.80	evap. crystal		-2.54	16.6	
3.05 - 6.1	soluble sulfate	7.5 (5)	-0.47	-9.0	-
5 (A3 - 5w)	soluble sulfate	68.1 (g)	1.23	-7.5	-21.5
Mean			0.38	-8.3	-21.5
Bedrock					
6.1 - 9.1	soluble sulfate (Sh/SS)	2.2 (5)	1.66	6.2	-
27.4 - 30.5	soluble sulfate (SS)	3.1 (5)	0.90	5.3	-
30 (A3 - 30)	soluble sulfate (SS)	22.6 (g)	-0.39	-8.5	-19.5
67.1 - 70.1	soluble sulfate (Sh)	3.1 (5)	1.25	7.6	-
69 (A3 - 69)	soluble sulfate (Sh)	12.0 (g)	-0.09	0.8	-15.3
Mean			0.67	3.5	-17.4

Sh/SS = Shale/Sandstone; SS = Sandstone; Sh = Shale
s = saturation paste extract; g = groundwater; 5 = 1:5(soil:water) extract

Table 4.2. Sulfur and oxygen isotopic composition of soluble sulfates, evaporite crystals, and groundwaters from the soil, drift, and bedrock deposits at Site C2.

Depth (m) or depth and piezometer	Sulfate form	SO_4 Ion Conc. mmole (-) / L	$\delta^{34}S$ (SO_4) (CDT)	$\delta^{18}O$ (SO_4) (SMOW)	$\delta^{18}O$ (H_2O) (SMOW)
				Per mil	
Soil					
0 - 0.07	evap. crystal		1.60	14.0	-
0.07 - 0.13	soluble sulfate	355.8 (s)	1.53	-3.8	-
0.13 - 0.24	soluble sulfate	492.0 (s)	1.03	-3.8	-
Mean			1.39	-3.8	-
Glacial					
1.60 - 1.75	soluble sulfate	113.4 (s)	1.06	-7.6	-
1.80 - 2.00	evap. crystal		-1.85	2.6	-
3 (C2 - 3w)	soluble sulfate	130.1 (g)	1.11	-7.5	-19.4
Mean			0.11	-7.6	-19.4
Bedrock					
3.7 - 4.0	soluble sulfate (SiS)	35.8 (5)	1.11	-7.5	-
7 (C2 - 7)	soluble sulfate (Sh)	126.6 (g)	0.94	-8.6	-18.9
10 (C2 - 10)	soluble sulfate (Sh/C)	105.0 (g)	0.81	-10.8	-19.7
10.1 - 10.7	soluble sulfate (Sh/C)	23.1 (5)	0.09	11.1	-
28.3 - 30.0	soluble sulfate (SS)	18.5 (5)	1.60	8.5	-
30 (C2 - 30a)	soluble sulfate (SS)	35.9 (g)	7.62	0.1	-19.4
Mean			2.03	-1.2	-19.3

SiS = Siltstone; Sh = Shale; Sh/C = Shale/Coal; SS = Sandstone
s = saturation paste extract; g = groundwater; 5 = 1:5(soil:water) extract

Table 4.3. Sulfur and oxygen isotopic composition of soluble sulfates, evaporite crystals, and groundwaters from the soil, drift, and bedrock deposits at Site A1.

Depth (m) or depth and piezometer	Sulfate form	SO_4 Ion Conc. mmole (-) / L	$\delta^{34}S$ (SO_4) (CDT)	$\delta^{18}O$ (SO_4)	$\delta^{18}O$ (H_2O)
				— (SMOW) —	
				Per mil	
Soil					
0 - 0.15	soluble sulfate	58.0 (s)	-1.98	-8.8	-
0.15 - 0.30	soluble sulfate	73.7 (s)	-3.13	-8.9	-
Mean			-2.56	-8.9	-
Glacial					
1.80 - 2.00	evap. crystal		1.86	11.5	-
Mean			1.86	11.5	-
Bedrock					
3.10 - 6.10	soluble sulfate (Sh)	11.9 (5)	0.01	-5.3	-
9 (A1 - 9)	soluble sulfate (SS)	251.3 (g)	2.02	-6.5	-18.5
21.3 - 24.4	soluble sulfate (SS/Sh)	7.4 (5)	-0.60	N. S.	-
24 (A1 - 24)	soluble sulfate (Sh)	10.6 (g)	2.97	9.8	-20.0
76 (A1 - 76)	soluble sulfate (Sh)	43.7 (g)	0.47	-2.1	-16.0
Mean			0.97	-1.0	-18.2

Sh=Shale; SS=Sandstone; SS/Sh=Sandstone/Shale
s=saturation paste extract; g=groundwater; 5=1:5(soil:water) extract

Table 4.4. Bromine and iodine concentrations of groundwaters in the Nobleford study area.

Piezometer or Well	Bromine (ppm)	Iodine (ppm)
A1 – 9	0.41	< 0.005
A1 – 76	0.11	0.041
A2 – 24	< 0.05	0.007
A2 – 42	< 0.05	< 0.005
A2 – 84	0.06	0.022
A3 – 5W	0.05	< 0.005
A3 – 30	< 0.05	< 0.005
A3 – 69	0.05	0.005
A4 – 20	< 0.05	0.005
A4 – 56	0.06	< 0.005
A4 – 99	< 0.05	0.006
B2 – 34	0.07	< 0.005
B2 – 63	0.07	0.011
B2 – 91	9.7	5.1
B3 – 6	0.06	0.018
B3 – 16	< 0.05	< 0.005
C1 – 3W	< 0.05	< 0.005
C1 – 7	< 0.05	0.005
C1 – 10	< 0.05	< 0.005
C1 – 25	< 0.05	< 0.005
C1 – 30a	0.05	< 0.005
C 1 35 a	< 0.05	< 0.005

Figure 4.1. Sulfur and oxygen isotopic composition of soluble-sulfates in relation to depth (.) at Site A3.

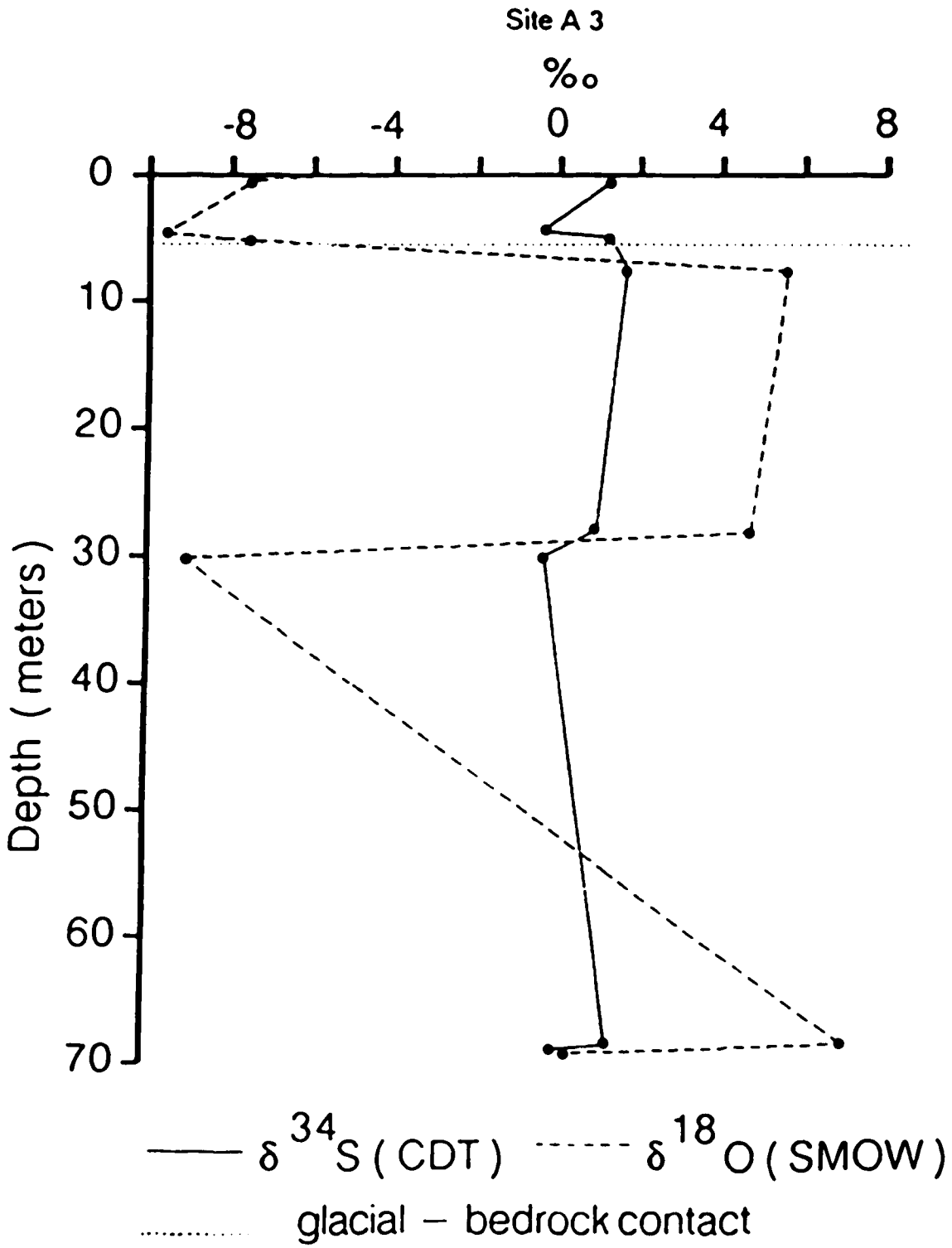

Figure 4.2. Sulfur and oxygen isotopic composition of soluble-sulfates in relation to depth (m) at Site C2.

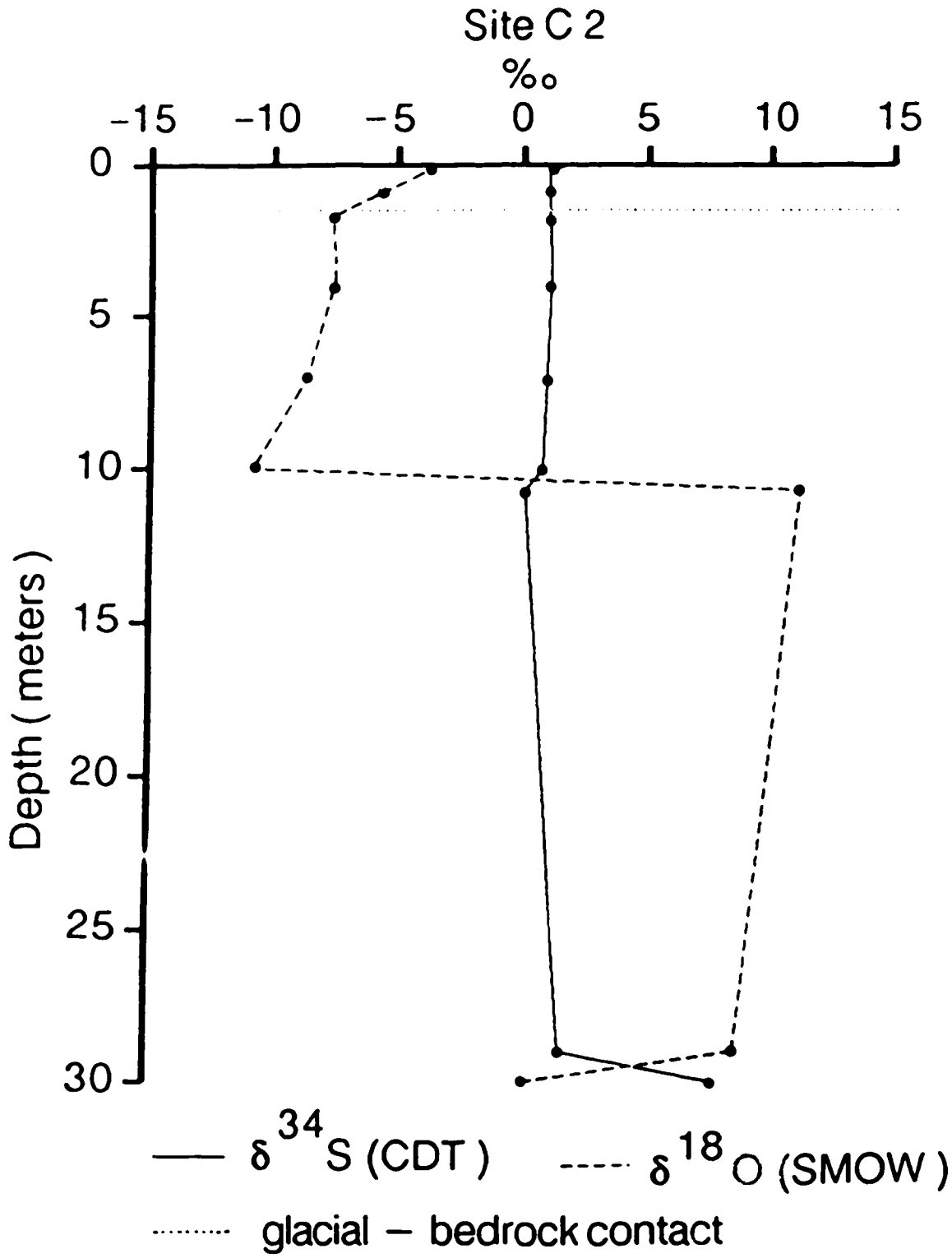

Figure 4.3. Sulfur and oxygen isotopic composition of soluble-sulfates in relation to depth (m) at Site A1.

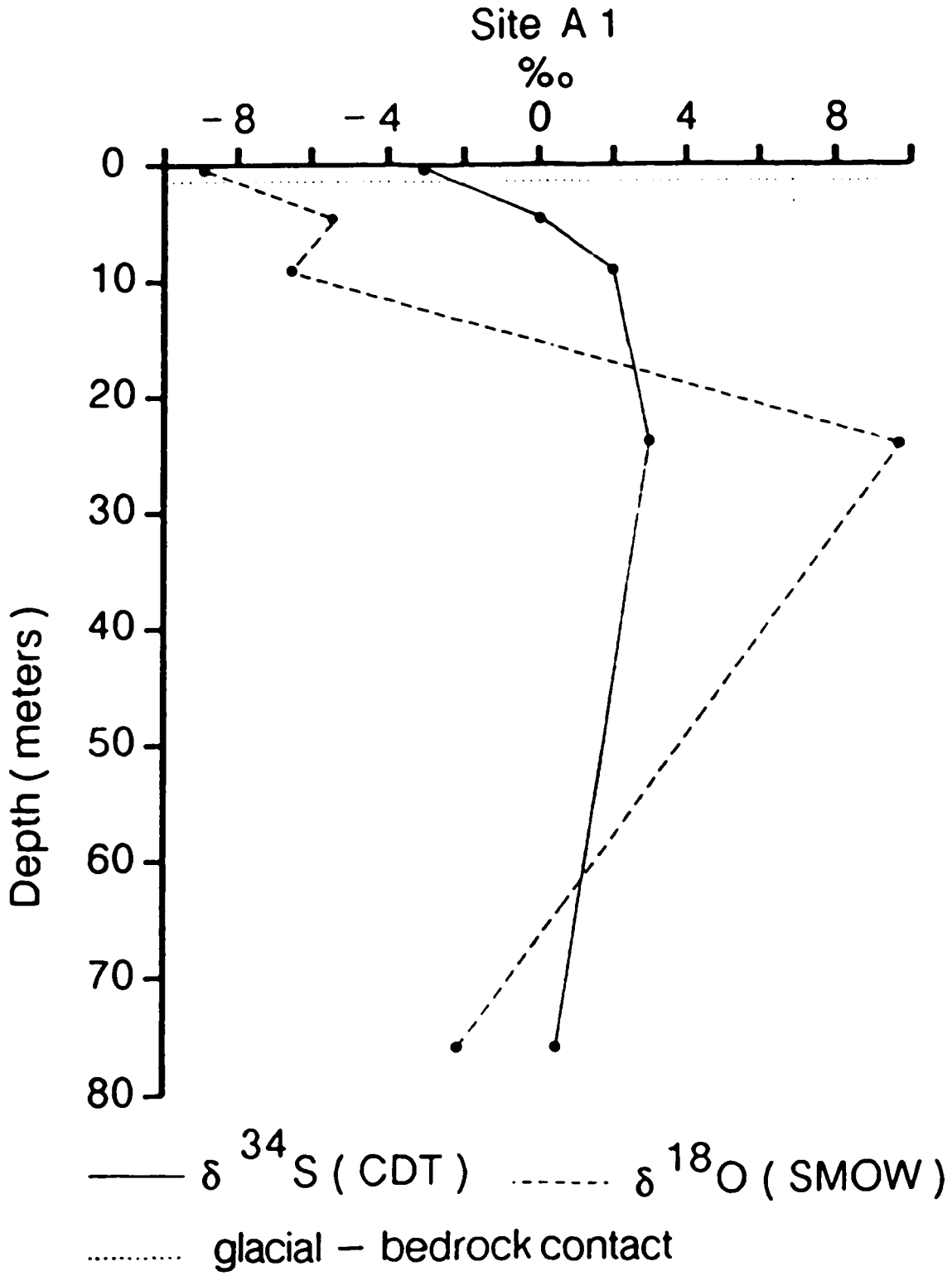

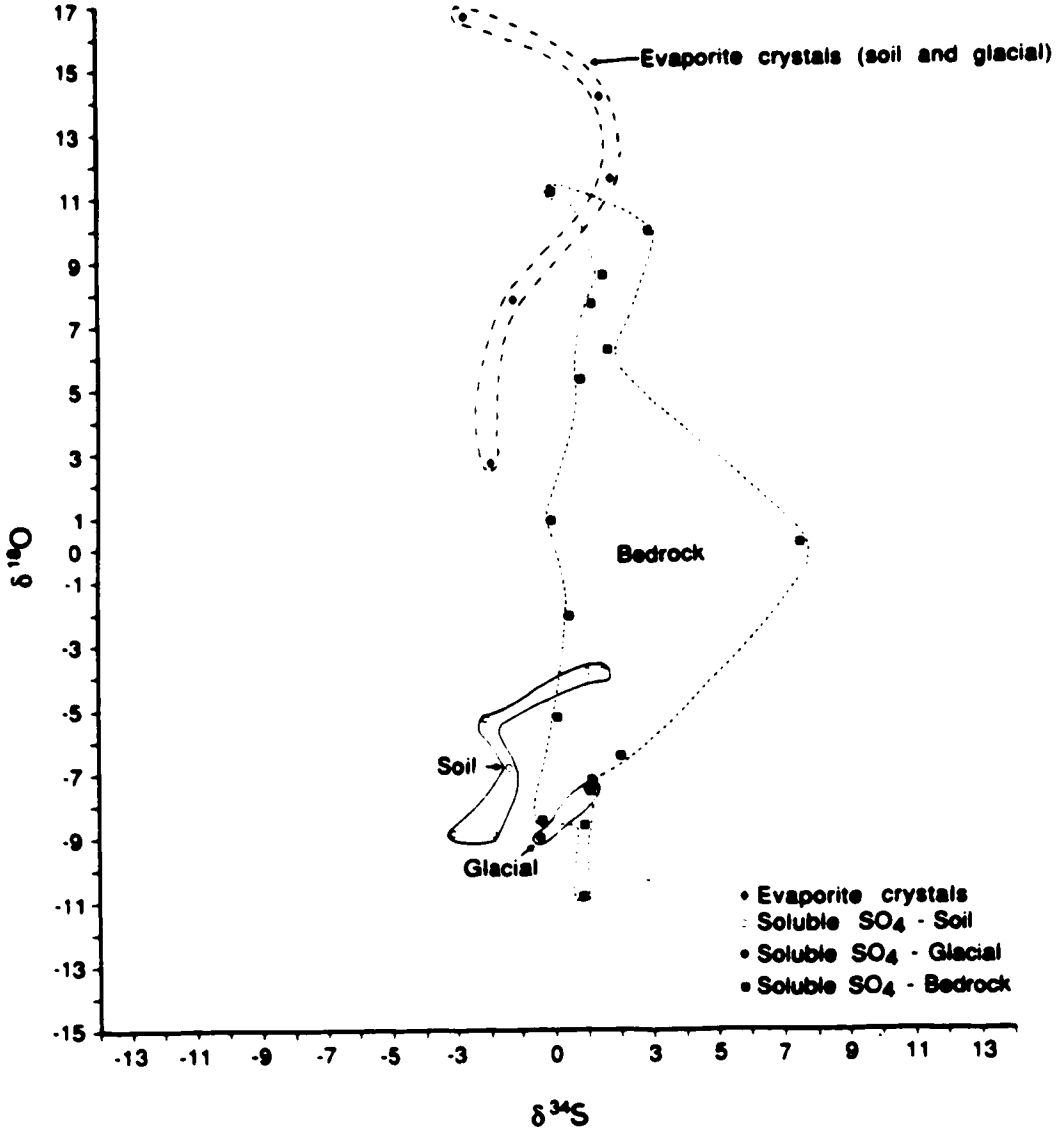

Figure 4.4. Scatter diagram of $\delta^{34}S$ (SO_4) versus $\delta^{18}O$ (SO_4) values of soluble-sulfates and evaporite crystals from soil, drift, and bedrock deposits at Sites A3, C2, and A1.

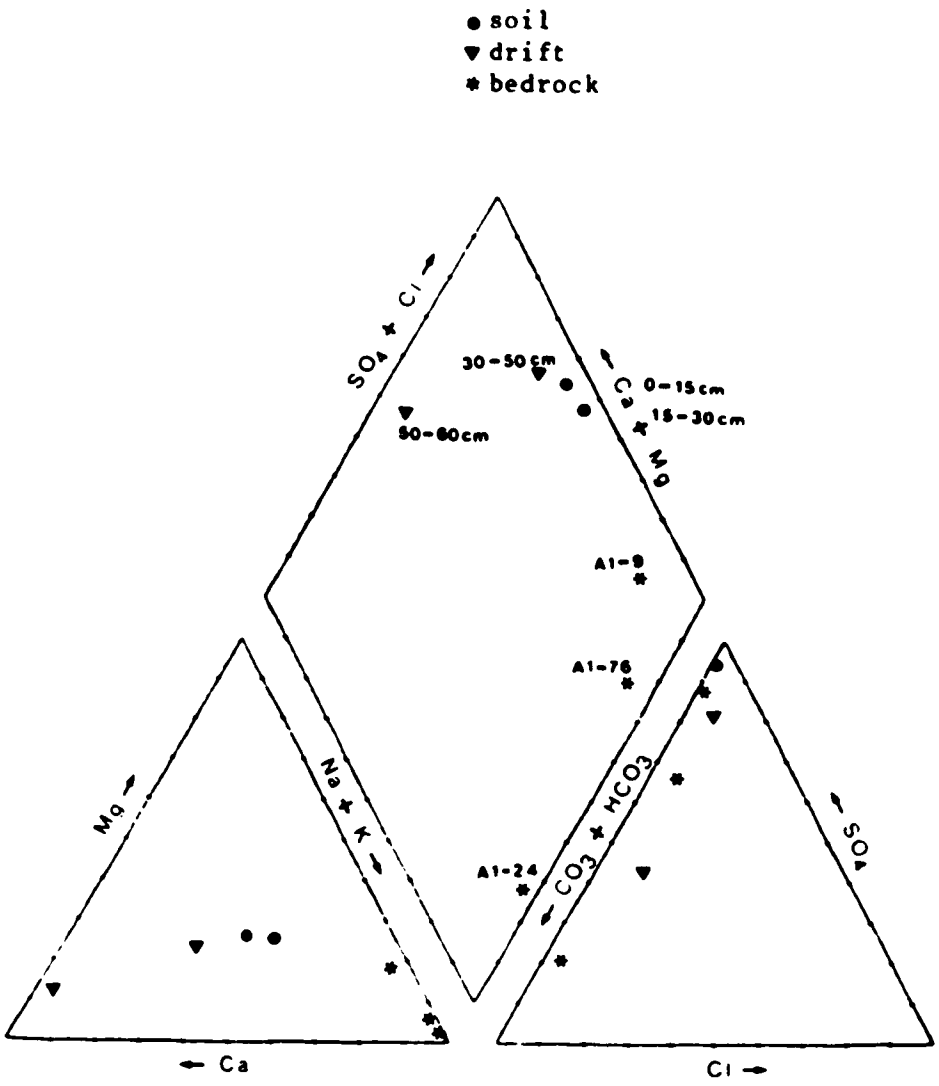

Figure 4.5. The relationship between the ion facies of saturation paste extracts of the soil, and groundwaters from the drift and bedrock deposits at Site A1 (Piper diagram).

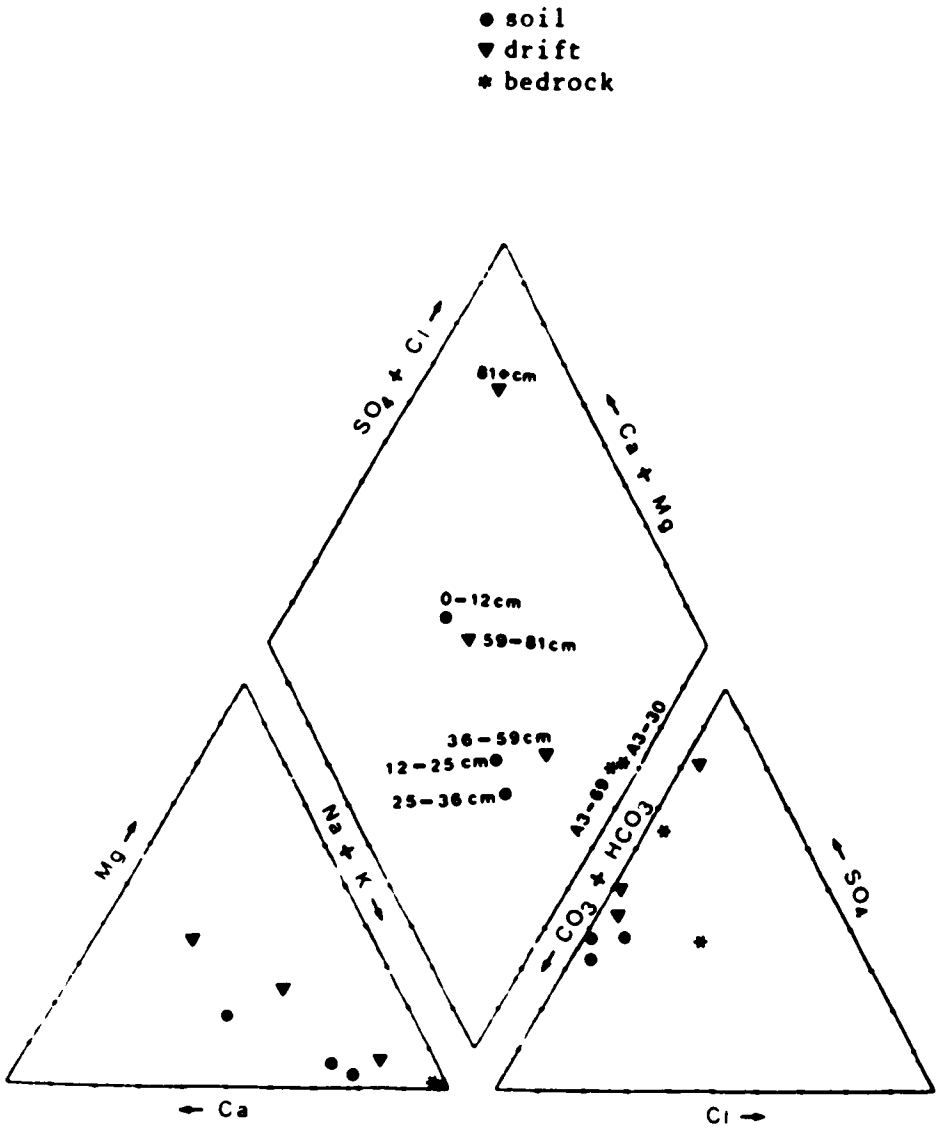

Figure 4.6. The relationship between the ion facies of saturation paste extracts of the soil, and groundwaters from the drift and bedrock deposits at Site A3 (Piper diagram).

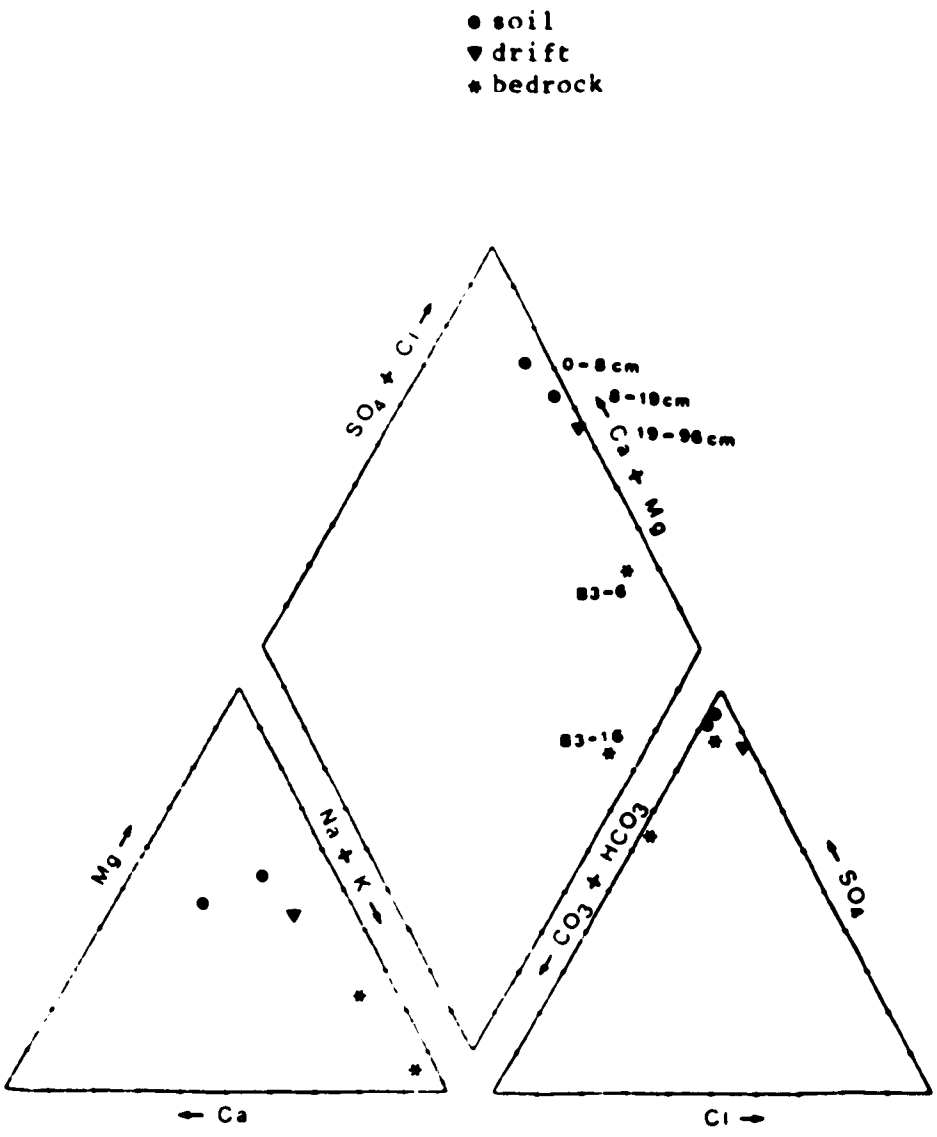

Figure 4.7. The relationship between the ion facies of saturation paste extracts of the soil, and groundwaters from the drift and bedrock deposits at Site B3 (Piper diagram).

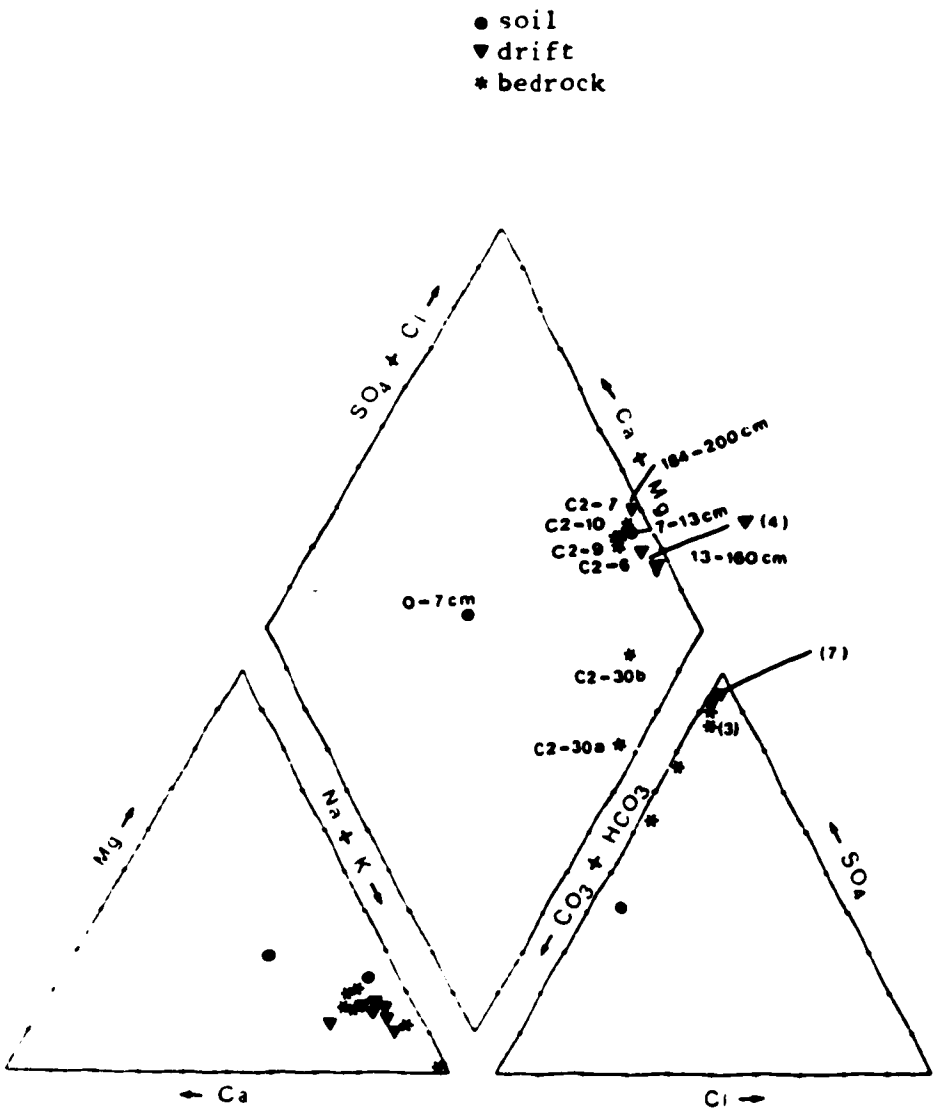

Figure 4.8. The relationship between the ion facies of saturation paste extracts of the soil, and groundwaters from the drift and bedrock deposits at Site C2 (Piper diagram).

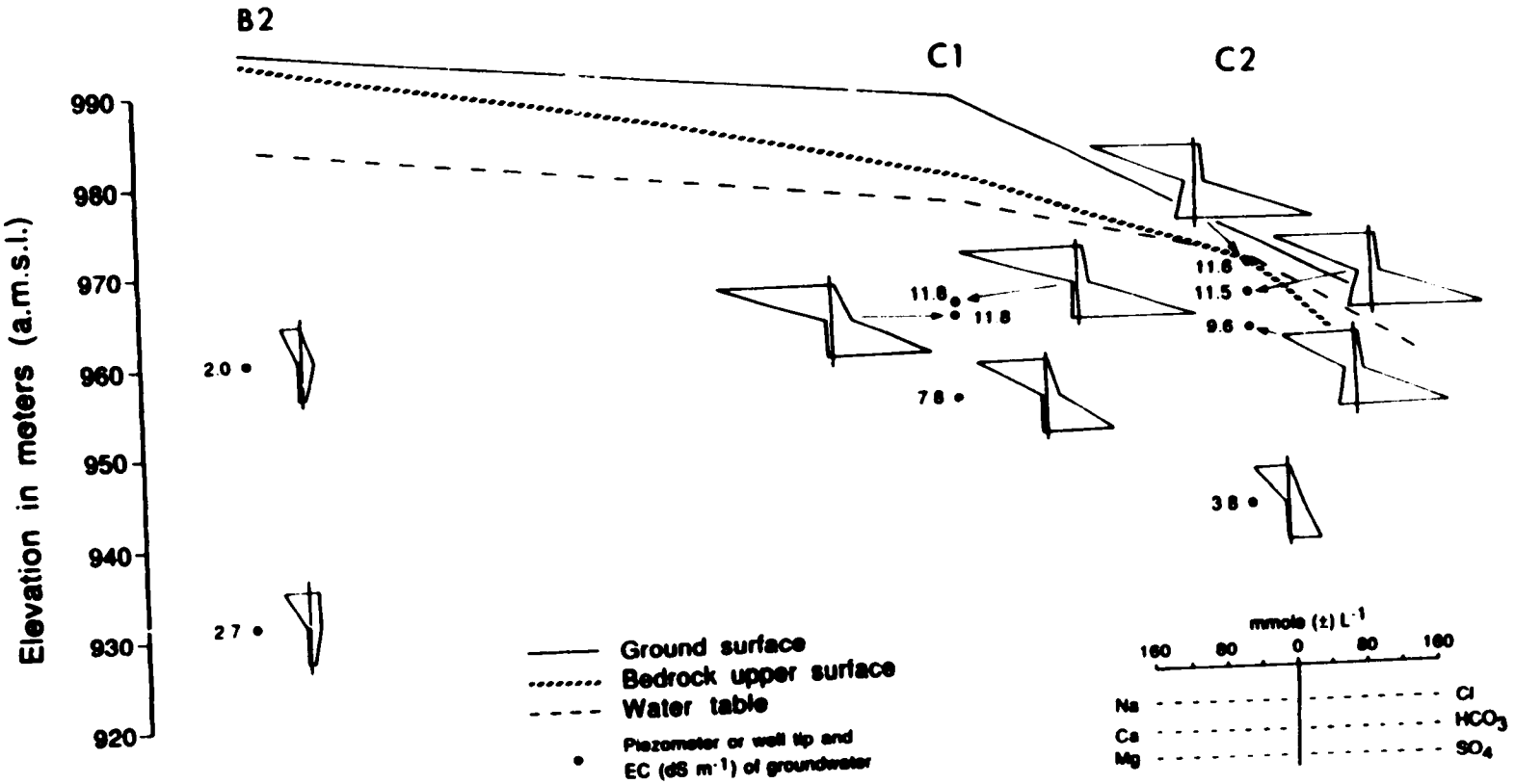

Figure 4.9. Ionic composition of groundwaters along the C-Line section (Stiff diagrams).

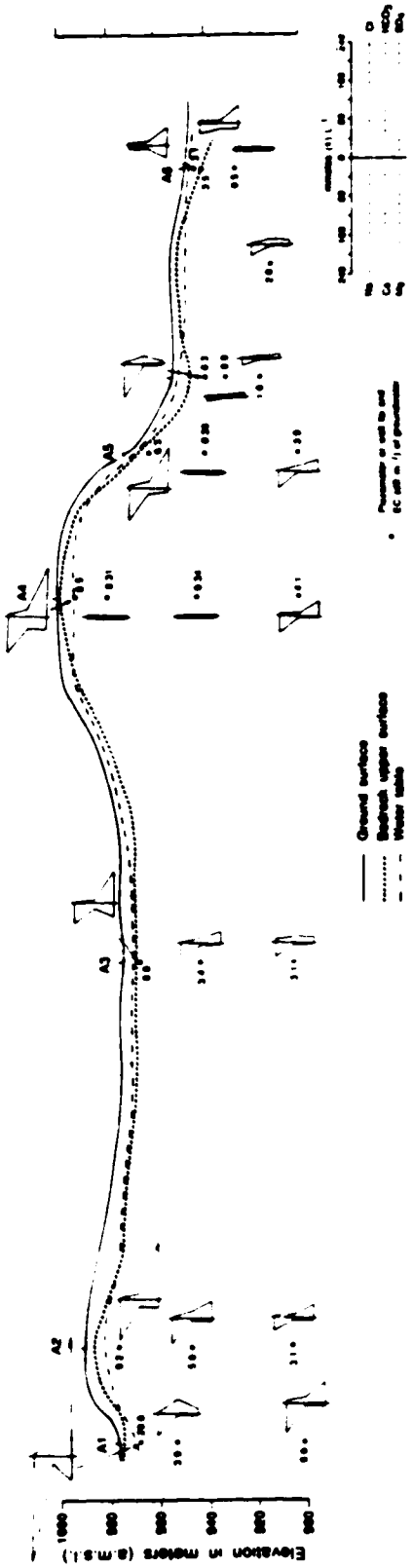

Figure 4.10. Ionic composition of groundwaters along the A-Line section (Stiff diagrams).

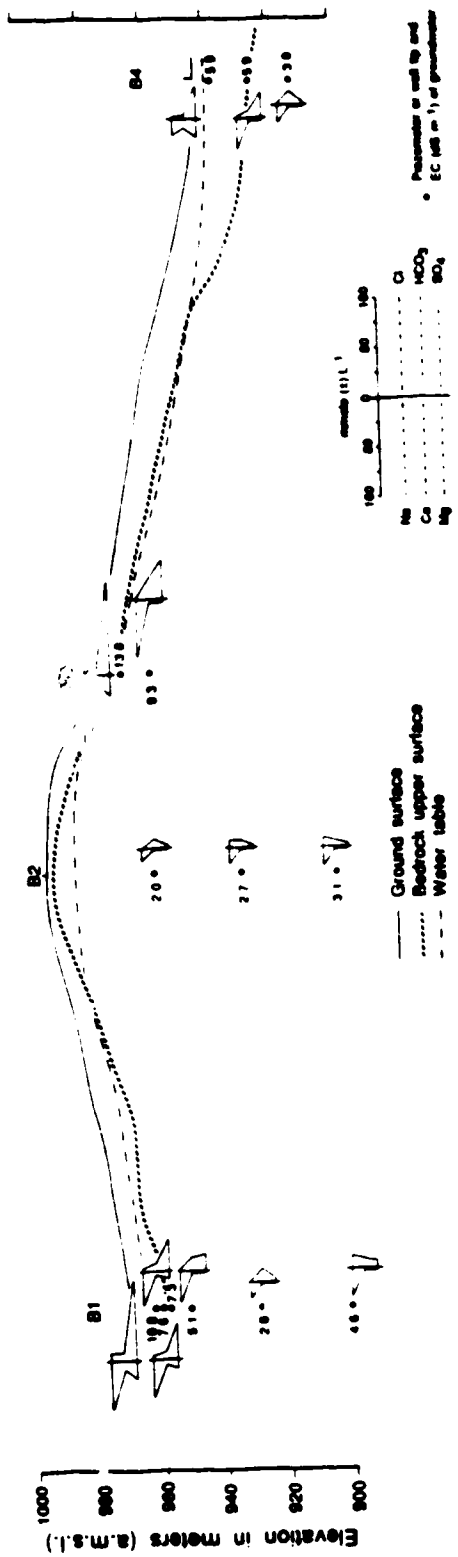

Figure 4.11. Ionic composition of groundwaters along the B-Line section (Stiff diagrams).

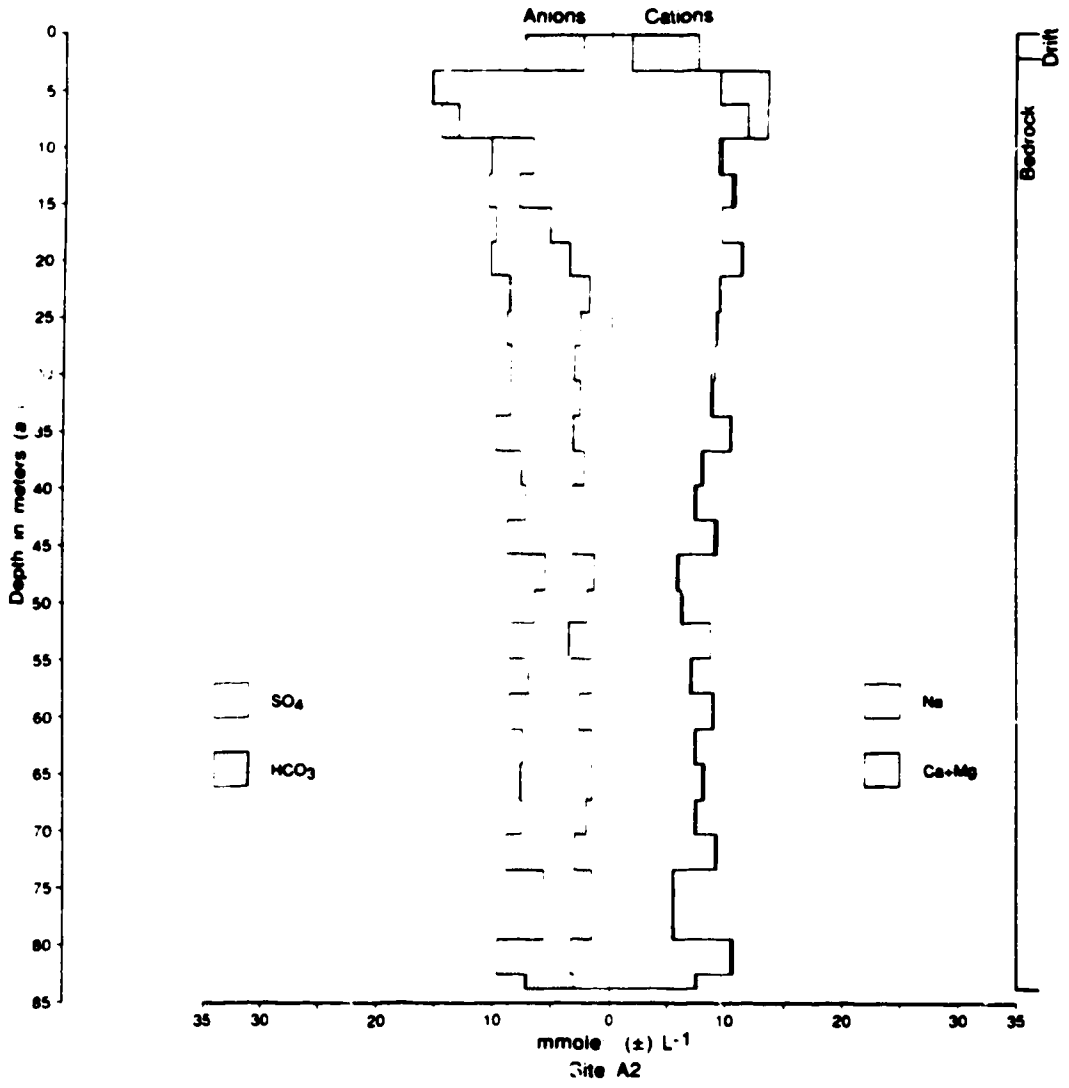

Figure 4.12. Ionic composition of 1:5 (soil:water) extracts in relation to depth (m) at Site A2 (recharge area).

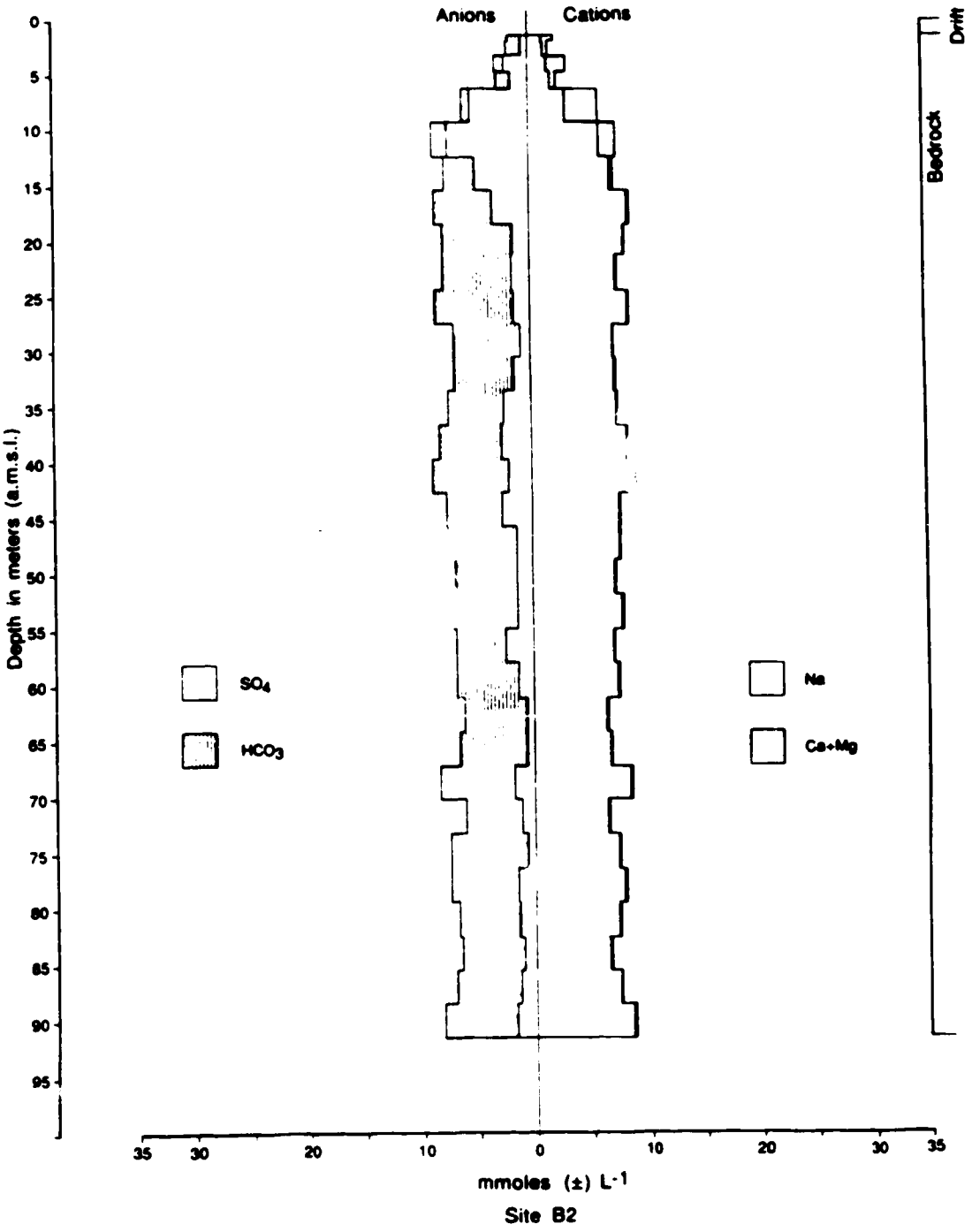

Figure 4.1 Ionic composition of 1:5 (soil:water) extracts in relation to depth (m) at Site B2 (recharge area).

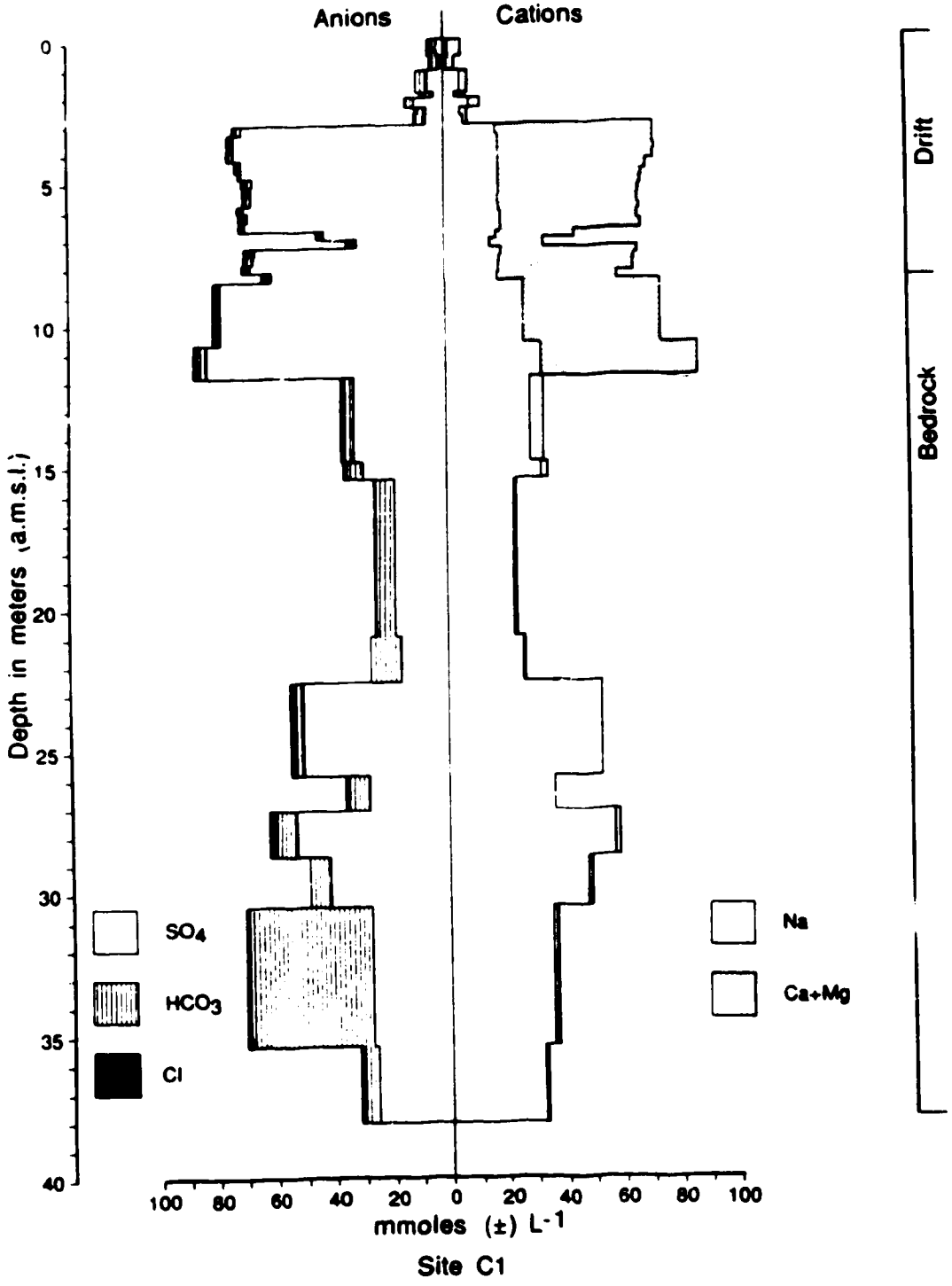

Figure 4.14. Ionic composition of saturation paste extracts in relation to depth (m) at Site C1 (recharge area).

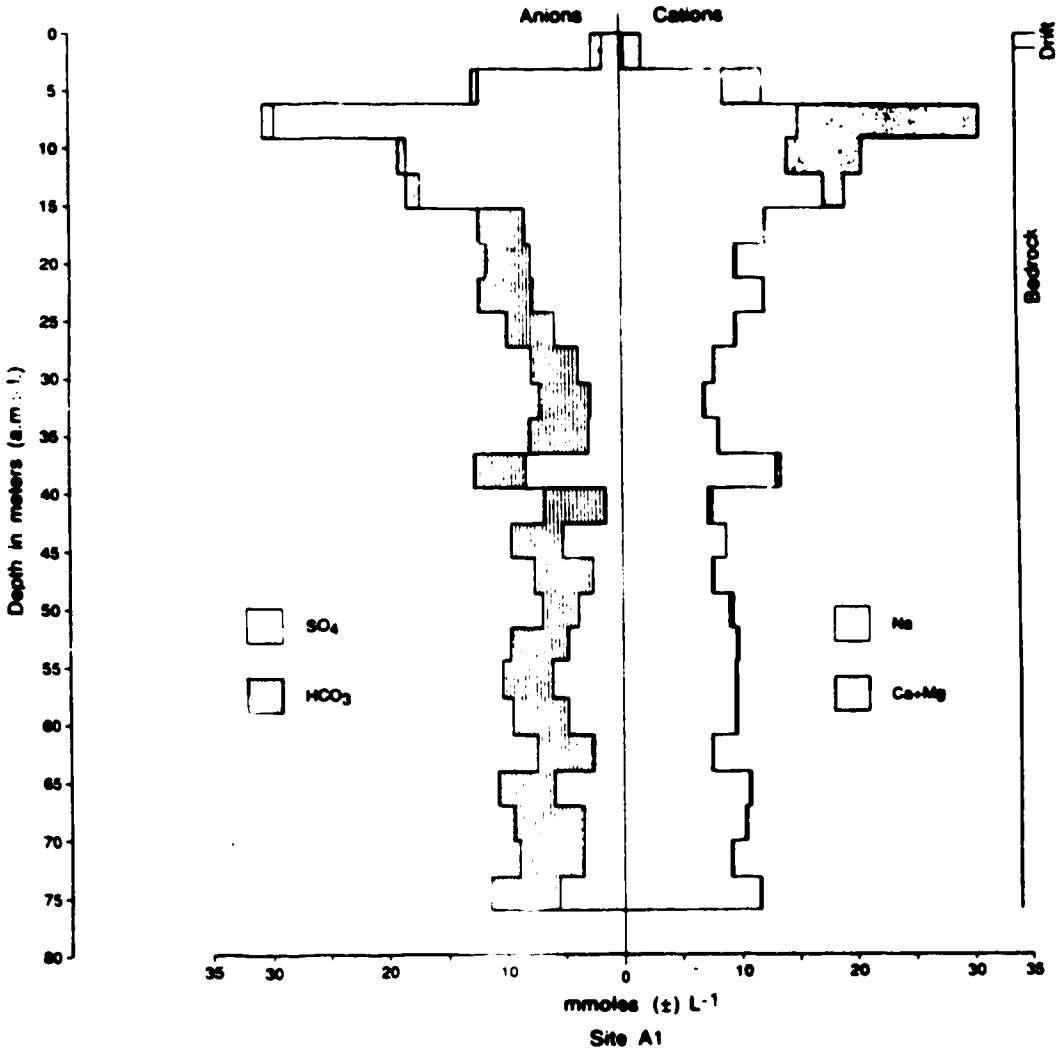

Figure 4.15. Ionic composition of 1:5 (soil:water) extracts in relation to depth (m) at Site A1 (discharge area).

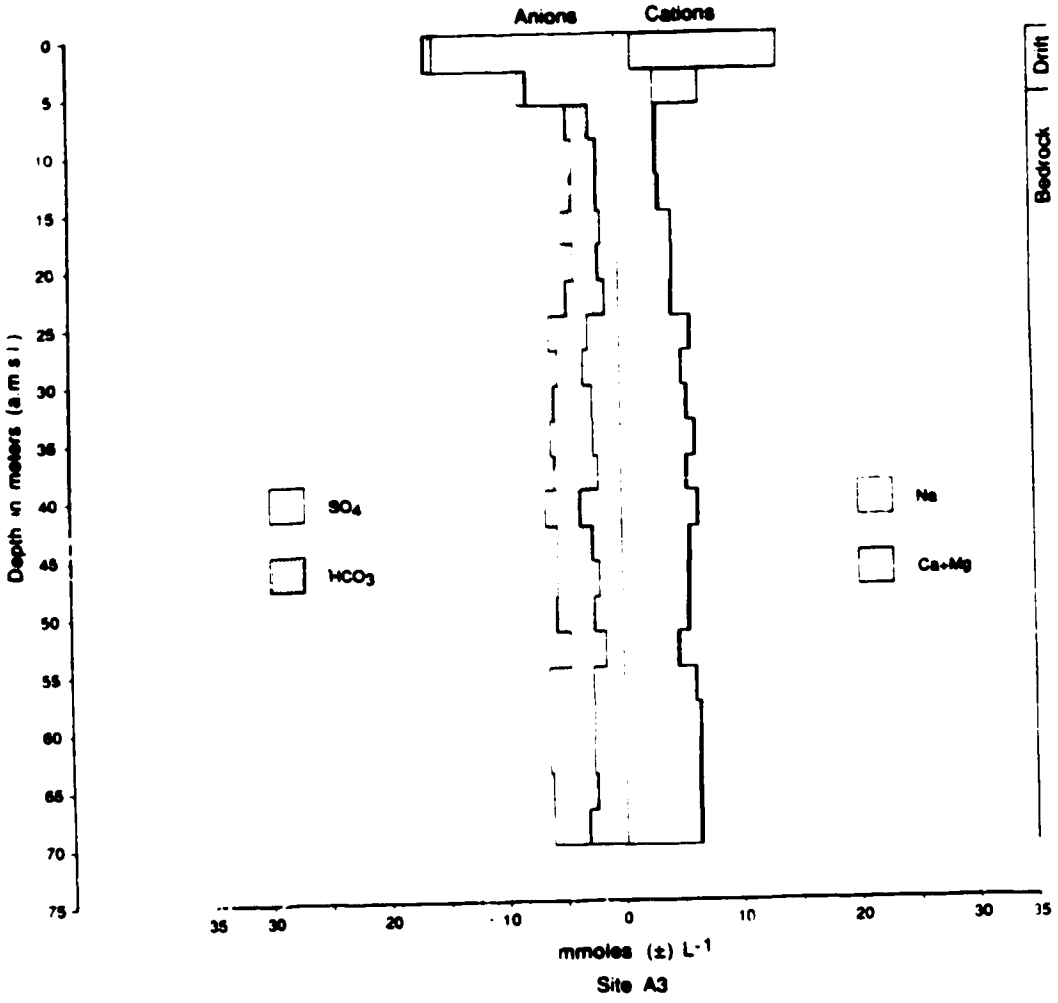

Figure 4.16. Ionic composition of 1:5 (soil:water) extracts in relation to depth (m) at Site A3 (discharge area).

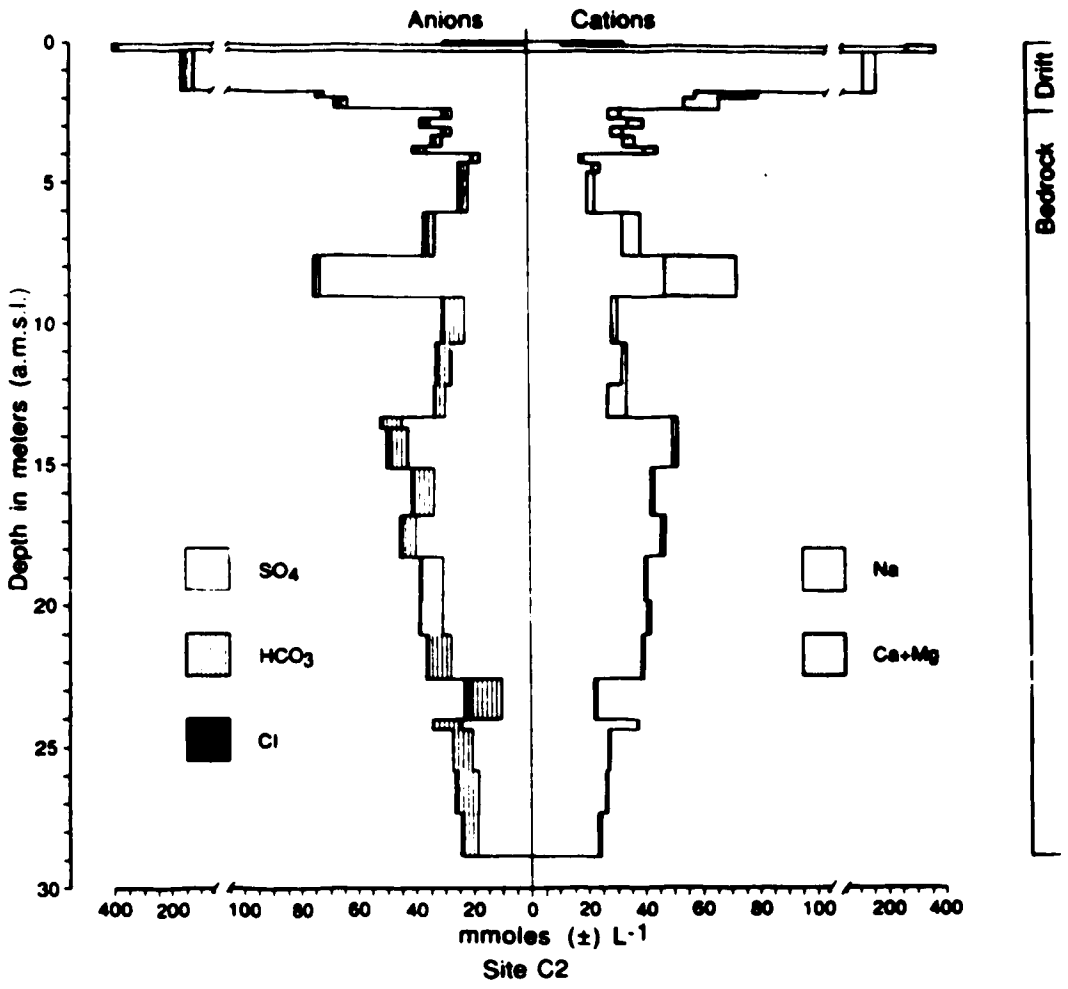

Figure 4.17. Ionic composition of saturation paste extracts in relation to depth (m) at Site C2 (discharge area).

5. SUMMARY AND SYNTHESIS

5.1 DISCUSSION AND SUMMARY

The objective of this study was to determine the origin of dryland salinity. The approach used was to examine the evaporite mineralogy, soil solution and groundwater chemistry of one saline seep in detail, and to determine the possible sources of excess water and salts causing soil salinization at various sites within the study area.

The mineralogy and chemistry of one saline seep (Site C2) was studied in detail. The ionic composition of the soil solution and groundwater was dominated by Na and SO_4 ions. Solution of $CaSO_4$ evaporite minerals (gypsum and bassanite) occurred both above and below the water table and may be a major source of soluble SO_4 ions.

Gypsum, bassanite, and calcite were the only evaporite minerals identified in this soil profile. Simulations with a geochemical model (SOLMNEQ) revealed that the more soluble Na and Mg minerals such as mirabilite and epsomite may theoretically form in this soil, but only in soil solutions of extremely high ionic strength. This would occur in very dry soils, in soil solutions containing high concentrations of soluble salts, or possibly during the winter (mirabilite only).

The common-ion effect involving calcite dissolution and

gypsum and/or bassanite precipitation may be an important factor controlling the occurrence of evaporite minerals. This process is relevant to soil salinity. Decalcification adds the common-ion Ca to the soil solution or groundwater. This causes precipitation of gypsum and/or bassanite, thereby decreasing soil or groundwater salinity with respect to the SO_4 ion.

Many of the microcrystalline bassanite crystals in the upper soil horizons were found as coatings or infillings along root channels. It is hypothesized that high partial pressures of carbon dioxide associated with root respiration may have enhanced decalcification and precipitation of bassanite along root channels. This suggests that plant roots may increase the common-ion effect, and decrease the concentration of soluble sulfate. Seeding saline soils with plants with extensive root systems should not only utilize excess water, but also decrease the quantity of SO_4 ions in solution. This is assuming that abundant carbonates are present in the saline soil, which is usually the case.

A genetic connection between the soil solution and groundwater was inferred by the similar ion chemistry (dominantly Na and SO_4 ions), and by the increase in soluble-salts with decreasing depth to a maximum at the 13 to 24 cm depth. Net upward movement of water and salts in this seep was consistent with this soil being classified as a saline Gleyed Regosolic soil. This soil profile had very minimal pedogenic development that reflected the influence of groundwater discharge and a shallow water table (1.68 - 2.34 m). Some pedogenic processes (decalcification), however, were active in

the soil. Decalcification was reported in this first paper and pedogenic carbonates have been previously identified in this soil by Miller et al. (1987).

An interesting question is whether or not this saline Gleyed Regosolic soil could develop into a Solonetzic soil? Three conditions must generally be met before solonization can proceed (Pawluk 1982). These are: (1) salt accumulations in saline soils must contain a significant content of sodium ions; (2) the clay mineral suite requires a significant component of expandable constituents; and (3) there must be a net adjustment in environmental conditions to favor gradual desalinization.

The first condition was met because the saline seep at Site C2 was sodic (SAR > 15). Greater ion pairing of Ca and Mg relative to Na in the soil solution of this profile also favored increased sodicity. A maximum ESP of 68.3% was determined for the 24 to 30 cm depth. The second condition was also met because this soil contained clay minerals (sandy loam to clay loam textures); and expandable clays such as montmorillonite are a significant component in drift deposits overlaying Cretaceous bedrock in southern Alberta (Pawluk and Bayrock 1969). The third condition was most likely the reason why solonization has not proceeded in this soil. Gradual desalinization of this profile was evident by leaching of soluble-salts from the surface horizon by surface water, by vegetation and an absence of a salt crust on the soil surface, and by tile drainage of the seep downslope. However, desalinization has not been sufficient to initiate formation of a Solonetzic B horizon

(solonization). This is primarily due to a shallow water table (1.68 to 2.34 m) inhibiting leaching of excess soluble salts from the soil.

Solonetzic soils were found in this study area. Dark Brown Solodized Solonetz soils were found adjacent to Studhorse Lake (Site A3) and Dark Brown Solonetz soils were found southeast of Site A5. Areas where Solonetzic soils were found have also been mapped as major artesian basins (Tokarsky 1973). Groundwater discharge from confined bedrock aquifers may keep the water table close to the soil surface, and may also be a major source of sodium, thereby encouraging the formation of Solonetzic soils.

The second paper in this study examined the possible sources of excess water causing soil salinization at four saline seeps (Sites A1, A3, B3 and C2). The results were used to derive five possible models representing various sources of excess water. Discharge below closed topographic depressions from deep (30 and > 69 m) confined bedrock aquifers, under near-flowing artesian conditions, was evident in the Studhorse Lake basin (Site A3). The volume of groundwater discharge was found to be 3.7 m^3 yr^{-1} (1.2 mm yr^{-1}). Discharge from shallow (< 20 m), confined sandstone aquifers was another possible source of excess water (Sites C2, B3). The volume of groundwater discharged from two sandstone aquifers below Site C2 was calculated to be 25.6 m^3 yr^{-1} (88 mm yr^{-1}). Therefore, greater quantities of groundwater were discharged from shallow depths via local flow systems than from artesian discharge from deeper bedrock aquifers.

Shallow groundwater flow through the upper weathered bedrock zone was also found to be a possible source of excess water (Sites A1, A3, B3). It was not clear, however, if this flow was unconfined or confined. Evidence for confined flow through coarse-textured drift deposits was found at Site C1. This included a perched water table and a high soil water content in the sand and gravel layer. Net downward and/or lateral drainage of soil water from the drift overlaying the fluvial layer at Site C1 may have been a possible source of excess water contributing to confined saturated flow through these coarse-textured deposits. Net downward and/or lateral drainage of water from the soil profile at Site C1 was determined to be approximately 122.1, 87.2 and 2.0 mm in 1985, 1986, and 1987, respectively. Similar geological conditions were also observed at Sites A1 and B3.

Finally, infiltration of surface water from snowmelt and precipitation was also found to be a possible source of excess water at Sites A3, B3 and C2. This confirmed similar findings by previous workers (Sommerfeldt and MacKay 1982; Stein 1987). This contribution may be significant because saline soils at lower elevations have shallow water tables; and the possibility of a water table rise (recharge) is greater for shallow rather than deep water tables (Freeze and Cherry 1979). The role of surface water in soil salinization has been underestimated in the past, probably because the emphasis has been on groundwater as the major cause of salinity.

All four saline seeps investigated had more than one possible source of excess water. Site A1 had two possible sources

of excess water, Sites A3 and C2 had three, and Site B3 had four possible sources of excess water. This illustrated the complexity and variety of the causes of salinity. These findings are in agreement with those of Stein (1987), who found that the relatively simple salinity models presently being used cannot be applied to such a complex system because of the many different causes of salinity and the unknown interactions between these sources.

The possible sources of excess salts at three saline seeps (Sites A1, A3 and C2) was addressed in the third paper. The generation and transport of soluble-salts occurred from relatively shallow depths (< 20 m) and from short distances away at Sites A1 (< 1,000 m) and C2 (< 2,000 m). The main salt reservoir for Ca, Mg and SO_4 ions was the drift and upper bedrock (< 10-20 m), whereas Na was derived mainly from the bedrock.

The generation and transport of salts at Sites A1 and C2 followed the classic seep model. Surface water infiltrated into the drift on the bedrock ridge and leached soluble-salts downward. The water and salts percolated to a shallow, coarse-textured drift layer, and then flowed laterally downslope under temporarily saturated conditions (perched water table). Excess water and salts may have also been transported laterally through the upper weathered bedrock zone.

Groundwater that discharged from shallow bedrock aquifers was also considerably mineralized. This was the case for the sandstone aquifer at 12 m below Site C2. Thus, salts may be derived from shallow bedrock aquifers as well as drift deposits. In

addition, salts may possibly be derived from deep bedrock aquifers via fracture-dominated flow. Calculations of salt fluxes and times required for soil salinization at Site A3 revealed that, only by assuming fracture-dominated flow, could significant salt be transported from considerable depth (69 m). It was calculated that the soil at Site A3 could become salinized to an EC of 4 dS m^{-1} in as little as 44 years, if fracture-flow was assumed.

The $\delta^{18}O$ content of soluble sulfates from the soil, drift and bedrock were similar. This suggested that salts in saline soils within the Nobleford area were derived from the drift and/or bedrock. Similar oxygen and sulfur isotope values in the drift and bedrock indicated that the drift was probably derived from the local, underlying bedrock.

Some other interesting trends, however, were observed in the isotope data. These were the heterogeneous $\delta^{18}O$ contents, and homogeneous $\delta^{34}S$ contents of soluble sulfates and evaporite crystals in the soil, drift and bedrock. Negative $\delta^{18}O$ (SO_4) values of soluble sulfates may be due to interaction with lighter meteoric groundwater, and/or reoxidation of sulfides; whereas positive $\delta^{18}O$ (SO_4) values of evaporite crystals may be due to repeated cycles of dissolution-reprecipitation. The relatively constant $\delta^{34}S$ (SO_4) values (close to or above 0‰) may possibly be explained by reduction of sulfate.

5.2 SYNTHESIS

The focus in this section is to combine the significant findings of the three papers in this thesis so as to form a synthesis of the origin of dryland salinity near Nobleford, Alberta. During the development of this thesis, two conceptual models for the origin of salinity became apparent. The first model was applicable to saline seeps associated with bedrock ridges (side-hill seeps) (Fig. 5.1); the second model was applicable to saline seeps found in closed topographic depressions (Fig. 5.2).

The model for side-hill seep (Fig. 5.1) shows the various possible sources of excess water and salt contributing to the formation of a saline seep. Considerable excess water at the seep may originate from surface runoff water to lower elevations and/or infiltration by precipitation. Excess water that percolates below the root zone in the local recharge area on the bedrock ridge acquires Ca, Mg, and SO_4 ions from within the drift, and then moves laterally downslope via perched water tables through permeable coarse-textured fluvial layers to the seep. Excess water and salts (Ca, Mg, Na, SO_4) may also be transported laterally through the upper weathered bedrock zone. Finally, local flow systems may contribute excess water and salts (mainly Na) by concentrating flow laterally through permeable, sandstone aquifers.

At side-hill seeps the excess water and salts were derived mainly from shallow depths (< 20 m) and from short distances away (< 2,000 m). This finding has favourable implications with respect

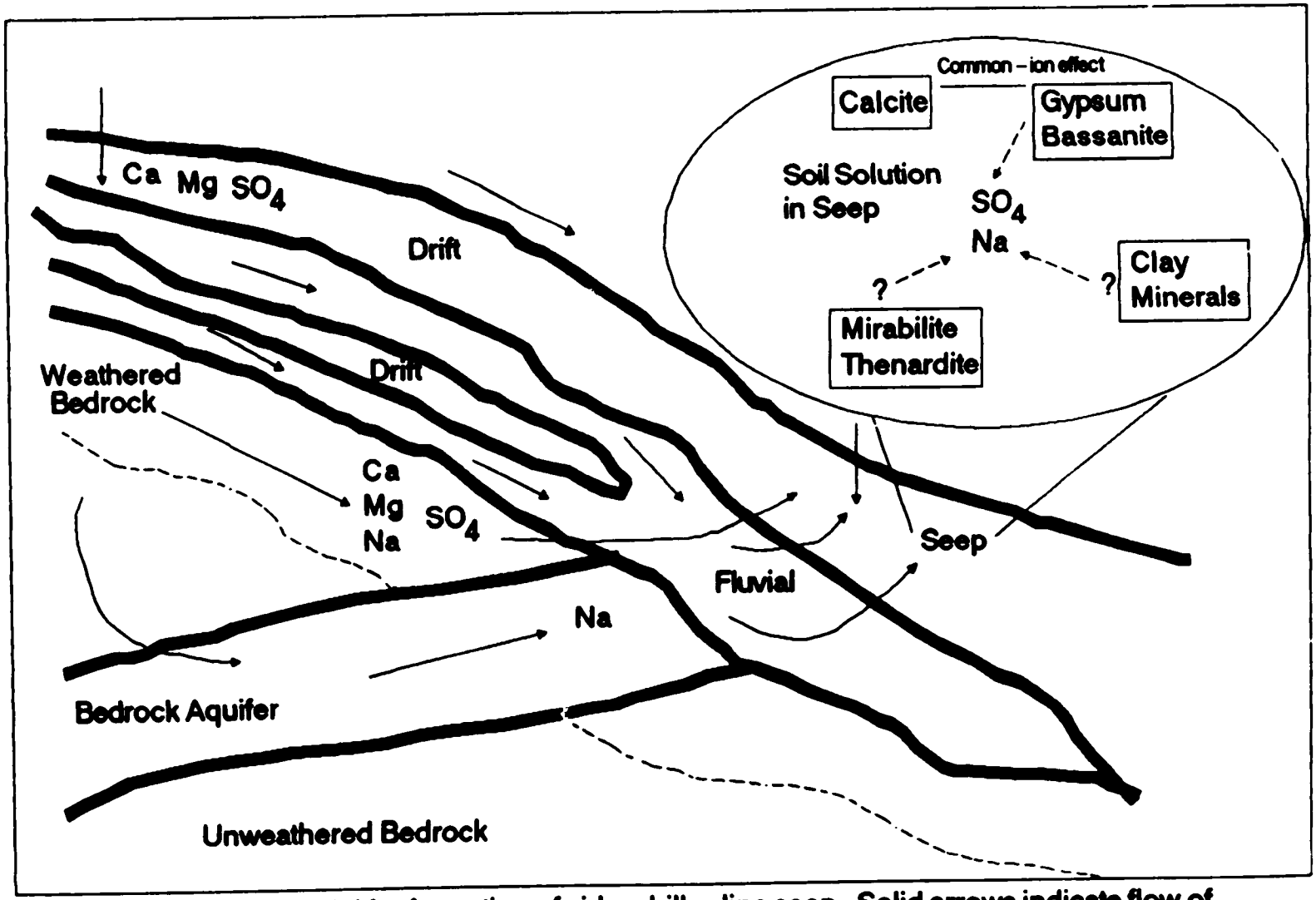

Fig. 5.1. Conceptual model for formation of side – hill saline seep. Solid arrows indicate flow of water and/or salts; dashed arrows in circle indicate possible sources of the dominant soluble salts.

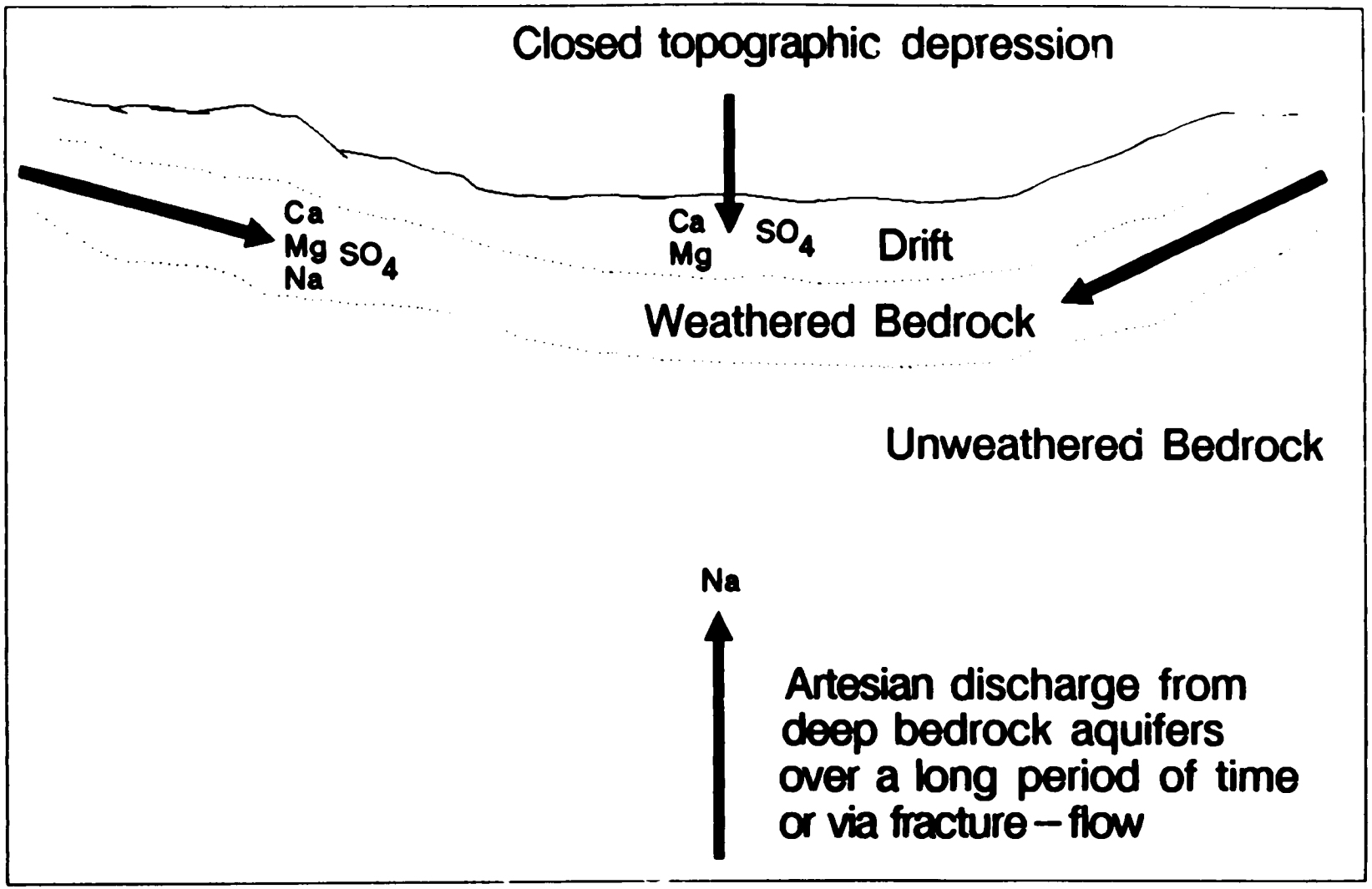

Figure 5.2. Conceptual model for formation of saline seep in closed topographic depression. Arrows indicate flow of water and/or salts.

to development of management practices for preventing the buildup of excess water in the seep area. Management practices are much more difficult and costly when the source of excess water is from considerable depth.

Soil water and groundwater flowed through the drift and bedrock and contributed excess salts to the side-hill seep. The ionic composition of the soil solution and shallow groundwater at the seep were dominated by Na and SO_4 ions. The most likely source of Na in the seep was from groundwater discharge from the bedrock; however, dissolution of mirabilite, and exchange reactions with clay minerals within the soil and drift, may also have contributed some Na. The source of the SO_4 ion in the seep was most likely from dissolution of gypsum and/or bassanite found within the soil and drift.

The conceptual model for formation of saline seeps within closed topographic depressions (Fig. 5.2) differs from the side-hill seep model (Fig. 5.1), mainly in the contribution of artesian discharge from deeper (30 to 69 m) bedrock aquifers. As noted by Freeze and Cherry (1979), the primary control on artesian conditions is topography; this is reflected in the large numbers of flowing wells that occur in valleys of rather marked relief.

Excess water in the closed depression may be derived from infiltration of precipitation and/or surface runoff water. Percolation of this water through the soil and drift above the water table results in dissolution of Ca, Mg, and SO_4 ions found within the drift. In addition, excess water and salts (Ca, Mg, Na, SO_4)

may have originated from lateral flow through the upper, weathered bedrock zone.

Artesian discharge from depth (30 or 69 m) could salinize the soil above to an EC of 4 dS m^{-1}, but only over a long period of time (10^4 to 10^5 years). If fracture-dominated flow was assumed, salinization could occur with[illegible] to 150 years. The crucial factor determining water and [illegible] movement upward from depth is probably the hydraulic conductivity of the intervening [illegible] strata. Similar findings have been reported by Stein (1987). The accumulation of Ca, Mg, and SO_4 ions near the soil surface, however, suggested that the most likely source of excess salts in the closed topographic depression was from depths < 10 m. Generally, much greater quantities of groundwater flow through shallow depths as local flow compared to groundwater discharge from deep bedrock aquifers.

An interesting question is what were the soil moisture conditions under which the evaporite minerals were found? Bassanite was only found in the upper soil horizons (0 to 30 and 88 to 160 cm depths), whereas both bassanite and gypsum were found at depths > 160 cm. Bassanite was associated with extremely variable soil moisture conditions that ranged from very dry (< -1,500 kPa) to saturated (0 kPa). In contrast, gypsum was found only in horizons that were saturated. Thus, the water of hydration of $CaSO_4$ minerals may be an indirect indicator of soil moisture conditions: bassanite reflecting extremely variable soil moisture levels and gypsum reflecting saturated conditions.

The evaporite minerals exhibited a unique "isotopic signature": variable but enriched $\delta^{18}O$ (SO_4) values and constant $\delta^{34}S$ (SO_4) values. The high $\delta^{18}O$ content of gypsum and bassanite may possibly be due to repeated cycles of dissolution-reprecipitation. Precipitation of $CaSO_4$ favours enrichment of sulfur and oxygen isotopes, particularily the latter isotope. Dissolution would tend to occur when the soil was wet, and re-precipitation when the soil was dry. Bassanite in the upper horizon of this study showed evidence of slight dissolution; whereas "comb-like" features on gypsum found below the water table reflected strong dissolution. Seasonal sampling of evaporite minerals would be required to ascertain the dissolution or reprecipitation status of evaporite minerals throughout the year.

In summary, generation, transport and accumulation of soluble salts, and formation of side-hill seeps occurred from local flow systems at relatively shallow depths (< 20 m). In closed topographic depressions, excess water and salts may originate from artesian discharge from depth (30 to 69 m); however, the volume of water discharged is relatively small, and only over a long period of time or by assuming fracture-flow can the soil be salinized. Greater quantities of groundwater were discharged from local flow systems at shallow depths compared to artesian discharge from deep bedrock aquifers.

5.3 CONCLUSIONS

1. Dissolution of gypsum and bassanite contributed Ca and SO_4 ions to the soil solution and shallow groundwater of a saline seep soil.

2. The more soluble Na and Mg evaporite minerals such as mirabilite and epsomite were not identified in the saline seep investigated. These minerals may possibly precipitate in the upper soil horizons, but only in soil solutions of extremely high ionic strength (dry and/or highly saline soils), or possibly during the winter (mirabilite only).

3. Possible sources of soluble Na in the soil solution and shallow groundwater of the saline seep investigated were groundwater discharge from the underlying bedrock, dissolution of mirabilite, or cation exchange within the drift.

4. The mineral sequence observed in a saline seep could not be explained by the Hardie-Eugster model of closed-basin brine evolution. The common-ion effect involving decalcification and gypsum or bassanite precipitation, however, may partially explain the mineral sequence observed.

5. The common-ion effect may decrease soil salinity with respect to the SO_4 ion and may be enhanced by root respiration.

6. An increase in $CaSO_4$ crystal size with depth could be related to the following changes with depth: a shift from variable to constant soil moisture and temperature conditions, and a shift from higher to lower soluble Na concentrations.

7. Greater ion pairing of Ca and Mg relative to Na in the soil solution and shallow groundwater of a saline seep favored increased sodicity.

8. Net upward movement of water and salts in a saline seep profile was consistent with this soil being classified as a saline Gleyed Regosolic soil. This soil probably could not evolve into a Solonetzic soil because it lacks a significant quantity of expandable clay minerals.

9. Five possible sources of excess water were found to have contributed to soil salinity in the study area: artesian discharge from shallow and deep bedrock aquifers; shallow flow through the upper weathered bedrock zone; confined flow through coarse-textured drift deposits; and infiltration of surface water at lower elevations.

10. Major contributing factors to soil salinity at some sites were: a sharp break in topographic gradient (from steep to shallow); a change from coarse to finer textured drift deposits, from upper to lower slope positions; and thin drift deposits (< 2.5 m) on the bedrock ridges.

11. Greater quantities of groundwater were discharged at saline seeps on bedrock ridges (side-hill seeps) from local flow at shallow depths (< 20 m), compared to artesian discharge from deep (30 to 69 m) bedrock aquifers below closed topographic depressions. Significant quantities of soil water may have drained downwards and/or laterally on the bedrock ridges, and contributed to perched water tables and high soil water contents in coarse-textured drift layers. Lateral, confined flow through these permeable fluvial layers would therefore contribute excess water and salts to saline seeps on the lower slopes of the bedrock ridges.

12. The oxygen isotopic technique for assessing possible source areas of salt (drift or bedrock) was applied in this study; however, the two source areas could not be differentiated because the $\delta^{18}O$ content of soluble sulfates in the drift and bedrock were similar. Therefore, possible sources of soluble salts in the saline soils studied were the drift and/or bedrock. The similar $\delta^{18}O$ and $\delta^{34}S$ contents of soluble sulfates in the drift and bedrock inferred that the drift was derived from the local, underlying bedrock.

13. Some other interesting trends, however, were observed in the isotope data. These were the heterogeneous $\delta^{18}O$ content and homogeneous $\delta^{34}S$ content of soluble sulfates and evaporite crystals from the soil, drift and bedrock. An explanation for these trends is not known.

14. A comparison between the ion facies of saline soils (saturation extracts), and associated groundwaters from the drift and bedrock, revealed that at some saline seeps, the source of salts was the drift. At other seeps, however, the source of salts was the drift and bedrock. The dominance of SO_4, HCO_3 or SO_4 type, anion facies in the soil and drift groundwaters, suggested the presence of local or intermediate flow systems (inferred from Chebotarev sequence). No mixing of drift and bedrock groundwaters was evident on the Piper diagrams.

15. The ion composition and concentrations of the groundwater showed that the shallow groundwater was the major reservoir for Na and SO_4 ions. Deeper groundwater had relatively low concentrations of soluble salts. The salts in the saline seeps were generated and transported over relatively short distances (< 2,000 m), and from shallow depths (< 20 m).

16. The soluble-salt profiles of the lithology showed leaching of salts from soils in recharge areas and redistribution of salts to saline soils in discharge areas. High Ca, Mg and SO_4 ion contents appeared to be derived from the drift and shallow bedrock (< 10-20 m). Sodium ions generally originated from the bedrock.

17. The Br and I contents of the groundwaters in the study area were generally low or non-detectable. This implied a relatively shallow source of salinity in the study area.

18. Calculations of salt fluxes and times required for soil salinization showed that, only by assuming fracture-dominated flow from considerable depth (69 m), could any significant salt be transported to the soil surface by artesian discharge.

5.4 RECOMMENDATIONS FOR FUTURE RESEARCH

Various recommendations for future research arose during the progress and completion of this study.

1. Evaporite mineralogy, soil solution and groundwater chemistry should be examined seasonally to characterize the dynamic nature of the minerals and chemistry.

2. Recently developed geochemical models that can accurately simulate soil solutions and groundwaters of high ionic strength should be applied to this type of study to improve predictions of evaporite mineral dissolution and precipitation. In addition, reliable thermodynamic data bases are needed for the evaporite minerals.

3. There is a need to quantify the possible sources of excess water contributing to soil salinity and to characterize the interactions between these sources. This could be done using a water balance approach.

4. There is a need to determine the role of fracture-flow in the transport of salts. As shown in this study, significant quantities of salts can be transported from depth if fracture-flow is assumed.

5. The deep drainage component of the soil water budget on different textured, drift deposits in local recharge areas should be determined. This would yield valuable information about potential groundwater recharge and would provide a data base for management practices designed to prevent percolation of excess soil water in local recharge areas.

6. The groundwater contribution from bedrock aquifers should be quantified. More information is needed to answer the question of whether deep drilling (> 30 m) is required in dryland salinity investigations. The results from this study revealed that, except for major closed topographic depressions, the origin of water and salts was from relatively shallow depths (< 20 m). This suggests that deep drilling is probably not required; however, more benchmark sites should be examined to answer this question.

7. In the Nobleford study area, similar ^{18}O (and ^{34}S) contents of soluble sulfates in both the drift and bedrock prevented identification of possible source areas of salts (drift or bedrock) contributing to soil salinity. The oxygen isotope

technique proposed by Hendry and Krouse (1987), however, should be applied at other geographic locations where the ^{18}O content of sulfates in the drift and bedrock are different. Possible source areas of salt (drift or bedrock) could then be differentiated.

8. Some interesting trends were observed in the isotope data. These were the large variability in $\delta^{18}O$ (SO_4) values, and relatively constant $\delta^{34}S$ (SO_4) values of soluble sulfates and evaporite crystals (gypsum and bassanite). An explanation for these trends is unknown, and merits future research.

5.5 BIBLIOGRAPHY

FREEZE, R.A. and CHERRY, J.A. 1979. Groundwater. Prentice-Hall, Inc., Englewood Cliffs, N.J. p. 286.

HENDRY, M.J. and KROUSE, H.R. 1987. A technique to identify source areas of groundwater causing saline seeps. Alberta Soil Sci. Workshop, Calgary, Alberta. p. 164-169.

MILLER, J.J., DUDAS, M.J. and LONGSTAFFE, F.J. 1987. Identification of pedogenic carbonate minerals using stable carbon and oxygen isotopes, x-ray diffraction and SEM analyses. Can. J. Soil Sci. 67: 953-958.

PAWLUK, S. 1982. Salinization and solonetzic formation. Proc. 19th Annual Alberta Soil Sci. Workshop, Edmonton, Alberta. p. 1-24.

PAWLUK, S. and BAYROCK, L.A. 1969. Some characteristics and physical properties of Alberta tills. Res. Council Alberta Bull. 26. p. 22.

SOMMERFELDT, T.G. and MacKAY, D.C. 1982. Dryland salinity in a closed drainage basin at Nobleford, Alberta. J. Hydrol. 55: 25-41.

STEIN, R. 1987. A hydrogeological investigation of the origin of saline soils at Blackspring Ridge, southern Alberta. Unpubl. M.Sc. Thesis. Dept. of Geology, Univ. of Alberta, Edmonton, Alberta. 272 pp.

TOKARSKY, O. 1973. Hydrogeology of the Lethbridge-Fernie area, Alberta. Alberta Research Council Report 74-1, Edmonton, Alberta. 18 pp.

6. APPENDIX

6.1. Lithologic drill logs

Legend

Sh=shale

SiS=siltstone

SS=sandstone

cSh=carbonaceous shale

bSS=bentonitic sandstone

mudS=mudstone

TESTHOLE NUMBER A1
(SW 34 – 11 – 23 – 4)

Depth (meters)	Dominant Geology	Subdominant Geology	Color	Remarks
0–0.91			10YR6/3d	
0.91 – 1.22			10YR6/3d	SiCL – SiC
1.22 – 3.05	Sandstone		10YR6/3d	Soft, brown color
3.05 – 7.32	Shale		2.5Y6/3d	Soft, fractrured
7.32 – 8.53	Sandstone	Sh	2.5Y5/2d	
8.53 – 9.45	Sandstone		2.5Y5/2d	Soft
9.45 – 11.58	Shale		2.5Y5.5/2d	Hard
11.58 – 12.80	SiS	Sh	2.5Y5.5/2d	Oxidized
12.80 – 15.24	Shale	SiS,SS	2.5Y5.5/2d	
15.24 – 16.46	cSh		10YR4.5/2d	
16.46 – 17.98	Shale	cSh	10YR4.5/2d	Oxidized
17.98 – 20.73	Shale	SiS,SS	2.5Y5/2d	Hard
20.73 – 22.64	Sandstone		2.5Y5/2d	
21.64 – 24.69	Shale	SiS,SS	2.5Y5.5/2d	
24.69 – 25.30	Sandstone		2.5Y5/2d	Hard
25.30 – 27.43	Shale	SiS,SS	2.5Y5/2d	
27.43 – 28.35	Sandstone		2.5Y6/2d	
28.35 – 28.96	Sandstone	Sh	2.5Y6/2d	Hard
28.96 – 32.00	Sandstone	Sh	2.5Y6/2d	Hard

TESTHOLE NUMBER A1 (Continued)

(SW 34 – 11 – 23 – 4)

Depth (meters)	Dominant Geology	Subdominant Geology	Color	Remarks
32.00 – 39.01	Shale	SS	2.5Y5/2d	Hard
39.01 – 39.62	Sandstone		2.5Y5/2d	Hard
39.62 – 41.76	bSS		2.5Y6/2d	
41.76 – 44.81	Shale		2.5Y5.5/2d	Hard
44.81 – 45.11	bSS		2.5Y5.5/2d	
45.11 – 45.72	Shale		2.5Y5.5/2d	Hard
45.72 – 48.77	bSS	Sh,SS,SiS	2.5Y5.5/2d	Hard Sh
48.77 – 52.43	bSS	Sh,SiS	2.5Y6/2d	
52.43 – 54.25	Shale		2.5Y5/2d	Hard
54.25 – 55.78	bSS	SS,Sh	2.5Y5/2d	Hard SS
55.78 – 56.39	Shale		2.5Y5/2d	
56.39 – 57.91	Sandstone		2.5Y5/2d	
57.91 – 59.13	Shale		2.5Y5/2d	Hard
59.13 – 60.96	bSS	SS,Sh,SiS	2.5Y5/2d	Hard SS
60.96 – 62.18	Sandstone	bSS,Sh	2.5Y6/2d	Hard SS
62.18 – 64.01	Shale		2.5Y4.5/2d	Hard
64.01 – 67.06	Shale	SS	2.5Y4.5/2d	Hard SS
67.06 – 70.10	Shale	SiS	2.5Y5/2d	Hard
70.10 – 73.15	Shale	SiS	2.5Y5.5/2d	Hard

TESTHOLE NUMBER A2
(EC28–11–23–4)

Depth (meters)	Dominant Geology	Subdominant Geology	Color	Remarks
0–1.83			2.5Y6/2	SiC
1.83–2.13	Sand		2.5Y6/2	
2.13–12.80	Shale	cSh	2.5Y5.5/3	Soft, fractured
12.80–16.76	Shale		2.5Y6/2	Fractured
16.76–17.68	Shale		2.5Y5/2	Hard,
17.68–19.20	Sandstone		2.5Y5/2	Hard, grey
19.20–19.81	Shale		2.5Y5.5/2	
19.81–20.73	Sandstone		2.5Y5.5/2	Hard, grey
20.73–22.86	Shale	SS	2.5Y5/2	
22.86–24.69	Sandstone	Sh	2.5Y5/2	
24.69–25.91	cSh		2.5Y4/2	
25.91–28.65	Shale		2.5Y4/2	
28.65–32.31	Shale		2.5Y5/2	
32.31–35.05	Sandstone		2.5Y4/2	Hard, grey
35.05–40.54	Shale		2.5Y5/2	
40.54–41.76	Sandstone		10YR6/1	Hard, grey
41.76–45.11	Shale	SS	10YR6/1.5	
45.11–45.72	Sandstone		10YR6/1.5	Hard, grey
45.72–46.94	Shale		10YR6/1	Hard

TESTHOLE NUMBER A2 (Continued)
(EC28–11–23–4)

Depth (meters)	Dominant Geology	Subdominant Geology	Color	Remarks
46.94–48.16	Sandstone		10YR6/1	
48.16–50.90	Shale		10YR6/1	
50.90–53.64	Sandstone		10YR6/1.5	Hard, grey
53.64–56.39	Shale		2.5Y5.5/2	
56.39–57.61	Shale		2.5Y5.5/2	Green color
57.61–61.87	Shale		2.5Y5.5/2	
61.87–62.18	cSh		2.5Y6/2	
62.18–62.48	Shale		2.5Y6/2	
62.48–63.09	Sandstone		2.5Y6/2	
63.09–72.24	Shale	SS	2.5Y5.5/2	
72.24–78.94	Sandstone		10YR6.5/1	
78.94–81.38	Shale		10YR5.5/1	Hard, Grey
81.38–83.52	Sandstone		10YR5.5/1	Hard
83.52–83.82	Shale		10YR5.5/1	

TESTHOLE NUMBER A3
(NW10-11-23-4)

Depth (meters)	Dominant Geology	Subdominant Geology	Color	Remarks
0-3.05	Glacial		2.5Y6/3	FSL-FSCL
3.05-5.49	Glacial		2.5Y6/3	FSL
5.49-7.92	Shale		2.5Y6/2	Hard
7.92-8.53	bSS		2.5Y6/2	Soft
8.53-8.84	cSh		2.5Y6/2	
8.84-10.97	Shale		10YR6/1	Hard
10.97-12.80	cSh		10YR6/1	Water
12.80-14.33	bSS	SS	10YR6/1	Soft
14.33-16.46	Shale		10YR6/1	Hard
16.46-18.59	Shale	bSS	10YR6/1.5	Hard Sh
18.59-19.51	Shale		10YR6/1	Hard
19.51-20.73	Sandstone		10YR6/1	Hard
20.73-22.25	Shale		10YR6/1	Hard
22.25-22.56	Sandstone		10YR6/1	Soft, grey
22.56-23.77	Shale	SS	10YR6/1	
23.77-24.08	Sandstone		10YR6/1	Soft, grey
24.08-27.74	Shale		10YR6/1	Hard,Water
27.74-30.48	Sandstone	cSh,Sh	10YR6.5/1	
30.48-33.53	Shale	SS,cSh	10YR6/1.5	Hard Sh

TESTHOLE NUMBER A3 (Continued)
(NW10-11-23-4)

Depth (meters)	Dominant Geology	Subdominant Geology	Color	Remarks
33.53-36.58	Shale		2.5Y6/2	Hard
36.58-38.71	Shale	SS	2.5Y6/2	Hard
38.71-41.76	Sandstone		2.5Y6/2	Hard
41.76-42.67	Shale	SS	2.5Y6/2	Hard
42.67-45.72	Shale		2.5Y6/2	Hard
45.72-48.77	Shale		2.5Y6/2	Hard
48.77-50.29	Shale		2.5Y6/2	Hard
50.29-51.21	Sandstone		2.5Y6/2	Hard
51.21-51.82	Sandstone		2.5Y6/2	Hard
51.82-54.86	Shale	SS,cSh	2.5Y5.5/2	Hard
54.86-57.91	Shale	SS,cSh	2.5Y6/2	Hard
57.91-60.96	Shale	SS,cSh	2.5Y5.5/2	Hard
60.96-68.58	Shale	SS,cSh	2.5Y5.5/2	Hard

TESTHOLE NUMBER A4

(EC32-10-23-4)

Depth (meters)	Dominant Geology	Subdominant Geology	Color	Remarks
0–0.61	Till		2.5Y6/2	
0.61 – 1.83	Sandstone		2.5Y6/2	Hard,brown
1.83 – 3.35	Shale	cSh	2.5Y6/2	Hard
3.35 – 3.96	Sandstone		2.5Y6/4	Hard
3.96 – 5.79	Shale		2.5Y6/4	
5.79 – 6.10	Sandstone		2.5Y6/4	Hard
6.10 – 7.01	Shale		2.5Y6/2	Hard
7.01 – 7.32	cSh		2.5Y6/2	
7.32 – 8.23	Shale		2.5Y6/2	Hard
8.23 – 9.75	Shale		2.5Y6/2	Hard
9.75 – 10.67	Sandstone		2.5Y6/2	Hard
10.67 – 12.19	Shale		2.5Y6/2	Hard
12.19 – 17.07	Shale		10YR6/1	Hard
17.07 – 18.29	Sandstone	Sh	10YR6/1	Hard
18.29 – 19.81	Shale		10YR6.5/1	Hard
19.81 – 20.12	Sandstone		10YR6.5/1	Hard
20.12 – 23.77	Shale		10YR6/1	Hard
23.77 – 24.38	cSh		10YR6/1	
24.38 – 24.99	Sandstone	Sh	2.5Y5.5/2	Hard

TESTHOLE NUMBER A4 (Continued)

(EC 32 – 10 – 23 – 4)

Depth (meters)	Dominant Geology	Subdominant Geology	Color	Remarks
24.99 – 26.52	Shale		2.5Y5.5/2	Hard
26.52 – 26.82	Shale		2.5Y5.5/2	Hard
26.82 – 28.04	Shale		2.5Y5.5/2	Hard
28.04 – 30.18	Shale	SS	10YR6/1	
30.18 – 31.09	Sandstone	Sh	10YR6/1	
31.09 – 35.05	Shale	SS	2.5Y5.5/2	
35.05 – 36.27	Sandstone	Sh	2.5Y5.5/2	
36.27 – 42.37	Shale	SS	2.5Y5.5/2	Brown, hard SS
42.37 – 44.50	Shale		2.5Y5.5/2	Hard
44.50 – 48.46	Shale		2.5Y5/2	Hard
48.46 – 49.99	Shale		2.5Y5/2	Hard
49.99 – 50.60	Sandstone		2.5Y5/2	Hard
50.60 – 54.56	Shale	SS	10YR5/1	SS lenses
54.56 – 57.30	Shale	SS	10YR5/1	
57.30 – 57.91	Sandstone		10YR5/1	
57.91 – 59.74	bSS		10YR5/1	
59.74 – 61.26	Shale	bSS	10YR5/1	
61.26 – 63.40	Shale	bSS,SiS	10YR5.5/1	
63.40 – 64.31	bss		10YR5.5/1	

TESTHOLE NUMBER A4 (Continued)
(EC 32-10-23-4)

Depth (meters)	Dominant Geology	Subdominant Geology	Color	Remarks
64.31-66.75	Shale	SS	10YR6/1	
66.75-68.28	Shale	cSh, SS	2.5Y5.5/2	
68.28-70.10	Shale		2.5Y5.5/2	Hard
70.10-71.02	Sandstone	Sh, SiS	2.5Y5.5/2	Hard SS and Sh
71.02-72.85	Shale	SS	2.5Y5.5/2	
72.85-75.59	Shale	SS	2.5Y5.5/2	
75.59-78.94	Mudstone	bss, Sh	2.5Y5.5/2	Soft, brown mudS
78.94-81.08	Sandstone	Sh	2.5Y5.5/2	
81.08-83.82	Shale		2.55.5/2	
83.82-85.04	bSS	Sh, SiS, SS	10R6/1	
85.04-91.14	Shale	SiS, bSS, SS	2.5Y5.5/2	Green-blue SiS
91.14-96.93	Shale	SiS	10YR6/1	
96.93-99.06	Shale	SiS, mudS	10YR6/1	

TESTHOLE NUMBER A5
(NE 29 – 10 – 23 – 4)

Depth (meters)	Dominant Geology	Subdominant Geology	Color	Remarks
0–2.44	Glacial		2.5Y5.5/2	PSL–PSCL
2.44–3.35	Glacial		2.5Y5.5/2.5	C–CL
3.35–4.57	Shale		2.5Y6/3	Fractured
4.57–5.49	Sandstone		2.5Y6/3	Soft, tan color
5.49–6.40	Sandstone		2.5Y6/3	Hard
6.40–8.23	Shale		2.5Y6/2	Soft, fractured
8.23–10.36	Sandstone	Sh	2.5Y6/2	SS soft, tan color
10.36–14.33	Shale		2.5Y6/2	Hard
14.33–16.76	Shale		2.5Y6/3	
16.76–17.98	cSh	SS	2.5Y6/4	SS ledge
17.98–18.29	Sandstone		2.5Y6/4	Hard
18.29–19.20	Sandstone		2.5Y6/1.5	Hard
19.20–21.34	Shale		2.5Y6/1.5	Hard
21.34–24.38	Shale		2.5Y/1.5	Hard
24.38–27.43	Shale		2.5Y5.5/2	Hard
27.43–30.48	Shale		10YR6/1	Hard
30.48–33.53	Shale		10YR6/1.5	Hard
33.53–36.58	Shale		10YR6/1.5	
36.58–40.84	Shale	SiS	10YR6/1.5	

TESTHOLE NUMBER A5 (Continued)
(NE 29 – 10 – 23 – 4)

Depth (meters)	Dominant Geology	Subdominant Geology	Color	Remarks
40.84 – 42.37	Shale		2.5Y6/2	
42.37 – 42.67	Shale		2.5Y6/2	
42.67 – 47.24	Sandstone	bSS	10YR6/1	Hard SS
47.24 – 49.99	Shale		10YR6/1.5	Hard
49.99 – 51.82	Shale	SiS	10YR6/1.5	
51.82 – 54.86	Shale	SiS	10YR6/1.5	
54.86 – 55.17	Sandstone		10YR6/1	Hard
55.17 – 57.61	Shale	SiS	10YR6/1	Hard
57.61 – 58.22	Sandstone		10YR6/1	Hard
58.22 – 60.96	Shale		10YR6/1	Hard
60.96 – 62.18	Sandstone	bSS	2.5Y6/2	Hard SS
62.18 – 63.09	Shale		2.5Y6/2	
63.09 – 67.06	Shale		2.5Y6/2	
67.06 – 68.58	Sandstone		2.5Y5.5/2	

TESTHOLE NUMBER B1
(SW24–11–23–4)

Depth (meters)	Dominant Geology	Subdominant Geology	Color	Remarks
0–3.05	Till		2.5Y6/4	CL–C
3.05–6.10	Till		2.5Y5/2	Oxidized zones
6.10–11.58	Till		2.5Y5.5/2.5	Silty lenses
11.58–13.11	Mudstone	SiS	2.5Y5/2	MudS soft,brown
13.11–14.02	Mudstone	SiS	2.5Y5/2	MudS soft,brown
14.02–17.07	Sandstone	SiS	2.5Y5/2	SS grey and fine
17.07–18.29	Sandstone	SiS	2.5Y5/2	SS hard
18.29–19.20	Shale	SiS	2.5Y5/2	Sh hard
19.20–19.81	Sandstone	Sh,SiS	2.5Y5/2	SS fine
19.81–21.34	Shale	SiS	2.5Y5/2	
21.34–24.38	Shale	SS,cSh,SiS	2.5Y5/2	cSh increasing
24.38–27.74	Shale	cSh,SiS,bSS	2.5Y5/2	Hard Sh
27.74–28.35	Sandstone	Sh,SiS	2.5Y5/2	
28.35–30.48	Shale	SiS,SS	2.5Y5/2	Hard black Sh
30.48–35.05	Shale	SiS	2.5Y5/2	Hard light brown
35.05–36.27	Sandstone	Sh,bSS	10YR6/1.5	Good SS
36.27–36.58	Coal		10YR6/1.5	
36.58–39.32'	Shale		10YR5/2	Hard

TESTHOLE NUMBER B1 (Continued)
(SW24-11-23-4)

Depth (meters)	Dominant Geology	Subdominant Geology	Color	Remarks
39.32-39.62	Shale	cSh,SS	10YR5/2	
39.62-42.67	Sandstone	Sh,bSS	10YR5.5/1	Mainly SS
42.67-45.42	Shale	bSS	10YR5/1	
45.42-45.72	Sandstone		10YR5/1	
45.72-48.77	Sandstone	bSS,Sh	10YR5.5/1	Good SS
48.77-52.43	bss	SS,Sh	10YR6/1	
52.43-54.86	Shale	bss,SS	10YR5/1	
54.86-56.08	Shale	SS	10YR4/2	Light bronw Sh
56.08-60.96	bss	SS	10YR6/1	
60.96-64.01	bss	SS	2.5Y6/2	Hard SS
64.01-67.06	bss	SS	2.5Y6.5/2	Hard SS
67.06-69.19	bss	SS	2.5Y6/2	Hard SS

TESTHOLE NUMBER B2
(NE2-11-23-4)

Depth (meters)	Dominant Geology	Subdominant Geology	Color	Remarks
0-1.22				
1.22-1.83	Sandstone		2.5Y6/2	Brown, oxidized
1.83-3.05	Sandstone	Sh	2.5Y7/2	
3.05-4.57	Sandstone	Sh	2.5Y6/3	
4.57-6.10	Sandstone	Sh	2.5Y6/3	
6.10-7.62	Sandstone	Sh	2.5Y6/2	
7.62-7.92	Shale		2.5Y6/2	
7.92-9.14	Sandstone		2.5Y6/2	Hard
9.14-12.19	Sandstone		2.5Y5.5/2	Hard
12.19-13.72	Sandstone		2.5Y5.5/2	Grey
13.72-14.63	cSh		2.5Y5.5/2	
14.63-15.24	cSh		2.5Y5.5/2	
15.24-18.29	Sandstone		2.5Y4.5/2	Grey
18.29-21.34	Sandstone	bSS	10YR6/1	
21.34-24.38	Sandstone	bSS	10YR5.5/1	
24.38-25.91	Sandstone	bSS	10YR5/1	
25.91-27.74	Shale	ss	10YR5/1	Shaly SS
27.74-31.39	Sandstone		10YR5.5/1	Grey shaly
31.39-33.53	Sandstone		10YR6/1	Sticky, moist

TESTHOLE NUMBER B2 (Continued)
(NE2–11–23–4)

Depth (meters)	Dominant Geology	Subdominant Geology	Color	Remarks
33.53–36.58	Sandstone		10YR6/1	Sticky,moist
36.58–39.32	Shale	SS	10YR5.5/1	
39.32–41.15	Sandstone	Sh	10YR5/2	
41.15–42.67	Shale	SS	10YR5/2	
42.67–48.77	Shale	SS,SiS	10YR6/1	
48.77–50.60	Shale	SiS	10YR6/1	
50.60–51.21	Sandstone		10YR6/1	Hard
51.21–54.25	Shale		10YR6/1	
54.25–55.47	Sandstone		10YR6/1	Hard
55.47–56.39	Shale	SiS,SS	10YR6/1	
56.39–57.61	Sandstone		10YR6/1	
57.61 [illegible]	Shale	cSh	10YR6/1	Brown Sh
5[illegible]	Shale	SiS	10YR6/1	
[illegible]	Shale	SiS	10YR6/1	
[illegible]	Sandstone	Sh	10YR6/1	
62.[illegible]	Shale	SS	10YR6/1	
62.48–62.79	cSh	Sh,SS	10YR6/1	
62.79–63.09	Sandstone	cSh,Sh	10YR6/1	
63.09–64.62	Shale	SS	10YR6/1	

TESTHOLE NUMBER B2 (Continued)

(NE2–11–23–4)

Depth (meters)	Dominant Geology	Subdominant Geology	Color	Remarks
64.62–67.36	Shale	SS	10YR6/1	
67.36–69.19	Shale	SiS	2.5Y5.5/2	
69.19–69.49	cSh	SiS,Sh	2.5Y5.5/2	
69.49–69.80	Sandstone		2.5Y5.5/2	
69.80–71.02	Shale	cSh,SiS	2.5Y6/2	Hard Sh
71.02–71.93	SiS	Sh	2.5Y6.5/2	
71.93–72.54	Shale	SiS	2.5Y6.5/2	
72.54–74.23	SiS	Sh	2.5Y6.5/2	
74.23–75.59	Shale	SiS	2.5Y6/2	
75.59–77.11	cSh	SiS,Sh	2.5Y6/2	
77.11–78.33	Shale	SiS	2.5Y5.5/2	
78.33–79.86	Shale	SiS,SS	2.5Y6/2	
79.86–81.69	Sandstone	Sh,bSS	2.5Y6/2	
81.69–86.26	SiS	Sh	2.5Y6/2	
86.26–87.48	bSS	SiS	2.5Y5.5/2	
87.48–90.22	Shale		2.5Y5.5/2	
90.22–90.83	SiS	Sh,SS	2.5Y5.5/2	

TESTHOLE NUMBER B4
(SE22-10-23-4)

Depth (meters)	Dominant Geology	Subdominant Geology	Color	Remarks
0–3.08	Glacial		2.5Y4.5/2	C–GL
3.08–18.29	Glacial		2.5Y4.5/2	
18.29–19.20	Sandstone	bSS	2.5Y5/2	
19.20–24.99	Shale		2.5Y5/2	Hard
24.99–30.18	Sandstone	Sh	2.5Y5/2	Hard SS

TESTHOLE NUMBER C1

(SC2-11-23-W4)

Depth (meters)	Dominant Geology	Subdominant Geology	Color	Remarks
0–0.6	Lacustrine		Dark Brown	Clayey,Moist
0.6–2.13	Lacustrine		Beige	Silty Clay,Moist
2.13–3.35	Fluvial	Gravel/Bedrock	Brown	Moist,fluvial
3.35–6.10	Till		Red Brown	Moist,clayey
6.10–7.62	Till		Dark Brown	Moist,clayey
7.62–8.23	Fluvial	Sand Lenses	Brown	Moist,sandy
8.23–8.53	Till		Dark Brown	Clayey,Moist
8.53–9.14	Sandstone		Beige	Soft,Moist
9.14–10.97	Shale		Olive	Sandy,Moist
10.97–11.89	Shale	cSh	Very Dark Brown	Moist,cSh
11.89–16.15	Sandstone	Shale	Grey	Moist
16.15–16.76	Sandstone	Shale,cSh	Dark Brown	Moist
16.76–17.68	Sandstone	Shale	Grey	Moist
17.68–17.98	Sandstone	Shale	Black	Moist
17.98–23.77	Sandstone	Shale	Grey	Slightly Moist
23.77–24.38	Coal/cSh		Black	Copious Water
24.38–24.69	Sandstone		Grey	Moist
24.69–25.91	Sandstone	cSh/Coal	Grey–Black	Water
25.91–27.43	Sandstone		Grey	Moist

TESTHOLE NUMBER C1 (Continued)

(SC2–11–23–W4)

Depth (meters)	Dominant Geology	Subdominant Geology	Color	Remarks
27.43–33.83	Shale		Dark Grey	Sandy,Moist
33.83–35.66	cSh	Coal	Grey–Black	Water
35.66–38.10	Sandstone		Grey	Slightly Moist

TESTHOLE NUMBER C2
(NW34-10-23-4)

Depth (meters)	Dominant Geology	Subdominant Geology	Color	Remarks
0-0.46	Glacial		Dark Brown	Moist
0.46-1.83	Glacial		Brown	Saturated
1.83-2.44	Glacial	Gravel/Bedrock	Mottled	Sandy,Saturated
2.44-3.66	Sandstone/Shale	Coal	Mottled	Moist,Weathered
3.66-4.57	Siltstone		Beige	Moist,Weathered
4.57-5.49	Shale	cSh	Dark Red Brown	Sandy, Moist
5.49-6.40	Sandstone		Olive	Water
6.40-7.92	Shale		Reddish	Oxidized
7.92-9.75	Shale		Grey	Slightly Oxidized
9.75-10.67	Shale/Coal	cSh	V.D. Brown-Black	Copious Water
10.67-13.41	Sandstone		Dark Grey	Slightly Moist
13.41-13.72	Sandstone		Grey	Hard,Dry
13.72-19.51	Sandstone		Dark Grey	Sandy,Moist,

TESTHOLE NUMBER C2 (Continued)

(NW34 – 10 – 23 – W4)

Depth (meters)	Dominant Geology	Subdominant Geology	Color	Remarks
19.51 – 19.66	Shale			Hard,Dry
19.66 – 23.47	Shale		Dark Grey	Slightly Moist
23.47 – 24.69	Shale		Dark Grey	Slightly Moist
24.69 – 30.48	Sandstone		Grey	Water

6.2. Piezometer and water-table well completion details.

Piezometer	Date completed	Surface Elevation (mamsl)	Top Pipe Elevation (mamsl)	Height Above Ground (m)	Total Length Pipe (m)	Screened Interval (m)
A1 – 4 w	Fall,1981	976.61	977.03	0.42	3.99	0.50
A2 – 84	Dec. 13,1985	989.70	990.24	0.52	84.66	0.84
A2 – 42	Dec. 13,1985	989.70	990.14	0.52	42.51	0.66
A2 – 14	Dec. 13,1985	989.70	990.24	0.52	14.19	0.71
A2 – 3w	Dec. 13,1985	989.70	990.26	0.54	3.42	slotted
A3 – 69	Dec. 11,1985	972.50	973.08	0.53	69.30	0.84
A3 – 30	Dec. 11,1985	972.50	973.01	0.53	30.81	0.84
A3 – 5w	Dec. 11,1985	972.50	973.01	0.54	5.83	slotted
A4 – 99	Dec. 4,1985	999.36	1000.45	1.02	100.33	0.91
A4 – 56	1984	999.36	1000.07	0.64	56.78	0.60
A4 – 39	1984	999.36	1000.20	0.82	39.55	0.60
A4 – 20	1984	999.36	1000.22	0.87	21.20	0.60
A4 – 7w	1984	999.36	999.92	0.65	7.70	slotted
A5 – 69	Dec. 13,1985	970.13	970.92	0.87	69.71	0.66
A5 – 30	1984	970.13	970.73	0.68	31.06	0.60
A5 – 8	1984	970.13	971.02	0.91	8.90	0.60
A5 – 2	1984	970.13	971.02	0.86	2.80	0.60
A5 – 3w	1984	970.13	970.93	0.63	3.73	slotted
A6 – 41	1984	947.11	947.91	0.76	41.49	0.60

Piezometer	Date Completed	Surface Elevation(mamsl)	Top Pipe Elevation(mamsl)	Height Pipe Above Ground(m)	Total Length Pipe(m)	Screened Interval(m)
A6 – 20	1984	947.11	947.87	0.79	21.00	0.60
A6 – 7	1984	947.11	947.82	0.72	7.73	0.60
A6 – 3w	1984	947.11	947.68	0.57	3.80	slotted
B1 – 69	Dec. 3,1985	969.80	970.24	0.64	69.17	0.91
B1 – 41	Dec. 3,1985	969.60	970.25	0.65	42.01	0.91
B1 – 19	1981	969.60	970.37	0.64	19.17	0.50
B1 – 11	1981	969.60	970.14	0.64	11.44	0.50
B1 – 9	1981	969.60	970.24	0.62	9.64	0.50
B1 – 6	1981	969.60	970.09	0.67	6.69	0.50
B1 – 3w	1981	969.6 – 0	970.12	0.64	3.52	0.50
B2 – 91	Dec. 1,1985	994.38	995.39	0.97	91.80	1.52
B2 – 63	Dec. 1,1985	994.38	995.28	0.87	64.27	1.52
B2 – 34	Dec. 1,1985	994.38	995.34	0.99	35.13	0.91
B2 – 5w	Dec. 1,1985	994.38	995.33	1.00	5.57	slotted
B3 – 16	1973	976.55	977.18	0.63	16.91	no screen
B3 – 6	1973	976.55	977.14	0.59	6.57	no screen
B3 – 3w	1973	976.55	977.16	0.61	3.29	slotted
B4 – 30	Dec. 12,1985	942.55	943.50	0.80	30.68	0.66
B4 – 18	Dec. 12,1985	942.55	943.25	0.55	18. 86	0.66
B4 – 4W	Dec. 12,1985	942.55	943.00	0.76	4.98	slotted

Piezometer	Date Completed	Surface Elevation (mamsl)	Top Pipe Elevation (mamsl)	Height Pipe Above Ground (m)	Total Length Pipe (m)	Screened Interval (m)
C1 - 35	May 14,1985	988.60	989.06	0.53	35.01	1.41
C1 - 25	May 14,1985	988.60	989.04	0.49	25.38	1.41
C1 - 9a	May 14,1985	988.60	989.18	0.64	9.19	1.44
C1 - 6w	May 14,1985	988.60	989.14	0.57	6.09	slotted
C1 - 24	May 14,1985	988.60	989.06	0.40	24.77	1.45
C1 - 34	May 14,1985	988.60	989.08	0.40	34.66	1.42
C1 - 9b	May 14,1985	988.60	1.13	0.43	8.89	1.42
C2 - 30a	May 15,1985	971.03	971.56	0.45	29.54	3.00
C2 - 10	May 15,1985	971.03	971.59	0.57	10.53	1.50
C2 - 7	May 15,1985	971.03	971.50	0.54	7.02	1.50
C2 - 3w	May 15,1985	971.03	971.61	0.58	3.64	slotted
C2 - 30b	May 15,1985	971.03	971.45	0.42	29.61	3.00
C2 - 9	May 15,1985	971.03	971.55	0.50	10.47	1.46
C2 - 6	May 15,1985	971.03	971.53	0.54	6.90	1.50
A1 - 76	Dec. 5,1985	976.61	977.10	0.49	76.86	0.84
A1 - 24	Fall,1981	976.61	977.09	0.48	24.19	0.50
A1 - 9	Fall,1981	976.61	977.06	0.45	9.17	0.50
A1 - 5	Fall,1981	976.61	977.04	0.43	5.99	0.50
A1 - 3	Fall,1981	976.61	977.00	0.39	3.77	0.50

6.3. Hydraulic conductivity (horizontal) values of piezometers.

Geologic Unit	Piezometer	Horizontal hydraulic conductivity(m/s)
Shale(high K values)	B1 – 69	6.0×10^{-8}
	A5 – 30	1.3×10^{-7}
	A6 – 41	1.8×10^{-7}
	B3 – 16 *	5.8×10^{-6}
	B4 – 30	1.7×10^{-7}
Geometric Mean		3.2×10^{-7}
Shale (low K values)	B2 – 91	1.4×10^{-9}
	A1 – 76	2.1×10^{-12}
	A2 – 84	1.6×10^{-10}
	A3 – 69	9.3×10^{-10}
	A4 – 99	4.1×10^{-11}
	A4 – 56	4.3×10^{-12}
	A4 – 20	2.5×10^{-11}
	B2 – 63	4.4×10^{-9}
Geometric Mean		3.9×10^{-11}

* Vertical hydraulic conductivity

Geologic Unit	Piezometer	Horizontal hydraulic conductivity(m/s)
Carbonaceous shale and/or coal	C1 – 35	7.4×10^{-8}
	C1 – 34	1.1×10^{-6}
	C1 – 24	9.5×10^{-8}
	C2 – 10	1.1×10^{-7}
	C2 – 9	2.0×10^{-6}
Geometric Mean		3.0×10^{-7}

Geologic Unit	Piezometer	Horizontal hydraulic conductivity (m/s)
Sandstone (unweathered and/ or bentonitic)	A3 – 30	8.1×10^{-8}
	A1 – 24	4.3×10^{-7}
	A2 – 42	1.3×10^{-7}
	A5 – 69	1.3×10^{-9}
	B1 – 41	1.1×10^{-6}
	B1 – 19	1.1×10^{-8}
Geometric Mean		4.6×10^{-8}

Geologic Unit	Piezometer	Horizontal hydraulic conductivity (m/s)
Lacustrine		
	B1 – 9	2.8×10^{-11}
	B1 – 6	4.9×10^{-11}
	A6 – 7	8.6×10^{-10}
	B4 – 18	5.5×10^{-9}
	B1 – 11	1.2×10^{-8}
Geometric Mean		6.0×10^{-10}
Sandstone (fractured and/or weathered	B2 – 34	8.9×10^{-7}
	C1 – 25	1.1×10^{-7}
	C2 – 30a	1.1×10^{-5}
	C2 – 30b	2.4×10^{-7}
	C 2 – 7	5.0×10^{-6}
	C2 – 6	1.4×10^{-5}
	A1 – 9	6.4×10^{-5}
	A5 – 8	6.3×10^{-8}
	B3 – 6	3.0×10^{-5}
Geometric Mean		2.7×10^{-6}

6.4. Hydrographs

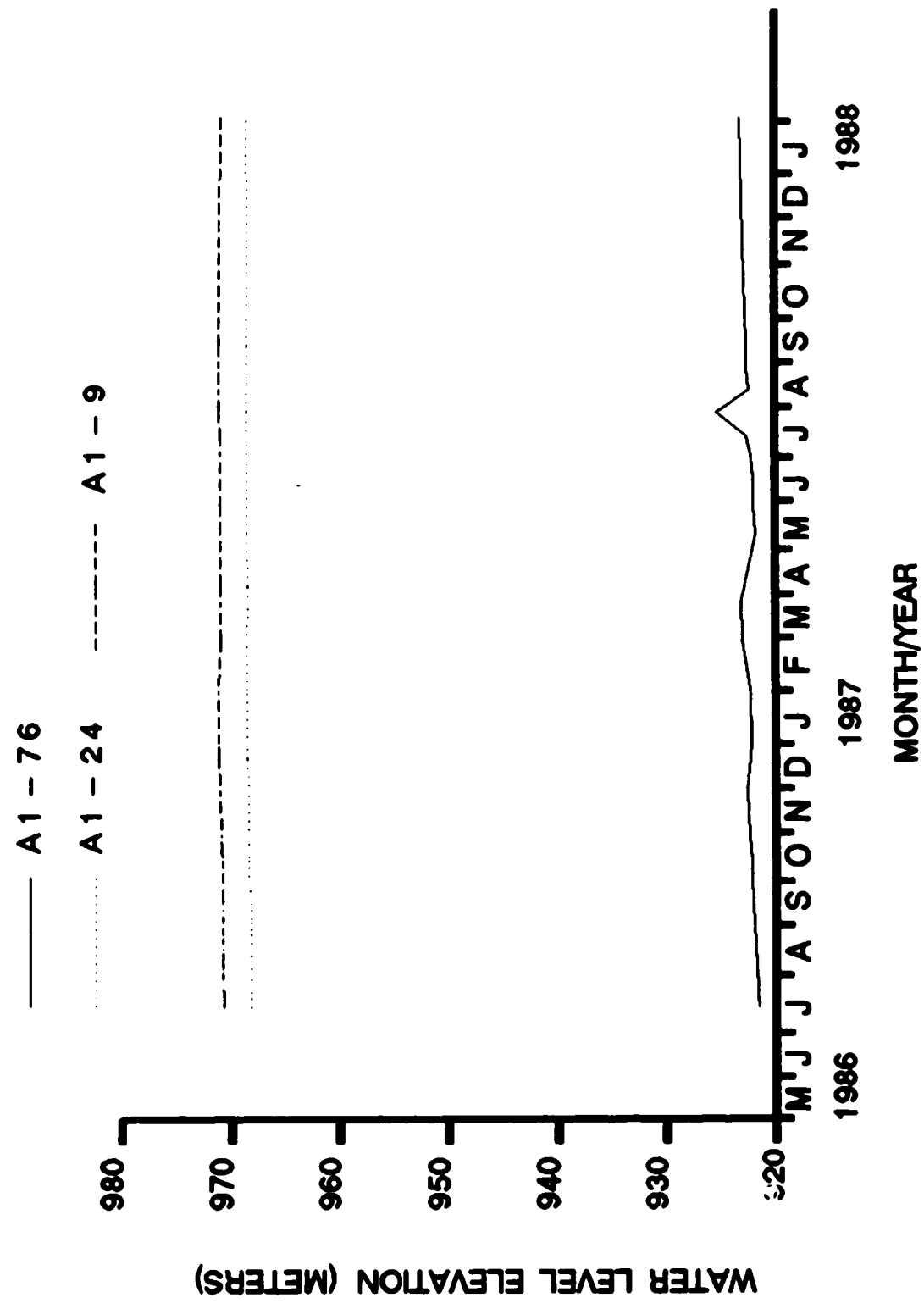
A1 - 76
A1 - 24
A1 - 9
980
970
960
950
940
930
920
WATER LEVEL ELEVATION (METERS)
M J J A S O N D J F M A M J J A S O N D J
1986
1987
1988
MONTH/YEAR

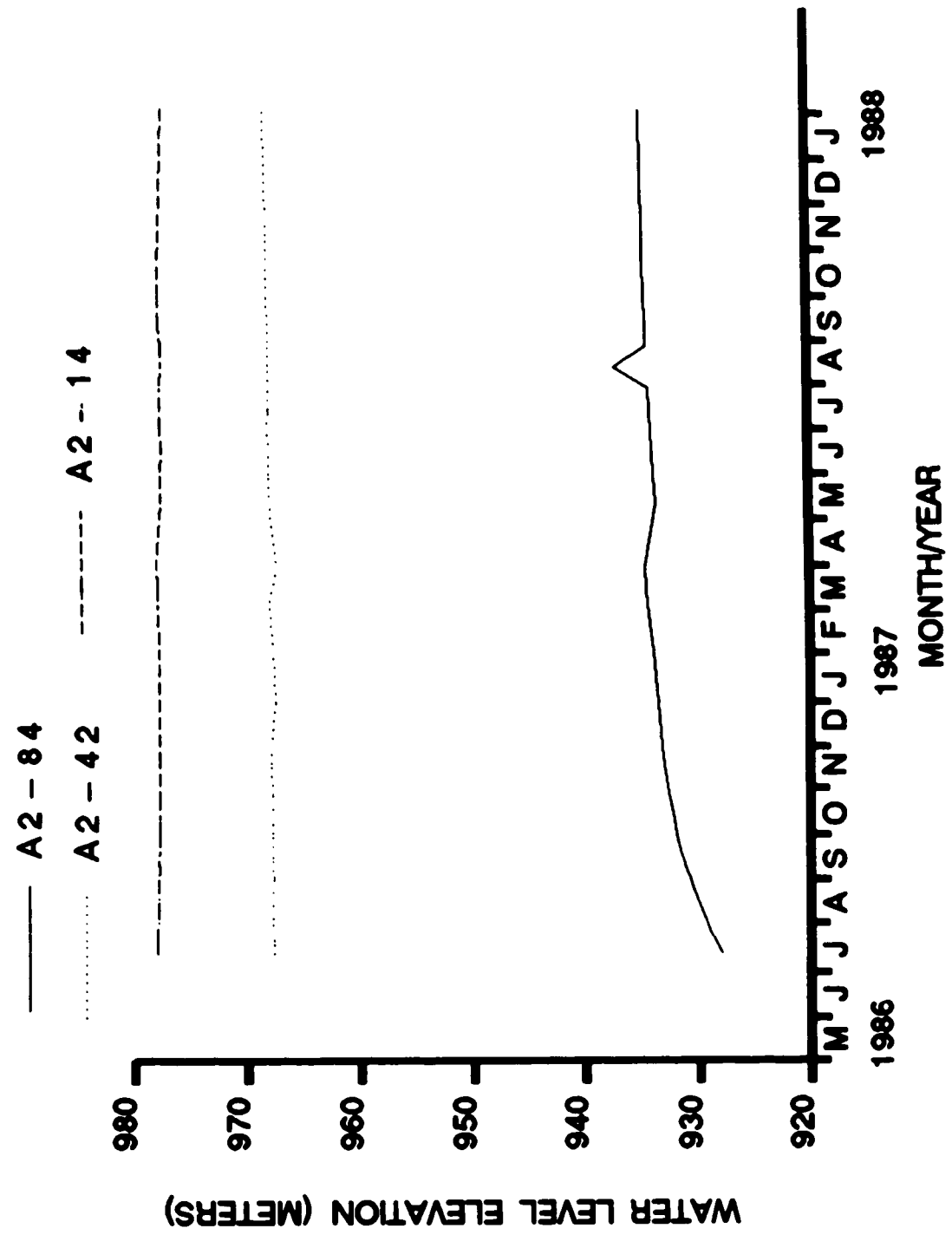
A2-84
A2-42
A2-14
WATER LEVEL ELEVATION (METERS)
980
970
960
950
940
930
920
M J J A S O N D J F M A M J J A S O N D J
1986
1987
1988
MONTH/YEAR

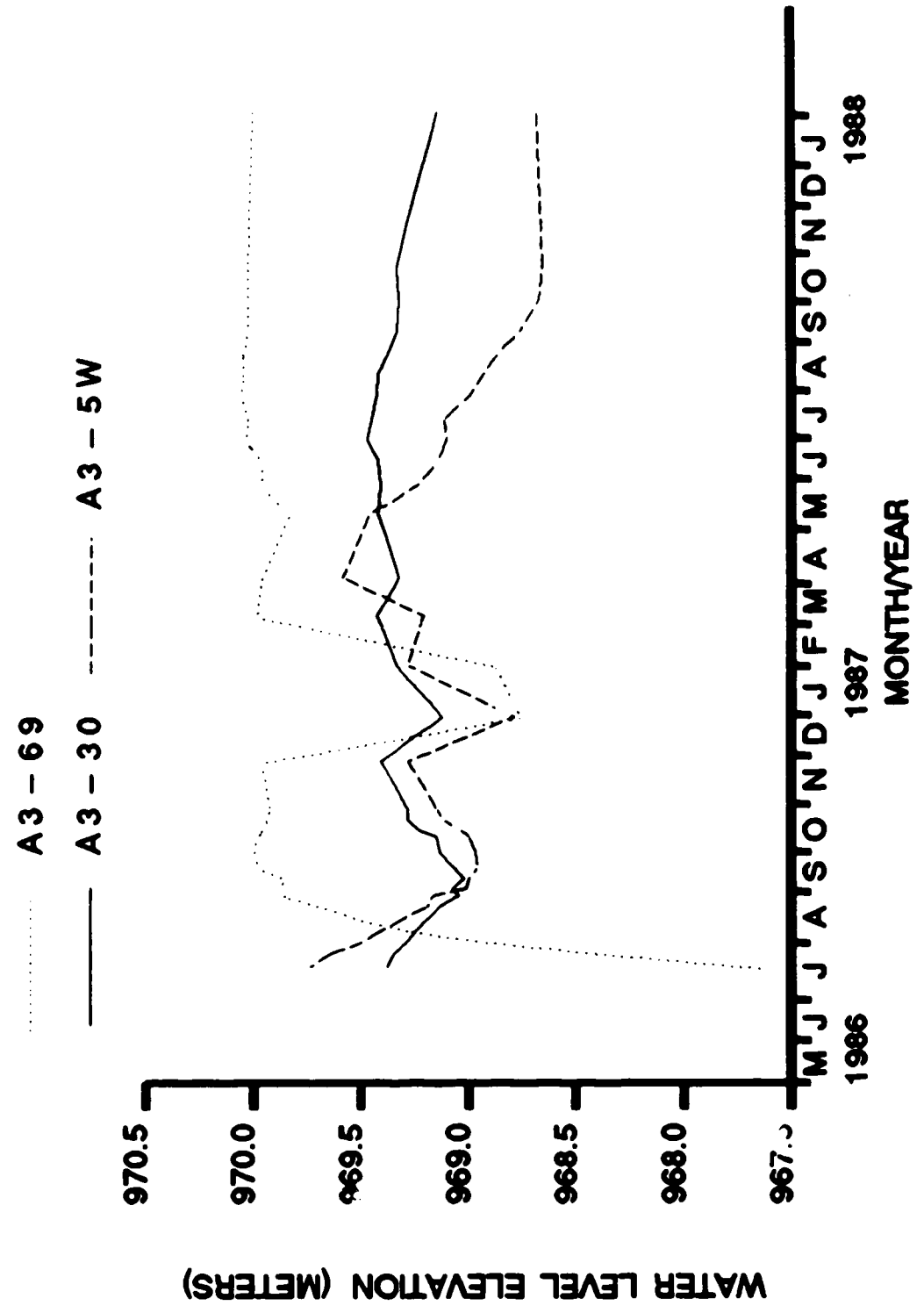
A3 – 69
A3 – 30
A3 – 5W
970.5
970.0
969.5
969.0
968.5
968.0
967.5
WATER LEVEL ELEVATION (METERS)
M J J A S O N D J F M A M J J A S O N D J
1986
1987
1988
MONTH/YEAR

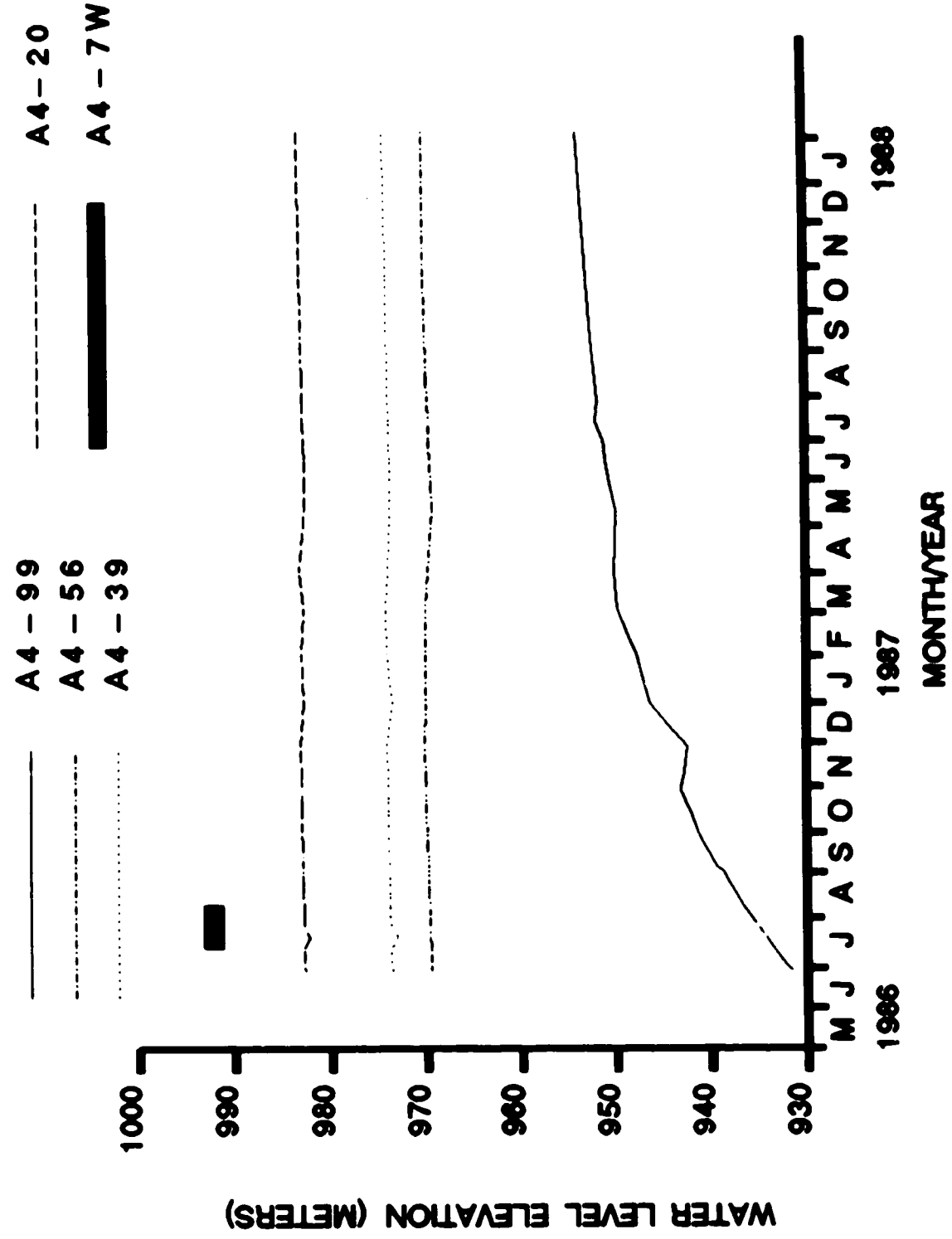
A4-99
A4-56
A4-39
A4-20
A4-7W
1000
990
980
970
960
950
940
930
WATER LEVEL ELEVATION (METERS)
M J J A S O N D J F M A M J J A S O N D J
1986
1987
1988
MONTH/YEAR

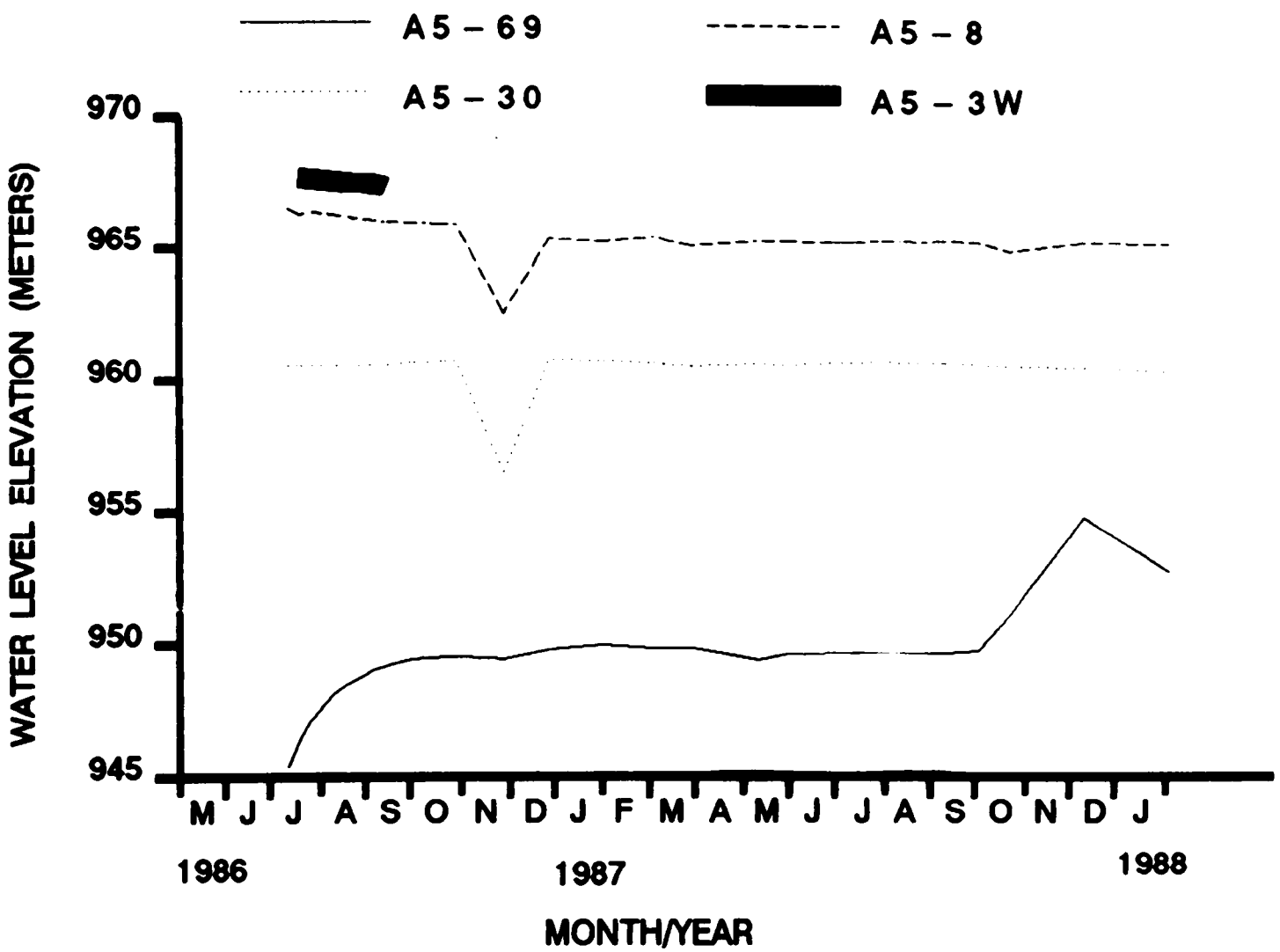
A5 – 69
A5 – 8
A5 – 30
A5 – 3W
970
965
960
955
950
945
WATER LEVEL ELEVATION (METERS)
M J J A S O N D J F M A M J J A S O N D J
1986
1987
1988
MONTH/YEAR

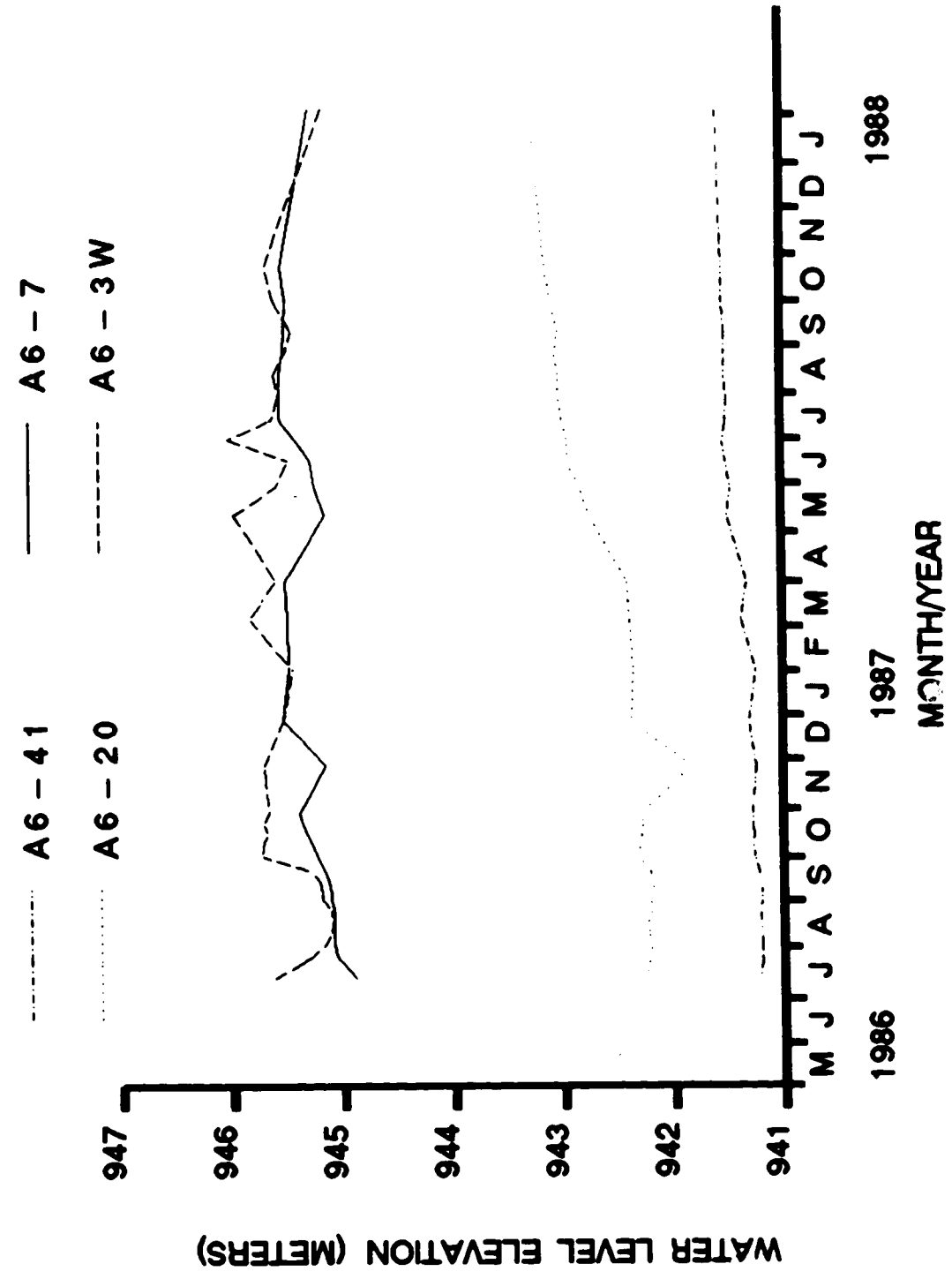
A6 – 41
A6 – 20
A6 – 7
A6 – 3W
947
946
945
944
943
942
941
WATER LEVEL ELEVATION (METERS)
M J J A S O N D J F M A M J J A S O N D J
1986
1987
1988
MONTH/YEAR

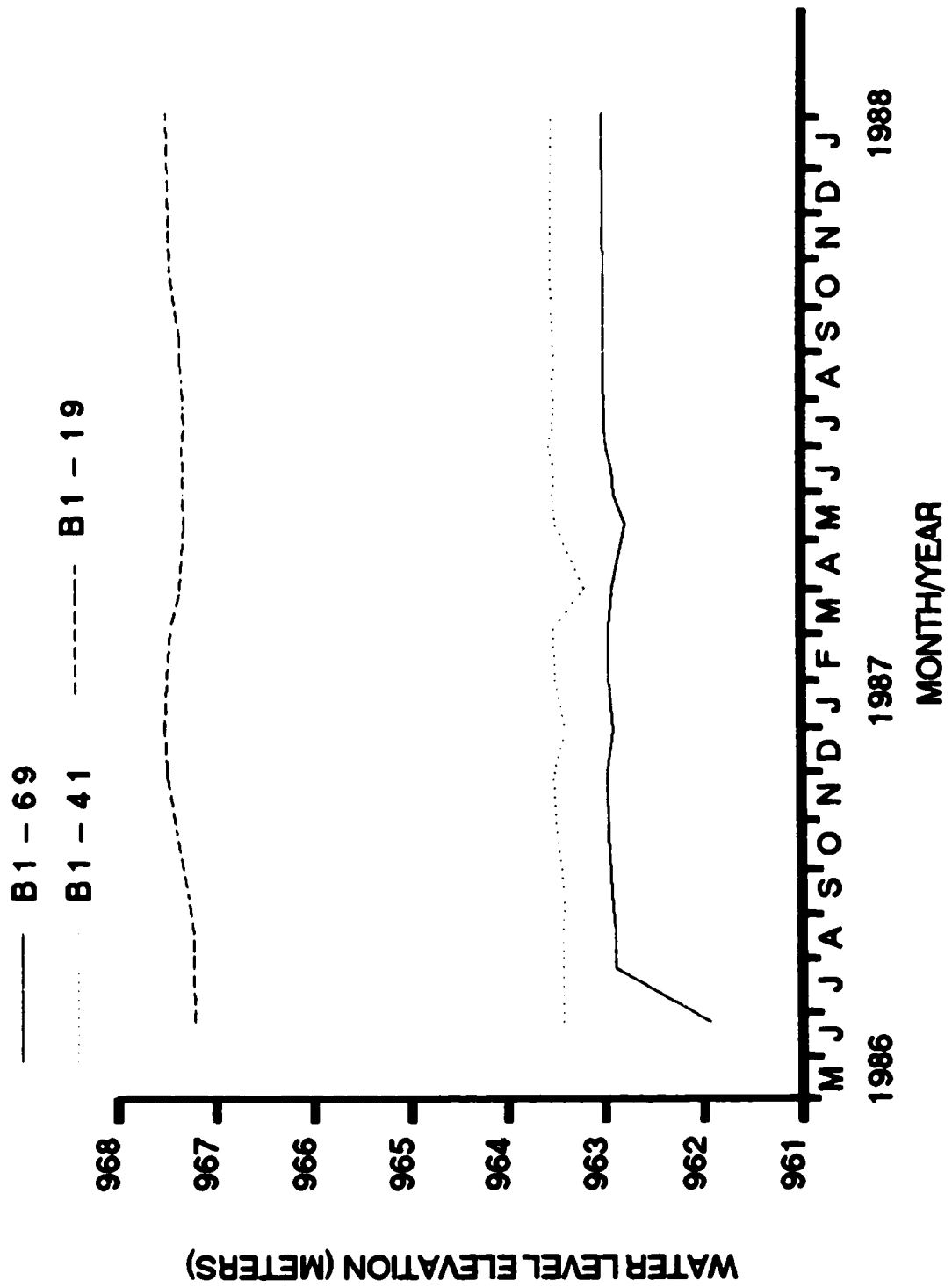
B1 – 69
B1 – 41
B1 – 19
968
967
966
965
964
963
962
961
WATER LEVEL ELEVATION (METERS)
M J J A S O N D J F M A M J J A S O N D J
1986
1987
1988
MONTH/YEAR

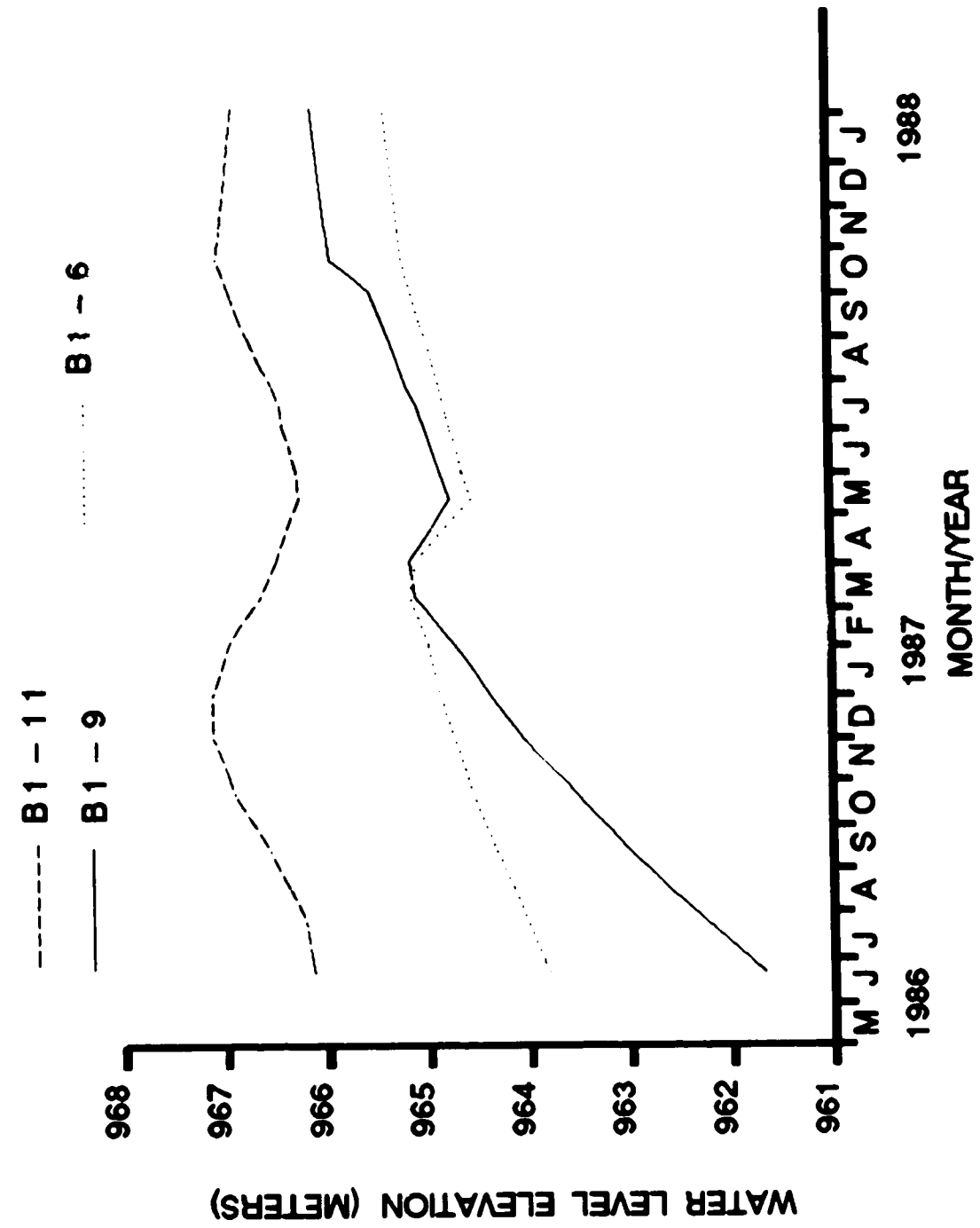
B1 - 11
B1 - 9
B1 - 6
968
967
966
965
964
963
962
961
WATER LEVEL ELEVATION (METERS)
M J J A S O N D J F M A M J J A S O N D J
1986
1987
1988
MONTH/YEAR

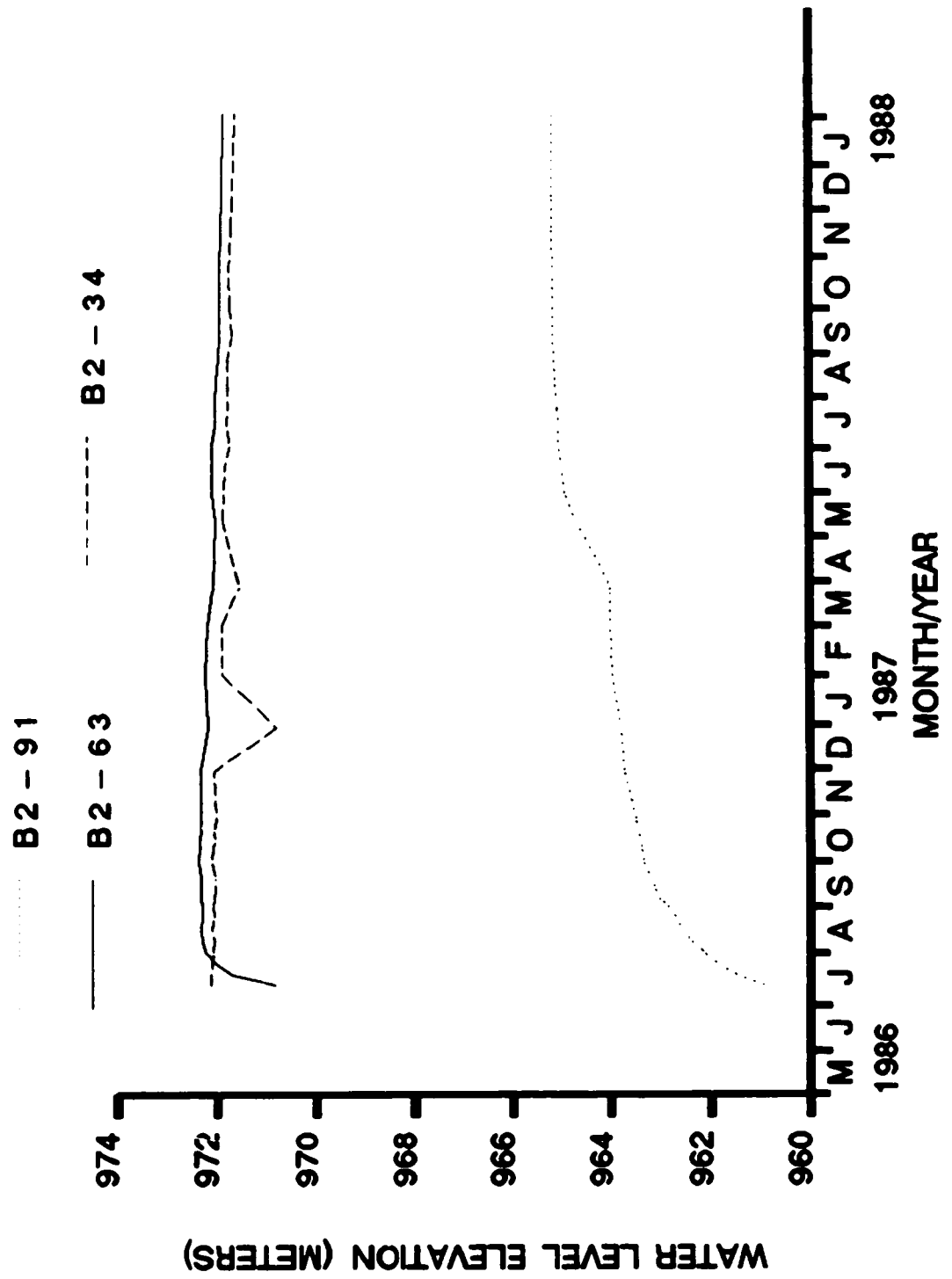
B2 - 91
B2 - 63
B2 - 34
974
972
970
968
966
964
962
960
WATER LEVEL ELEVATION (METERS)
M J J A S O N D J F M A M J J A S O N D J
1986
1987
1988
MONTH/YEAR

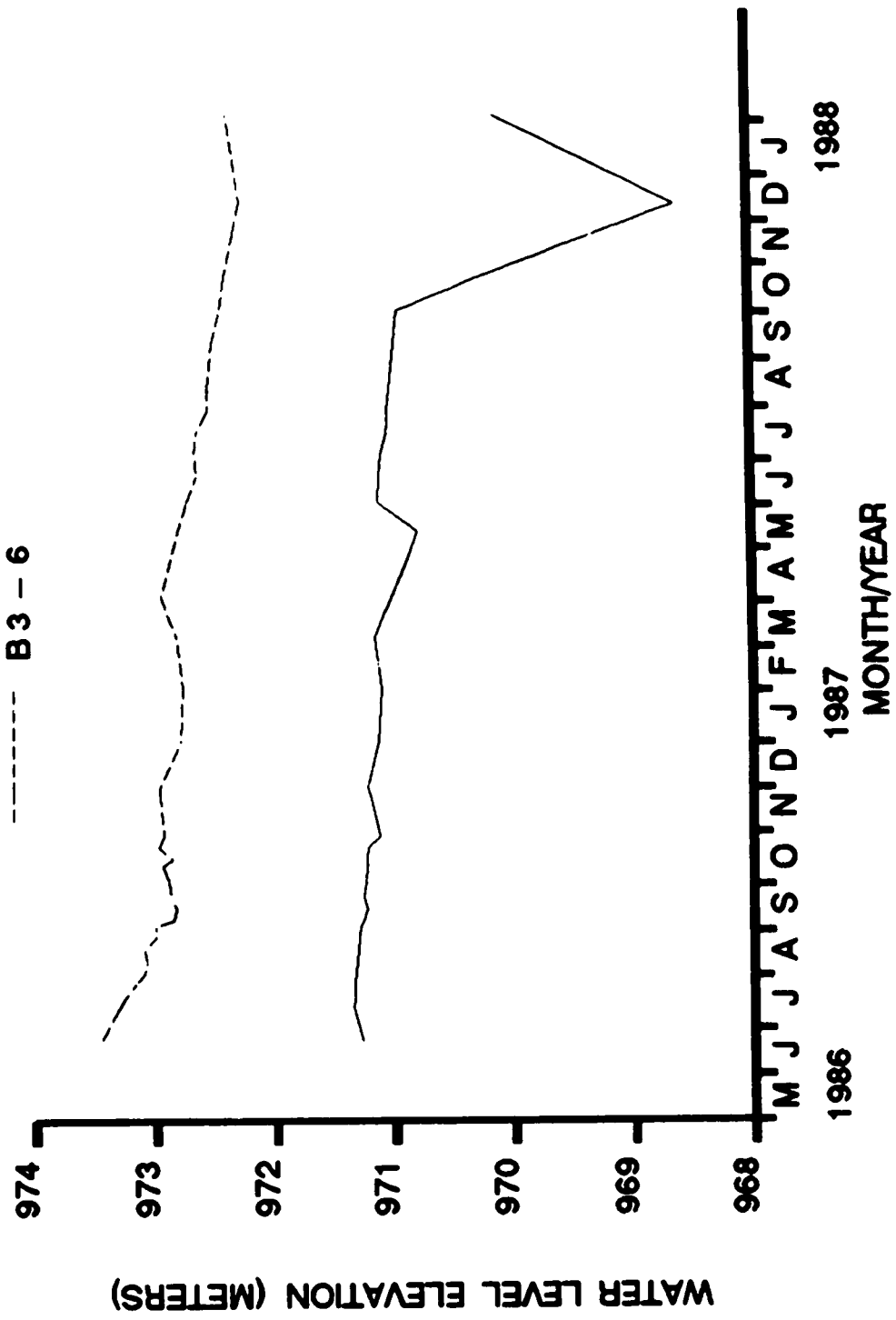
B3 – 16
B3 – 6
974
973
972
971
970
969
968
WATER LEVEL ELEVATION (METERS)
M J J A S O N D J F M A M J J A S O N D J
1986
1987
1988
MONTH/YEAR

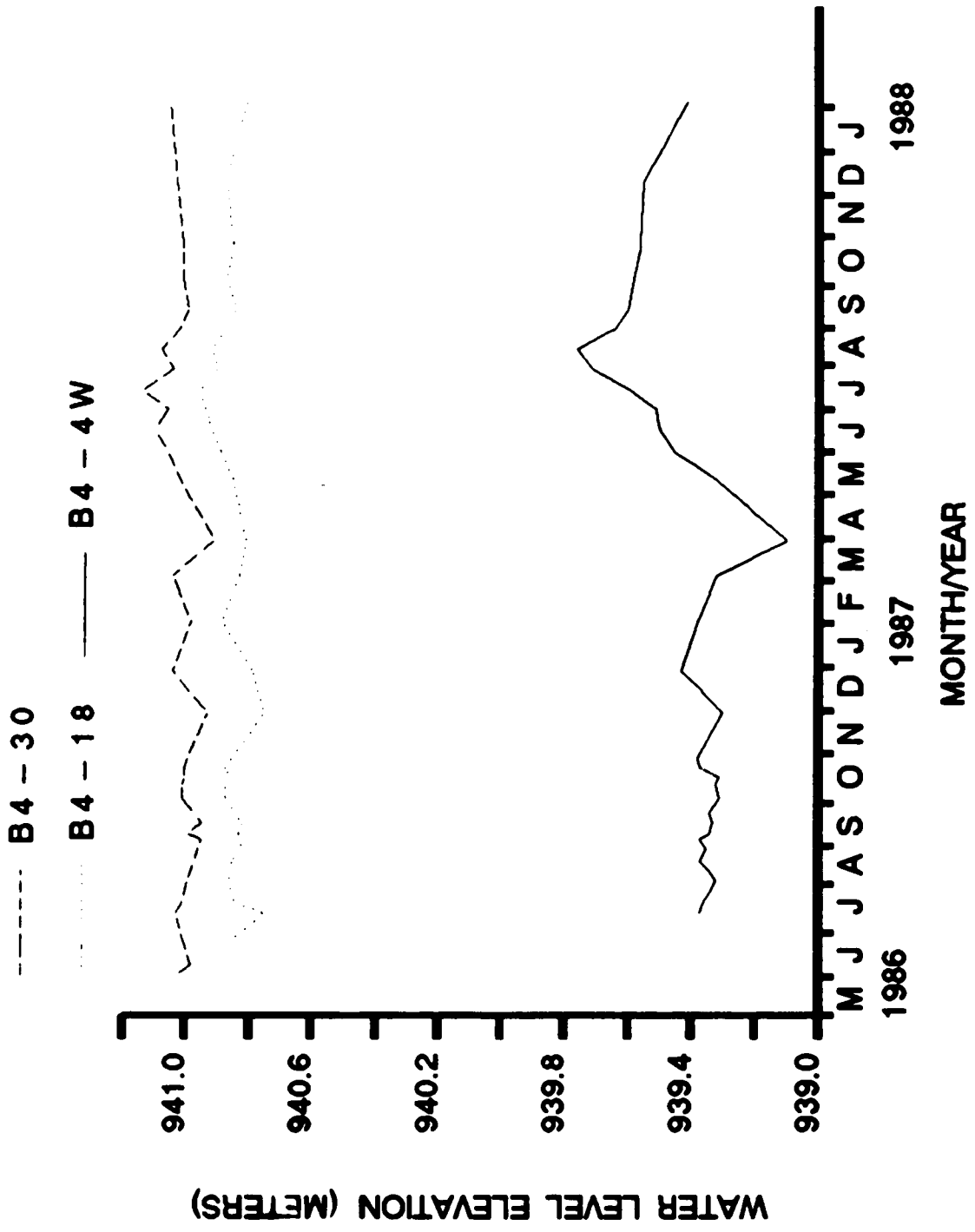
B4 - 30
B4 - 18
B4 - 4W
941.0
940.6
940.2
939.8
939.4
939.0
WATER LEVEL ELEVATION (METERS)
M J J A S O N D J F M A M J J A S O N D J
1986
1987
1988
MONTH/YEAR

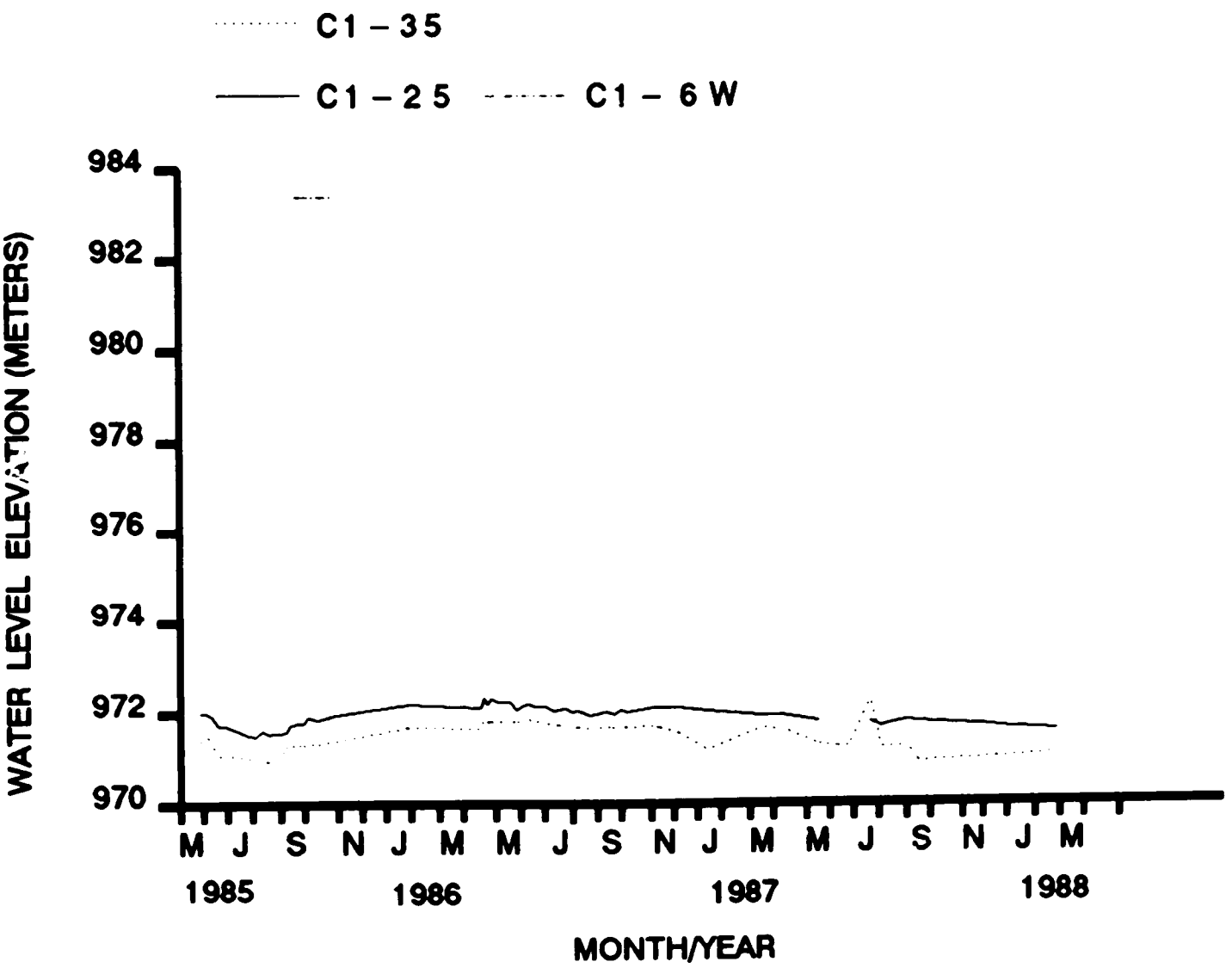
C1 – 35
C1 – 25
C1 – 6 W
WATER LEVEL ELEVATION (METERS)
984
982
980
978
976
974
972
970
M J S N J M M J S N J M M J S N J M
1985
1986
1987
1988
MONTH/YEAR

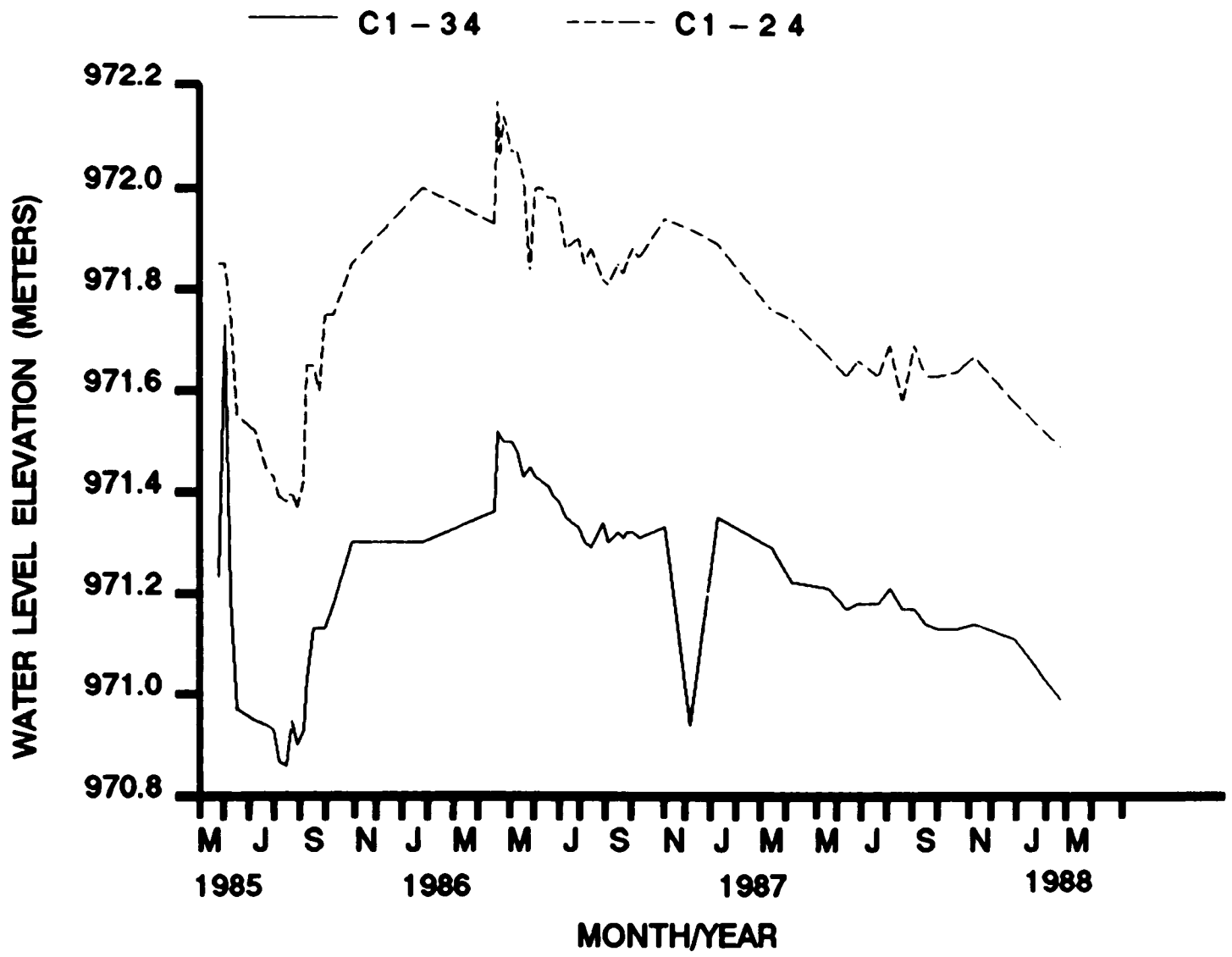
C1 – 34
C1 – 24
WATER LEVEL ELEVATION (METERS)
972.2
972.0
971.8
971.6
971.4
971.2
971.0
970.8
M J S N J M M J S N J M M J S N J M
1985
1986
1987
1988
MONTH/YEAR

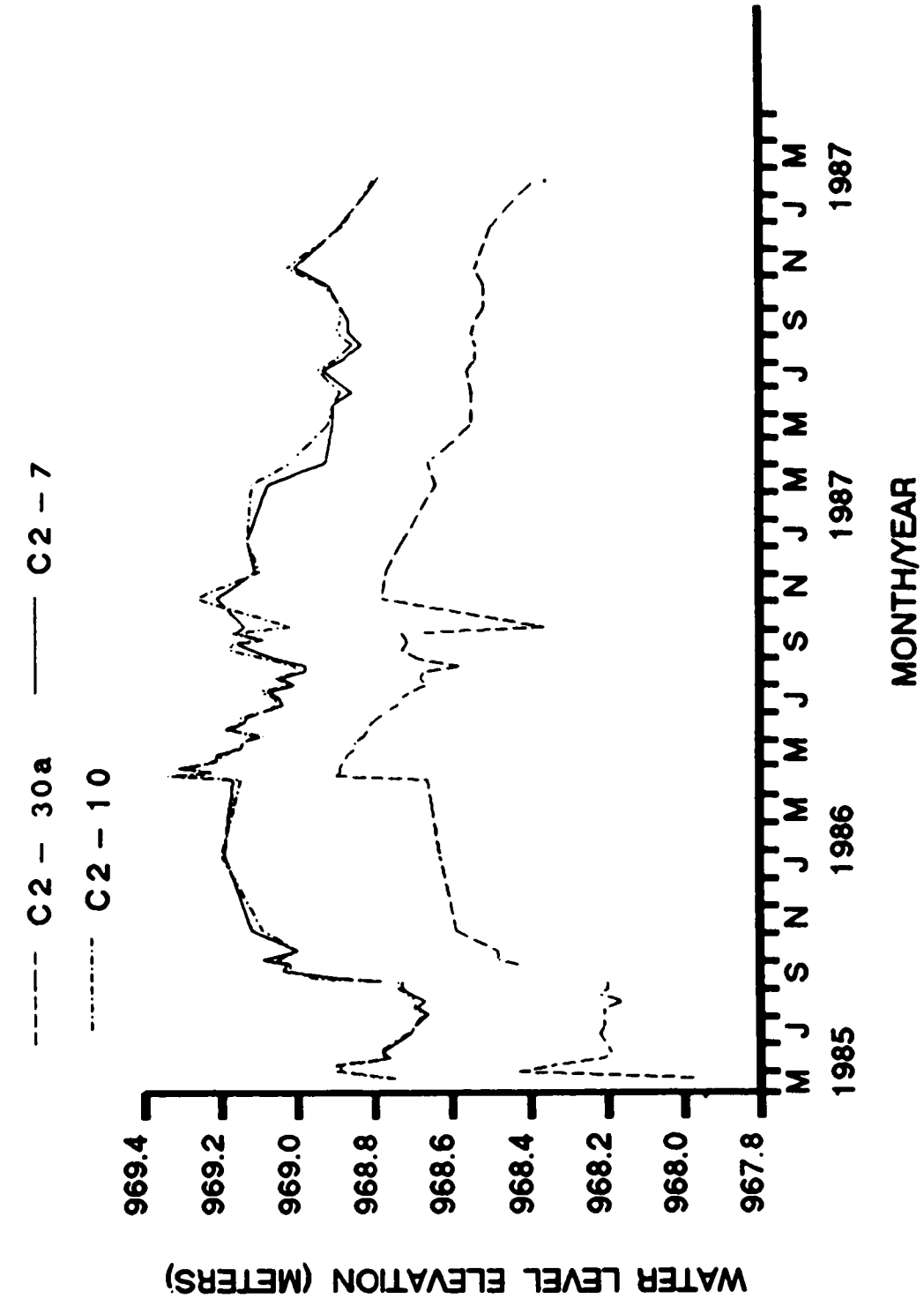
C2 – 30a
C2 – 7
C2 – 10
969.4
969.2
969.0
968.8
968.6
968.4
968.2
968.0
967.8
WATER LEVEL ELEVATION (METERS)
M J S N J M M J S N J M J S N J M
1985
1986
1987
1987
MONTH/YEAR

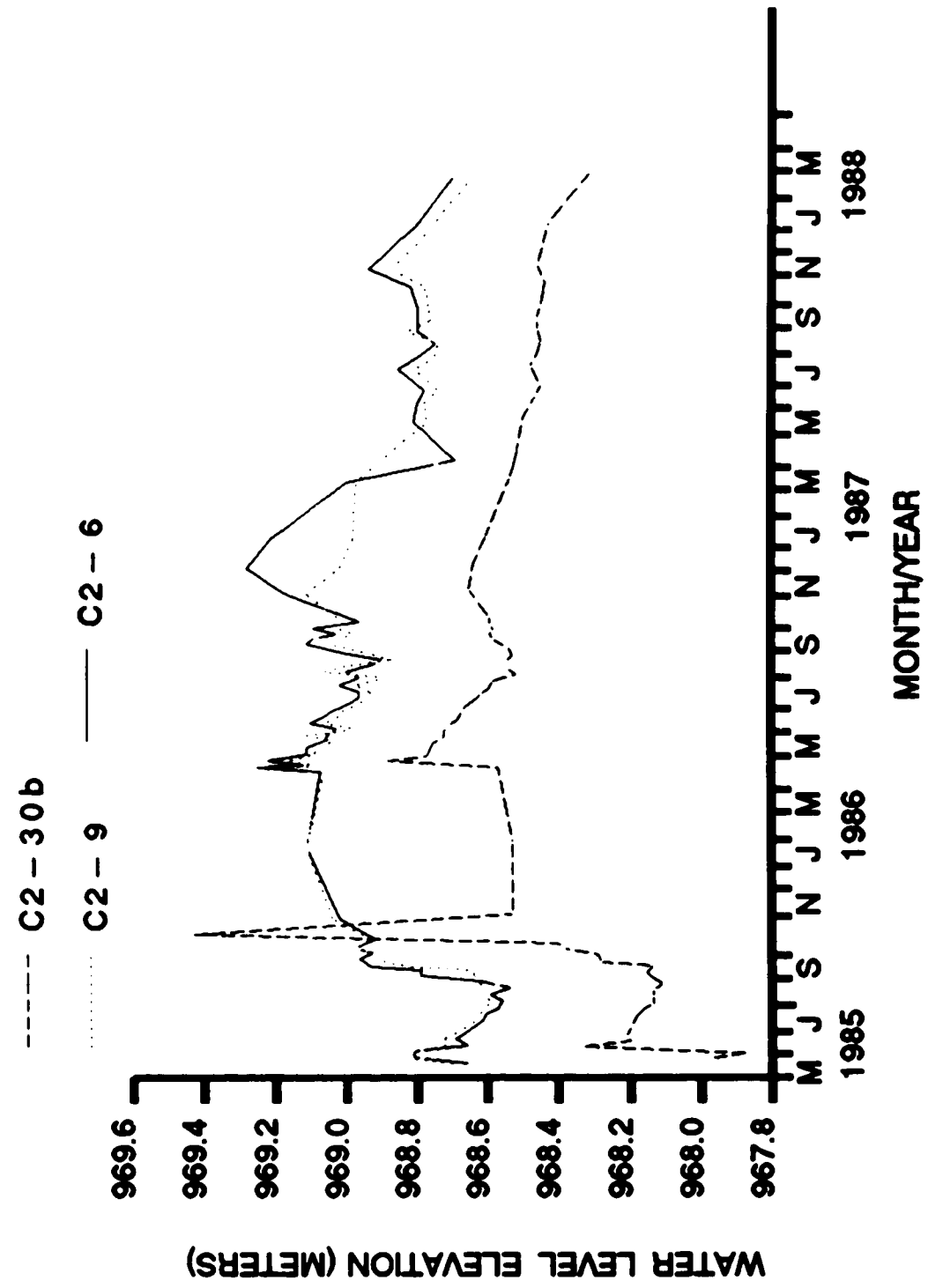
C2 – 30b
C2 – 9
C2 – 6
WATER LEVEL ELEVATION (METERS)
969.6
969.4
969.2
969.0
968.8
968.6
968.4
968.2
968.0
967.8
M J S N J M M J S N J M M J S N J M
1985
1986
1987
1988
MONTH/YEAR

6.5. Tritium content of groundwaters.

Tritium activity (TU = Tritium Units) of water samples taken in May, 1987, from A – line piezometers and water – table wells.

Piezometer or Well	Activity (TU)
A1 – 76	10 (+/– 1)
A1 – 24	<2
A1 – 9	<2
A2 – 84	20 (+/– 1)
A2 – 42	16 (+ –1)
A2 – 14	95 (+ –8)
A3 – 69	2 (+/– 1)
A3 – 30	<2
A3 – 5W	46 (+/– 1)
A4 – 99	28 (+/– 7)
A4 – 56	53 (+/– 8)
A4 – 39	46 (+/– 8)
A4 – 20	19 (+/– 8)
A5 – 69	20 (+/– 7)
A5 – 30	<2
A6 – 41	<2
A6 – 20	16 (+ –1)
A6 – 7	6 (+/– 1)
A6 – 3W	41 (+/– 2)

Tritium activity (TU = Tritium Units) of water samples taken in May, 1987, from B – line piezometers and water table wells.

Piezometer or Well	Activity (TU)
B1 – 69	2(+/–1)
B1 – 41	2(+/–1)
B1 – 19	<3
B1 – 11	<2
B1 – 9	<2
B1 – 6	<2
B2 – 91	9(+/–1)
B2 – 63	<17
B2 – 34	29(+/–9)
B3 – 16	<2
B3 – 6	18(+/–1)
B4 – 30	<20
B4 – 18	<20
B4 – 4W	58(+/–10)

Tritium activity (TU = Tritium Units) of water samples taken in May, 1987, from C – line piezometers and wells.

Piezometer or Well	Activity (TU)
C1 – 35a	<2
C1 – 25	<2
C1 – 24	<2
C1 – 35b	3(+/–1)
C2 – 30a	<2
C2 – 10	7(+/–1)
C2 – 7	10(+/–1)
C2 – 3w	11(+/–1)
C2 – 30b	<2
C2 – 9	11(+/–1)
C2 – 6	11(+/–1)

6.6. Chemistry of saturation paste extracts from soil profiles.

Horizon	Depth (cm)	EC (dS m^{-1})	pH (H_2O)	Na	K	Ca	Mg	SO_4	CO_3	HCO_3	Cl
				mmole (±) L^{-1}							
Site A1. Calcareous Dark Brown Chernozem											
Apk	0- 15	4.9	7.5	26.5	0.47	22.0	17.5	58.0	0.0	2.5	1.1
Bmk	15- 30	5.9	7.6	37.8	0.62	23.4	19.7	73.7	0.0	2.9	1.6
Cca	30- 50	2.5	7.6	8.6	0.38	14.0	6.4	20.3	0.0	2.6	2.1
Ck	50- 60	1.1	7.5	0.3	0.41	8.7	1.2	3.1	0.0	3.7	0.8
Site A2. Orthic Dark Brown Chernozem											
Ap	0- 30	0.7	7.0	0.3	0.96	4.5	1.1	2.9	0.0	3.7	0.2
Bm1	30- 44	0.4	7.2	0.6	0.09	3.0	0.7	3.4	0.0	2.5	0.1
Bm2	44-56	0.5	7.6	0.5	0.10	3.9	1.1	3.3	0.0	3.3	0.1
Cca	56- 85	0.6	7.9	1.4	0.12	3.4	1.6	3.3	0.0	2.6	0.1
Site A3. Saline Calcareous Dark Brown Chernozem											
Apksa	0- 13	--	--	13.7	1.33	29.1	36.2	96.6	0.0	3.6	4.9
Bmksa	13- 27	--	--	50.7	0.31	17.7	69.9	151.4	0.0	2.8	1.2
Ccasa	27- 60	--	--	84.3	0.19	22.9	110.2	224.8	0.0	2.8	11.8
Cksa	60+	--	--	40.1	0.15	16.8	118.1	187.9	0.0	1.5	9.4
Site A4. Calcareous Dark Brown Chernozem											
Apk	0- 20	0.7	7.8	0.4	0.32	5.6	0.7	3.4	0.0	3.5	0.2
Bmk	20- 36	0.4	8.0	0.4	0.11	3.0	0.7	3.0	0.0	2.8	0.1
Cca	36- 43	0.5	8.1	0.5	0.13	2.8	1.4	3.0	0.0	3.2	0.1
R	43- 56	0.5	7.9	1.1	0.18	2.0	1.9	3.4	0.0	2.8	0.2
Site A5. Orthic Dark Brown Chernozem											
Ap	0- 16	1.5	8.0	2.2	0.15	12.4	3.3	10.9	0.0	2.5	0.6
Bm	16- 34	6.7	7.7	0.7	0.62	5.2	1.2	3.4	0.0	6.1	0.2
Ck	34-100	5.0	8.7	46.8	0.13	2.3	6.2	48.1	0.0	3.0	0.9
Site A6. Calcareous Dark Brown Chernozem											
Ap	0- 17	1.4	7.2	1.5	1.03	10.8	3.6	3.9	0.0	10.7	0.5
Bmk	17- 36	3.0	7.8	21.5	0.15	9.1	4.2	24.2	0.0	3.8	2.2
Cca	36- 90	1.2	8.4	6.6	0.15	1.5	4.5	7.7	0.0	3.5	0.7
Site B1. Orthic Dark Brown Chernozem											
Ap	0- 7	1.4	7.8	15.1	0.70	3.9	0.9	9.0	0.0	5.1	0.3
Bm1	7- 34	0.6	7.1	0.7	0.24	4.7	1.2	4.8	0.0	3.4	0.3
Bm2	34- 58	0.5	7.4	1.1	0.12	3.4	1.3	4.0	0.0	3.8	0.1
Bm3	58- 74	0.7	7.5	1.8	0.17	4.3	1.8	4.4	0.0	4.9	0.1
Ck	74+	3.6	7.7	8.4	0.27	23.6	21.5	49.0	0.0	2.3	0.9

Horizon	Depth (cm)	EC (dS m^{-1})	pH (H_2O)	Na	K	Ca	Mg	SO_4	CO_3	HCO_3	Cl
				mmole (+) L^{-1}							
Site B2. Orthic Dark Brown Chernozem											
Ap	0- 8	0.7	7.8	3.8	0.34	4.0	0.6	4.6	0.0	5.9	0.2
Bm	8- 16	0.5	7.6	0.6	0.13	4.1	0.5	4.1	0.0	3.8	0.4
Ck	16- 49	0.4	7.9	1.3	0.12	2.7	0.5	4.0	0.0	3.4	0.1
IICk	49- 92	0.6	8.0	1.3	0.13	2.5	2.6	3.5	0.0	4.4	0.2
Site B3. Saline Calcareous Dark Brown Chernozem											
Apks	0- 8	6.0	7.8	21.8	0.93	31.7	46.1	87.5	0.0	6.2	1.1
Bmksa	8- 19	9.2	8.0	47.0	0.48	25.6	76.7	119.1	0.0	3.7	2.9
Cksa	19- 96	11.1	8.3	70.2	0.64	25.2	68.5	103.4	0.0	1.5	14.3
Site B4. Orthic Dark Brown Chernozem											
Ap	0- 13	1.3	7.7	6.3	0.48	5.4	2.6	9.0	0.0	3.4	0.3
Bm	13- 33	1.1	7.5	1.8	0.76	7.0	2.7	7.2	0.0	4.7	0.3
Ck	33-110	0.7	8.0	1.6	0.12	2.8	2.8	4.0	0.0	2.5	0.6
Site C1. Orthic Dark Brown Chernozem											
Ap1	0- 10	1.3	7.7	2.1	0.95	8.5	1.6	4.9	0.0	4.3	0.4
Ap2	10- 21	0.4	7.7	0.6	0.27	3.3	0.7	1.0	0.0	2.6	0.2
Bm1	21- 44	0.4	7.7	0.8	0.04	2.3	1.0	1.2	0.0	1.6	0.2
Bm2	44- 59	0.4	7.8	0.5	0.03	3.0	0.8	1.0	0.0	2.3	0.2
BC	59- 72	0.5	7.9	0.7	0.06	3.3	1.0	1.5	0.0	1.7	0.2
Cca1	72-115	0.4	8.3	0.8	0.04	1.8	1.2	1.1	0.0	3.5	0.2
Cca2	115-152	0.9	8.6	5.2	0.05	1.5	2.9	6.0	0.0	3.2	0.2
Ck	152-180	0.8	8.8	6.6	0.05	0.2	1.3	4.0	0.0	4.0	0.2
Site C2. Saline Carbonated Gleyed Regosol											
Apksgj	0- 7	2.8	7.5	13.5	1.84	10.1	9.9	12.5	1.5	14.2	1.4
AC	7- 13	23.5	8.0	246.6	1.66	27.8	81.7	355.8	0.2	8.6	8.5
Ccasa1	13- 24	32.5	8.6	347.6	0.59	35.8	95.7	492.0	0.0	3.7	18.4
Ccasa2	24- 30	21.1	8.6	256.2	0.23	17.1	44.4	288.0	0.0	2.2	10.2
Ccasa3	30- 49	15.6	8.6	181.2	0.21	13.5	28.1	199.0	0.0	2.0	6.8
Cksa1	49- 63	13.2	8.7	149.4	0.22	12.6	24.9	154.8	0.0	1.7	6.6
Cksa2	63- 88	12.4	8.5	133.8	0.26	15.5	28.4	149.4	0.0	1.6	5.3
Cksa3	88-160	11.1	8.5	114.6	0.29	16.4	26.4	132.0	0.0	1.4	5.3
ICksag	160-175	9.4	8.2	97.2	0.37	19.0	13.9	113.4	0.0	1.7	2.7
IICksg	175-184	4.7	8.3	42.5	0.18	4.6	4.1	47.0	0.0	1.8	1.1
IICksa	184-200	7.8	8.0	75.6	0.39	24.8	12.0	95.0	0.0	1.5	1.3
IVCks	200+	5.7	8.4	53.1	0.16	5.0	5.7	58.5	0.0	2.0	2.0

Horizon	Depth (cm)	EC (dS m^{-1})	pH (H_2O)	Na	K	Ca	Mg	SO_4	CO_3	HCO_3	Cl
				- - - - - - - - - - - - mmole ($\pm$) L^{-1} - - - - - - - - - -							
EC 10-11-23-4. Saline Orthic Dark Brown Chernozem											
Ap	0- 13			199.1	1.43	16.7	31.1	229.9	0.0	4.9	14.9
Bm	13- 28			440.9	1.31	30.5	174.6	615.2	0.0	3.2	44.4
Ck	28+			635.0	1.19	9.2	487.0	1095.1	0.0	5.1	101.4
NE 27-10-23-4. Saline Rego Dark Brown Chernozem											
Apk	0- 15			89.8	13.62	29.5	48.3	159.6	1.0	11.6	9.2
Cksa	15- 45			263.8	2.99	75.3	45.8	353.8	0.0	3.3	21.1
Ck1	45- 65			185.8	0.63	11.5	65.4	244.5	0.0	2.1	16.2
Ck2	65- 90			160.7	0.38	5.3	53.0	209.3	0.0	2.1	13.2
NW 21-10-23-4. Alkaline Solonetz or Solonetz											
Ap	0- 3			24.9	1.13	5.5	4.5	21.0	0.7	13.3	0.5
Bn	3- 16			93.1	0.55	13.5	7.7	128.2	0.0	4.4	0.7
Bnj	16- 40			532.3	0.46	16.3	94.0	649.7	0.0	4.0	2.1
Cksa	40+			622.7	0.49	12.3	190.3	823.2	0.0	4.2	1.8
WC 10-11-23-4. Solodized Solonetz											
Ap	0- 10			137.8	3.62	17.5	27.2	165.2	0.0	7.2	16.5
Ae	10- 13			269.1	3.12	18.4	41.3	302.5	0.0	4.4	17.8
Bnt	13- 32			345.4	3.52	11.8	138.0	483.1	0.0	3.0	21.8
Cksa	32+			486.7	4.92	33.5	322.5	830.5	0.0	2.3	22.0
SE 29-10-23. Saline Orthic Dark Brown Chernozem											
Apsa	0- 10			23.0	4.60	10.7	24.8	81.0	0.0	6.5	1.1
Bmsa	10- 15			55.8	0.56	11.4	27.5	109.0	0.0	2.2	2.9
Bmksa	15- 25			145.7	0.14	14.1	41.0	200.4	0.0	2.1	2.8
Cca	25- 50			331.2	0.27	21.0	90.2	546.5	0.0	2.5	11.8
Ck	50+			392.6	0.48	21.4	144.7	436.3	0.0	2.6	10.8

6.7. Piper-diagrams

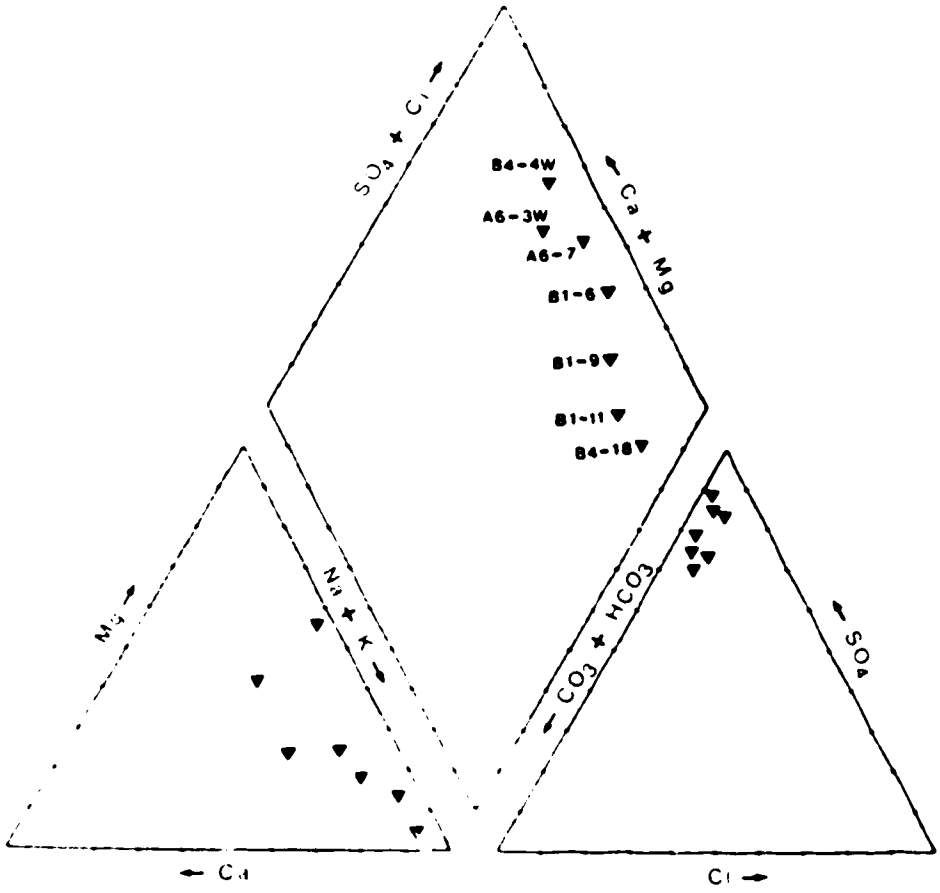

Piper diagram-ion facies of groundwaters from the drift along the A-,B-, and C-Line sections.

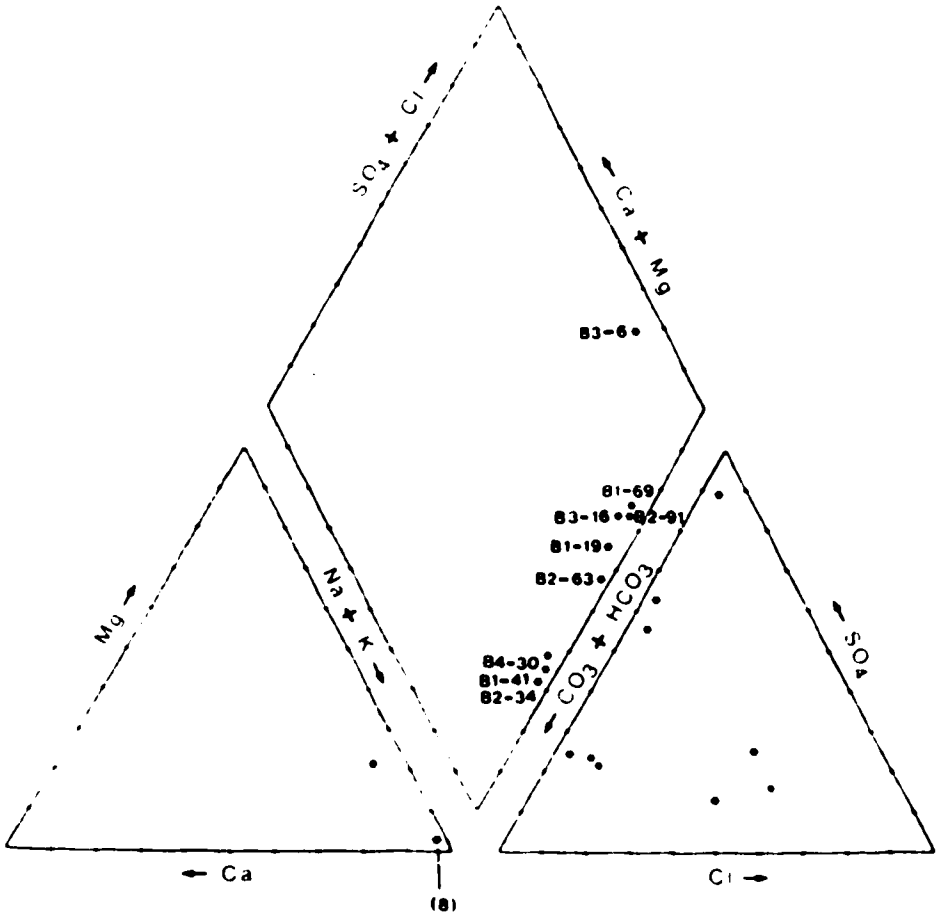

Piper diagram-ion facies of groundwaters from the bedrock along the B-Line section.

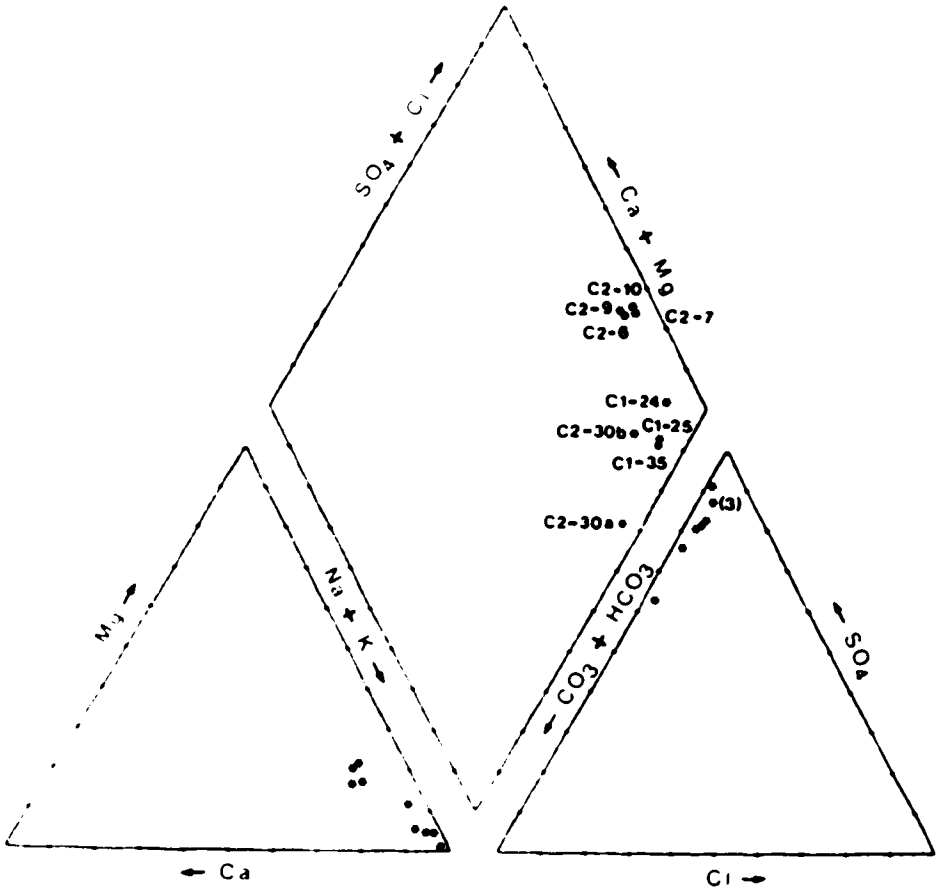

Piper diagram-ion facies of groundwaters from the bedrock along the C-Line section.

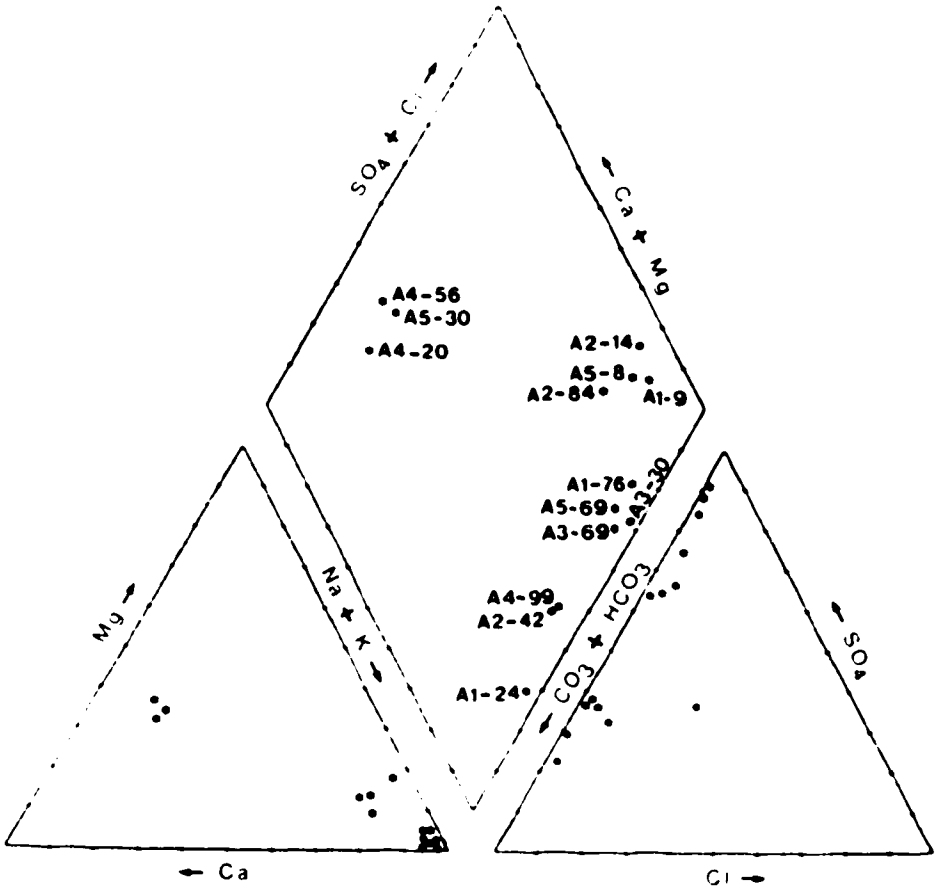

Piper diagram-ion facies of groundwaters from the bedrock along the A-Line section.

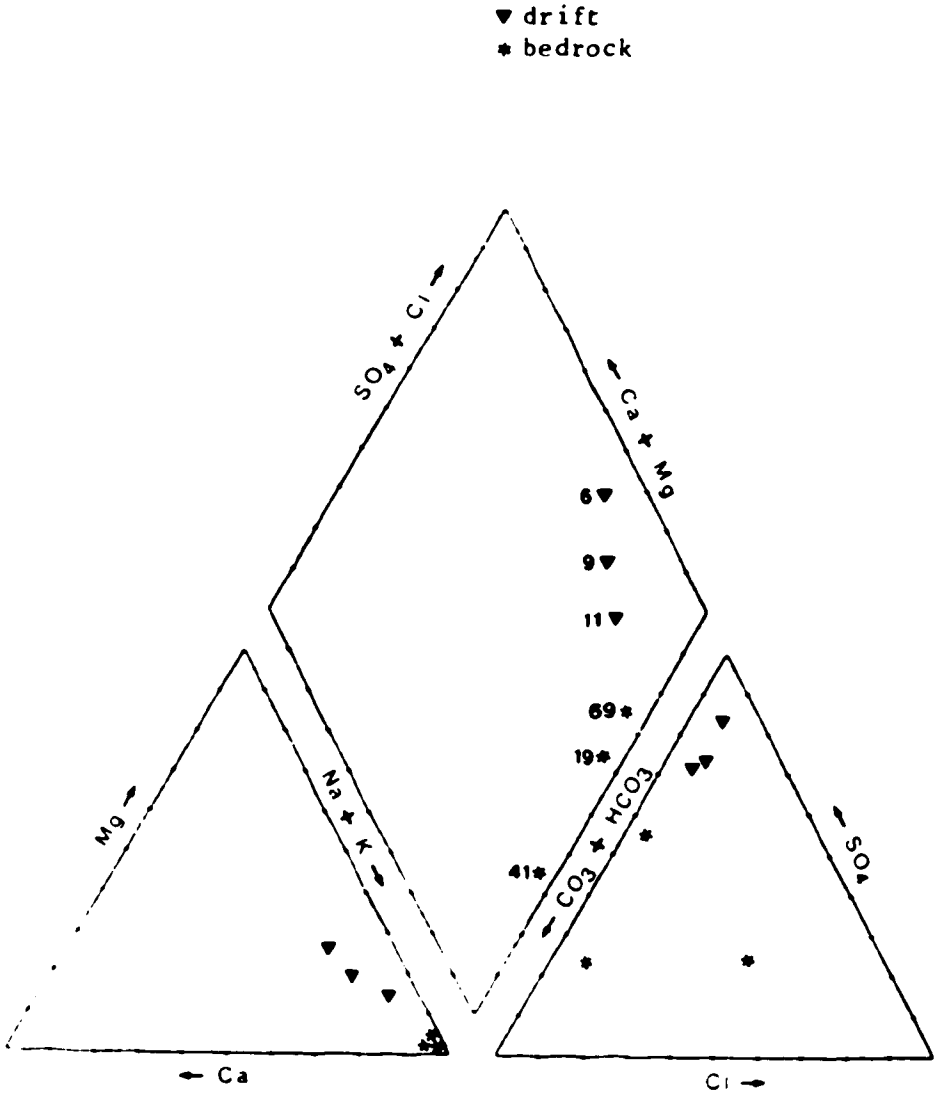

Piper diagram-ion facies of groundwaters from the drift and bedrock at Site B1.

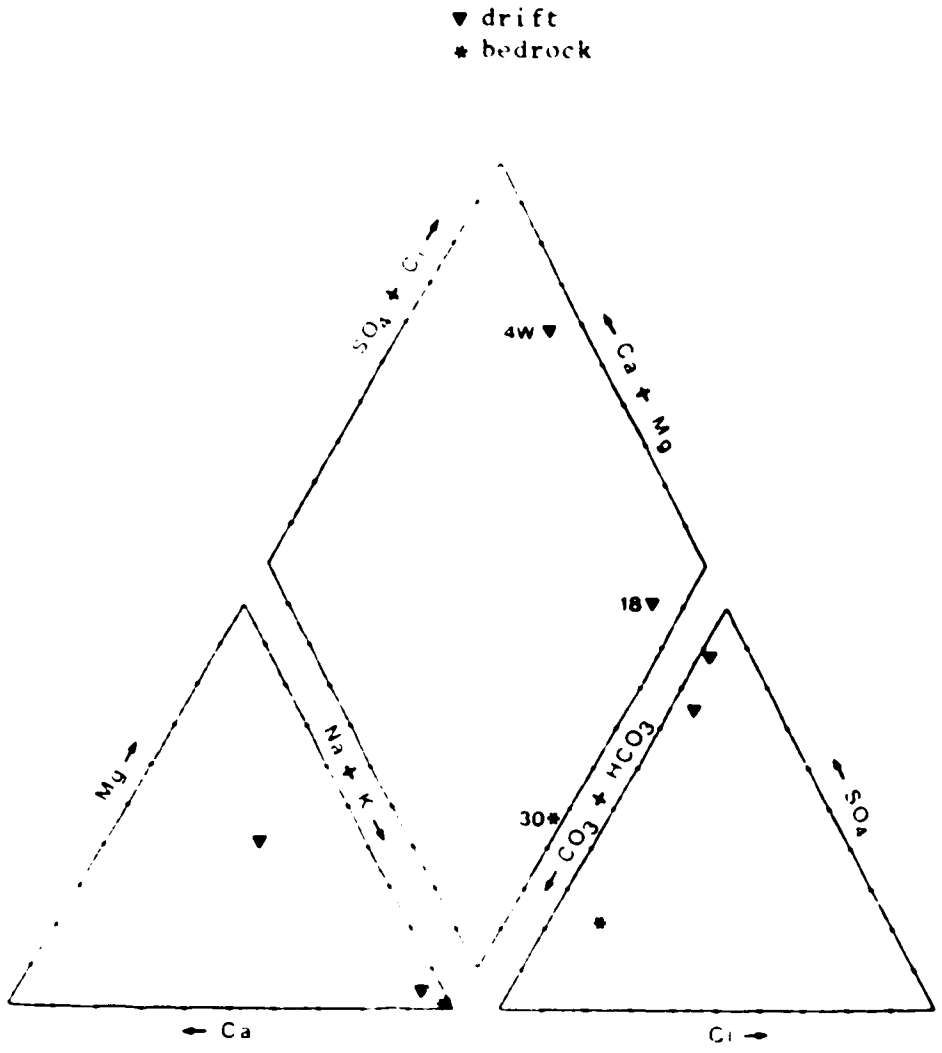

Piper diagram-ion facies of groundwaters from the drift and bedrock at Site B4.

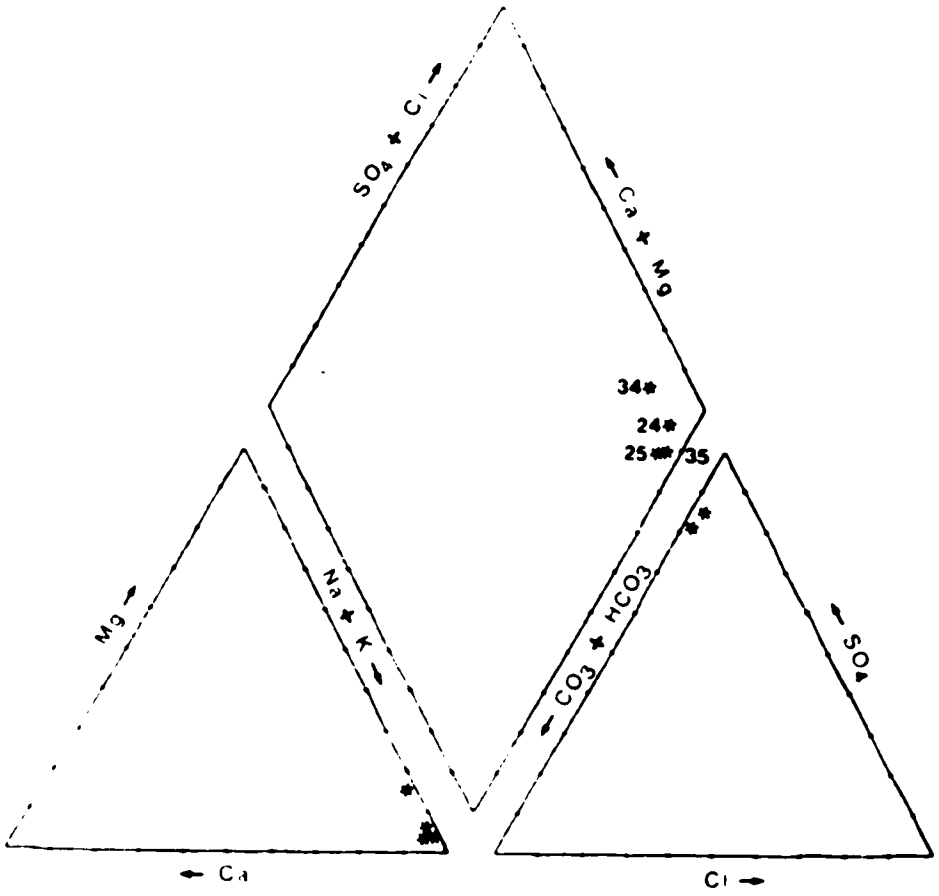

Piper diagram-ion facies of groundwaters from the bedrock at Site C1.

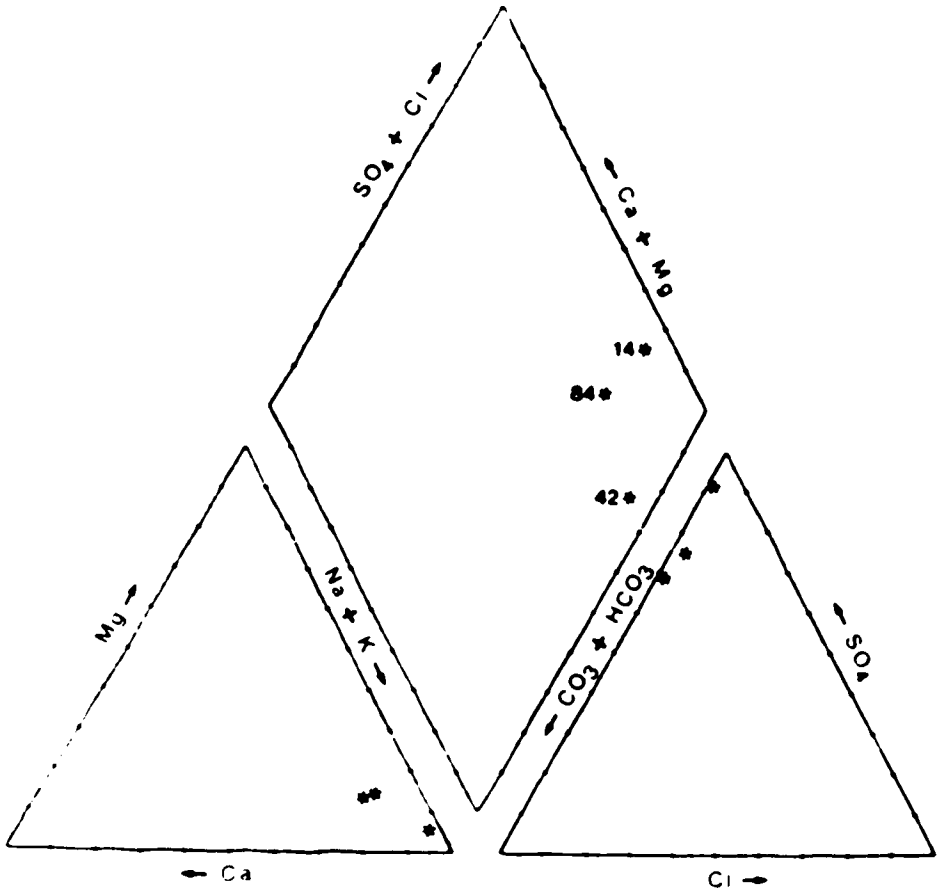

Piper diagram-ion facies of groundwaters from the bedrock at Site A2.

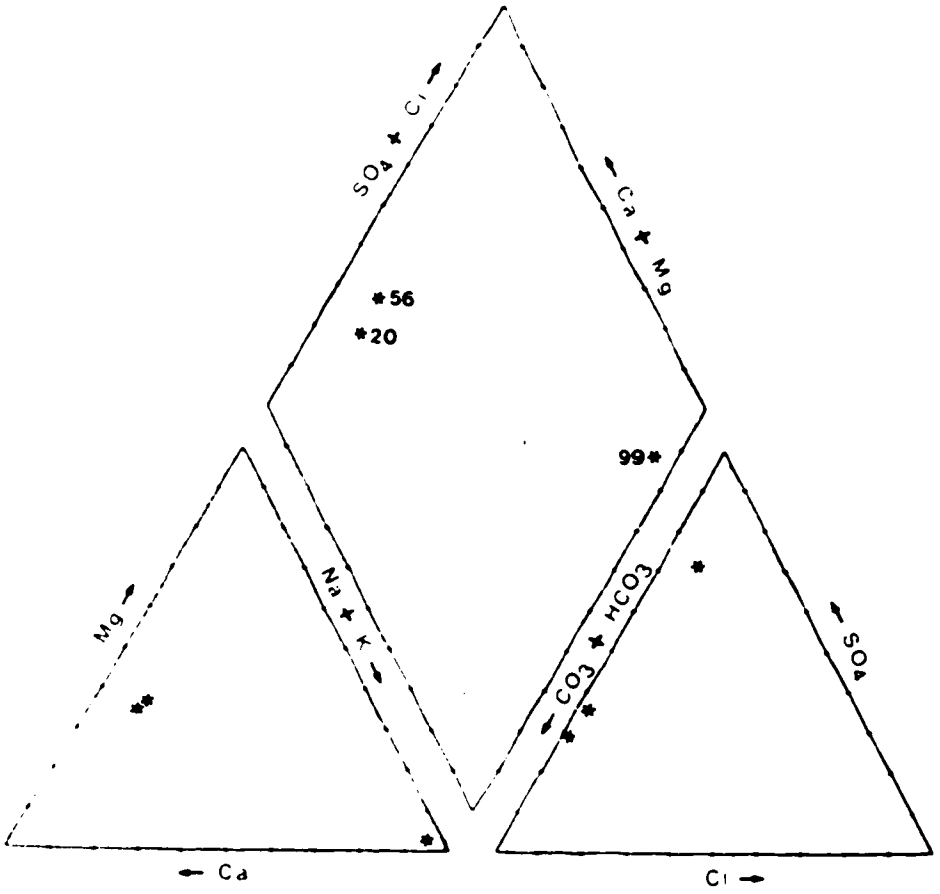

Piper diagram-ion facies of groundwaters from the bedrock at Site A4.

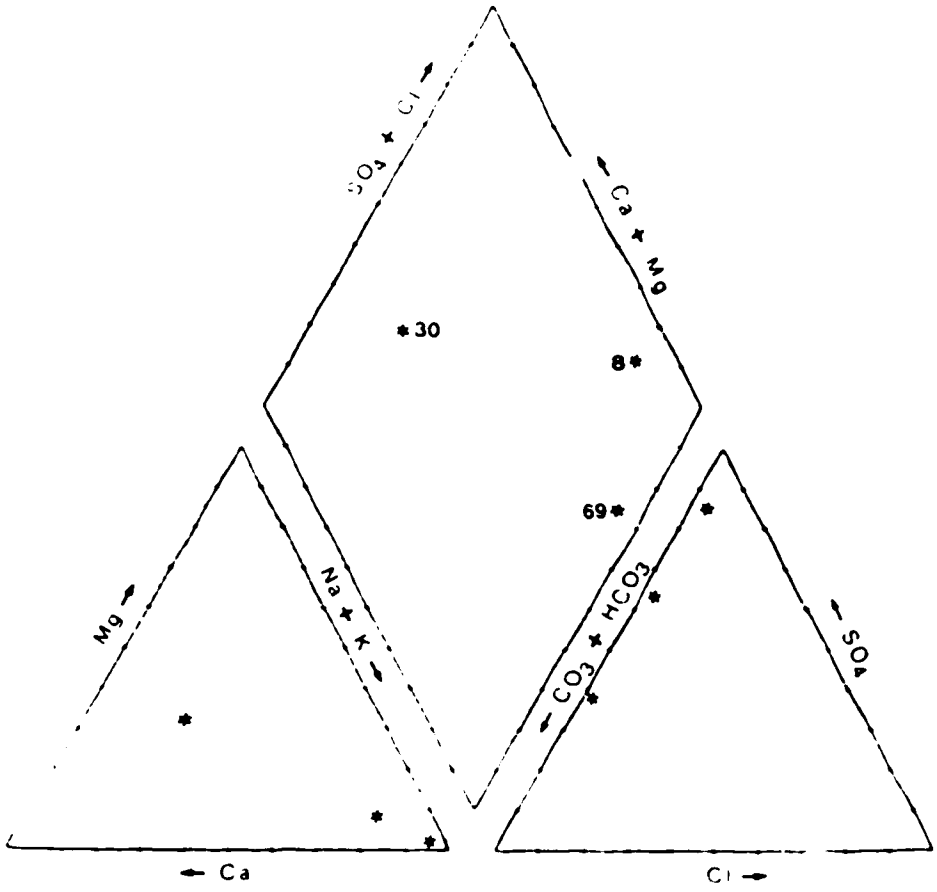

Piper diagram-ion facies of groundwaters from the bedrock at Site A5.

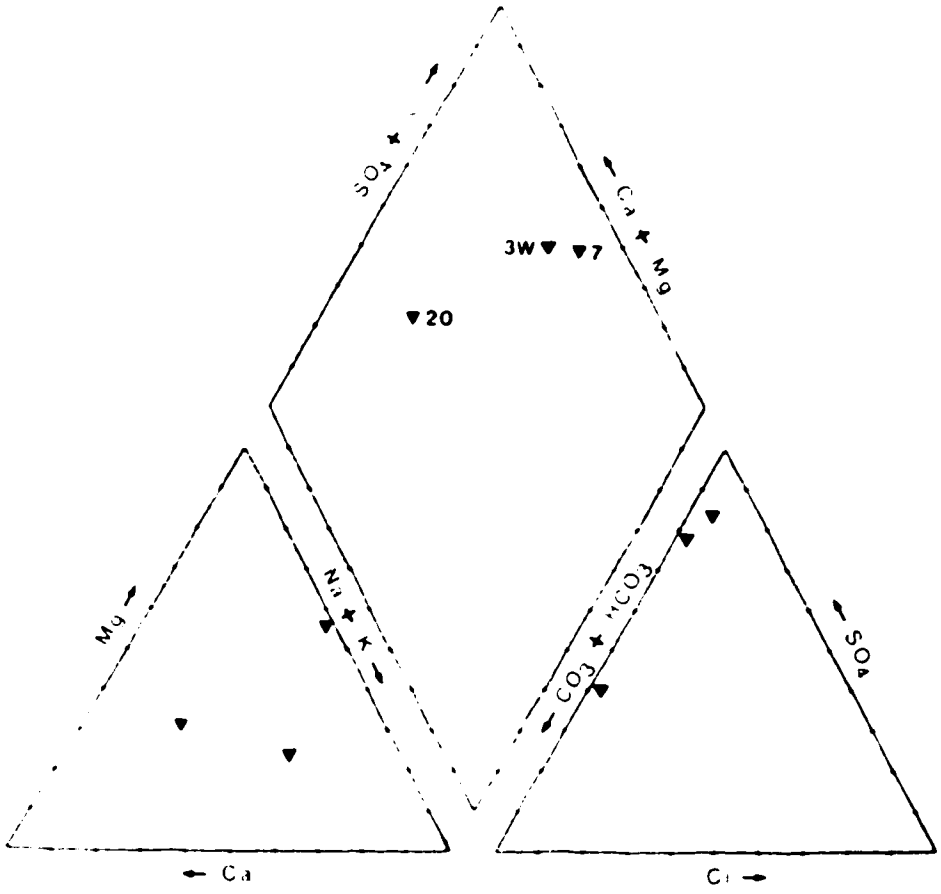

Piper diagram-ion facies of groundwaters from the drift at Site A6.

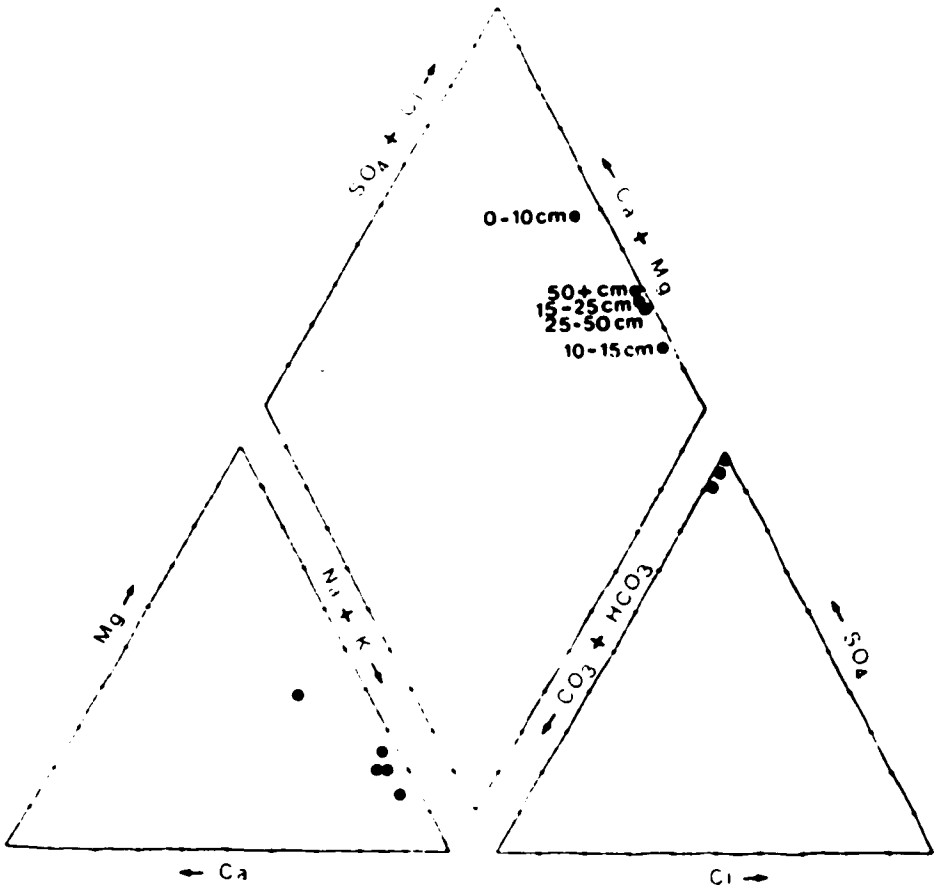

Piper diagram-ion facies of saturation paste extracts from soil horizons in a saline soil (SE 29-10-23-W4).

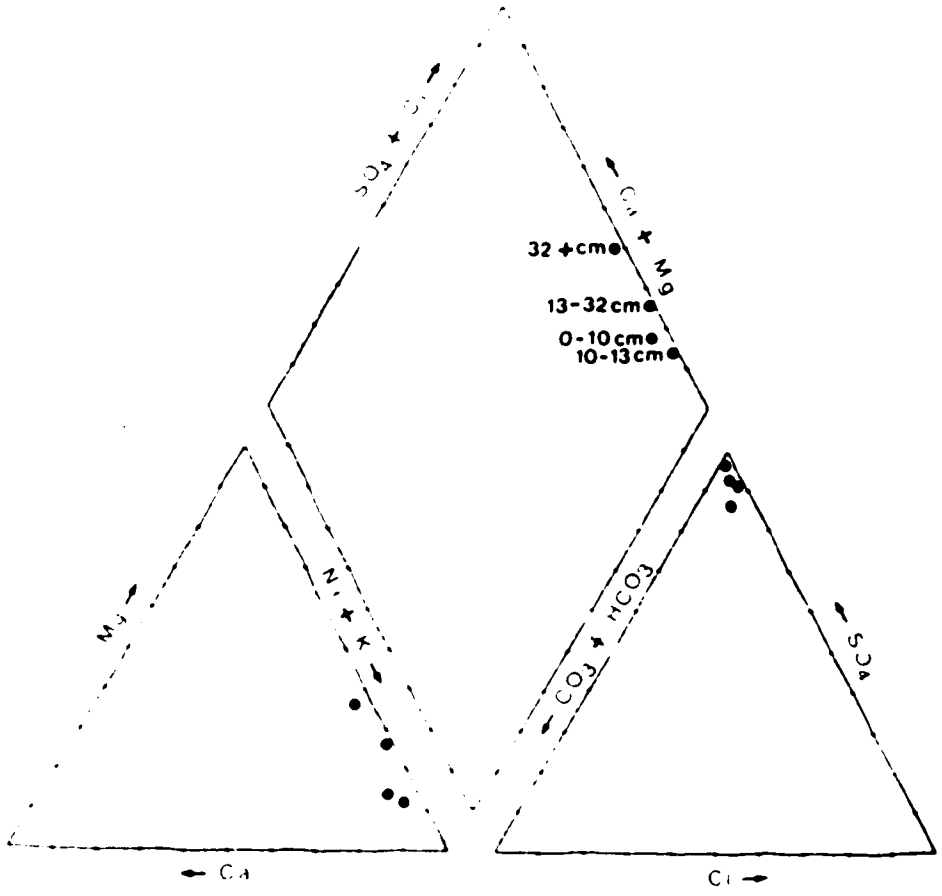

Piper diagram-ion facies of saturation paste extracts from soil horizons in a saline soil (WC 10-11-23-W4).

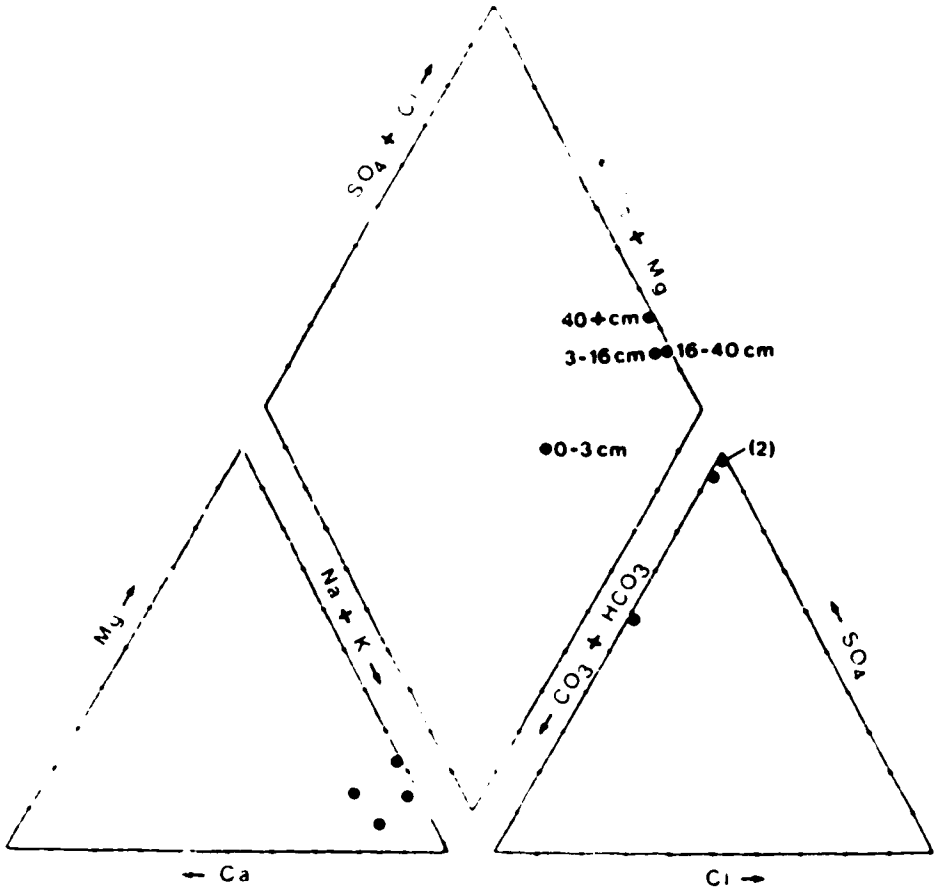

Piper diagram-ion facies of saturation paste extracts from soil horizons in a saline soil (NW 21-10-23-W4).

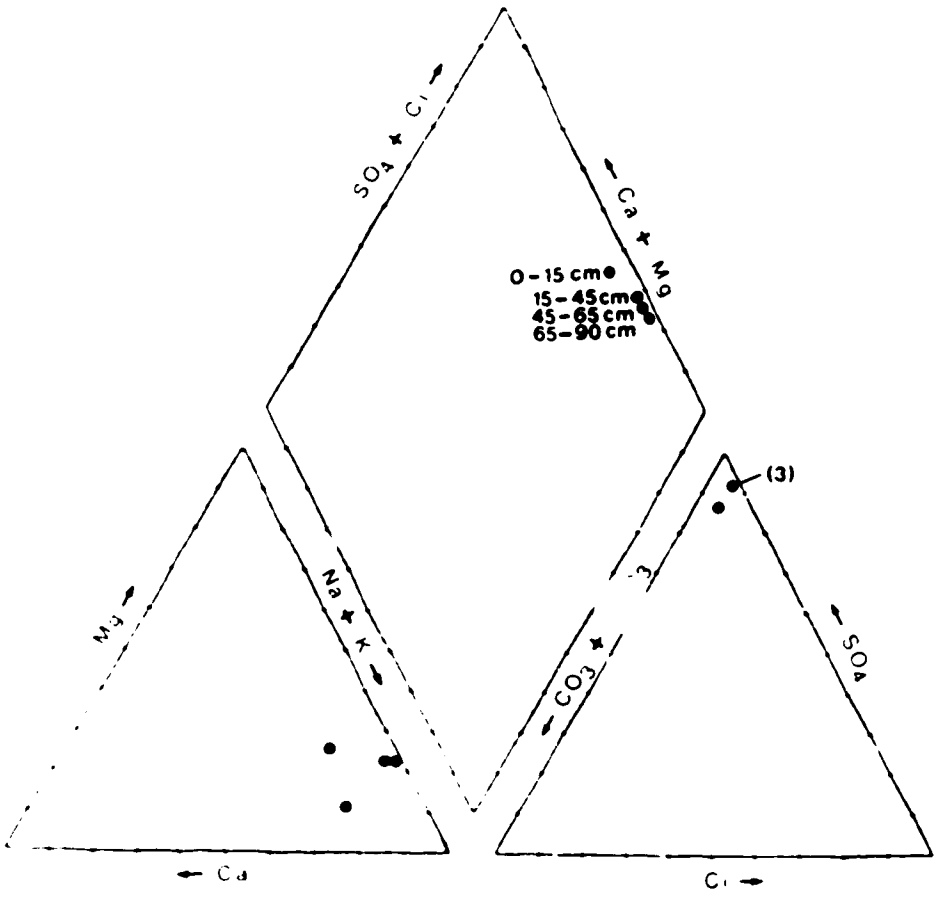

Piper diagram-ion facies of saturation paste extracts from soil horizons in a saline soil (NE 27-10-23-W4).

6.8. Groundwater chemistry.

Piezometer or Well	EC (dS m^{-1})	pH (H_2O)	Na	K	Ca	Mg	SO_4	CO_3	HCO_3	Cl
			- - - - - - - - - - mmole ($\pm$) L^{-1} - - - - - - - - - -							
A1-76	6.0	7.1	60.1	0.24	1.4	3.5	43.7	1.7	14.9	5.6
A1-24	3.9	7.2	43.7	0.15	0.4	1.0	10.6	5.7	29.9	2.2
A1- 9	20.8	6.8	222.8	0.64	15.4	55.2	251.3	2.2	23.5	4.2
A2-84	3.1	7.4	23.9	0.15	4.8	3.8	26.7	0.0	7.6	1.5
A2-42	5.0	7.1	50.1	0.13	1.5	2.2	38.5	0.0	16.2	1.1
A2-14	9.2	7.0	85.0	0.38	13.8	14.2	119.9	0.0	12.4	0.6
A3-69	3.1	7.4	29.6	0.14	1.1	0.7	12.0	0.0	11.8	8.7
A3-30	3.4	7.3	32.7	0.08	0.5	0.2	22.6	0.0	11.8	1.1
A3-5W	6.8	7.3	42.3	0.28	11.9	28.7	68.1	0.7	5.5	1.7
A4-99	4.1	7.3	36.6	0.13	2.0	1.0	31.5	0.0	8.1	4.2
A5-69	3.9	7.3	35.6	0.13	1.7	0.8	26.5	2.1	11.9	1.4
B1-69	4.6	7.2	43.5	0.37	1.0	0.8	11.6	1.5	14.5	21.0
B1-41	2.8	7.4	28.5	0.09	0.2	0.1	7.1	3.2	17.5	2.9
B1-19	5.1	7.2	48.4	0.24	0.4	1.5	29.3	4.2	17.9	2.2
B1-11	7.3	7.2	58.0	0.38	5.0	10.9	50.6	1.3	13.3	5.0
B1- 9	7.6	7.1	60.7	0.36	10.1	15.7	58.0	0.0	13.1	6.5
B1- 6	10.8	7.0	80.5	0.53	16.9	30.7	125.3	0.0	12.6	10.8
B2-91	3.1	7.4	26.5	0.10	0.7	0.2	4.7	0.8	9.6	16.2
B2-63	2.7	7.5	24.4	0.08	0.1	0.1	3.7	2.3	11.2	12.0
B2-34	2.0	7.5	20.6	0.07	0.1	0.4	5.8	2.2	16.2	0.6
B3-16	9.3	6.9	94.5	0.21	2.7	2.2	60.3	5.0	28.6	1.5
B3- 6	13.8	7.0	107.3	0.44	12.2	33.2	153.5	1.4	11.6	6.6
B4-30	3.0	7.3	29.6	0.07	0.2	0.1	7.0	2.8	19.4	3.8
B4-18	5.9	7.2	52.5	0.18	3.4	2.8	42.6	1.7	10.5	3.1
B4-4W	5.9	7.3	24.5	0.20	18.0	29.9	58.0	0.0	6.5	2.1
C1-35	7.8	7.8	78.7	0.37	2.0	2.5	76.5	1.1	14.9	3.1
C1-34	4.0	8.3	97.9	0.44	3.0	17.5	113.8	1.7	14.3	4.8
C1-25	11.2	7.7	128.0	0.45	3.9	3.8	112.0	3.5	19.4	4.3
C1-24	11.4	7.7	137.4	0.40	4.6	8.9	129.1	1.6	15.5	5.0
C2-30a	3.8	8.1	38.3	0.19	0.8	0.7	35.9	1.9	16.5	1.8
C2-30b	6.1	7.9	58.9	0.31	3.0	7.1	60.3	1.3	13.9	2.5
C2-10	9.6	7.4	80.8	0.44	16.2	20.6	105	1.7	8.7	3.9
C2- 9	11.4	7.3	99.3	0.45	18.1	29.8	123.9	0.8	9.8	4.3
C2- 7	11.5	7.5	107.6	0.38	17.8	26.6	128.6	0.6	8.8	4.5
C2- 6	11.2	7.5	97.0	0.44	18.1	29.0	126.0	0.7	10.2	4.8

6.9. Lithologic chemistry of saturation paste extracts from Sites C1 and C2.

Depth (m)	EC (dS m^{-1})	pH (H_2O)	Na	K	Ca	Mg	SO_4	CO_3	HCO_3	Cl
						mmole (±) L^{-1}				
Site C1										
0.00- 0.10	1.32	7.7	2.1	0.95	8.5	1.6	4.9	0.00	4.34	0.39
0.10- 0.21	0.41	7.7	0.6	0.27	3.3	0.7	1.0	0.00	2.56	0.19
0.21- 0.44	0.37	7.7	0.8	0.04	2.3	1.0	1.2	0.00	1.62	0.20
0.44- 0.59	0.39	7.8	0.5	0.03	3.0	0.8	1.0	0.00	2.27	0.15
0.59- 0.72	0.45	7.9	0.7	0.06	3.3	1.0	1.5	0.00	1.66	0.20
0.72- 1.15	0.37	8.3	0.8	0.04	1.8	1.2	1.1	0.00	3.45	0.18
1.15- 1.52	0.93	8.6	5.2	0.05	1.5	2.9	6.0	0.00	3.21	0.20
1.52- 1.80	0.84	8.8	6.6	0.05	0.2	1.3	4.0	0.00	3.98	0.22
1.52- 1.83	0.79	8.2	3.0	0.22	2.5	2.5	5.0	0.00	2.60	0.28
1.83- 2.13	0.75	8.6	4.3	0.14	1.0	2.2	3.3	0.00	3.82	0.42
2.13- 2.44	1.29	8.3	9.3	0.31	1.5	2.0	9.9	0.00	3.29	0.35
2.44- 2.74	0.89	8.5	6.0	0.14	0.5	1.8	5.5	0.00	3.37	0.29
2.74- 3.05	0.95	8.3	7.1	0.21	0.2	1.4	6.5	0.00	3.13	0.35
3.05- 3.35	4.96	7.8	18.0	1.40	29.1	25.9	68.9	0.00	2.27	1.55
3.35- 3.66	4.96	7.8	18.8	1.26	28.9	25.6	72.0	0.00	1.87	0.40
3.66- 3.96	4.96	7.8	[illegible]	1.21	29.1	25.5	72.3	0.00	1.91	0.48
3.96- 4.27	5.02	7.8	19.5	1.21	27.8	25.9	72.0	0.00	2.03	0.46
4.27- 4.57	4.85	7.7	19.4	1.11	[illegible]	23.2	69.0	0.00	1.87	0.70
4.57- 4.88	4.85	7.7	19.4	1.08	[illegible]	3.0	69.0	0.00	0.77	0.79
4.88- 5.18	4.74	7.8	19.3	1.19	[illegible]	.6	66.1	0.00	2.72	1.04
5.18- 5.49	4.74	7.8	19.7	1.14	26.6	21.1	66.0	0.00	1.83	1.05
5.49- 5.79	4.69	7.7	19.2	1.06	27.6	20.6	66.0	0.00	1.79	1.14
5.79- 6.10	4.80	7.7	19.8	1.11	28.7	20.0	67.9	0.00	1.75	1.46
6.10- 6.40	4.74	7.7	20.0	1.16	27.2	20.1	67.0	0.00	1.75	1.61
6.40- 6.71	4.80	7.8	20.0	1.28	29.1	19.5	67.5	0.00	1.66	1.35
6.71- 7.01	3.62	7.9	17.8	0.92	15.2	12.4	41.8	0.00	1.75	1.14
7.01- 7.32	2.88	8.0	15.8	0.69	9.7	9.0	30.9	0.00	1.87	1.06
7.32- 7.62	4.74	7.8	20.0	1.06	27.9	19.2	65.2	0.00	1.62	1.87
7.62- 7.92	4.59	7.9	19.2	1.02	28.1	18.8	65.2	0.00	1.95	1.65
7.92- 8.23	4.74	7.9	19.3	0.97	27.5	19.0	66.5	0.00	1.66	1.74
8.23- 8.53	4.40	7.9	19.0	0.89	23.7	16.8	59.1	0.00	1.73	1.57
9.14-10.67	5.34	7.8	27.3	0.95	26.5	20.9	77.0	0.00	1.58	0.52
11.28-11.89	6.19	6.5	34.2	0.79	27.2	26.3	82.0	0.00	3.57	0.60
13.72-14.94	3.41	8.2	29.8	0.86	2.9	2.1	31.7	0.00	3.45	0.38
15.24-15.54	3.50	8.2	33.3	0.59	1.3	1.0	29.0	0.00	5.85	0.78
19.81-21.03	2.43	8.7	24.0	0.27	0.1	0.5	18.0	0.00	6.41	0.50
21.34-22.56	2.54	8.8	26.1	0.35	0.1	0.5	16.1	0.00	9.99	0.60
24.69-25.91	5.20	8.7	53.3	0.48	0.1	0.6	50.0	0.00	2.92	1.30
26.52-27.13	3.56	8.7	36.2	0.28	0.1	0.5	27.8	0.00	7.31	0.44
27.13-28.65	5.47	8.7	57.7	0.44	0.8	0.6	53.0	0.00	5.28	1.70
28.96-30.48	4.64	8.6	48.8	0.37	0.5	0.5	41.1	0.00	7.02	0.45
33.83-35.36	3.47	8.5	35.8	0.32	0.2	0.5	27.0	0.00	7.75	0.53
36.58-38.10	3.28	8.6	32.9	0.37	0.5	0.5	25.9	0.00	5.36	0.54

Depth (m)	EC (dS m^{-1})	pH (H_2O)	Na	K	Ca	Mg	SO_4	CO_3	HCO_3	Cl
			- - - - - - - - - - - - mmole (±) $l.^{-1}$ - - - - - - - - - - - -							
Site C2										
0.00- 0.07	2.78	7.5	13.5	1.84	10.1	9.9	12.5	1.46	14.21	1.36
0.07- 0.13	23.46	8.0	246.6	1.06	27.8	81.7	355.8	0.24	8.61	8.52
0.13- 0.24	32.48	8.6	347.6	0.59	35.8	95.2	492.0	0.00	3.69	18.36
0.24- 0.30	21.11	8.6	256.2	0.23	17.1	44.4	288.0	0.00	2.23	10.20
0.30- 0.49	15.64	8.6	181.2	0.21	13.5	28.1	189.0	0.00	1.95	6.84
0.49- 0.63	13.19	8.7	149.4	0.22	12.6	24.9	134.8	0.00	1.71	6.60
0.63- 0.88	12.42	8.5	133.8	0.26	15.5	28.4	149.4	0.00	1.62	5.28
0.88- 1.60	11.11	8.5	114.6	0.29	16.4	26.4	132.0	0.00	1.38	5.28
1.60- 1.75	9.38	8.2	97.2	0.37	19.0	13.9	113.4	0.00	1.66	2.68
1.75- 1.84	4.74	8.3	42.5	0.18	4.6	4.1	47.0	0.00	1.83	1.13
1.84- 2.00	7.82	8.0	75.6	0.39	24.8	12.6	95.0	0.00	1.54	1.29
1.83- 2.13	5.71	8.4	53.1	0.16	5.0	5.7	58.5	0.00	1.95	1.95
2.13- 2.44	5.95	8.3	55.0	0.20	5.8	5.9	63.0	0.00	1.95	1.80
2.44- 2.74	3.20	8.4	28.7	0.16	2.1	2.0	26.5	0.00	2.35	0.85
2.74- 3.05	3.91	8.4	35.2	0.22	3.5	2.8	34.5	0.00	2.15	1.00
3.05- 3.35	3.20	8.4	29.7	0.16	1.7	1.6	26.2	0.00	2.80	0.90
3.35- 3.66	3.55	8.3	33.7	0.19	2.1	1.7	30.0	0.00	3.13	1.00
3.66- 3.96	4.26	8.1	40.5	0.19	2.9	2.4	35.8	0.00	3.33	1.27
3.96- 4.27	2.11	8.5	18.4	0.16	0.7	0.8	16.1	0.00	2.96	0.55
4.27- 4.57	2.57	8.4	23.2	0.22	1.3	1.1	20.8	0.00	2.72	0.70
5.49- 6.10	2.45	8.2	21.5	0.14	1.4	1.2	20.6	0.00	2.31	0.70
4.01- 7.62	3.74	7.8	32.5	0.25	3.8	3.5	33.0	0.00	2.44	0.98
8.53- 9.14	5.86	7.7	47.0	0.34	17.3	8.7	72.8	0.00	1.66	0.55
10.06-10.67	2.97	8.2	27.0	0.28	0.9	1.0	23.1	0.00	7.02	0.31
11.58-12.19	3.35	8.5	33.0	0.34	0.8	0.6	27.8	0.00	4.51	0.30
12.19-13.41	3.30	8.0	27.3	0.86	3.3	3.7	29.7	0.00	3.53	0.35
13.11-13.72	4.74	8.6	50.5	0.53	..0	0.5	44.9	0.00	5.89	0.47
14.63-15.24	4.74	8.5	50.6	0.37	1.0	0.4	42.4	0.00	6.41	0.50
16.15-16.76	4.14	8.7	42.6	0.27	0.4	0.5	34.0	0.00	6.82	0.70
17.68-18.29	4.49	8.7	46.6	0.26	0.6	0.6	40.0	0.00	4.79	0.36
19.51-19.81	3.95	8.6	40.7	0.36	0.4	0.6	31.1	0.00	6.82	0.43
20.73-21.03	3.95	8.8	41.2	0.31	0.3	0.6	30.9	0.00	7.31	0.54
22.25-22.56	3.77	8.7	38.9	0.38	0.3	0.7	28.4	0.00	7.67	0.54
22.86-24.08	2.27	8.8	22.8	0.31	0.1	0.6	10.0	0.00	11.77	1.92
23.77-24.38	3.58	8.7	37.1	0.44	0.2	0.6	24.5	0.00	9.70	0.58
25.30-25.91	2.78	8.9	27.3	0.22	0.1	0.5	20.7	0.00	6.37	0.54
26.82-27.43	2.64	8.9	26.3	0.19	0.2	0.6	18.5	0.00	7.19	0.61
28.35-28.96	2.48	8.9	24.3	0.20	0.1	0.5	18.5	0.00	5.64	0.54

Depth (m)	EC (dS m^{-1})	pH (H_2O)	Na	Ca + Mg	K	SO_4	CO_3	HCO_3	Cl
			mmole (±) L^{-1}						
24.38-27.43	0.82	9.8	8.7	0.1	0.1	1.4	0.0	6.9	0.1
27.43-30.48	0.67	9.8	7.1	0.1	0.1	0.9	0.0	5.9	0.2
30.48-33.53	0.70	9.9	7.3	0.1	0.1	1.4	0.0	5.4	0.2
33.53-36.58	0.74	9.9	7.5	0.1	0.1	2.3	0.0	4.9	0.1
36.58-39.62	0.84	9.8	8.5	0.1	0.1	2.5	0.0	5.6	0.1
39.62-42.67	0.89	9.6	9.2	0.1	0.1	2.0	0.0	6.8	0.1
42.67-45.72	0.76	9.8	7.8	0.1	0.1	2.5	0.0	5.0	0.1
45.72-48.77	0.72	9.9	7.7	0.1	0.1	1.4	0.0	5.9	0.1
48.77-51.82	0.69	9.8	7.1	0.1	0.1	1.2	0.0	5.5	0.2
51.82-54.86	0.76	9.9	7.9	0.1	0.1	1.3	0.0	6.4	0.2
54.86-57.91	0.71	9.8	7.0	0.1	0.1	2.3	0.0	4.5	0.1
57.91-60.96	0.71	9.7	7.3	0.1	0.1	1.3	0.4	5.4	0.1
60.96-64.01	0.60	9.8	6.3	0.1	0.1	0.6	0.0	5.5	0.2
64.01-67.06	0.65	9.8	6.8	0.1	0.1	0.8	0.0	5.7	0.2
67.06-70.10	0.82	9.9	8.5	0.1	0.1	1.7	0.0	6.5	0.2
70.10-73.15	0.61	9.9	6.4	0.1	0.1	1.1	0.0	4.9	0.2
73.15-76.20	0.71	9.9	7.5	0.1	0.1	0.7	0.0	6.6	0.2
76.20-79.25	0.75	9.9	7.9	0.1	0.1	1.5	0.0	5.9	0.2
79.25-82.30	0.71	9.9	7.4	0.1	0.1	1.4	0.0	[illegible]	0.2
82.30-85.34	0.67	9.9	6.5	0.1	0.1	1.0	0.0	5.4	0.1
85.34-88.39	0.74	9.9	7.5	0.1	0.1	1.3	0.0	5.7	0.1
88.39-91.44	0.84	9.9	8.6	0.1	0.1	1.8	0.0	6.3	0.1
Site B4									
0.00- 3.05	0.25	8.6	0.5	1.9	0.2	0.4	0.0	1.5	0.2
3.05- 6.10	1.19	8.1	1.4	11.2	0.3	11.9	0.0	0.9	0.1
6.10- 9.14	1.52	8.1	4.3	12.7	0.3	14.8	0.0	1.2	0.1
9.14-12.19	1.12	8.2	3.4	8.7	0.3	10.7	0.0	0.9	0.2
12.19-15.24	1.78	8.0	3.1	18.5	0.3	19.1	0.0	0.9	0.2
15.24-18.29	2.13	8.0	3.5	25.0	0.3	24.4	0.0	0.7	0.2
18.29-21.34	1.26	9.5	12.0	0.2	0.1	7.1	0.0	4.8	0.1
21.34-24.38	1.42	9.2	8.6	0.2	0.1	8.2	0.0	3.5	0.1
24.38-27.43	1.12	9.6	11.0	0.1	0.1	5.9	0.0	4.8	0.1
27.43-30.48	0.89	9.6	8.6	0.1	0.1	4.5	0.0	3.8	0.1

6.10. Lithologic chemistry of 1:5 (soil:water) extracts from sites on the A- and B-Lines.

Depth (m)	EC (dS m^{-1})	pH (H_2O)	Na	Ca + Mg_R	K	SO_4	CO_3	HCO_3	Cl
			- - - - - - - - - mmole (±) L^{-1} - - - - - - - - -						
Site A1									
0.00- 3.05	0.26	8.4	0.3	1.7	0.2	1.4	0.0	0.8	0.1
3.05- 6.10	1.17	7.5	8.9	3.3	0.2	11.9	0.0	0.6	0.1
6.10- 9.14	2.71	7.9	15.3	15.6	0.3	29.6	0.0	0.7	0.1
9.14-12.19	2.11	8.4	14.3	5.6	0.2	18.1	0.0	0.8	0.1
12.19-15.24	2.11	8.6	17.5	1.8	0.2	17.0	0.0	1.1	0.1
15.24-18.29	1.24	9.4	12.3	0.2	0.1	8.1	0.2	4.0	0.3
18.29-21.34	1.17	9.6	9.8	0.2	0.1	7.8	0.0	3.7	0.2
21.34-24.38	1.24	8.9	12.2	0.1	0.2	7.4	0.2	4.7	0.3
24.38-27.43	1.06	9.0	9.8	0.1	0.1	5.7	0.2	4.1	0.2
23.43-30.48	0.84	9.1	7.9	0.1	0.1	3.8	0.0	4.0	0.2
30 48-33.53	0.73	9.3	7.0	0.1	0.2	2.7	0.0	4.3	0.1
33.53-36.58	0.8	9.4	8.2	0.1	0.1	2.8	0.0	5.1	0.7
36.58-39.62	1.41	9.0	13.1	0.5	0.2	8.1	0.0	4.5	0.2
39.62-42.67	0.68	9.4	7.2	0.5	0.1	1.5	0.1	5.2	0.4
42.67-45.72	0.96	8.7	8.9	0.1	0.1	5.0	0.0	4.4	0.2
45.72-48.77	0.75	9.4	7.6	0.1	0.1	2.5	0.0	5.0	0.2
48.77-51.82	0.92	9.2	9.1	0.4	0.2	3.9	0.0	3.0	0.9
51.82-54.86	0.98	9.8	9.8	0.1	0.1	4.6	0.3	5.0	0.3
54.86-57.91	1.06	9.9	9.7	0.1	0.1	6.0	0.0	4.2	0.2
57.91-60.96	0.98	9.2	9.6	0.1	0.1	4.8	0.2	4.5	0.5
60.96-64.01	0.78	9.8	7.5	0.1	0.1	2.5	0.0	4.8	0.1
64.01-67.06	1.11	9.3	10.8	0.1	0.2	5.9	0.0	4.8	0.2
67.06-70.10	1.01	9.7	10.3	0.1	0.1	3.3	0.3	6.1	0.3
70.10-73.15	0.92	9.7	9.1	0.1	0.1	3.3	0.0	5.6	0.2
73.15-76.20	1.17	9.6	11.7	0.1	0.4	5.5	0.2	5.8	0.2
Site A2									
0.00- 3.05	0.68	8.6	1.9	4.1	0.2	6.0	0.0	1.0	0.0
3.05- 6.10	1.46	8.4	9.4	4.3	0.2	14.2	0.0	1.2	0.1
6.10- 9.14	1.46	8.6	11.9	1.7	0.2	13.1	0.0	1.6	0.1
9.14-12.19	1.03	9.2	9.4	0.3	0.1	7.6	0.0	2.6	0.1
12.19-15.24	1.17	9.1	10.6	0.2	0.1	7.9	0.0	2.6	0.1
15.24-18.29	0.96	9.5	9.7	0.1	0.1	5.2	0.0	4.7	0.1
18.29-21.34	1.06	9.7	11.3	0.1	0.1	3.6	0.7	6.6	0.1
21.34-24.38	0.88	9.7	9.4	0.1	0.1	1.9	0.6	6.7	0.1
24.38-27.43	0.88	9.5	9.1	0.1	0.1	2.6	0.0	6.3	0.1
27.43-30.48	0.88	9.6	8.8	0.2	0.1	3.1	0.0	5.4	0.2
30.48-33.53	0.84	9.5	8.8	0.1	0.1	2.8	0.0	5.8	0.2
33.53-36.58	1.01	9.5	10.4	0.1	0.1	3.2	0.0	6.6	0.4
36.58-39.62	0.75	9.6	7.9	0.1	0.1	2.3	0.0	5.4	0.1
39.62-42.67	0.75	9.6	7.3	0.1	0.1	3.3	0.0	3.9	0.1
42.67-45.72	0.92	9.5	9.0	0.3	0.1	3.2	0.0	5.5	0.-

Depth (m)	EC (dS m^{-1})	pH (H_2O)	Na	Ca + Mg	K	SO_4	CO_3	HCO_3	Cl
			- - - - - - - - - -		mmole (±) L^{-1}		- - - - - - - - - -		
45.72-48.77	0.59	10.0	5.9	0.1	0.1	1.4	0.0	4.2	0.2
48.77-51.82	0.62	10.0	6.2	0.1	0.1	2.0	0.0	4.3	0.2
51.82-54.86	0.88	9.9	8.7	0.1	0.1	3.5	0.0	5.0	0.3
54.86-57.91	0.68	10.0	7.0	0.1	0.1	1.5	0.0	5.5	0.2
57.91-60.96	0.88	10.0	8.9	0.1	0.1	2.6	0.0	6.0	0.2
60.96-64.01	0.73	10.1	7.4	0.1	0.1	1.6	0.0	5.7	0.2
64.01-67.06	0.75	10.2	8.0	0.1	0.1	1.5	0.0	6.1	0.2
67.06-70.10	0.72	10.0	7.3	0.1	0.1	2.0	0.0	5.2	0.1
70.10-73.15	0.92	9.9	9.1	0.1	0.1	3.0	0.3	5.8	0.2
73.15-79.25	0.57	10.2	5.6	0.1	0.1	1.5	0.0	4.1	0.2
79.25-82.30	1.06	9.7	10.7	0.1	0.1	3.2	0.6	6.5	0.2
82.30-83.82	0.78	9.9	7.5	0.1	0.1	3.1	0.0	4.1	0.2
Site A3									
0.00- 3.05	1.32	8.3	1.4	12.5	0.2	15.6	0.0	0.6	0.1
3.05- 6.10	0.78	8.6	3.2	4.0	0.2	9.5	0.0	0.7	0.1
6.10- 9.14	0.41	9.2	3.3	0.3	0.1	2.2	0.0	2.0	0.1
9.14-12.19	0.39	9.4	3.3	0.2	0.2	1.6	0.0	2.2	0.1
12.19-15.24	0.43	9.5	3.6	0.2	0.2	1.8	0.0	2.2	0.1
15.24-18.29	0.47	9.8	4.6	0.1	0.1	1.4	0.0	3.5	0.1
18.29-21.34	0.51	9.8	4.7	0.1	0.1	1.8	0.0	3.0	0.1
21.34-24.38	0.47	10.0	4.5	0.1	0.1	1.2	0.0	3.3	0.1
24.38-27.43	0.65	9.8	6.0	0.1	0.2	2.7	0.0	3.3	0.2
27.43-30.48	0.57	9.7	5.2	0.1	0.1	3.1	0.0	2.2	0.1
30.48-33.53	0.60	10.1	5.7	0.1	0.1	2.3	0.0	3.5	0.1
33.53-36.58	0.62	10.1	6.3	0.1	0.1	2.3	0.0	3.7	0.2
36.58-39.62	0.58	10.1	5.6	0.1	0.1	2.0	0.0	3.8	0.1
39.62-42.67	0.68	10.0	6.5	0.1	0.1	3.5	0.0	3.0	0.1
42.67-45.72	0.60	9.9	5.8	0.1	0.1	2.6	0.0	3.1	0.1
45.72-48.77	0.57	10.1	5.7	0.1	0.1	2.0	0.0	3.6	0.2
48.77-51.82	0.62	10.0	5.7	0.1	0.1	2.5	0.0	3.3	0.2
51.82-54.86	0.49	10.1	4.8	0.1	0.1	1.6	0.0	3.0	0.1
54.86-57.91	0.64	9.9	6.1	0.1	0.1	2.6	0.0	3.7	0.1
57.91-60.96	0.66	10.0	6.5	0.1	0.1	2.6	0.0	3.7	0.2
60.96-64.01	0.66	10.0	6.4	0.1	0.1	2.8	0.0	3.5	0.2
64.01-67.06	0.66	10.0	6.3	0.1	0.1	2.4	0.0	3.8	0.1
67.06-70.10	0.68	9.8	6.4	0.1	0.1	3.1	0.0	3.1	0.1
Site A4									
0.00- 3.05	0.45	9.4	3.6	0.4	0.1	2.2	0.0	1.8	0.2
3.05- 6.10	0.73	9.6	6.8	0.2	0.1	3.9	0.0	3.0	0.1
6.10- 9.14	0.84	9.6	7.5	0.2	0.1	4.6	0.0	2.6	0.2
9.14-12.19	0.70	10.0	6.7	0.1	0.1	2.7	0.0	4.1	0.2
12.19-15.24	0.70	10.1	7.0	0.1	0.1	2.0	0.0	4.9	0.2

Depth (m)	EC (dS m^{-1})	pH (H_2O)	Na	Ca + Mg	K	SO_4	CO_3	HCO_3	Cl
			- - - - - - - - - -	mmole (+) L^{-1}			- - - - - - - - - -		
15.24-18.29	0.74	10.2	7.4	0.1	0.1	1.8	0.0	5.5	0.2
18.29-21.34	0.59	10.3	6.1	0.1	0.1	1.0	0.0	5.0	0.2
21.34-24.38	0.67	10.1	6.6	0.1	0.1	2.3	0.0	4.3	0.1
24.38-27.43	0.74	10.3	7.4	0.1	0.1	1.8	0.2	5.4	0.2
27.43-30.48	0.59	10.3	6.0	0.1	0.1	1.4	0.0	4.6	0.2
30.48-33.53	0.69	10.2	6.9	0.1	0.1	2.0	0.0	5.0	0.2
33.53-36.58	0.72	10.1	7.0	0.1	0.1	2.9	0.0	3.9	0.2
36.58-39.62	0.89	9.8	8.4	0.2	0.2	4.5	0.0	4.1	0.3
39.62-42.67	0.72	9.9	7.1	0.1	0.1	2.7	0.0	4.3	0.2
42.67-45.72	0.82	10.0	7.9	0.1	0.1	3.1	0.0	3.6	0.3
45.72-48.77	0.84	9.7	8.2	0.1	0.1	3.4	0.0	4.8	0.2
48.77-51.82	0.89	9.8	8.5	0.1	0.1	4.7	0.0	3.8	0.3
51.82-54.86	0.74	9.9	7.3	0.1	0.1	2.4	0.0	4.7	0.2
54.86-57.91	0.67	9.8	6.4	0.1	0.1	2.2	0.0	4.1	0.2
57.91-60.96	0.85	9.9	8.2	0.1	0.1	3.9	0.0	4.4	0.1
60.96-64.01	0.85	10.1	8.5	0.1	0.1	2.7	0.0	5.7	0.2
64.01-67.06	0.76	10.0	7.6	0.1	0.1	2.6	0.0	4.7	0.1
67.06-70.10	0.97	10.0	9.4	0.1	0.2	4.0	0.0	5.4	0.3
70.10-73.15	0.81	10.0	7.8	0.1	0.1	3.2	0.0	4.5	0.1
73.15-76.20	0.69	10.1	6.8	0.1	0.1	2.2	0.0	4.5	0.1
76.20-79.25	0.91	10.0	8.8	0.1	0.1	4.8	0.0	4.1	0.1
79.25-82.30	0.77	10.0	7.6	0.1	0.1	3.3	0.0	4.2	0.2
82.30-85.34	0.95	9.9	9.4	0.1	0.2	4.8	0.0	4.6	0.3
85.34-88.39	0.89	10.1	9.0	0.1	0.1	3.7	0.0	5.1	0.2
88.39-91.44	0.84	10.2	8.4	0.1	0.1	2.5	0.0	5.7	0.2
91.44-94.49	0.87	10.2	8.7	0.1	0.1	3.3	0.0	5.2	0.1
94.49-97.54	0.99	9.9	9.5	0.1	0.2	5.0	0.0	4.5	0.2
97.54-99.06	0.99	9.9	9.7	0.1	0.1	4.5	0.0	4.8	0.2
Site A5									
0.00- 3.05	1.74	8.5	10.2	7.6	0.2	18.8	0.0	0.9	0.1
3.05- 6.10	1.39	8.6	8.0	6.1	0.2	15.2	0.0	0.8	0.1
6.10- 9.14	0.77	9.3	6.7	0.6	0.1	5.4	0.0	1.7	0.1
9.14-12.19	0.72	9.8	6.8	0.3	0.1	3.4	0.0	3.5	0.2
12.19-15.24	0.84	10.1	8.7	0.1	0.1	2.4	0.0	5.7	0.2
15.24-18.29	0.75	10.0	7.5	0.1	0.1	2.1	0.0	5.2	0.2
18.29-21.34	0.67	10.1	7.0	0.1	0.1	1.6	0.0	5.3	0.2
21.34-24.38	0.84	10.2	8.6	0.1	0.1	2.2	0.2	5.8	0.2
24.38-27.43	0.80	10.1	8.3	0.1	0.1	2.4	0.0	5.6	0.2
27.43-30.48	0.84	10.2	8.7	0.1	0.1	2.3	0.2	6.0	0.2
30.48-33.53	0.72	10.2	7.3	0.1	0.1	1.9	0.0	5.0	0.2
33.53-36.58	0.80	10.1	7.9	0.1	0.1	2.6	0.0	5.2	0.2
36.58-39.62	0.80	10.0	8.4	0.1	0.1	1.8	0.2	6.2	0.2
39.62-42.67	0.82	10.1	8.5	0.1	0.1	1.6	0.2	6.4	0.2
42.67-45.72	0.70	10.0	7.0	0.1	0.1	2.5	0.0	4.3	0.2

Depth (m)	EC (dS m^{-1})	pH (H_2O)	Na	Ca + Mg	K	SO_4	CO_3	HCO_3	Cl
			- - - - - - - - - -	mmole (±) L^{-1}			- - - - - - - - - -		
45.72-48.77	0.87	9.3	8.9	0.1	0.1	1.8	0.2	5.7	0.2
48.77-51.82	0.89	10.0	9.3	0.1	0.1	2.5	0.2	6.1	0.2
51.82-54.86	0.89	9.9	8.9	0.1	0.1	3.0	0.0	5.6	0.2
54.86-57.91	0.76	10.0	7.8	0.1	0.1	2.4	0.0	5.0	0.4
57.91-60.96	0.85	10.0	8.7	0.1	0.1	2.8	0.0	5.4	0.4
60.96-64.01	0.70	10.0	6.9	0.1	0.1	2.6	0.0	4.2	0.2
64.01-67.06	0.89	9.9	8.8	0.1	0.1	3.7	0.3	4.6	0.2
67.06-70.10	0.70	9.9	7.2	0.1	0.1	2.8	0.0	4.5	0.1
Site B1									
0.00- 3.05	1.20	8.6	7.3	8.2	0.3	13.3	0.0	1.2	0.2
3.05- 6.10	1.86	8.3	8.3	10.9	0.4	13.3	0.0	0.9	0.2
6.10- 9.14	0.91	8.7	6.5	2.4	0.0	5.7	0.0	1.3	0.2
9.14-12.19	0.85	9.0	7.5	0.6	0.2	8.0	0.0	2.8	0.2
12.19-15.24	0.85	9.1	7.9	0.3	0.2	5.1	0.0	3.2	0.1
15.24-18.29	0.95	9.2	8.9	0.3	0.2	6.6	0.0	3.0	0.1
18.29-21.34	1.05	9.4	15.6	0.2	0.1	7.2	0.0	3.9	0.1
21.34-24.38	0.97	9.5	10.4	0.1	0.1	3.7	0.2	6.0	0.1
24.38-27.43	1.07	9.7	11.8	0.1	0.1	4.0	0.5	6.6	0.1
27.43-30.48	0.99	9.7	11.1	0.1	0.1	2.1	0.9	7.6	0.2
30.48-33.53	1.04	9.9	11.6	0.1	0.1	2.1	1.1	8.0	0.2
33.53-36.58	0.89	10.0	9.7	0.1	0.1	1.5	0.7	7.5	0.1
36.58-39.62	0.99	10.0	11.0	0.1	0.1	1.4	0.8	8.3	0.1
39.62-42.67	0.95	10.0	9.8	0.1	0.1	1.5	1.3	7.3	0.1
42.67-45.72	1.27	9.8	12.9	0.1	0.1	6.4	0.0	6.6	0.1
45.72-48.77	1.04	9.9	11.2	0.1	0.1	2.8	0.0	7.7	0.1
48.77-51.82	1.10	9.9	11.0	0.1	0.1	4.3	0.0	5.9	0.1
51.82-54.86	1.31	9.7	13.1	0.1	0.1	9.5	0.0	5.3	0.1
54.86-56.08	1.31	9.7	13.1	0.1	0.1	9.7	0.0	5.3	0.1
56.08-57.91	0.77	10.1	7.9	0.1	0.1	1.2	0.0	6.5	0.2
57.91-60.96	0.91	10.0	9.0	0.1	0.1	3.0	0.0	5.8	0.1
60.96-64.01	0.80	10.1	8.3	0.1	0.1	2.2	0.0	5.9	0.2
64.01-67.06	0.84	10.1	8.4	0.1	0.1	1.9	0.0	6.3	0.2
67.06-70.10	0.80	10.1	8.1	0.1	0.1	2.1	0.0	5.7	0.2
Site B2									
1.22- 1.83	0.23	9.2	1.3	1.1	0.1	0.6	0.0	1.0	0.1
1.83- 3.05	0.21	9.3	1.4	0.5	0.1	0.6	0.0	1.2	0.1
3.05- 4.57	0.35	9.0	1.7	1.7	0.1	2.0	0.0	0.9	0.1
4.57- 6.10	0.30	8.9	2.0	0.6	0.1	1.4	0.0	1.3	0.0
6.10- 9.14	0.65	8.6	3.2	2.9	0.2	5.1	0.0	0.7	0.1
9.14-12.19	0.85	8.8	6.2	1.5	0.2	7.2	0.0	1.3	0.1
12.19-15.24	0.79	9.3	7.1	0.3	0.1	4.7	0.0	2.8	0.1
15.24-18.29	0.89	9.6	8.7	0.2	0.1	3.1	0.0	5.3	0.1
18.29-21.34	0.79	10.0	8.2	0.1	0.1	1.5	0.0	6.3	0.2
21.34-24.38	0.74	9.8	7.5	0.1	0.1	1.6	0.0	5.5	0.1

6.11. Soil moisture status at Sites C1 and C2.

	MOISTURE (percent by volume)											
	DEPTH (cm)											
Date	23	31	46	61	76	91	107	122	150	200	250	292
Site C1												
May 16/85	35.11	33.19	30.40	31.30	33.59	32.16	28.10	26.66	—	—	—	—
May 23/85	35.82	33.42	30.92	31.77	34.34	32.71	30.38	28.90	—	—	—	—
May 30/85	35.23	34.42	31.91	31.87	34.83	32.57	29.46	28.29	—	—	—	—
Jun 6/85	35.49	33.87	31.27	32.06	34.35	33.55	30.51	28.59	—	—	—	—
Jun 13/85	34.30	32.25	31.20	30.91	34.26	32.46	29.48	29.18	—	—	—	—
Jun 20/85	34.51	32.26	30.61	32.03	33.99	32.81	29.99	29.74	—	—	—	—
Jun 27/85	33.74	31.86	30.07	31.40	33.71	32.23	29.67	28.66	—	—	—	—
Jul 4/85	33.11	32.25	30.05	30.95	33.64	31.86	29.60	28.41	—	—	—	—
Jul 11/85	31.87	30.66	29.75	30.90	33.34	31.36	29.55	29.03	—	—	—	—
Jul 18/85	31.60	30.48	28.54	30.32	33.30	31.22	29.12	28.41	—	—	—	—
Jul 25/85	31.80	29.90	28.30	30.41	32.58	30.00	28.39	28.48	—	—	—	—
Aug 1/85	31.61	30.19	28.33	31.19	32.93	30.31	28.55	28.22	—	—	—	—
Aug 9/85	31.22	30.07	28.56	30.75	32.82	30.60	29.01	28.29	—	—	—	—
Aug 16/85	31.77	30.22	28.24	31.04	33.38	30.08	27.80	27.93	—	—	—	—
Aug 22/85	32.25	30.02	28.04	31.01	33.11	29.84	28.22	28.21	—	—	—	—
Aug 29/85	32.13	30.10	28.19	30.88	32.68	29.74	28.71	27.75	—	—	—	—
Sep 5/85	32.62	30.45	28.85	31.74	34.09	30.04	20.47	20.79	—	—	—	—
Sep 13/85	36.01	31.64	29.59	32.39	33.63	30.21	28.01	28.43	—	—	—	—
Sep 20/85	35.16	32.41	29.72	32.34	33.74	29.57	27.88	28.80	27.94	24.48	37.50	38.70
Sep 26/85	33.68	31.58	29.11	31.81	33.71	29.25	27.60	28.23	27.17	25.85	27.99	36.91
Oct 3/85	33.07	30.76	29.35	31.73	32.55	29.67	27.74	29.11	27.69	24.97	34.79	38.27
Oct 25/85	36.31	32.93	30.85	33.17	34.08	30.26	28.70	29.31	—	—	—	—

	MOISTURE (percent by volume)											
	DEPTH (cm)											
Date	23	31	46	61	76	91	107	122	150	200	250	292
Site C1 (continued)												
May 16/86	37.71	34.91	31.51	33.70	32.75	29.69	27.90	29.81	26.64	24.76	35.21	35.76
May 21/86	35.76	33.28	32.45	35.15	34.75	31.57	29.79	31.64	27.83	25.58	36.61	38.17
May 29/86	34.16	32.48	31.53	34.69	34.67	31.36	29.85	31.56	28.25	24.81	35.44	37.66
Jun 5/86	33.05	31.07	31.44	34.55	34.09	31.62	31.03	31.93	28.82	25.02	37.22	37.84
Jun 12/86	31.54	31.16	30.81	34.34	34.25	31.17	30.11	31.66	28.35	24.94	37.86	—
Jun 19/86	30.11	29.44	30.47	34.39	33.83	31.44	30.18	31.02	28.78	25.36	37.54	37.87
Jun 26/86	29.58	29.44	28.29	33.07	34.48	33.25	29.99	29.40	28.59	26.02	37.04	—
Jul 3/86	28.93	28.81	27.86	32.71	34.09	33.05	29.92	29.16	30.27	27.98	37.57	—
Jul 10/86	28.07	27.76	26.98	32.56	33.39	31.93	29.59	29.07	28.92	26.40	36.54	—
Jul 17/86	23.86	24.45	24.07	29.86	31.05	29.42	27.31	27.28	26.65	24.32	34.35	—
Aug 28/86	18.47	18.72	18.45	20.30	21.41	20.60	19.60	21.10	25.88	26.46	32.26	—
Sep 4/86	19.19	18.82	17.91	19.48	21.18	19.42	18.56	20.34	25.30	25.19	36.21	—
Sep 11/86	24.74	20.40	18.35	19.97	21.20	19.45	18.37	20.21	25.03	23.70	35.66	—
Sep 18/86	26.60	21.51	17.41	19.22	19.88	18.92	17.21	19.13	23.67	22.76	33.00	—
Sep 25/86	33.29	25.38	17.83	19.02	20.24	19.20	17.83	20.39	24.15	23.24	33.12	—
Oct 2/86	35.37	32.96	28.48	23.92	20.58	19.59	18.13	20.67	24.83	24.76	31.56	—
Oct 9/86	34.30	33.02	28.38	23.87	21.69	19.21	18.41	20.37	24.84	23.76	32.52	—
Oct 16/86	33.57	30.88	27.98	25.32	21.30	19.24	18.06	20.87	25.53	24.95	35.51	—
Oct 23/86	33.01	30.72	28.00	25.30	21.39	19.42	18.21	20.80	25.21	23.70	36.04	—

	MOISTURE (percent by volume)											
	DEPTH (cm)											
Date	23	31	46	61	76	91	107	122	150	200	250	292
Site C1 (continued)												
Jun 4/87	28.22	28.19	25.25	28.98	29.06	27.12	22.92	23.23	25.83	23.95	35.08	—
Jun 25/87	33.45	31.20	27.07	28.86	29.41	27.91	23.47	23.92	25.25	25.02	33.91	—
Jul 9/87	27.18	26.99	25.78	27.97	28.81	27.30	22.89	23.59	24.99	24.50	30.04	—
Jul 23/87	37.18	34.69	26.52	25.80	26.93	25.50	22.00	23.43	24.96	24.31	28.65	—
Aug 7/87	24.64	24.32	22.85	25.38	25.30	23.64	20.06	22.12	24.84	24.50	30.21	—
Aug 17/87	26.85	24.76	22.36	25.28	25.29	23.75	20.49	22.30	24.84	24.82	30.47	—
Aug 31/87	23.38	22.99	20.08	23.47	24.88	22.47	20.26	21.74	24.34	25.07	31.66	—
Sep 14/87	21.48	21.47	19.69	22.95	23.28	22.00	20.41	22.36	24.	24.44	31.11	—
Sep 28/87	19.98	20.04	18.96	22.79	23.57	21.11	17.88	21.64	24	24.18	35.71	—
Feb 26/88	38.77	31.03	20.11	24.72	24.02	20.84	19.74	22.02		24.29	29.58	—
Mar 23/88	34.65	31.15	22.51	23.45	24.34	21.11	20.01	22.05	23.91	24.53	27.95	—
Apr 26/88	32.36	30.33	24.47	25.22	25.22	22.09	20.35	22.70	24	33.20	34.69	—
May 9/88	30.15	28.45	24.56	25.69	25.18	23.45	21.94	20.35	25.28	23.57	32.09	—

	MOISTURE (percent by volume)											
	DEPTH (cm)											
Date	23	31	46	61	76	91	107	122	150	200	250	300
Site C2												
May 16/85	43.41	42.21	37.79	35.54	34.28	37.20	40.82	45.94	—	—	—	—
May 23/85	41.78	41.50	37.14	34.56	33.42	37.25	40.72	45.90	—	—	—	—
May 30/85	43.09	40.93	37.47	34.68	34.12	37.14	40.62	44.67	—	—	—	—
Jun 13/85	41.80	41.07	37.15	33.90	33.10	37.27	39.75	45.85	—	—	—	—
Jun 20/85	41.88	40.86	37.05	34.27	33.61	37.53	41.13	47.65	—	—	—	—
Jun 27/85	34.60	33.40	31.31	31.45	31.37	34.03	38.01	37.73	39.58	41.04	40.24	—
Jul 4/85	33.79	33.86	31.65	31.31	31.37	34.27	37.57	37.38	39.55	40.77	44.55	44.33
Jul 11/85	33.68	32.69	31.27	30.92	31.04	34.16	38.04	37.50	39.98	40.97	43.84	43.47
Jul 18/85	34.30	32.57	30.73	31.26	31.58	34.77	38.22	37.51	40.99	41.62	44.99	44.61
Jul 25/85	33.49	32.40	30.83	31.39	30.99	34.76	38.23	37.63	40.00	41.44	43.36	44.57
Aug 1/85	33.90	32.19	31.11	31.49	31.52	34.35	37.69	36.88	40.39	40.93	43.56	44.16
Aug 9/85	34.40	32.65	31.25	31.45	30.97	34.64	37.97	36.08	40.73	41.14	42.08	43.99
Aug 16/85	37.27	35.49	31.69	31.44	31.34	34.82	38.25	36.75	40.21	40.85	42.92	43.91
Aug 22/85	36.29	34.75	31.97	31.72	31.89	35.65	37.83	37.38	41.37	42.93	43.28	44.80
Aug 29/85	35.80	33.76	31.22	31.91	31.18	34.71	38.18	36.71	40.34	41.42	43.28	43.81
Sep 5/85	35.42	33.72	31.63	32.81	32.00	36.50	39.35	37.81	41.48	43.25	43.76	46.03
Sep 13/85	40.89	39.70	40.60	42.09	39.66	40.56	42.01	40.66	42.51	43.74	43.03	44.58
Sep 20/85	37.01	35.54	36.80	37.63	39.13	39.01	41.47	41.09	44.02	44.43	44.58	47.49
Sep 26/85	36.09	34.11	35.38	38.49	36.42	38.42	40.16	39.75	42.90	43.00	43.49	46.65
Oct 3/85	35.53	33.70	34.92	37.04	36.07	37.89	39.83	39.03	42.05	43.28	43.20	45.47
Oct 25/85	36.39	34.41	36.12	38.92	37.78	40.26	41.46	41.60	44.30	45.35	45.17	47.61

	MOISTURE (percent by volume)											
	DEPTH (cm)											
Date	23	31	46	61	76	91	107	122	150	200	250	300
Site C2 (continued)												
May 16/86	37.41	34.09	34.30	38.02	36.54	39.03	41.31	42.27	43.99	44.43	46.81	—
May 21/86	37.19	35.52	35.49	38.23	36.73	39.40	41.92	41.56	43.98	44.38	45.75	—
May 29/86	36.11	33.77	35.11	37.14	35.91	38.42	41.28	41.37	43.11	44.06	44.81	—
Jun 5/86	35.76	34.21	35.11	37.30	36.40	38.63	41.69	41.51	44.18	43.66	46.00	—
Jun 12/86	34.60	33.25	34.27	37.26	35.88	38.15	40.89	41.08	43.58	43.77	45.24	—
Jun 19/86	34.12	33.29	34.62	36.54	36.09	39.02	40.73	40.89	43.41	43.58	45.56	—
Jun 26/86	33.45	32.69	32.78	35.65	35.10	35.58	39.36	40.13	42.21	43.08	45.01	—
Jul 3/86	34.39	33.13	33.37	36.02	35.72	35.68	38.89	39.89	41.77	43.93	46.02	—
Jul 10/86	34.53	33.04	32.77	36.16	36.66	35.99	38.94	40.94	41.78	43.13	45.27	—
Jul 17/86	34.97	33.29	33.15	36.62	36.03	36.67	39.19	40.02	42.76	43.34	46.22	—
Aug 21/86	33.31	32.24	31.37	33.77	33.89	34.83	37.45	38.73	40.03	42.44	44.53	—
Aug 28/86	34.28	32.93	33.42	35.57	35.84	35.75	39.14	40.81	42.00	42.50	45.23	—
Sep 4/86	34.68	32.67	32.55	35.11	35.55	35.54	38.40	49.90	40.64	43.21	44.56	—
Sep 11/86	34.91	33.86	33.78	35.68	36.07	36.89	39.29	39.31	40.92	41.23	43.35	—
Sep 18/86	34.06	32.72	31.87	34.67	34.67	34.88	37.45	38.37	39.07	40.56	43.72	—
Sep 25/86	34.82	33.19	32.76	35.50	35.63	36.14	38.73	38.98	41.63	40.57	42.72	—
Oct 2/86	38.03	36.17	34.05	36.57	36.25	36.53	39.65	40.02	42.16	42.69	45.03	—
Oct 9/86	37.76	35.27	33.74	36.52	36.27	36.50	39.52	39.75	41.49	42.27	44.98	—
Oct 16/86	37.42	34.83	33.83	36.48	36.16	37.40	39.96	40.83	42.16	43.18	44.31	—
Oct 23/86	36.14	34.52	33.05	36.53	36.68	36.74	39.34	39.60	39.99	41.14	44.80	—

Date	MOISTURE (percent by volume) DEPTH (cm) 23	31	46	61	76	91	107	122	150	200	250	300
Site C2 (continued)												
Jun 4/87	25.26	26.89	31.16	33.97	34.54	34.21	36.92	38.25	40.55	42.27	43.36	—
Jun 25/87	27.01	28.03	31.04	34.38	34.79	35.15	38.27	39.23	40.77	42.11	44.46	—
Jul 9/87	27.40	28.17	30.36	34.19	34.50	34.26	37.98	38.09	40.44	43.52	46.31	—
Jul 23/87	37.50	32.42	30.10	33.53	33.45	33.74	37.37	38.42	40.25	42.46	45.69	—
Aug 7/87	29.69	29.74	30.49	33.27	34.15	33.77	37.37	38.18	40.88	42.39	45.74	—
Aug 17/87	30.05	30.09	31.58	34.41	34.74	34.63	37.19	38.24	41.09	42.20	44.91	—
Aug 31/87	30.22	29.86	31.22	33.82	33.90	35.76	38.40	38.51	40.72	42.89	46.58	—
Sep 14/87	29.36	29.44	31.33	34.26	34.09	35.34	38.68	38.93	41.23	43.34	45.92	—
Sep 28/87	29.32	29.34	31.08	34.41	34.22	35.76	39.17	38.60	40.67	42.30	44.94	—

6.12. Soil moisture status at saturation, field capacity (-33 kPa), and permanent wilting point (-1,500 kPa) in the soil horizons at Sites C1 and C2.

Horizon Depth (cm)	% Moisture (v/v)		
	Saturation	- 33 kPa	-1,500 kPa
Site C1			
0 - 21	47.17	34.58	22.19
21 - 44	51.56	30.45	19.88
44 - 59	51.43	28.25	18.94
72 - 115	45.17	28.19	19.35
115 - 152	48.67	32.20	20.82
152 - 180	44.97	29.96	17.54
Site C2			
0 - 7	46.78	36.78	31.39
13 - 24	48.95	37.55	30.50
30 - 49	45.69	28.15	17.90
63 - 88	41.82	24.60	13.06
88 - 160	43.58	25.88	14.41
175 - 184	38.12	34.19	23.17
184 - 200	37.77	26.71	17.49